SYNTHESIS, CHARACTERISATION AND DRUG RELEASE FROM A RANGE OF

NOVEL "SMART"-CO-BIODEGRADABLE DELIVERY SYSTEMS

BY

FIONA NÍ CHEARÚIL (B.A.)

being a thesis submitted for the degree of

Doctor of Philosophy

in Pharmaceutics

at

University of Dublin

Trinity College

Under the direction and supervision of

Professor O.I. Corrigan, B.SC. (Pharm.), M.A., Ph.D., F.T.C.D., F.P.S.I.
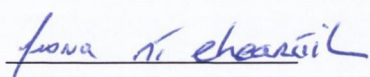
January 2008
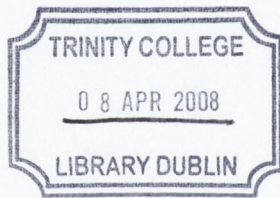
DECLARATION

This thesis is submitted by the undersigned to the University of Dublin for examination for the degree of Doctor of Philosophy. It has not been submitted as an exercise for a degree at any other university. I carried out all the practical work except where duly acknowledged. I wrote this manuscript with the aid of editorial advice from Professor O.I. Corrigan. I agree that the library may lend or copy the thesis upon request.

Fiona Ní Chearúil

To my parents

SUMMARY:

In recent years many biodegradable polymers have been investigated particularly for controlled delivery of drugs or proteins/peptides. The most commonly studied biodegradable polymers for controlled drug delivery are based on poly (esters), such as poly (lactides) of poly (glycolic acid). Limited research of environmentally sensitive and degradable systems capable of controlling drug release in response to a specific stimulus has been undertaken. The present thesis investigates the potential application of a novel intelligent biodegradable hydrogel.

A series of novel multifunctional hydrogels that combined the merits of both thermoresponsive and biodegradable polymeric materials were designed by varying both the composition ratios and the molecular weight of the precursor unit. The hydrogels were composed of N-isopropylacrylamide as a thermoresponsive unit and chemically modified poly (lactic acid) (PLA) as a hydrolytically degradable and hydrophobic unit. The chemical structures of the hydrogels were characterised using nuclear magnetic resonance (NMR), Fourier transform infrared spectroscopy (FTIR) and gel permeation chromatography (GPC). The hydrogels were thermoresponsive, with an increase in the lower critical solution temperature (LCST) the higher the percent of lactic acid diacrylate macromoer (PLAM) incorporated into the hydrogels. Swelling properties were dependant on temperature as well as the PLAM content. Increasing the molecular weight of PLAM resulted in both larger pores and a decrease in the crosslinking density; the effect being magnified by the higher molar ratio of PLAM to poly N-isopropylacrylamide (PNIPAAM).

The degradation behaviour of the three-dimensional polymeric networks formed was dependent on both structural (mesh size, cross-linking density, molecular weight (MW) distribution) and environmental parameters (temperature). Swelling, and in vitro biodegradation-induced morphological structure changes were characterised using scanning electron microscopy (SEM). A greater rate of degradation and disruption to the porous network could be seen with increasing PLAM. In the case of hydrogel series containing lower MW PLAM, degradation was faster below the LCST due the increased hydrophilicity of the network leaving it more susceptible to solute diffusion, thus increasing the hydrolytic cleavage of PLAM.

Increasing the MW of PLAM unit during polymerisation affected the cross-linking density and therefore the resulting water content of the degradable gel. A more open network led to an increase in the hydrolytic degradation rate of the PLAM ester bonds above the LCST however a trend emerged whereby the higher the percent of PLAM incorporated into the gel the faster the rate of degradation. Polymeric systems composed of lower molecular weight PLAM displayed a faster rate of degradation in comparison to that of the larger MW PLAM. However by co-

polymerisation, reversal in temperature control on the rate of degradation was achieved; whereby the gels displayed faster degradation relative to the linear PLA at 20°C.

The potential use of these novel biodegradable thermoresponsive hydrogels was also evaluated by using a range of model drugs with a variety of physicochemical properties. Drug release profiles as well as the mechanism of release were examined as a function of both temperature and composition. Mathematical models were employed to fit the data and obtain model parameters for the prediction of drug release profiles. Drug release was examined both above and below the LCST of the hydrogel series. The mechanism of release could be tailored as well as the rate of release by altering the hydrogel composition. An increase in temperature resulted in a decrease in both rate and extent of hydrogel swelling with an effective reversal of thermal control of drug release. The extent of thermal control depended on physicochemical properties of the drugs used. The loaded drug was shown to influence the swelling depending on solubility and polymer-drug interactions. The resulting release rates of the drugs were dependent on swollen state of hydrogel and the relationship between pore size and molecular diameter of the probe molecule.

The application of a thermoresponsive semi-biodegradable gel in pulsatile release studies was also examined. The rate of swelling was affected by the extent of deswelling or contraction on switching the external temperature. The hydrogel shrank to 80% its original volume on temperature switch indicative of a dense skin layer on the surface of the gel. The incorporation of a hydrophobic unit PLA appears to have strengthened the dense layer, which is further demonstrated by the effectiveness of "on-off" regulation of small molecular weight compounds in response to external temperature changes.

The current thesis therefore explores the use of a novel degradable smart gel in the role of controlled drug delivery. It can be concluded that degradation of hydrogels series can be manipulated by controlling monomer molar ratios of the reactants and the temperature at which experiments were conducted. A combination of characteristics such as the chemical nature of the polymer, rate of degradation, swelling characteristics and therefore pore size affected the release profiles of the model drugs. Drug physicochemical properties such as solubility, size and pKa played an important role in drug delivery.

TABLE OF CONTENTS

INTRODUCTION

Chapter 1: Design and Applications of "Smart" Polymers in Drug Delivery

Chapter 2: Biodegradable Hydrogels for Drug Delivery: Swelling kinetics and Mechanisms of Drug Release

EXPERIMENTAL

Chapter 3: Materials and Experimental methods

RESULTS AND DISCUSSION

Chapter 4: Polymer, Drug and Hydrogel Characterisation

Chapter 5: An Investigation of the Degradation and Release Kinetics from a Series of Gels Synthesised by Varying the Molar Ratios of PNIPAAM to PLA (MW 2000).

Chapter 6: An Investigation of the Degradation and Release Kinetics from a Series of Gels Synthesised by Varying the Molar Ratios of PNIPAAM to PLA (MW 12000).

Chapter 7: Effect of Drug Physiochemical Properties on Swelling/Deswelling kinetics and Pulsatile Drug release from PNP2$_{-2}$

Chapter 8: General Discussions

ACKNOWLEDGEMENTS

PRESENTATIONS ASSOCIATED WITH THIS THESIS

Poster presentations:

Synthesis, characterisation and drug release from a series of biodegradable thermoresponsive polymers, F. Ní Chearúil, O.I Corrigan, 26th Annual joint Research Seminar, Queens University, Belfast, March 2004.

The effect of the molecular weight of poly- L-lactic acid on the swelling behaviour, degradation and release kinetics from thermoresponsive NIPAAM-PLA co-polymers. F. Ní Chearúil, O.I Corrigan, 27th Annual joint Research Seminar, Trinity College Dublin, March 2005.

Oral presentations:

The influence of polymer composition and network structure on the degradation and release of indomethacin from PNIPAAM-co-PLA hydrogels. F Ní Chearúil and O.I. Corrigan, Socrates Intensive Programme: "Innovative therapeutics: from molecules to drugs" Université Catholique de Louvain, Belgium, July 2005.

Abbreviations and symbols

X	Flory interaction parameter
ξ	Mesh/Pore size
<C>	Correction factor
δ	Solubility parameter
μm	Micrometer
∞	Infinity
±	Plus or minus
TM	Trademark
~	Approximately
O	Degree
°C	Degree Centigrade
Å	Angstrom
A	Area
AA	Acrylic acid
Aam	Acrylamide
AIBN	Azobisisobutylonitrile
APS	Ammonium Persulfate
AUC	Area under the curve
BA	Benzoic acid
BIS	(N,N methylenebisacrylamide)
BMA	Butyl methacrylate
BSA	Bovine serum albumin
CD	Coefficient of Determination
$CDCl_3$	Deuterated chloroform
Cm	Centimetre
cm^{-1}	Frequency
D	Diffusion coefficient
D4	Dextran MW~4000
D10	Dextran MW~10000
D40	Dextran MW~40000
D70	Dextran MW~70000
DB	Diltiazem base
DCM	Dichloromethane
DH	Diltiazem Hydrochloride
DMA	N,N'-dimethylacrylamide
DMF	Dichloromethane

DSC	Differential Scanning Calorimetry
F	Fraction drug released
FITC	Fluorescein isocyanate
FTIR	Fourier Transform Infrared Spectroscopy
g	Gram
g/L	grams per litre
GPC	Gel Permeation Chromoatography
h	hour
H_2O	water
IDM	Indomethacin
IPN	Intrapenetrating network
J	joule
K	kelvin
k_c	Cube root dissolution rate constant
k_{dh}	Diffusional release rate constant fitted to Higuchi (1961)
k_{dp}	Diffusional release rate constant fitted to Peppas (1985)
Kj	kilojoule
k_{MC}	Maximum contraction rate
k_S	Swelling rate constant
k_{Sh}	Swelling rate constant fitted to Higuchi (1961)
k_{Sp}	Swelling rate constant fitted to Peppas (1985)
K_{ss}	Quasi-steady state release constant
L	litre
LCST	Lower critical solution temperature
$LCST_d$	LCST as determined by DSC measurements
$LCST_t$	LCST as determined by transmittance measurements
$LCST_s$	LCST as determined by swelling measurements
M	moles per litre
MBA	N,N'methylbisacrylamide
Mc	Molecular weight between cross-links
mg	milligram
min	minutes
ml	millilitre
mm	millilimeter
mM	millimolar
mmol	millimole
mol	mole

Mn	Number average molecular weight
m.p.	Melting point
MW	Molecular weight
n	Diffusiona,l exponent
N	Number of replicates
NaCl	Sodium chloride
NIPAAM	N-isopropylacrylamide
nm	nanometre
NMR	Nuclear Magnetic Resonance
PEO	Poly (ethylene oxide)
pH	Minus Log of hydrogen ion concentration
PHEMA	Poly (2-hydroxyethyl mathacrylate)
PB	Phosphate buffer 7.4
pKa	Dissociation constant for a weak acid
PLA	Poly (Lactic acid)
PLA$_{-2}$	Poly (Lactic acid) (MW 2000)
PLA$_{-12}$	Poly (Lactic acid) (MW 12000)
PLGA	Poly (Lactic-co-glycolic acid)
PNIPAAM	Poly (N-isopropylacrylamide)
PNP	Poly (N-isopropylacrylamide) hydrogel
PNP1$_{-2}$	PNIPAAM-co-PLA (MW2000) hydrogel[95-5 Molar Ratio]
PNP2$_{-2}$	PNIPAAM co-PLA (MW2000) hydrogel[90-10 Molar Ratio]
PNP3$_{-2}$	PNIPAAM co-PLA (MW2000) hydrogel[80-20 Molar Ratio]
PNP1$_{-12}$	PNIPAAM co-PLA (MW12000) hydrogel[95-5 Molar Ratio]
PNP2$_{-12}$	PNIPAAM co-PLA (MW12000) hydrogel[90-10 Molar Ratio]
PNP3$_{-12}$	PNIPAAM co-PLA (MW12000) hydrogel[80-20Molar Ratio]
PNP-PLA$_{-2}$	PNIPAAM-co-PLA (MW2000) hydrogel systems
PNP-PLA$_{-12}$	PNIPAAM co-PLA (MW12000) hydrogel systems
PNP-L	Linear Poly (N-isopropylacrylamide)
PNP-L1$_{-2}$	Linear PNIPAAM co-PLA (MW2000) hydrogel[95-5 Molar Ratio]
PNP-L2$_{-2}$	Linear PNIPAAM co-PLA (MW2000) hydrogel[90-10Molar Ratio]
PNP-L3$_{-2}$	Linear PNIPAAM co-PLA (MW2000) hydrogel[80-20Molar Ratio]
PNP-L1$_{-12}$	Linear PNIPAAM co-PLA (MW2000) hydrogel[95-5 Molar Ratio]
PNP-L2$_{-12}$	Linear PNIPAAM co-PLA (MW2000) hydrogel[90-10 Molar Ratio]
PNP-L3$_{-12}$	Linear PNIPAAM co-PLA (MW2000) hydrogel[80-20Molar Ratio]
PPO	Poly (propylene oxide)
P$_x$	Crosslinking density

Q	Fraction drug released at time t
R^2	Correlation coefficient
r.p.m	Revolutions per minute
s	Second
SA	Salicylic acid
s.d.	Standard deviation
S.R.	Swelling ratio
SEM	Scanning Electron Microscopy
t	Time
T	Temperature
TEMED	N,N,N,N,'-Tetramethylenediamine
Tg	Glass transition temperature
THF	Tetrahydrofuran
UCST	Upper critical solution temperature
UV	Ultraviolet
V_{2r}	Volume fraction in the relaxed state
V_{2s}	Volume fraction in the swollen state
Vs.	Versus
w/v	Weight per volume
w/w	Weight per weight
XRD	X-ray diffraction

CHAPTER 1:

DESIGN AND APPLICATIONS OF "SMART" POLYMERS IN

DRUG DELIVERY

1.1 INTRODUCTION

A polymer is a substance with a high molecular weight made up of many repeating smaller chemical units or molecules. Hydrogels are water-swollen polymeric networks containing chemical or physical cross-links (Peppas, 1986). It is the inherent properties of the cross-linker that maintains the three-dimensional swollen structure. Cross-linking can be in the form of covalent bonds or cohesion forces such as hydrogen bonding, Van der Waals, ionic or hydrophobic interactions (Qiu and Park 2001).

Intelligent drug delivery systems (DDS) demonstrate the ability to sense the environmental changes, judge the degree of the signal and react by producing a useful effect (Kost and Langer 2001). Such intelligent or "smart" DDS may be achieved by using stimuli responsive polymeric hydrogels, which alter their structure and physical properties in response to external stimuli. "Smart" hydrogels undergo reversible volume phase transitions upon changes in the environmental conditions. Many chemical and physical stimuli have been employed to induce these responses. The physical stimuli include temperature, electric fields, solvent composition, light, pressure and magnetic fields. Examples of chemical stimuli are pH, ions or specific molecules (Gupta et al., 2002). Due to the dynamic properties of hydrogels, they are a promising option in drug delivery applications.

The physical and mechanical properties of hydrogels are dependent upon the chemical composition as well as the physical structure. Improved biocompatibility and flexibility by controlling network properties can be achieved by modification of the hydrogel. Such modifications include addition of monomer(s), degree of crosslinking and the introduction of biodegradable hydrophilic and hydrophobic segments. A combination of permeability, biocompatibility, sensitivity to environmental changes and rates of enzymatic and hydrolytic degradation of the hydrogels play an important role in the swelling kinetics and thereby can control the rate and extent of drug release.

In the current niche of drug delivery technologies, hydrogels have made an irreplaceable space because of their unique characteristics. Traditional drug delivery systems developed can maintain drug levels within the therapeutic range and need fewer administrations thereby achieving effective therapies and increasing patient compliance. While these advantages can be significant, in many cases, such consistent drug release profiles may not be desirable e.g. insulin for diabetics, antiarrhythmics for heart rhythm disorders, gastric acid inhibitors for ulcer control, nitrates for angina pectoris, birth control, hormone replacement, immunisation, cancer chemotherapy and selective β-blockade (Kost and Langer, 1991). Intelligent controlled release

1

systems are more sophisticated and can respond to environmental changes and deliver or cease to deliver drugs. In addition smart polymers have been developed to achieve drug targeting to a specific part of the body. These self-regulating drug delivery systems or temporal systems are achieved by using stimuli responsive hydrogels by on-off switches (e.g. increase or decrease in temperature) resulting in pulsatile drug delivery (Kikuchi and Okano 2002).

Pulsatile drug delivery is receiving a major impetus towards the development of new or improved drug therapies. It has the advantage of avoiding drug tolerance as well as reducing the cost of medication. Peptides, which easily degrade under physiological conditions and encounter absorption problems due to their large molecular weight, cannot be used effectively in conventional dosage forms. However, maximising the therapeutic effects can be achieved by intelligent DDS, which protect the drug native structure and confirmation (Bromberg and Ron 1998).

Biodegradable polymers offer two further advantages; firstly there is no need to remove residual biomaterial from the implantation site and secondly drug release profiles have more versatility and are therefore beneficial to a wider range of compounds. For example hydrogels that degrade by microbial enzymes in the colon are used for colon specific delivery (Ghandehari et al., 1997, Maris et al., 2001). Hydrogels can also be fabricated as microparticles and used for injection (Chenite et al., 2000). The use of natural polymers in the preparation of these intelligent drug delivery systems are also beneficial since many natural polymers are inherently biodegradable and posses the ability to self-assembly, specific recognition of other molecules and the formation of reversible bonds (Park et al, 1993).

1.2 PHYSICAL FORMS OF STIMULI-RESPONSIVE POLYMERS

Stimuli-responsive polymers have been utilised in various forms such as crosslinked hydrogels (permanently), reversible hydrogels, micelles, modified interfaces and conjugated solutions (stimuli responsive) (Park et al., 1993, Qiu and Park 2001,Kost and Langer 2001).

- Hydrogels are called permanent or chemical gels when they are covalently cross-linked gels. Chemical gels will not dissolve in water or organic solvents unless covalent cross-links are cleaved. The gels may be synthesised by polymerisation or co-polymerisation of a variety of monomers with minor amounts of crosslinkers. Based on these cross-linked networks, drug release and associated swelling characteristics of the hydrogels can be significantly changed by altering the delicate balance of hydrophobic and hydrophilic moieties (Hennink and van Nostrum 2002; Kopecek 2003). Also the presence of the stimulus responsive component within the polymer network allows dramatic change in the swelling properties when an environmental stimulus is initiated (Qiu and Park 2001).

- Associative forces capable of forming non-covalent cross-links form reversible gels or physical networks (Jeong et al, 2002). A degree of the polymer is involved in the formation of stable contacts within between polymer chains. Since these networks are not covalently cross-linked, they display weaker and reversible chain-chain interactions forming solution-gelation (sol-gel) transitions. Therefore, these types of stimuli responsive polymers have been developed for a phase change rather then a dimensional change.

- Polymeric micelles are another form of stimuli responsive systems. An AB-type polymer incorporating both hydrophilic and hydrophobic segments forms polymeric micelles. This is due to their amphiphilic nature. The micellization/demicellization formed by the alteration of the hydrophilicity or hydropobicity, can be modulated by stimuli (mostly temperature) (Lin and Cheng, 2001, Zhang et al., 2002, Jeong et al., 1999).

Alternatively a stimulus responsive polymer may be modified by the addition of either the hydrophilic or hydrophobic segment leading to an improved targeting system, capable of actively targeting due to their switchable thermo-responsive physical-chemical characteristics, while they maintain the passive targeting ability (Chung et al., 1998, Kohori et al., 1998). However, it is ambiguous to distinguish these micelle

structures from reversible hydrogels as micelles form hydrogels above a specific temperature (micelle gelation concentration).

- Matrix surfaces, such as polymer (Peng et al., 2001), silica (Rama et al., 2002) and metal (Nath et al., 2001) can be functionalised with stimuli responsive polymers to produce intelligent interfaces between solid and liquid phases. (Extrinsic, triggered control of interfacial properties is attractive for the development of regenerable biosensers and proteomic chips, interfacial control of microfluidics that enable the dynamic presentation of cell specific ligands on their surface). The properties of the modified interface can result in a dynamic on-off system by changing the hydrophobic/hydrophilic surface function and the pore size of the porous membranes.

- Changing simuli can control the solubility of stimuli responsive polymers. As a result, their conjugates can be modulated to have stimuli responsive solubility. The conjugates can be obtained by a covalent bond or secondary bond (Gil and Hudson 2004, Nath et al., 2001). Once the conjugation of stimuli responsive polymer and conjugates such as drugs and proteins is developed, the activity of the conjugates depends on the hydrophobic and hydrophilic changes of the polymer chain induced by stimuli.

1.3 Smart polymers:

Delivery systems whereby a drug can be activated by external stimuli are still largely experimental. Enteric coating as reviewed by Dittgen, (1997), is an established method of bypassing the stomach only releasing the active substance when reaching the relatively alkaline pH of the small intestine. There are only a few commercially successful hydrogel-based drug delivery systems; most of which are over the counter dressings and surgical aids (Aquatrix II^{TM} a chitosen-PVP hydrogel, Smart hydrogel^{TM} poly (acrylic acid) and poly (oxypropylene-co-glycol) (Gupta et al., 2002). Some aspects of the various potential stimuli are discussed in the following section.

1.31 pH sensitive hydrogels:

The pH responsive polymers consist of ionisable pendants that can accept and donate protons in response to an environmental change in pH. Polyacids will swell to a greater extent at high pH as they are transformed into electrolytes resulting in electrostatic repulsion forces between molecular chains. On the other hand polybases have amine groups in their side chain, which

release protons under basic conditions and gain protons under acidic conditions. This gives a momentum along with the hydrophobic interaction to govern swelling/deswelling, hydrophobic/hydrophilic characteristics and volume phase transition temperature of the polymer. Drug release from such devices will display release rates dependant on pH (Gupta et al., 2002, Kost and Langer, 1991, Qui and Park, 2001).

Hydrogels, which are pH sensitive and biodegradable, have also been synthesised. Poly (ortho esters) have shown fast degradation kinetics under mildly acidic conditions while they are relatively stable at physiological pH (Seymour et al., 1994). The pH responsive degradation profiles of poly (ortho esters) has been used as a hydrogel matrix for pulsatile insulin delivery (Heller et al., 1990) and has also been applied as triggered sustained drug release systems targeted to weak acidic environments (Guo et al., 2001). Attention has also been focused on the development of biodegradable, pH sensitive hydrogels based on polypeptides, proteins and polysaccharides.

1.3.2 Light Sensitive Hydrogels:

Light sensitive hydrogels can be separated into UV-sensitive and visible sensitive hydrogels. The UV-sensitive hydrogels are synthesised by the introduction of a leuco derivative molecule, bis (4-di-methylamino) phenylmethyl leucocyanide into the polymer network (Mamada et al., 1990). The light induced swelling was due to an increase in osmotic pressure within the gel due to an appearance of cyanide ions formed by UV irradiation (Figure 1.1).
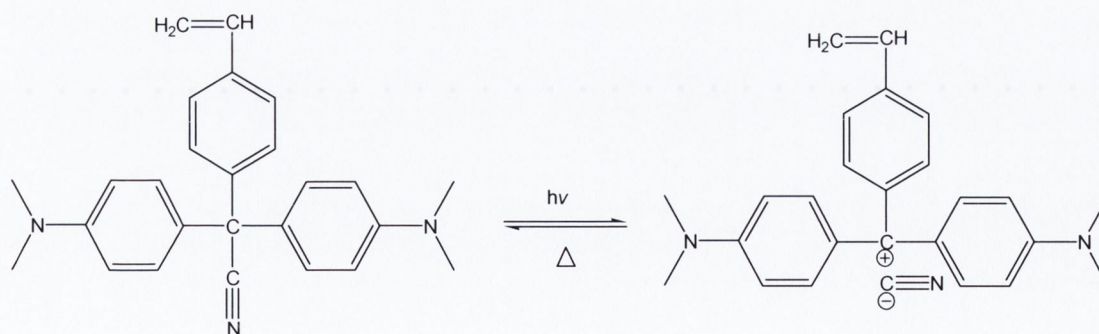
Figure 1.1: Structure of a leuco derivitive molecule bis(4-(dimethylamino)phenyl)(4-vinylphenyl)methylleucocyanide.

Visible light sensitive hydrogels were prepared by introducing a light sensitive chromophore (e.g. trisodium salt of copper chlorophyllin) to poly (N-isopropylacrylamide) hydrogels (Suzuki and Tanaka, 1990). The chromophore absorbs light, which is then dissipated locally as heat. The temperature increase alters the swelling behaviour of the thermoresoponsive N-isopropylacrylamide unit. In the absence of any chromophores poly (n-isopropylacrylamide) hydrogels display a volume phase transition by the formation of a temperature gradient due to a CO_2 laser infrared beam. Yiu et al., 1993 examined the application of visible light sensitive hydrogels for temporal drug delivery based on crosslinked hyaluronic acid hydrogels that undergo photosensitised degradation in the presence of methylene blue.

1.3.3 Electric sensitive hydrogels:

Hydrogels sensitive to electric current are usually made of polyelectrolytes, as are pH sensitive hydrogels. Their ability to convert chemical energy to mechanical energy have demonstrated their suitability for selective controlled transport of both neutral and charged compounds across hydrogel membranes. In the case of a hydrated polyelectrolyte membrane such as poly (methyl methacrylate) (PMMA) application of an electric field gives rise to a net force on the space charge in the fluid phase, which contains an excess of counterions over co-ions. This force is transferred to the solvent resulting in electrosmotic fluid flow relative to membrane matrix (Kost and Langer, 2001).

In addition to hydrogel swelling and contraction electric fields have also been used to control the erosion of hydrogels made of poly (ethyloxazoline)-poly (methacrylic acid) (PMA) complex in a saline solution (Kwon and Bae, 1991). The co-polymer (formed via intermolecular hydrogen bonding between the carboxylic and oxazoline groups) disintegrated into water-soluble polymers at the gel surface on application of the electric current. By altering the applied electrical stimulus the surface erosion of this polymer was controlled in a step wise or continuous fashion. Pulsatile release of insulin was achieved by applying a step function of electric current.

1.3.4 Biomolecule sensitive hydrogels:

Biomolecule-sensitive hydrogels undergo swelling in response to specific biomolecules such as glucose, enzymes, and antigens (Miyata et al., 2002). Glucose sensitive gels are useful for the development of self-regulated insulin delivery systems, which can be categorised into three types.

6

Glucose oxidase-loaded hydrogels combine glucose oxidase with pH sensitive hydrogels to sense glucose and regulate insulin release. Within the pH-sensitive hydrogel glucose is converted to gluconic acid by glucose oxidase thus lowering the pH in the hydrogels (Ito et al., 1989, Hassan et al., 1997). The second type of glucose sensitive gel involves lectin. Lectins are carbohydrate-binding proteins, which interact with gycloproteins and glycolipids. Concanavalin A (Con A) is the most frequently used glucose binding protein in modulated insulin delivery (Brownlee and Cerami, 1979). A stable biologically active glycosylated insulin derivative able to form a complex with con A was synthesised. The glycosylated insulin derivative could be released from its complex with con A in the presence of free glucose based on the competitive and complementary binding properties of glcosylated insulin and glucose to con A. The third example of glucose sensitive gel involves complex formation between a phenylboronic acid group and glucose as opposed to biological components (proteins) as previously described (Figure 1.2) (Kitano et al., 1992). Glucose having pendant hydroxyl groups competes with polyol polymers for the borate crosslinkages. Since glucose is mono-functional it cannot function as a crosslinking agent as polyol polymer does. Thus as glucose concentration increases the crosslinking density of the gel decreases and the gel swells/erodes to release more insulin.
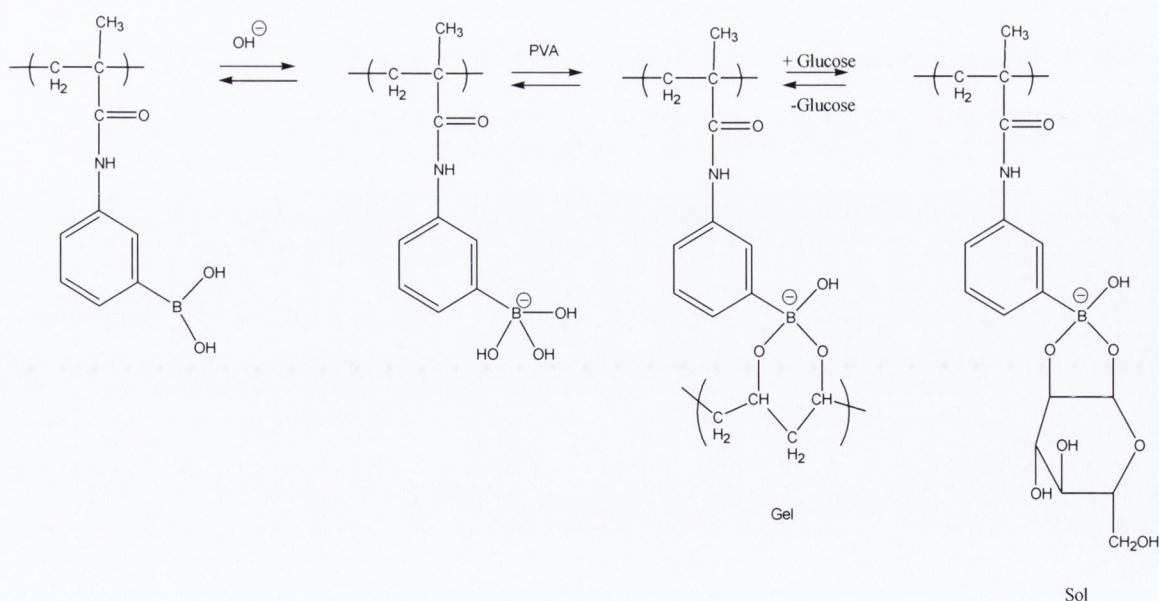
Figure 1.2: Sol-gel phase transition of a phenylborate polymer. At alkaline pH, Phenylborate polymer interacts with PVA to form a gel. Glucose replaces PVA to induce a transition from the gel to the sol phase.

Enzyme-sensitive hydrogels have also become increasingly important since specific enzymes can digest some biodegradable polymers. Enzymatically degradable cross-links were introduced into weak polyacid-based hydrogels for colon specific drug delivery (Ghandehari et al., 1997 Maris et al., 2001). Cross-linking agents containing azoaromatic moieties are degradable by the azoreductase activity in the colon thereby initiating drug release.

1.3.5   Temperature responsive polymers

Thermoresponsive polymers are the most extensively studied class of environmental sensitive polymers (Bromberg and Ron, 1998). Poly N-isopropylacrylamide is the most extensively studied in the field of controlled drug delivery due to its lower critical solution temperature (LCST). The LCST is the critical temperature at which a polymer solution undergoes a phase transition from soluble to insoluble state above the critical temperature. Systems, which become soluble upon heating, have an upper critical solution temperature (UCST). Examples of polymers possessing a LCST in water are tabulated below;

Table 1.1:Polymers showing an LCST in water (Jeong et al., 2002)

Polymer	LCST ($^{\circ}$C)	Polymer	LCST ($^{\circ}$C)
Poly (N-isopropylacrylamide)	~32	Poly (siloxyethylene glycol)	10-60
Poly (vinyl methyl ether)	~40	Poly (silamine)	~37
Poly (N-vinylcaprolactam)	~30	Methylcellulose	~80
Poly (propylene glycol)	~50	Hydroxypropylcellulose	~55
Poly (methacrylic acid)	~75	Polyphosphazene derivatives	33-100
Poly (vinyl methyl oxazolidone)	~65		

The behaviour of the temperature sensitive polymer in a solvent is a balance of solvent-solvent interactions, solvent-polymer interactions and polymer–polymer interactions. In water PNIPAM has water molecules bonded by hydrogen bonds to the amide side of the chain as well as structured water around the isopropyl groups. This effect of structured water is known as the hydrophobic effect.

Linear Poly (N-isopropylacrylamide) chains in dilute aqueous solutions appear to exist as isolated, flexible but extended coils due to dominant solvent-polymer interactions above polymer-polymer interactions (Schild, 1992). At higher temperatures the interactions between hydrogen bonds and water molecules weaken leading to an entropically favoured release of water. This leads to a phase separation whereby the polymer-polymer interactions become stronger causing the polymer to precipitate. The temperature at which the phase transition

occurs is called the LCST. These temperature sensitive systems undergo a sol-gel phase transition instead of a swelling/deswelling transition. Block co-polymers like poly (ethylene oxide)-poly (propylene oxide) (PEO-PPO) (Pluronics®, poloxamers®, tetronics®) possess an inverse temperature sensitive property based on a sol-gel phase conversion around body temperature (Figure 1.3) (Bromberg and Ron, 1998).
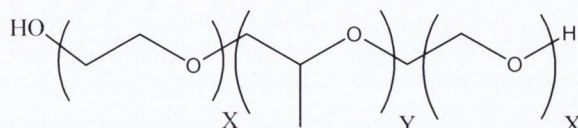
Figure 1.3: Structure of poly (ethylene oxide)-poly (propylene oxide)(PEO-PPO-PEO) block copolymer; where x is the number of repeating PEO units and y is the number of repeating PPO units (Bromberg and Ron, 1998).

In the case of a hydrogel where polymer chains are covalently crosslinked, this phenomenon leads to sharp volume changes at the LCST. A hydrophilic swollen polymer is observed below the LCST and above this temperature a collapse/deswelling in the polymer network is observed due hydrophobic interactions and interpolymer chain association.
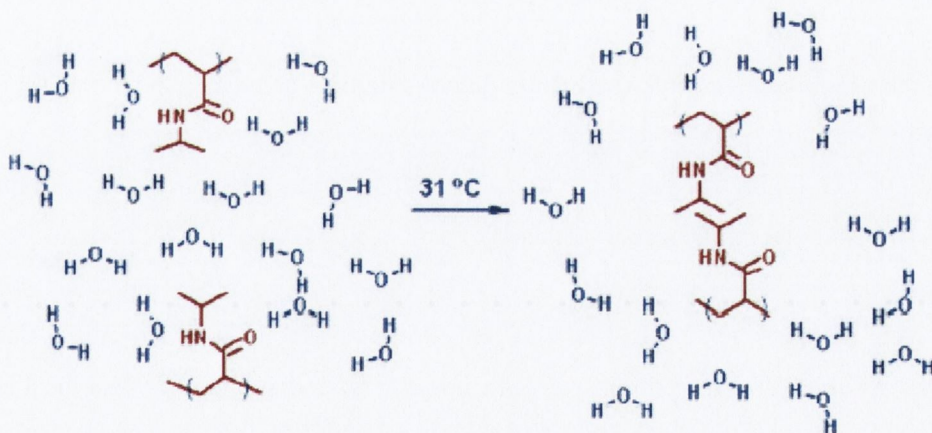
Figure 1.4: Volume phase transition in PNIPAAM gels. At temperatures below the LCST of PNIPAAM (~31^{0}C), water is bonded to the amide side chains of PNIPAAM, there is also structured water around the isopropyl group. Hence the gel is in the swollen state due to strong polymer-solvent interactions. At temperatures above the LCST there is an entropically favoured release of water from the interior of the gel and polymer-polymer interactions become stronger thereby deswelling the gel (Nayak, 2004).

9

Covalently cross-linked thermoresponsive hydrogels synthesised using PNIPAAM are the most extensively studied (Hoffman et al., 1986, Bae et al., 1987, Makino et al., 2001). In the case of thermoreversible gels, a hydrogel is formed by placing/injecting the polymer solution into an aqueous environment. Jeong et al., (1997) reported a polymer consisting blocks of poly (ethylene oxide) and poly (L-lactic acid). The polymer (at 45°C), upon subcutaneous injection and subsequent rapid cooling to body temperature, undergoes a sol-gel transition. The entrapped drug was released at first by diffusion and then at a faster rate as degradation mechanisms started operating.

1.3.6 Others:

Other types of stimuli responsive hydrogels, which have been reported, include magnetic, ultrasound, pressure or radiation. Ultrasound is mostly used as an enhancer for the improvement of drug permeation through biological barriers such as skin, lungs, intestinal wall, and blood vessels. Kost et al., (1989) described ultrasound-enhanced polymer degradation system. During polymer degradation, incorporated drug molecules were released by repeated ultrasonic exposure. As degradation of biodegradable matrix was enhanced by ultrasonic exposure the rate of drug release also increased.

Kost et al., (1985) investigated magnetically controlled drug delivery from a polymer matrix incorporating a small magnet. Release studies of BSA (bovine serum albumin) increased 5 to 10 fold by subjecting the matrix to an oscillating magnetic field. Kost et al., (1987) reported the exposure to an oscillating field induced insulin delivery to diabetic rats.

Zhong et al., (1996) found that the phase transition of temperature sensitive gels were pressure dependent with potential implications for the degree of swelling.

Juodkazis et al., (2000) reported reversible phase transitions in polymer gels induced by radiation. The volume phase transitions were attributed to the radiation rather than local heating.

10

1.4 Synthesis and Chemistry of Poly (N-isopropylacrylamide) networks.

Poly (N-isopropylacrylamide) (PNIPAAM) has been synthesised by a variety of techniques resulting in many different architectures. Such polymerisation methods employed include free radical initiation in organic solution, redox initiation in aqueous media, ionic polymerisation and synthesis by radiation. The chemical and physical properties of PNIPAAM are diverse depending on the process adapted and conditions employed (Schild 1992). Furthermore by addition of co-monomers, diverse labels and functional groups have been introduced.

One of the most common techniques used in drug delivery is redox initiation in aqueous media. Redox polymerisation of PNIPAAM is typically carried out using either ammonium persulfate (APS) or potassium persulfate (KPS) as the initiator and either NNNN-tetramethylenediamine (TEMED) or sodium metabisulfite as the accelerator (Schild, 1992). N, N methylene-bisacrylamide is used as the cross-linker in many of these reactions.

n-isopropylacrylamide

N,N-methylenebisacrylamide

Poly (N-isopropylacrylamide)
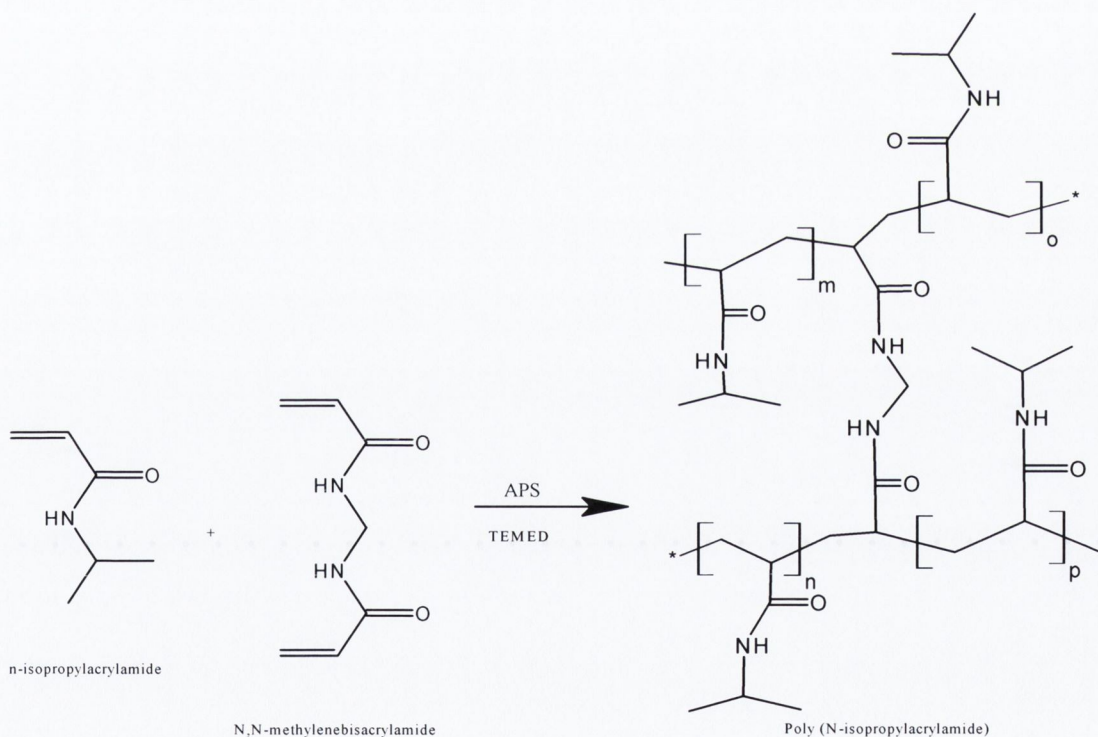
Figure 1.5: synthesis of poly (N-isopropylacrylamide) hydrogel. The reaction is initiated using ammonium persulfate (APS) and propagated with tetramethylethylenediamine (TEMED). Value of integers (m,n,o,p) depend on crosslinking density.

Free radical polymerisation in organic solution has been widely used in polymer chemistry for drug delivery applications. There are limitations to hydrogels composed of only PNIPAAM, such as biocompatibility, swelling/deswelling rate and mechanical properties. The need to

11

improve these required properties led to other functionalities being incorporated by co-polymerisation and IPNs (interpenetrating networks), which is mainly carried out by free radical polymerisation in organic solution. Many hydrophobic monomers have been introduced such as butyl methacrylate, which necessitates the use of organic solutions.

Acrylic acid (anionic)

N,N'-diethylaminoethyl methacrylate (cationic)

di-dodecylacrylamide

Butyl methacrylate

Hydrophobic co-monomers

Acrylamide

Dextran

Hydrophilic co-monomers
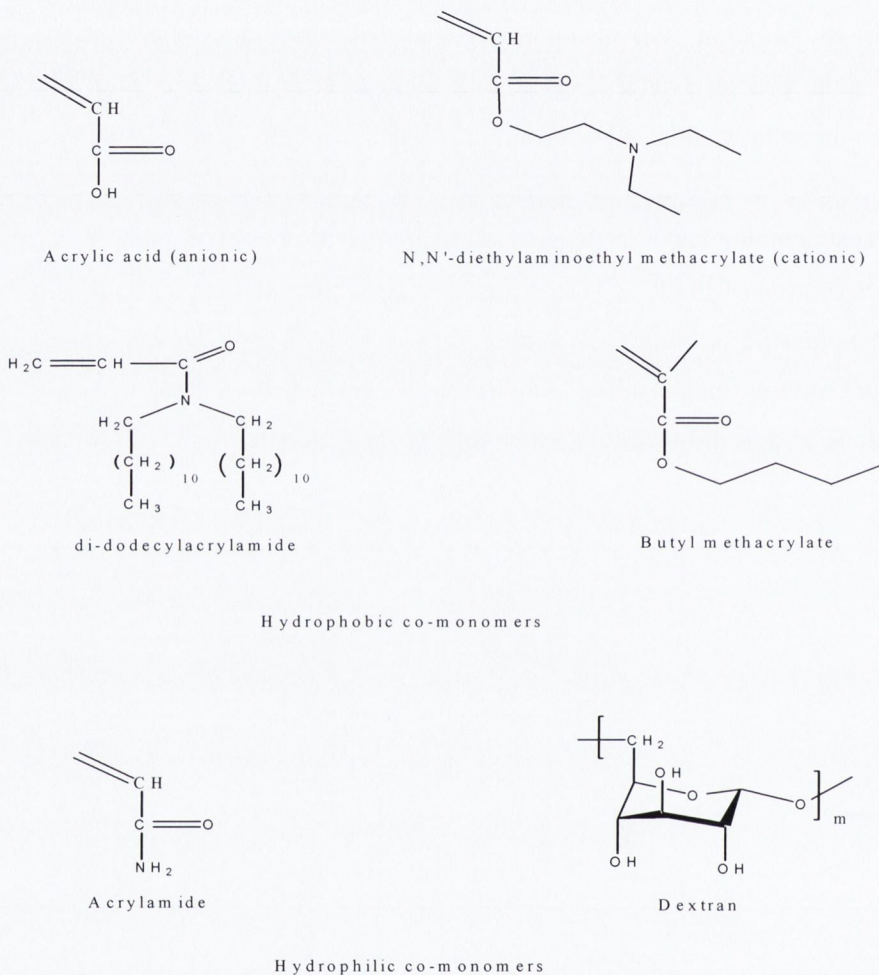
Figure 1.6 shows some of the various functional groups; hydrophobic/hydrophilic, degradable and ionic monomers that have been used in synthesis by free radical polymerisation to form PNIPAAM gels.

Reports of ionic and radiation polymerisation have been reported. Radiation polymerisation has facilitated grafting NIPAAM onto substrates of biological interest, motivated by the subsequent control of the hydrophilic/hydrophobic balance of the resulting surface (Uenoyama, and Hoffman, 1988, Yamada et al., 1990).

1.5 Designs for temperature sensitivity of poly (N-isopropylacrylamide) networks:

Architecture diversity or modification is important as properties such as hydrophobicity/hydrophilicity and the degradation profile can be modified so that the role of molecules in medical technologies can thus be extended (Section 1.2).

Temperature sensitive hydrogels can be classified into negatively and positively thermoresponsive systems. The majority of thermoresponsive systems, including both linear and cross-linked systems exhibit a LCST and thus display negative temperature dependency (Yoshida et al., 1994). Negative temperature systems can be described as systems, which are insoluble or shrink in water above the LCST. In drug delivery this would result in a negative thermoresponsive release. N-isopropylcrylamide and methacrylic acid (MAA) has been extensively studied. It has been found that the temperature response disappears with high-enough content of MAA. On the other hand bock co-polymers with the same composition of NIPAAM to MAA can retain both temperature and pH responsiveness which is attributed to the microphase separation of both units (Peng et al., 2001). Wu et al., (1992) prepared thermally reversible poly (N-isopropylacrylamide) gels with macroporous structures by polymerising gels at a temperature above their LCST and evacuating the reactor near the end of the polymerisation (Figure 1.7 (II)). Similarly Cheng et al., (2003) synthesised macroporous gels for protein controlled release by carrying out polymerisation in aqueous sodium chloride solution. By controlling the temperature, the release of the model protein, BSA, could be modulated with entrapment of the BSA above the LCST and diffusion below the LCST. The obtained macroporous hydrogels had higher swelling ratios at temperatures below the LCST and exhibited faster swelling/deswelling kinetics although the LCST was the same for the conventional and macroporous gels.

(I)   (II)   (III)
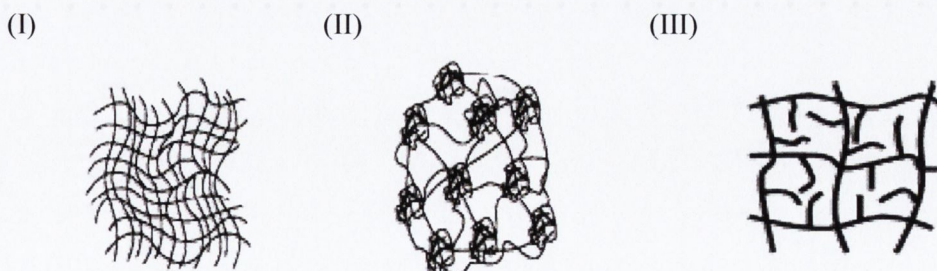
Figure 1.7: Diagram of (I) conventional gel (II) heterogeneous structure of a macroporous LCST hydrogel and (III) Structure of a comb type grafted poly (N-isopopylacrylamide) gel (Wu et al., 1992).

Comb-type PNIPAAM hydrogel has been recently prepared exhibiting a fast acceleration of the shrinking rate compared to that of a linear type PNIPAAM gel (Figure 1.7). Within its novel architecture, dangling PNIPAAM chains in a hydrogel can easily collapse above the LCST due to the strong shrinking tendency of PNIPAAM chains that bear free ends (Yoshida et al., 1995). Regulation of water content of thermoresponsive hydrogels is an important subject for controlled drug release. Copolymerisation of PNIPAAM and hydrophobic butyl methacrylate has been widely investigated and displayed a fall in the LCST and a reduction in the degree of swelling. As a technique to control the degree of swelling without affecting the LCST, Bae et al., (1991) modified poly (N-isopropylacrylamide) with hydrophobic components via formation of interpenetrating polymer networks (IPNs). The release of herapin was investigated at various temperatures. (IPNs are formed when one crosslinked network is intertwined with another independent network.) IPNs of crosslinked PNIPAAM and linear poly (ether (urethane-urea) have shown greater mechanical strength and faster deswelling rates than croslinked PNIPAAM alone (Gutowska et al., 1994). Okano et al., (1990) and Bae et al., (1991) both investigated the on- off pulsatile release of indomethacin from IPNs of PNIPAAM and polytetramethylene ether glycol (PTMEG).

Biodegradability has been given to the hydrogels, while keeping their temperature responsive properties. PNIPAAM chains were grafted to biodegradable biopolymers such as zein protein and Chitosan (Ju et al., 2001, Bromberg, 1997). Bromberg (1997) synthesised thermo and pH-sensitive comb type graft and semi-IPN hydrogels were prepared by using alginate and PNIPAAM. Comb type gel responded rapidly to changes in temperature due to the freely mobile PNIPAAM-NH$_2$ chains. In the pH sensitive swelling behaviour, the swelling ratio of comb-type graft hydrogels increased continuously with increasing pH. However the swelling ratio of semi IPN decreased at pH ranging between 3 and 5 because of the compact structure resulting from formation of a polyelectrolyte complex.

PNIPAAM-based networks have been chemically incorporated with enzymatically biodegradable poly (amino acid) or dextran. Huang et al., (2004), Zhang and Chu, (2002) designed a triblock polymer containing PNIPAAM, PLA and dextran which were thermoresponsive and partially hydrolytically degradable. Novel thermoresponsive and biodegradable hydrogels were designed and prepared in aqueous phosphate buffer (PB) solvent by copolymerisation NIPAAM and Dex-lactate-HEMA, (hydroxyethyl methacrylate) a dextran methacrylate macromer containing a hydrolysable oligolactate spacer with different weight ratios (Huang and Lowe, 2005). Two hydrophilic drugs BSA and methylene blue were loaded during the synthesis process into a gel consisting of a weight ratio 5:4 NIPAAM: DEX-lactate-Hema. The release of methylene blue was slower below the LCST than at 37°C, while the

14

release of BSA at these two temperatures showed the opposite trend. This was attributed to drug release kinetics been strongly dependent on environmental temperature, swelling and degradation of the gel and interactions of the loaded drugs within the gel network.

A few polymeric micelle systems have been reported using N-isopropylacrylamide with degradable components such as PLA, polylactide-co-glycolide (Liu et al., 2005, Kohori et al., 1998). Liu et al., (2005) fabricated Poly (PNIPAAM-co-DMAAm)-b-PLGA micelles containing doxorubicin (DOX) that were stable at body temperature but deformed at 39.5^0C thus triggering DOX release.

Other temperature sensitive systems can display a positive temperature dependency. The polymer systems display an upper critical solution temperature (UCST) and swell at higher temperature. This results in positive thermoresponsive release whereby drug release is faster at higher temperature. Limited systems have been reported (Katono et al., 1991). Coughlin et al., (2004) achieved positive thermoresposive release using negative thermoresponsive gels by incorporating dextran fractions into PNIPAAM. A squeezing effect was observed on increasing the temperature and the off state was seen below LCST due to the larger molecular diameter of the model drug in comparison to that of pore size. Ichikawa and Fukumori (2000) designed a positive thermoresponsive drug release microcapsule. Its thermosensitive coat was composed of ethylcellulose containing PNIPAAM hydrogel "particles". The release rate of the model drug (carbazochrome sodium sulfonate) increased on increasing temperature due to the shrinkage of the thermosensitive hydrogel particles within the coating of the microcapsule. The resultant voids in the coating facilitated diffusion of drug from the core.

1.6 Designs for LCST control:

The LCST of a temperature responsive polymer is influenced by hydrophobic or hydrophilic moieties in its molecular chain. In general, to increase the LCST of thermoresponsive polymers such as PNIPAAM, random co-polymerisation with hydrophilic monomers will result in an increase in LCST. In contrast hydrophobic constituents have been reported to decrease the LCST of PNIPAAM (Xue and Hamley, 2002, Feil et al., 1993, Yoshida et al., 1994). Another aspect in the design and control of the LCST is introducing a hydrophobic biodegradable segment. A hydrolytically sensitive lactate ester side group was introduced to control the LCST of temperature senstitve NIPAAM-based gels. An increase in the LCST was observed after the hydrolysis of the hydrophobic lactate groups (Huang and Lowe, 2005). Figure 1.6 displays such monomers that may increase (acrylic acid) or decrease (buthylmethacrylate) the LCST.

Okano et al., (1990) studied the relationship between the alkyl group length in cross-linked poly (N,N-alkyl substituted acrylamides) and their aqueous swelling as a function of temperature. It was found that a more pronounced deswelling or gel collapse with increased temperature followed the trend shown in Figure 1.8. The thermosensitivity of the swelling was attributed to the delicate balance of hydrophobicity/hydrophilicity of the polymer chains and was affected by the size, configuration and mobility of the alkyl side chains.

Poly(N-isopropylacrylamide)   Poly(N,N diethylacrylamide)   Poly (acryloyl pyrrolidine)   Poly(N-ethylacrylamide)   Poly(N,N dimethylacrylamide)
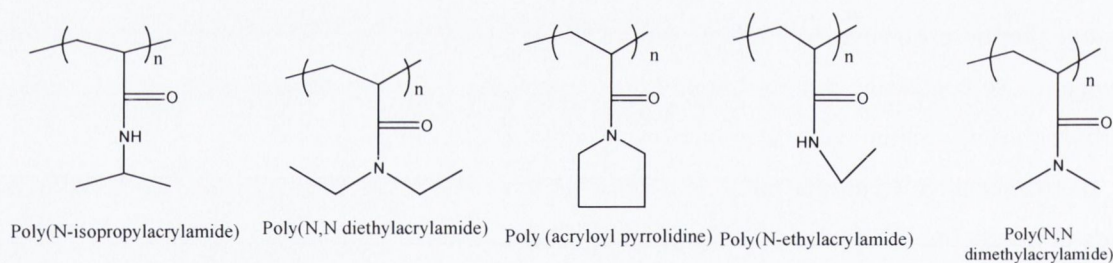
Figure 1.8: series of poly (N, N-alkyl substituted acrylamides) in order of magnitude of collapse on increasing the temperature (Okano et al., 1990).

When ionisable groups such as AAc (poly acrylic acid) or N, N-dimethylacrylamide (DMAAm) are co-polymerised with PNIPAAM, the LCST shows a discontinuous alteration or even disappearance at the pKa of the ionisable groups (Beltran et al., 1991). The ability of ionised co-monomers to remain charged and interact electrostatically with aqueous media and themselves within the copolymer network over a wide range of ionic strengths and pH values is proposed to explain significantly increased swelling and collapse behaviour in crosslinked gel systems over that of pure PNIPAAM (Yu and Grainger, 1993).

16

Co-polymerisation of PNIPAAM with different types of monomers results in hydrogels with more versatile properties such as faster rates of shrinking when heated through the LCST and sensitivity to additional stimuli. Okano et al., (1990) have studied the relationship between copolymers of PNIPAAM with alkyl methacrylates. They found larger alkyl groups led to stronger hydrophobic interaction promoting aggregation of the polymer chains leading to a sharp phase transition temperature. Feil et al., (1992) examined the influence of pH and temperature on the swelling of ionisable thermoresponsive poly (NIPAAm-co-BMA-co-DEAEMA) hydrogels. Increasing the ionisable monomer, DAEMA led to a strong increase or disappearance of the gel collapse temperature. In addition, the LCST increased with decreasing pH (increasing charge on DAEMA) indicating charge may be dominant factor in controlling the LCST.

1.7 Effect of additives on phase transition temperature:

Since the thermoresponsive behaviour depends on the solvent interaction with the polymer and the hydrophilic/hydrophobic balance within the polymer molecules, additives to the polymer/solvent system can influence the position of the phase transition. Such additives include salts, surfactants (Saito et al., 1992, Eeckman et al., 2001) and the addition of co-solvent (Lee et al., 2000).

1.7.1 Inorganic salt:

Hydrogen bonding plays an important role in the phase transition of thermoresponsive polymers as described in Section 1.2 and disruption of this hydrogen bonding will alter the phase transition temperature. The addition of a simple salt generally results in a decrease in the LCST ("salting out" effect) as a function of the salt concentration (Saito, 1971, Eliassaf, 1978, Ataman, 1987, Schild, 1990, Park and Hoffman, 1993). Exceptions are known such as certain thiocynates or quaternary ammonium salts (Saito, (1971), Suwa et al., (1998), Baltes et al., (1999), Schild, (1990)). These exceptions result in a "salting in" effect increasing the phase transition temperature. The observed "salting out" / "salting in" effect can be explained as a combination of several effects i.e. changes in the water structure in the polymer hydration sheath and changes in the interactions between the polymer and solvent due to the presence of the salts.

According to the model of Frank and Wen (Ataman, 1987) for aqueous salt solutions, water consists of three regions: (a) is the region that is permanently associated with the ion (b)

consists of water molecules partially ordered by the electric field of the region and (c) the structure of water is normal. The proportion of (b) is a measure of the ability of the ion to destroy water structure. Depending on whether the ion is a structure breaker or not, the normal hydrogen bonded structure of water is either destroyed or retained. The sudden removal of the protective hydration layer of molecules exposes the hydrophobic character of the polymer resulting in volume phase transition.

The co-solute effect was observed in 1888 and classified as the Hofmeister effect. The Hofmeister effect refers to an ordered sequence of ions (the Hofmeister series) categorised in regard to their "salting out" potential towards proteins from aqueous solutions. Eeckman et al., (2001), showed that the valence and size of the anion play an important role in the salting out process in respect to PNIPAAM polymers. Anions were classified on a molar concentration basis in accordance with the Hofmeister series (Ataman, 1987) with respect to the "salting out" effectiveness:

$$PO_4^{3-} > HPO_4^{2-} > SO_4^{2-} > OH^- > H_2PO_4^- > HCO_3^- > F^- > CH_3COO^- > Cl^- > Br^- > I^-$$
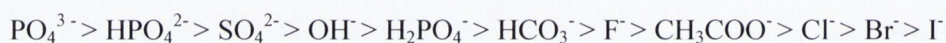
When the molecular weight was used instead of the molar concentration the order of ranking was:

$$OH^- > F^- > PO_4^{3-} >> SO_4^{2-} > HPO_4^{2-} > H_2PO_4^- > HCO_3^- > CH_3COO^- > Cl^- > Br^- > I^-$$
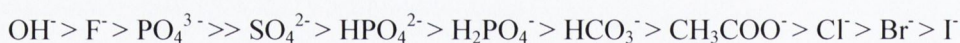
The phase transition temperature of PNIPAAM polymers was found to be independent of the cationic species (Saito et al., 1992).

1.7.2 Surfactants:

Surfactants, contrary to salts, are often used to obtain stable aqueous dispersion of hydrophobic solutes. Several studies revealed that surfactant molecules adsorb onto the polymer by means of their hydrophobic tails whereas salts are not thought to absorb into the polymer network but affect the phase transition temperature (Saito et al., 1992). In the presence of surfactants both the type of surfactant and its hydrocarbon chain length influences the phase transition temperature (Eeckman et al., 2001). Increasing or decreasing of the LCST in PNIPAAM is dependant on the hydrophobic chain length and the concentration of surfactant used. This behaviour has been explained as the result of two antagonistic phenomena: A salting out effect due to the anionic character of the free surfactant molecules and on the other hand a conversion of the originally hydrophobic character into a more hydrophilic complex by bonding of the long

aliphatic hydrocarbon chains of the surfactants with the polymer hydrophobic segments (Eeckman et al., 2001).

1.8 Potential uses of drug delivery systems:

Temperature responsive polymer networks undergo reversible change in properties in response to environmental conditions. This can be in conformation, change in solubility or alteration in the hydrophobicity/hydrophilicity balance. This response can be modified to respond to a small change in temperature as previously seen in Section 1.6. In drug delivery, stimuli responsive polymers have the potential to modulate drug release via temperature control. By altering the temperature, on-off release of the model compound can be achieved. Thus drug delivery patterns can be optimised by pulsatile or self-regulated delivery by adjustment of drug release rates in response to a physiological need. Potential uses of such systems are described in the following section.

1.8.1 Constant temperature:

In conventional drug delivery, the drug concentration in the blood rises when the drug is taken, then peaks and declines. Multiple doses are often required to keep a drug at a therapeutic plasma level, above an ineffective level but below a toxic level. Supplying the appropriate amount of drug to the body over a prolonged period led to the development of constant rate drug delivery systems. Current technology on sustained drug release devices has improved to such a level that delivery of drugs at a constant rate can be achieved for a period of time ranging from days to years (Park et al., 1993). Advantages of controlled drug release devices include delivery to the required site, delivery at a required rate, fewer applications, reduced dangers of overdose and economic advantages by the virtue of a more efficient dosage at the expense of a more complicated fabrication.

As a constant drug delivery device at body temperature (37°C), the properties of the thermosensitive hydrogels can be tailored to meet the desired release profile (Section 1.5). If the LCST of the polymer system is above body temperature, the gel will swell at a rate dependent on monomer composition, degree of crosslinking and/or rate of degradation. If the LCST is below 37°C, no swelling will occur. Similarly in the case of linear polymers, depending on the LCST relative to body temperature the polymer will either dissolve or precipitate delivering bioactive solutes to a location in the body. "Smart" polymers devices offer a feasible route of controlled drug delivery of larger molecules such as protein or peptides whereby their native structure can be protected from enzymatic attack.

1.8.2 Changing temperature:

Delivery systems in which drug release can be activated by an external stimulus can be classified as open loop or closed-loop systems. In controlled drug delivery open-looped systems are known as pulsed or externally regulated and closed loop systems as self regulated.

1.8.2 (a) Externally regulated delivery systems:

The use of external heat to modulate drug release has applications in any situation where the release of a substance is required at a critical temperature. Subdermal implants are a possible method of controlling the swelling state of an implanted hydrogel and subsequent release rate. Such an implant could be useful in patients where frequent but non-continuous drug release is desirable.

In anticancer therapy, it has been found that hyperthermia has a synergistic effect when used with chemotherapeutic agents for destruction of tumours. Hyperthermia preferentially increases the permeability of tumour vasculature over normal vasculature, which further enhances preferential delivery to tumours (Weidner, 2001). An implant containing chemotherapeutic agent in the tumour region and the whole area exposed to a slightly higher temperature would trigger drug release. Another application may be to implant a device containing an antipyretic drug. A responsive system could also be designed where a unit has a small heater incorporated into the design. Raising the temperature by a few degrees would trigger drug release. Meyer and co-workers (2001) have recently reported two thermally responsive polymeric drug carriers to target tumours. The LCST of the thermoresponsive polymer was chosen at 40°C because this is higher than the body physiological temperature but lower than 42°C, a temperature that is regularly used for hyperthermia treatments in cancer patients.

Thermoresponsive polymers have also been proposed as carriers for DNA delivery (Hinrichs et al., 1999, Kurisawa et al., 2000). Polymeric gene carriers have advantages over lipid systems i.e. high stability against nuclease, easy control of hydrophilicity of complex by co-polymerisation, relatively small size and narrow distribution of the complex. These cationic lipid and polymeric carrier systems have a common dilemma in that these systems must fulfil the following two requirements simultaneously (1) complex formation of cell uptake and prevention of DNA degradation (2) complex dissociation for transcription by RNA polymerase (Kurisawa et al., 2000). Since formation and dissociation are two different phenomena, an intelligent thermoresponsive system was used for cell entry and transcription. Kurisawa et al.,

(2000) showed enhanced reporter gene expression by lowering the incubation temperature from the ordinal incubation temperature (37°C).

1.8.2 (b) Auto regulation of drug release by change in body temperature:

The use of temperature as a signal has been justified by the fact that body temperature often deviates from the physiological temperature (37°C) in the presence of pathogens or pyrogens. This deviation sometimes can be a useful stimulus that activates the release of therapeutic agents from temperature responsive drug delivery systems for diseases accompanying fever. Two potential drug delivery systems could be possible. Firstly, a system that can respond to an increase in temperature (hyperthermia) by release of an antipyretic drug (paracetamol) to lower temperature. Drug release would cease once set temperature is reached. Such causes of hyperthermia may include diseased states (cancer, inflammation, stroke, blood clots, connective tissue disorders, central nervous system haemorrhage), drugs (antidepressants, antibiotics).

A second potential system could respond to a decrease in the body temperature by release of a stimulant drug or a potential drug to assist the body to recover its normal homeostatic state. The elderly, sick, frail and immunocompromised are particularly susceptible to hypothermia.

CHAPTER 2:

SWELLING KINETICS AND MECHANISMS OF DRUG

RELEASE FROM BIODEGRADABLE HYDROGELS

2.1 INTRODUCTION

In swellable drug delivery systems such as hydrogels, mathematical modelling plays an important role in facilitating hydrogel network design by identifying key parameters and molecule release mechanisms. In the following chapter the fundamentals in hydrogel network design as well as mathematical modelling approaches related to controlled molecule release from hydrogels will be reviewed. Section 2.2 describes the network structure, which determines the overall mobility of encapsulated molecules and their rates of diffusion within a swollen hydrogel matrix. Section 2.3 briefly describes the processes of drug dissolution and diffusion relevant to the present work. This is followed by the examination of diffusion in terms of swelling and drug release from hydrogels (Section 2.4). Finally section 2.5 deals with several mechanisms that have been elucidated to describe molecule release from polymer hydrogel systems including diffusion swelling and chemically controlled release.

2.2 STUDY OF HYDROGEL NETWORKS

As discussed in Section 1.2, hydrogels are hydrophilic polymer networks, which have the capacity of absorbing and retaining large amounts of water (Park et al., 1993). This three dimensional network can be constituted of homopolymers or copolymers and the presence of chemical (tie point junctions) and physical (entanglements) crosslinker rendering them insoluble. Figure 2.1 shows a representation of the effect of environmental changes on the hydrogel structure. In order to evaluate the feasibility of using a particular hydrogel as a drug delivery device, it is important know the structure and properties of the polymer network. The most important parameters that define the structure and properties of swollen hydrogels are the polymer volume fraction in the swollen state, $\upsilon_{2,s}$, effective molecular weight of the polymer chain between crosslinking points, $\overline{M}_c$, and network mesh or pore size, ξ.
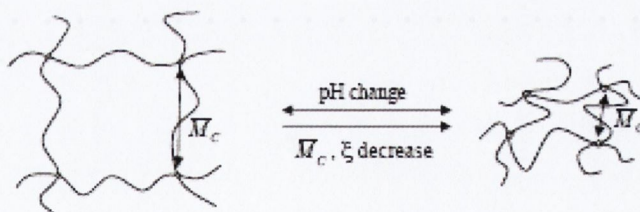
FIGURE 2.1   Schematic representation of the cross-linked structure of a hydrogels. $\overline{M}_c$ is the molecular weight of the polymer chains between crosslinks and ξ is the network mesh size.

The polymer fraction of the polymer in the swollen gel is a measure of the amount of fluid that a hydrogel can incorporate into its structure (Peppas et al., 2000).

$$\upsilon_{2,s} = \frac{volume \ of \ polymer}{volume \ of \ swollen \ gel} = \frac{V_p}{V_{gel}} = 1/Q \qquad \text{Equation 2.1}$$

This parameter can be determined using equilibrium swelling experiments. The molecular weight between crosslinks is the average molecular weight of the polymer chains between junction points, both chemical and physical. This parameter provides a measure of the degree of crosslinking in the gel. The correlation length (ξ) is a measure of the space available for diffusion between two macromolecular chains. Due to the extent of randomization produced during the polymerization, both the molecular weight between cross-links and the correlation length can only be evaluated as an average value. The determination of these parameters can be preformed through theoretical methods and experimental techniques i.e. equilibrium swelling studies (Canal and Peppas, 1989).

The structure of neutral hydrogels can be analysed by the Flory-Rehner theory. This combination of thermodynamic and elasticity theories states that a cross-linked polymer gel that is immersed in a fluid and allowed to reach equilibrium with its surroundings is subject only to two opposing forces: the thermodynamic force of mixing and the retractive force of the polymer chains. When equilibrium is reached, the contributions of the two forces are equal and the physical situation can be expressed in terms of Gibbs free energy:

$$\Delta G_{total} = \Delta G_{elastic} + \Delta G_{mixing} \qquad \text{Equation 2.2}$$

Where $\Delta G_{elastic}$ is the contribution due to the elastic retractive forces developed inside the gel and ΔG_{mixing} is the contribution of the spontaneous mixing of the fluid molecules with the polymer chains.

Differentiation of EQN. 2.2 with respect to the number of solvent molecules while keeping the pressure and temperature constant results in equation. 2.3

$$\mu_1 - \mu_{1,0} = \Delta\mu_{elastic} + \Delta\mu_{mixing} \qquad \text{Equation 2.3}$$

Where;

μ_1 is the chemical potential of the solvent in the polymer gel and

$\mu_{1,0}$ is the chemical potential of the pure solvent.

At equilibrium, the differences between the chemical potentials of the solvent outside and inside the gel must be zero. Therefore changes in the chemical potential due to mixing and elastic forces must balance each other. The change of chemical potential due to mixing can be expressed using heat and entropy of mixing.

The change in chemical potential due to the elastic retractive forces of the polymer chains can be determined from the theory of rubber elasticity. Peppas and Merrill (1977) modified the original Flory-Rehner theory for hydrogels prepared in the presence of a solvent. The presence of a solvent effectively modifies the change of chemical potential due to the elastic forces. This term must now account for the volume fraction density of the chains during cross-linking. According to this model the molecular weight between two subsequent cross-links in neutral gels prepared in a solvent can be expressed as:

$$\frac{1}{\overline{Mc}} = \frac{2}{Mn} - \frac{\left(\dfrac{\overline{v}}{V}\right)\left[\ln(1 - V_{2s}) + V_{2s} + \chi V^2{}_{2s}\right]}{V_{2r}\left[\left(\dfrac{V_{2s}}{V_{2r}}\right)^{1/3} - \left(\dfrac{V_{2s}}{2V_{2r}}\right)\right]}$$

Equation 2.4

Where:

Mn is the molecular weight of the polymer chains,

$\overline{v}$ is the specific volume of the polymer,

V is the molar volume of solvent,

χ is the Flory-Huggins polymer water interaction parameter,

V_{2s} is volume fraction of the swollen gel,

V_{2r} is the polymer volume fraction in the relaxed state (state of polymer after cross-linking but before swelling),

$\overline{Mc}$ is the average number molecular weight between the crosslinks.

On the other hand, assuming that all cross-linker molecules used in hydrogel synthesis participate in forming effective cross-links, theoretical $\overline{Mc}$ values of the hydrogels can be calculated by the following equation (Canal and Peppas, 1989):

$$\overline{Mc}(theor) = \frac{Mr}{2X}$$
Equation 2.5

Where:

X is the cross-linker ratio (mole ratio of crosslinker/monomer)

Mr is the molecular weight of one repeating unit of polymer.

The polymer volume fraction of the hydrogel in both the swollen state and relaxed state can be evaluated from swelling studies using equations 2.6 (a) and 2.6 (b) respectively (Caykara et al., 2005):

$$V_{2s} = \left[1 + \frac{\left(\frac{m_s}{m_d} - 1 \right) \rho_2}{\rho_1} \right]^{-1}$$
Equation 2.6 (a)
$$V_{2r} = \left[1 + \frac{\left(\frac{m_r}{m_d} - 1 \right) \rho_2}{\rho_1} \right]^{-1}$$
Equation 2.6 (b)

Where;

m_s is the mass of the swollen hydrogel,

m_d is the mass of the dry hydrogel disc

m_r is the mass of the hydrogel after polymerisation but before swelling

ρ_1 and ρ_2 are densities of the solvent and polymer respectively.

Alternatively V_{2r} can also be calculated from the knowledge of the initial monomer(s) concentration, Co (mol mL^{-1}) (Caykara et al., 2005):

$$V_{2r} = Co\overline{V}r$$
Equation 2.7

Where;

$\overline{V}r$ is the molar volume of monomer(s)

After the molecular weight between cross-links is determined using the swelling theory; the cross-linking density of the hydrogels P_x can be calculated using the following relationship (Canal and Peppas, 1989):

26

$$\rho_x = \frac{1}{\overline{v}\,Mc}$$

Equation 2.8

It should also be noted that <C> the correction factor for network imperfections resulting from chain ends is expressed as:

$$< C >= 1 - \frac{2\overline{M}c}{Mn}$$

Equation 2.9

This factor reduces to one for perfect networks (Jafari et al., 2005).

2.3 Drug dissolution and diffusion in hydrogels

The release of drugs from hydrogels results from a combination of classical diffusion mechanisms in the polymer network. In order to optimize a hydrogel system for a particular application, the fundamental mechanism of solute transport in the hydrogels must be understood completely. In this section, we focus on the mechanism of drug diffusion in hydrogels as well as the importance of network morphology in controlling the transport of drugs in hydrogels.

Molecular diffusion or permeation through non-porous media depends on the solubility of the permeating molecules in the bulk membrane, whereas a second process can involve passage of a substance through solvent-filled pores of a membrane and is influenced by the relative size of the penetrating molecules and the diameter and shape of the pores (Martin, 1993).

The transport or release of a drug through a polymeric controlled release device can be described by classical Fickian diffusion theory. This theory assumes that the governing factor for drug transport in the gels is ordinary diffusion. Drug delivery devices can be designed so that other mechanisms control the release rate such as gel swelling or polymer erosion. Fick's first law is described by Equation 2.10 where J is the flux, j is the flux per unit area, A is the area across the diffusional field, D is the diffusional co-efficient, c is the concentration of solute, x is the distance and $\partial c/\partial x$ is the concentration gradient along the x axis.

$$J = -Aj = -AD\frac{\partial c}{\partial x}$$

Equation 2.10

The negative sign indicates that diffusion occurs in a direction opposite to that of increasing concentration. The chemical nature of the diffusant as well as temperature, pressure and solvent can influence the diffusional co-efficient.

The law states that the flux of a component of concentration across a membrane of unit area, in a predefined plane, is proportional to the concentration differential across that plane. In the case of diffusion without convection and unitary area, equation 2.10 could be rewritten as described by equation 2.11, which is the starting point for numerous descriptions of diffusion behaviour in swellable polymers.

$$J = -D\frac{\partial c}{\partial x}$$
Equation 2.11

Fick's second law of diffusion examines the rate of change of diffusant concentration at a point in the system. The law with constant boundary conditions can successfully describe much of the observed solute transport in polymers. It states that the rate of change of concentration in a volume element in the membrane, within a diffusional field, is proportional to the rate of change of concentration gradient at that point in the field as is given by equation 2.12 where x is the distance of movement perpendicular to the surface of the barrier (Martin, 1993).

$$\frac{\partial c}{\partial t} = D\frac{\partial^2 c}{\partial x^2}$$
Equation 2.12

Where the boundary conditions are:

$t = 0$ $-1/2 < x < 1/2$ $C = C_1$
$t > 0$ $x = \pm 1/2$ $C = C_0$

Dissolution refers to the process by which a solid dissolves and enter the solution phase. The dissolution process can be diffusion controlled, surface reaction controlled or a combination of both processes. Diffusion controlled process is the standard in most cases of dissolution of solids in liquids. In this case, the liberation of the solute molecules at the interface is much faster than the diffusion of the solute from the interfacial boundary to the body of solution.

The first attempt to explain the dissolution rate of a solid was developed by Noyes and Whitney (1897). They claimed the dissolution rate to be proportional to the difference between bulk concentration and concentration at the dissolving interface. Nernst and Brunner (1904) introduced the diffusion layer model. They assumed that dissolution at the solid-liquid interface

is rapid and transport of the solute to the bulk is completely determined by diffusion through a stagnant boundary layer surrounding the dissolving interface. They applied Fick's law and developed Equation 2.13 (a) to describe the dissolution process at steady state:

$$\frac{dC}{dt} = \frac{DA}{Vh}(C_s - C_t)$$ Equation 2.13 (a)

$$\frac{dC}{dt} = \frac{DA}{Vh}C_s$$ Equation 2.13 (b)

Where:

dC/dt= rate of change of concentration with respect to time

C_s= saturation solubility of the solid

C_t= concentration of the solute in the bulk solution at time t

D= diffusion co-efficient

A= surface area

V=volume of dissolution medium

h =diffusion layer thickness

When the concentration of solute in the bulk solution is much less than drug solubility, sink conditions occur and C_t becomes negligible in comparison with C_s. In such circumstances, equation 2.13 (a) can be written as equation 2.13 (b).

Hixon and Crowell (1931) modified the above equation to develop an equation that expresses the rate of dissolution of uniformly sized spherical particles based on the cube root of the weight of particles:

$$W_o^{\frac{1}{3}} - W^{\frac{1}{3}} = kt$$ Equation 2.14

Where:

W_o= initial powder weight

W= powder weight at time t

This is known as the Hixson-Crowell cubic root law where k is the cube root dissolution rate constant.

Since the fraction dissolved is $F = \dfrac{W_o - W}{W_o}$ ($0 \leq F \leq 1$), then equation 2.14 can be expressed as (Rost and Quist, 2003):

$$F = 1 - \left(1 - \frac{kt}{W_o^{1/3}}\right)^3 \qquad \text{Equation 2.15}$$

Equation 2.15 gives the fraction dissolved of a number of particles, each having the initial weight W_o and can be used for non-linear fitting of the cube root law to dissolution profiles (Rost and Quist, 2003).

Diffusion controlled systems can be divided into reservoir systems and monolithic systems. In reservoir systems, the drug core is encapsulated by an inert membrane. The nature of the drug and membrane determines the drug diffusion process as described by Fick's laws of diffusion.

In the monolithic device, the drug is dispersed or dissolved in an inert polymer. Various configurations such as slab, cylindrical and spherical are commonly used for controlled release devices. Similar to that of reservoir systems, drug diffusion through the polymer matrix is the rate-limiting step. The release rates are determined by the nature of the polymer, diffusion and the partition co-efficient of the drug within the polymer.

Mathematical treatment of diffusion depends on whether the drug is dissolved or dispersed in the polymer. In a matrix system, where the drug is dissolved in the polymer matrix, release follows Fick's law of diffusion. Higuchi (1961, 1962) developed several theoretical models to study the release of water-soluble and drugs of low solubility incorporated into semi-solid and /or solid matrixes. Mathematical expressions were obtained for drug particles dispersed in a uniform matrix behaving as the diffusion media.

To study the dissolution from a planar system having a homogeneous matrix, equation 2.16 was proposed;

$$Q = [D(2C_0 - C_s)C_s t]^{1/2}$$

Equation 2.16

$$Q = (2C_0 DC_s t)^{1/2}$$

Equation 2.17

$$\frac{dQ}{dt} = (C_0 DC_s / 2t)^{1/2}$$

Equation 2.18

Where;

C_0= total concentration of drug per unit volume dissolved or undissolved in the matrix

C_s=solubility or saturation concentration of drug within the matrix

The drug in the inside is thus dissolved first and can diffuse out from the surface of the matrix. In a non-swellable system, this process continues between the boundary of the bulk solution and the receding depletion zone, which moves towards the centre of the tablet as the drug is released. Normally C_0 is a lot greater than C_s and the equation can be reduced to equation 2.17. This equation states that the amount of drug released is proportional to the square root of time. The rate of release (dQ/dt) can be derived from equation 2.17 to give 2.18. Therefore the rate of release can be altered by increasing or decreasing the drug's solubility, C_s, in the polymer by complexation or by changing the total concentration of the drug available, C_0.

Higuchi developed a second form of the diffusional model where the release of a solid drug is from a granular matrix. Then release of the solid drug involves the simultaneous penetration of the surrounding liquid, dissolution of the drug, and leaching out of the drug from the interstitial channels or pores. The volume and length of the opening is accounted for in the diffusional equation below;

$$Q = \frac{D\varepsilon}{\tau}(2C_0 - \varepsilon C_s)C_s t)^{1/2}$$ Equation 2.19

Where;

τ = the tortuosity of the capillary system

ε = porosity of the matrix

Equation 2.16 differs from equation 2.19 only in the addition of ε and τ. Equation 2.16 is applicable to release from a homogeneous system that gradually erodes and release the drug into the bathing medium. Equation 2.19 applies instead to a drug-release mechanism based on entrance of the surrounding medium into the polymer matrix where it dissolves and leaches out the soluble drug, leaving a shell of polymer and empty pores.

Higuchi (1962) proposed the following equation for the amount of drug released into the solution from a single surface of a homogeneous ointment;

$$Q = 2C_0 (\frac{Dt}{\pi})^{1/2}$$ Equation 2.20

$$Q = 2\varepsilon C_0 (\frac{Dt}{\tau\pi})^{1/2}$$ Equation 2.21

Where;

Q= amount of drug released per unit surface area

D= diffusion co-efficient of the drug in the matrix

C_0= initial concentration of the drug in the ointment

t= time

This equation holds for a homogeneous phase where the fraction released is less or equal to 60%. Equation 2.20 can be modified to describe drug release from a heterogeneous phase to give Equation 2.21.

In a general way it is possible to apply the Higuchi models to the following expression (generally known as the simplified Higuchi model, 1961);

$$Q=kt^{1/2}$$
<div align="right">Equation 2.22</div>

A plot of the amount of drug released versus the square root of time will be linear if the release of the drug from the matrix is diffusion controlled.

2.4 Drug release mechanisms from swellable devices

Drug release can be controlled by several means, such as diffusion through a rate limiting membrane or a matrix, osmosis, ion exchange or degradation of a matrix or part of a matrix (Park et al., 1993). In biodegradable hydrogels, drugs are in contact with water and thus the drug solubility is an important factor in drug release. In swelling drug delivery systems such as hydrogels, the release of water-soluble drugs from initially dehydrated hydrogel matrices involves the diffusion of the surrounding medium into the hydrogel containing the dispersed drug resulting in swelling of the system. The dissolved drug then diffuses through the swollen hydrogel into the external medium. However, expressions derived for diffusion-controlled and swelling controlled drug release can be used to describe drug release from biodegradable hydrogel systems provided the duration of the drug release is significantly faster with respect to the rate of the degradation of the matrix.

2.4.1 Diffusion and hydrogel Swelling

In the swelling process, following penetration of water into a glassy matrix, the following three steps are proposed to occur in succession (Yoshida et al., 1994(c));

Step 1: diffusion of water molecules into the polymer network
Step 2: relaxation of polymer chains with hydration
Step 3: Expansion of the polymer network into the surrounding bulk water upon relaxation.

A complicated process results, where the drug diffusion is coupled to the swelling kinetics of the system. The swelling behaviour differs depending on which step becomes dominant in determining the rate. Depending on the dominant factor, the mechanism of transport of the solvent penetrating media into the polymers can be classified as either Fickian diffusion (Case I) or Case II diffusion or non-Fickian/ anomalous diffusion. Much of the work on drug release described below has been undertaken on Case I or Fickian diffusion when the rate of diffusion is much less than that of the relaxation. The significance of this classification is that both Case I and Case II diffusion can be described in terms of a single parameter. The diffusion in case I systems is described by the diffusion co-efficient. The constant velocity of the advancing waterfront, which marks the boundary between the swollen hydrogel and the glassy core, describes case II diffusion. Non-Fickian or anomalous systems need two or more parameters to describe release resulting from both diffusion and polymer relaxation. The above classification of the diffusion of permeant can also be used to classify the drug release profiles from the swelling polymer (Park, 1993).

When the drug is loaded into the hydrogel by equilibrium swelling in the drug solution, drug release from the swollen gel follows Fick's law. Thus the rate of release from the equilibrated slab device can be described by equation 2.23 proposed by Crank (1975);

$$\frac{M(t)}{M(\infty)} = 4(\frac{Dt}{\pi d^2})^{1/2}$$
Equation 2.23

Where;
Mt/M∞ = is the fraction drug released at time t
D= the diffusion co-efficient of the drug in the matrix
l=the thickness of the slab device
t= time

In this case, it is noted again that drug release from case I systems are dependent on $t^{1/2}$. This equation is valid for the release of the first 60 percent of the drug total (early time approximation (Brazel and Peppas, 1999)).

In case II sytems, diffusion of water through the previously swollen shell is rapid compared with the swelling-induced relaxations of polymer chains. Thus, the rate of water penetration is controlled by the polymer relaxation. If the hydrogel contains a water-soluble drug, the drug is

34

essentially immobile in a glassy polymer, but begins to diffuse out as the polymer swells by absorbing water. Thus, the drug release depends on two simultaneous rate processes, water migration into the device and drug diffusion through the swollen gel. The mathematical analysis of Case II drug transport from a thin polymer film can be presented by the following equation:

$$\frac{Mt}{M\infty} = (\frac{2k_0}{C_0 l})t$$

Equation 2.24

Where;

k_0 = the relaxation constant

C_0 = equilibrium concentration of solvent in polymer

As indicated by the equation 2.22 drug release is characterised by square root of time. However, in many systems, the release rate is controlled by diffusion and some other physical phenomenon such as swelling and/or degradation. In order to determine whether a particular device is diffusion-controlled, the early-time release data can be fit to the following empirical relationship.

$$\frac{M_t}{M_\infty} = kt^n$$

Equation 2.25

Where;

k= kinetic constant characteristic of the drug polymer system

n= diffusional exponent characteristic of the release mechanism

It predicts that the fractional release is exponentially related to the release time and it adequately describes the release of drugs from slabs, spheres, cylinders and discs from swellable polymers. The slope (n) of the amount drug released versus time is 0.5 for pure Fickian diffusion. An anomalous non-Fickian diffusion pattern (n=0.5-1) is observed when the rates of the solvent penetration and drug release are in the same range. Zero order drug release can be achieved (n= 1) when drug diffusion is rapid compared to the constant rate of solvent induced relaxation and swelling in the polymer (Case II transport). Use of this equation to analyse data of drug release from a porous system will probably lead to n < 0.5 since the combined mechanisms (diffusuion through the matrix and partially through water filled pores) will shift the release exponent n towards smaller values (Peppas, 1985).

Table 2.1: Transport mechanisms of penetrant through a polymer slab. The table summaries a list of possible transport mechanisms with their characteristic n values and time dependence.

Diffusional Exponent, n	Type of Transport	Time Dependence
0.5	Fickian diffusion	$t^{1/2}$
0.5 < n < 1	Anomalous transport	t^{n-1}
1	Case II transport	time independent
n > 1	Super case II transport	t^{n-1}

A graphical representation of the each solute transport diffusion mechanism in swellable polymers in shown in Figure 2.2.The power-law model (EQN.2.25) generally accommodates only for $M_t/M_\infty \leq 0.6$. Thus where it is important to model the entire swelling or release curve more sophisticated models are used (Ritger and Peppas, 1987).
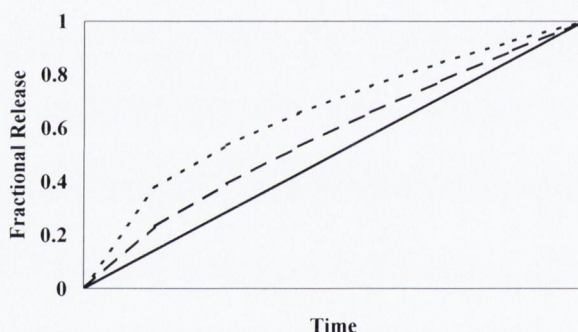
FIGURE 2.2: Comparison of the release profiles of systems exhibiting (- - -) classical Fickian diffusion behavior, (— —) anamolous release behavior and (——) zero-order release or Case II transport.

Hopfenburg and Hsu, (1978) observed that a glassy polymer which absorbed liquid at a constant rate (Case II transport) also release a drug at a constant rate. They proposed that the mechanism was analogous to that of surface eroding delivery systems in which the drug delivery was controlled by the chemical relaxation such as hydrolysis or dissolution of the polymer.

For Fickian release from a slab, fractional release can by characterised by some constant multiplied by the square root of time. Therefore Higuchi's diffusional equation can be expressed in terms of the fraction released (f) from a dosage form:

$$F = kt^{1/2}$$
<div align="right">Equation 2.26</div>

The generalised empirical equation (EQN.2.25) has been widely used to describe the water uptake through swellable glassy polymers as well as drug release from these devices whereby the weight gain (M_s) is replaced by Mt/M∞.

Swelling ratios have been used to characterise the swelling of hydrogels. The swelling ratio (S.R.) is the weight of the absorbed water per weight of dried polymer disc and has been defined in several ways. In the current work equation 2.27 was employed (Gutowska et al., 1992 and Mandel 2000)

$$S.R = \frac{W_s - W_d}{W_d}$$
<div align="right">Equation 2.27</div>

Where;

W_s= weight of swollen membrane at time t

W_d= weight of dry polymer disc

In each case, the swelling ratio produces a value for the actual swelling of the hydrogel relative to its original dry weight.

2.5 CLASSIFICATION OF DRUG RELEASE FROM HYDROGELS

The properties of a hydrogel network as well as the selection of drug loading techniques will determine the mechanism(s) by which the loaded drug is released from the cross- linked matrix. The incorporation of drugs into hydrogel delivery matrices can be undertaken by two methods; post-loading or in-situ loading.

Post–loading involves absorption of drugs after the hydrogel networks are formed. If an inert hydrogel system is used, diffusion is the major driving force for drug uptake and release and will be determined by diffusion and/or swelling. In the presence of hydrogels containing drug-binding ligands, bioerodible or pendant chain groups, the mechanism can be controlled by diffusion and/or degradation and drug-polymer interaction.

In-situ loading involves the drug or drug polymer conjugates mixed with polymer precursor solution and hydrogel network formation and drug encapsulation are accomplished

<div align="right">37</div>

simultaneously. In these systems, drug release can be controlled by diffusion, hydrogel swelling, reversible drug-polymer interactions or degradation of labile bonds.

Both sophisticated and simple models have been previously developed to predict the release of an active agent from a hydrogel device as a function of time. These models are based on a rate-limiting step for controlled release and can be classified as follows or as a combination of one or more mechanisms (Goperfich, 1997).

2.5.1 Diffusion/swellable controlled release

The release of water-soluble drugs from dehydrated hydrogel matrices generally involves the simultaneous absorption of water and desorption of drug via a swelling-controlled diffusion mechanism. In swelling-controlled release systems, the drug is dispersed within a glassy polymer. Upon contact with biological fluid, the polymer begins to swell. No drug diffusion occurs through the polymer phase. As the penetrant enters the glassy polymer, the glass transition of the polymer is lowered allowing for relaxations of the macromolecular chains. The drug is able to diffuse out of the swollen, rubbery area of the polymers. This type of system is characterized by two moving fronts; the front separating the swollen (rubbery) portion and the glassy regions which moves with velocity, (υ), and the polymer/fluid interface (Figure 2.3). The rate of drug release is controlled by the velocity and position of the front dividing the glassy and rubbery portions of the polymer.

For true swelling-controlled release systems, the diffusional exponent, n, is 1. This type of transport is known as Case II transport and results in zero-order release kinetics. However, in some cases, drug release occurs due to a combination of macromolecular relaxations and Fickian diffusion. In this case, the diffusional exponent is between 0.5 and 1.

Yoshida et al., (1991) achieved zero order release of indomethacin by using hydrophilic polymeric matrices. Regulating the zero–order release kinetics was achieved by using high swelling polymeric matrices and loading a large amount of hydrophobic drug.

Gutowska et al., (1992) studied the release of heparin from PNIPAAM based hydrogels containing hydrophobic or hydrophilic monomers. The study showed the release profiles correlated with the swelling kinetics governed by solute diffusion within the collapsed matrix at 37°C. Yoshida et al., (1994) showed that swelling of PNIPAAM-co-BMA gels above the phase transition temperature resulted in water uptake due to diffusion of water molecules into the polymer network. However below the phase transition temperature the swelling kinetics were

controlled by relaxation of the polymer chains (Case II transport) yielding a constant swelling rate. At 20°C, swelling increased linearly with time due to Case II transport mechanism. At 10°C a sigmoidal release pattern was observed. The difference in the swelling patterns below the LCST was attributed to different constraining forces for swelling.

A theoretical concentration profile of the solvent and the solute during the swelling-controlled release processes are shown in Figure 2.3 (b)-(c). Water concentration in the rubbery region increases with distance from the centre of the system. A corresponding drug concentration gradient would exist in the rubbery region and would depend on properties of the drug. Sink conditions are assumed in the bulk region.
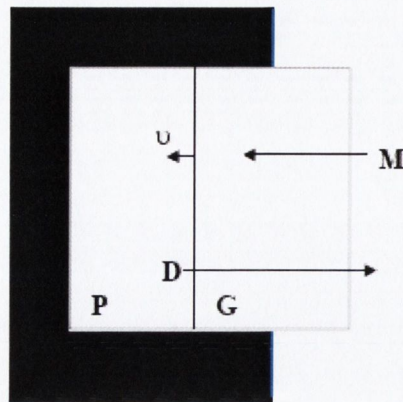
(B)
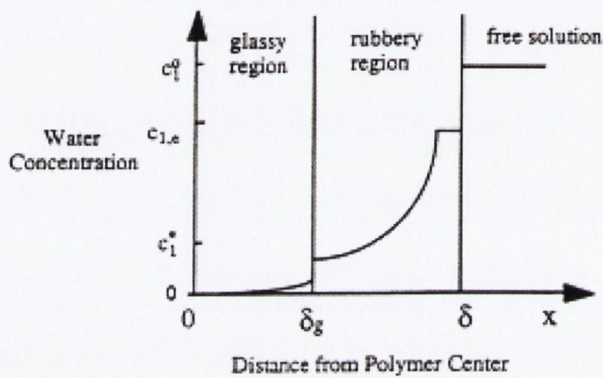
(C)
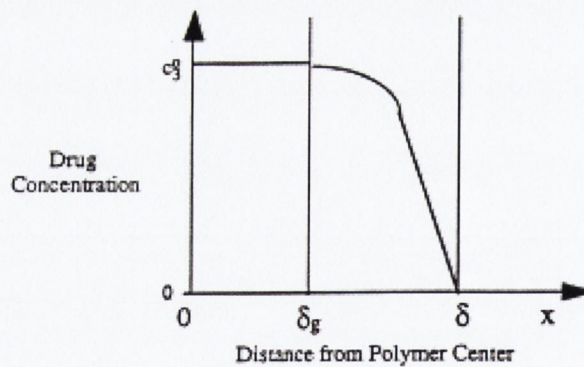
FIGURE 2.3: Schematic representation of the behavior of (A): a one-dimensional swelling controlled release system. The medium (M) penetrates the glassy polymer (P) to form a gel (G). The drug (D) is released through the swollen layer. A theoretical concentration profile of (B): the solvent where c_1^o is the concentration of medium at time zero, $c_{1,e}$ medium concentration normalized with respect to the equilibrium concentration, c_1^* is the boundary assumed to remain constant during the swelling process and ∂g is the distance from the center of the sample to the swelling front (C): the solute during the swelling controlled release process at a time t where the glassy/rubbery front still exists where c_3^o is the initial drug concentration in the system (Brazel and Peppas, 2000).

2.5.2 Chemically-controlled Release Systems

There are two major types of chemically controlled release systems; erodible drug delivery systems and pendant chain systems. In erodible systems, drug release occurs due to degradation or dissolution of the polymer. In pendant chain systems, the drug is affixed to the polymer backbone through degradable linkages. As these linkages degrade, the drug is released.

Erodible drug delivery systems, also known as degradable or absorbable release systems, can be either matrix or reservoir delivery systems. In reservoir devices, an erodible membrane surrounds the drug core. If the membrane erodes significantly after the drug release is complete, the dominant mechanism for release would be diffusion. Predictable, zero-order release could be obtained with these systems. In some cases, the erosion of the membrane occurs simultaneously with drug release. As the membrane thickness decreased due to erosion, the drug delivery rate would also increase.

For erodible matrix devices, the drug is dispersed within the three-dimensional structure of the hydrogel. Drug release is controlled by drug diffusion through the gel or erosion of the polymer. In true erosion controlled devices, the rate of drug diffusion will be significantly slower than the rate of polymer erosion and the drug is released as the polymer erodes.

In an erodible system, there are three major mechanisms for erosion of the polymer. The first mechanism for erosion is the degradation of the crosslinks. This degradation can occur by hydrolysis of water labile linkages, enzymatic degradation of the junctions, or dissolution of physical crosslinks such as entanglements or crystallites in semi-crystalline polymers. Torchilin et al., (1977) prepared hydrogels crosslinked with BIS. The polymer degraded slowly by hydrolysis of the crosslinker and degradation was sensitive to the concentration of BIS used in the hydrogel. Chymotrypsin was incorporated into the gel by physical entrapment during polymerization. The gels with very low crosslink density were unable to retain the entrapped chymotrypsin due to their high porosity. As a result the drug was rapidly release via a diffusion mechanism rather than degradation. Shalaby et al., (1992) loaded Flavin mononucleotide (FMN) in to albumin crosslinked PVP gels by swelling the gels in an FMN saturated solution. After the initial burst effect the drug release was zero order up to 300 hours.

The second mechanism for erosion is solubilization of insoluble or hydrophobic polymers. This could occur as a result of hydrolysis, ionization or protonation of pendant groups along the polymer chains. Zero-order release can be obtained with these systems, provided that the cleavage of the drug is the rate-controlling mechanism.

The final mechanism of erosion is the degradation of backbone bonds to produce small molecular weight molecules. Typically, the degradation products are water-soluble. This type of erosion can occur by hydrolysis of water-labile backbone linkages or by enzymatic degradation of backbone linkages. The most commonly studied erodible polymer systems are poly (lactic acid) (PLA), poly (glycolic acid) (PGA) and copolymers of PLA and PGA. Gallagher et al., (2000) studied the release of levamisole HCl, at low drug loadings from Poly-$_{DL}$-Lactide-co-glycolide matrices. The loading exhibited a significant burst release phase followed by a polymer degradation controlled phase.

Zhang and Chu, (2002 (b)) investigated the controlled release of insulin from a series of biodegradable hybrid hydogel networks containing dextran derivative of allyl isocyanate (dex-ai) and poly lactide diacrylate macromer over a wide range of composition ratios. Insulin release from these hydrogels was regulated by the (dextran allyl isocyanate) dex-ai to PDLLAM composition ratio. As the PDLLAM composition ratio increased insulin dispersion within the hydrogel became less homogeneous and the degradation extent of the hydrogl increased. This led to an initial burst effect followed by a higher insulin release rate due to the formation of a more open and lose 3D network structures at a later stage. The release kinetics involved a combination of diffusion and degradation controlled mechanisms.

Heller et al., (1983) prepared hydrogels in which degradable polyester prepolymers were crosslinked with PVP chains. The release of the physically entrapped BSA from these hydrogels was regulated by the amount of PVP which inturn depended solely on the rate of degradation. However the release kinetics were tailored by varying the crosslinking density of the gel or by the addition of electron withdrawing groups adjacent to the carboxyl groups. The duration of the BSA release could then be varied from 10 days to more than 12 weeks.

2.5.3 Environmentally Responsive Systems

Environmentally responsive materials show drastic changes in their swelling ratio due to changes in their external pH, temperature, ionic strength, nature and composition of the swelling agent, enzymatic or chemical reaction and electrical or magnetic stimulus. In most responsive networks, a critical point exists at which this transition occurs.

Responsive hydrogels are unique in that are many different mechanisms for drug release and many different types of release systems based on these materials. For instance, in most cases drug release occurs when the gel is highly swollen or swelling and is typically controlled by gel swelling, drug diffusion, or a coupling of swelling and diffusion. However, in a few instances, drug release occurs by a squeezing mechanism. Also, drug release can occur due to erosion of the polymer caused by environmentally responsive swelling.

Another interesting characteristic about many responsive gels is that the mechanism causing the network structural changes can be entirely reversible in nature. The ability of these materials to exhibit rapid changes in their swelling behavior and pore structure in response to changes in environmental conditions lend these materials favorable characteristics as carriers for bioactive agents, including peptides and proteins. This type of behavior may allow these materials to serve as self-regulated, pulsatile drug delivery systems. This type of behavior is shown in Figure 2.4 for pH or temperature-responsive gels. Initially, the gel is in an environment in which no swelling occurs. As a result, very little drug release occurs. However, when the environment changes and the gel swells, rapid drug release occurs (either by Fickian diffusion, anamolous transport or case II transport). When the gel collapses as the environment changes, the release can be turned off again. This can be repeated over numerous cycles. Such systems could be of extreme importance in the treatment of chronic diseases such as diabetes.
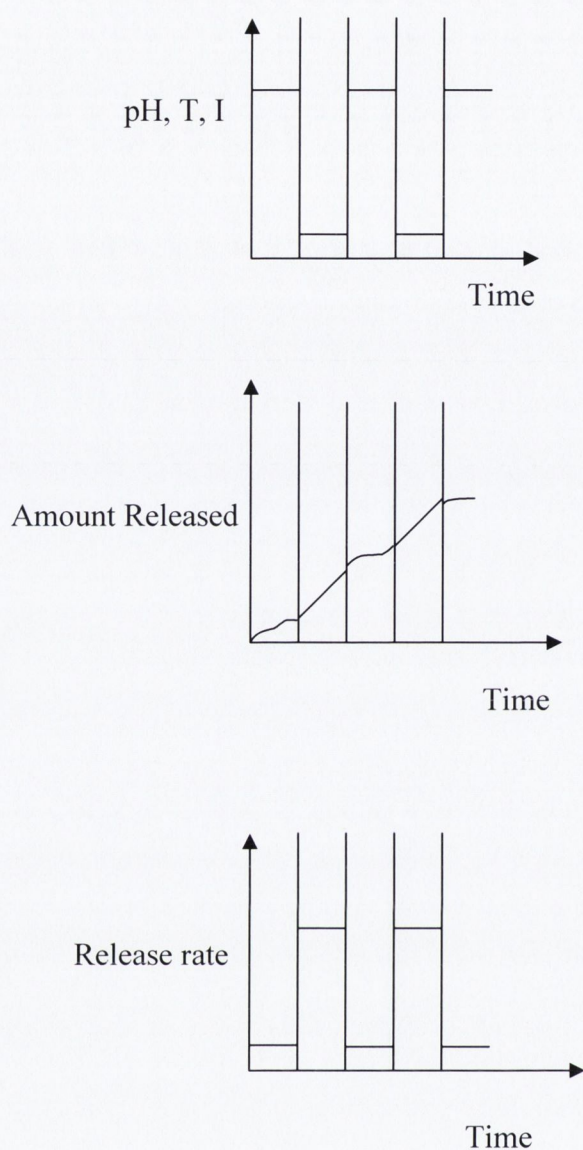
FIGURE 2.4: Cyclic change of pH, T or ionic strength (I) leads to abrupt changes in the drug release rates at certain time intervals in some environmentally responsive polymers.

Much of the work to date involving temporal drug release from thermoresponsive systems has been carried out on heterogeneous PNIPAAM gels using hydrophobic monomers such as BMA and RMA (Yoshida et al., 1992). Changing the length of alkyl side chains can control the gel skin formation process resulting in the formation of an " enhanced dense surface layer". This skin layer can be used in surface- regulated "on-off" release while the core remains swollen. On-off release profiles of indomethacin have been described in response to stepwise temperature change (Bae et al., 1987, Yoshida et al., 1992, Okano et al., 1990).

Coughlan et al., 2004 examined the effect of drug physiochemical properties on swelling/deswelling kinetics and drug release from homogeneous PNIPAAM. A dense layer was formed on the PNIPAAM gels upon temperature change above the LCST. Two series of drugs of contrasting hydrophilicity and physicochemical properties were examined. Drug release was controlled by diffusion below the LCST while solubility dependant drug pulse release on temperature switch was observed for the hydrophobic series. Effectiveness of thermal control of hydrophobic drug release increased with increasing solubility. The hydrophilic series (Dextran) produced a molecular size dependant drug pulse on temperature switch above the LCST.

Kaneko et al., (1995) reported a new method to accelerate swelling/deswelling kinetics based on the molecular design of the gel structure. Free mobile linear PNIPAAM chains were grafted within the PNIPAAM hydrogels. PNIPAAM-grafted gels showed rapid deswelling kinetics without the formation of a skin layer on the gel surface. The molecular weight of the graft chains had a significant effect on the deswelling kinetics and also on the drug release profiles especially for large molecular weight drugs. Sodium salicylate and dextran MW9300 showed a burst release on temperature increase with graft-type gels with a molecular weight of 9000 whereas incorporating graft type gels of MW 4000 formed a skin layer suppressing drug release.

Biodegradable temperature sensitive polymers have an advantage that the drug release rate can be controlled by changing the temperature. A hydrophilic drug, ketoprofen and a hydrophobic drug spirolactone were incorporated into PEG and PLGA tribolck copolymers with thermosensitive properties. The hydrophilic drug was predominately diffusion released whereas the hydrophobic drug showed a degradation controlled release after the initially diffusion dominant release (Jeong et al., 2000).

2.6 Influential factors in swelling controlled release systems:

The release of drug substances from initially dehydrated but swellable devices has been shown to follow mechanisms ranging from Fickian to case II through to super case II where the diffusional exponent is n>1. Materials and network fabrication governs the rate and mode of drug release from hydrogel matrices. Depending on the synthesis of a hydrogel matrix and the rate-limiting step for controlled drug release for a specific drug carrier, the desired release kinetics can be tailored considering the physical properties of the drugs and the loading level.

2.6.1 Effect of polymer composition;

The composition of the polymer defines its nature as a neutral or ionic network and furthermore its hydrophobic/hydrophilic characteristics. The presence of hydrophilic components in the polymer network enhances the swelling characteristics of the polymer. Hydrophobic moieties on the other hand reduces the swelling (Peppas and Khare, 1993) In addition the physical properties such as molecular weight and polymer/initiator concentrations influence swelling behaviour and degradation (Lin and Metters, 2006).

2.6.2 Effect of cross-linking density:

An increase in the cross-linking density through addition of crosslinking agents such as divinyl glycol, divinyl benzene, N-N methylenebisacrylamide or tripropyleneglycol diacrylate is known to reduce the equilibrium swelling (Peppas, 1986). Reduced swelling is often marked with a reduced diffusion co-efficient. Lee et al., (1978) in their study on the diffusion co-efficients in cross-linked PHEMA hydrogels found a reduction in the diffusion co-efficient values with increased cross-linking density.

2.6.3 Effect of the nature and size of the drug

The size and nature of the incorporated drug play a very important role in determining the efficiency of its release from the carrier. Yoshuda et al., (1968) (1969) found a linear dependence of the solute diffusion co-efficient in the swollen polymer system on the molecular size of the solute and the reciprocal of the degree of swelling. An increase in the molecular size of the drug reduces the drug release rate (Brazel and Peppas 1999, Peppas, 1986)

Swami, 2003 investigated the release of the model drug (vitamin b) in ionic hydrogels. It was found that the nature of the drug also affects the release properties of the carrier. They suggest that the columbic interactions between the charges borne by the vitamin and the hydrogel matrices are also influential in the release pattern of the drugs.

Makino et al., 2001 studied the release of dibucaine HCl, sodium benzoate and theophylline at $25^{\circ}C$ from the homo-polymer PNIPAAM. Differences in the release rates were attributed to electrostatic, attractive or repulsive forces between the polymer chains and drug molecules.

Origin and Scope

Biodegradable controlled drug delivery systems present unique advantages in drug delivery such as improved biocompatibility as well as improved flexibility in controlling stability and diffusion properties of model drugs.

Much of the research to date in our lab on biodegradable drug delivery systems has employed water-soluble polymers such as poly (glycolic acid) or poly (lactic acid). Fitzgerald and Corrigan (1996) investigated the controlled release and degradation behaviour from poly (lactide-co-glycolide) microspheres. Levamisole release profiles were sigmoidal and fitted to a model indicative of degradation-controlled release. Interestingly, once polymer hydrolysis had reached a critical MW, oligomer dissolution and drug release proceeded. Gallagher and Corrigan (2000) investigated the release of levamisole hydrochloride from poly (lactide-co-glycolide) compacts and found release profiles significantly different to those using the base form of the drug. A biphasic release pattern with an initial fast release followed by a slow degradation controlled release was observed.

Previous work undertaken in our lab explored the use of PNIPAAM; a temperature sensitive polymer, for drug delivery. Stimuli-responsive polymers show a sharp change in properties upon a small or modest change in environmental condition (e.g. temperature, pH etc.) (Hoffman, (1987), Gil and Hudson (2004), Kost and Langer, (1991)). Such behaviour can be utilised for the preparation of so-called "smart" drug delivery systems (DDS), which mimic biological response behaviour to a certain extent.

Coughlan and Corrigan (2004) investigated the potential use of PNIPAAM composed hydrogels in pulsatile drug delivery. They found drug release at $25^{\circ}C$ was approximately proportional to the square root of time while a solubility dependent drug pulse was observed on temperature switch. Effectiveness of thermal control or "on-off" drug delivery was dependent on the model drug's physiochemical properties. Not much work has been conducted on smart biodegradable hydrogel systems. Due to the unique properties of hydrogels, biodegradable gels are expected to find wide application in the improvement of existing dosage forms and the development of new and better drug delivery systems.

The aim of the present work was to synthesise a novel "smart" biodegradable hydrogel and to examine the ability of thermal controlled release from the heterogeneous gel. Much of the work examining drug release from thermoresponsive systems have focused on PNIPAAM hydrogels containing BMA as a hydrophobic monomer (Okano et al., 1990, Bae et al., 1987, Yoshida et al., 1994). Pulsatile drug delivery of indomethacin (IDM) has been achieved by Gutowska et al., (1997) due to the dense skin layer formed on temperature switch attributed to BMA. In the present work a hydrophobic and degradable monomer, PLA will be incorporated into the PNIPAAM network in an attempt to achieve a surface regulating system with semi-degradable properties. Co-polymerisation of a thermoresposive unit (PNIPAAM) and hydrolytically sensitive unit PLA was carried out by varying molar ratio compositions of the monomers. By varying the composition; the networks can be altered to accommodate drugs with different hydrodynamic radii, water affinity and desired release profiles.

In order to understand the mechanism of degradation, mechanism of swelling and drug release the following objectives were defined:

➢ To investigate the effect of monomer composition on the structural parameters of the hydrogel networks and in turn their influence on the rate of swelling as well as the thermal properties of the three dimensional networks.

➢ To examine the swelling kinetics and pore size in relation to hydrolytic degradation of the gels. In addition to examine the effect of both environmental parameters (temperature) and structural parameters (mesh size, crosslinking density, composition, molecular weight) on the rate of degradation.

➢ To investigate the mechanism of release both above and below the LCST. A study of the effect of a range of drug molecules on the swelling and release patterns from the matrices. In addition to examine the influence of PLA composition and the effect of increasing the MW of the PLA unit on the release profiles.

➢ To investigate the potential of the drug delivery system as "on-off" regulation systems for controlled drug delivery.

CHAPTER 3:

MATERIALS AND EXPERIMENTAL METHODS

3.1 Materials

Materials (abbreviation)	Supplier/Manufacturer
Acetone	Trinity stores
Acryloyl chloride	Aldrich
Azobisisobutylonitrile (AIBN)	Aldrich
2-Aminoethanol	Sigma
Chloroform	Trinity stores
Deionised water	------------
Deuterated Chloroform (CDCl$_3$)	Aldrich
Diltiazem Hydrochloride (DH)	Elan Pharmaceutical
Disodium hydrogen phosphate (anhydrous)	Merck
1,3-dicyclohexylcarbodiimide (DCC)	Aldrich
Dimethylformamide (DMF)	Trinity stores
Dichloromethane (DCM)	Trinity stores
Diltiazem base (DB)	Elan Pharmaceutical
Ethanol	Trinity stores
FTIC-Dextran MW 4000 (D4)	Sigma
FTIC-Dextran MW 9,500 (D10)	Sigma
FTIC-Dextran MW42000 (D40)	Sigma
FTIC-Dextran MW 77000 (D70)	Sigma
1-hydroxybenzotriazole (HOBT)	Aldrich
Hexane	Trinity stores
Indomethacin (IDM)	Sigma
Nitrogen Gas	Sigma
N, N, N, N Tetramethylenediamine (TEMED)	Aldrich
N-isoproplacrylamide (NIPAAM)	Aldrich
N, N methylenebisacrylamide (MBA)	Aldrich
Polylactic acid MW 2000 (PLA 2000)	Boehringer Ingelheim
Polylactic acid MW 12000 (PLA 12000)	Boehringer Ingelheim
Potassium bromide (KBr)	Aldrich
Phenolphthalein	Sigma
Polystyrene molecular weight standards (GPC)	Polymer Laboratories
Sodium Chloride	BDH

Materials (abbreviation)	Supplier/Manufacturer
Sodium dihydrogen phosphate (anhydrous)	Merck
Sodium Hydroxide pellets	Aldrich
Salicylic acid (SA)	Sigma
Tetrahydrofuran (THF)	Trinity stores
Triethylamine (Et$_3$N)	Aldrich

3.2 METHODS OF SYNTHESIS

3.2.1 Introduction:

A series of hydrogels were synthesised by changing the composition ratio of PNIPAAM / PLA and the molecular weight of the precursor, PLA (Table 4.2). To prepare the hydrogels designed in this study, PLA (1) had to be chemically modified so that the unsaturated functional groups could undergo cross-linking (See Figure 3.1). The hydrogel synthesis consisted of three steps.

3.2.2 STEP 1: Synthesis of the PLA diol:

The objective of this step was to prepare PLA with –OH end groups so that the resulting PLA diol could be converted to the PLA diacrylate macromer (Figure 3.1). The original PLA polymer (16g) was dissolved in a round-bottomed three-neck flask in THF (240ml) under a nitrogen purge. Once all of the polylactic acid was dissolved, the solution was cooled to $0^{\circ}C$ in a chilled ice-bath. The calculated amount of 1-hydroxybenzotriazole (HOBT) (1:1molar ratio HOBT/PLA) and 1,3-dicyclohexylcarbodiimide (DCC) (1:1molar ratio DCC/PLA) were carefully added and the reaction was allowed proceed with continuous stirring for 30min at $0^{\circ}C$. The mixture was then allowed to reach room temperature before the calculated amount of 2-aminoethanol (1.1:1molar ratio 2-aminoethanol/PLA) was added dropwise. The reaction was allowed proceed for another 30 min before the precipitated by-product, cyclohexylurea salt, was filtered off. The PLA diol product was obtained by pouring the filtrate into an excess of hexane and was purified by dissolution and precipitation in THF and hexane respectively. The PLA diol was dried under vacuum at room temperature for 1 day (Zhang et al., 1999).

3.2.3 STEP 2: Synthesis of the PLA diacrylate macromer:

The objective of this step was to introduce unsaturated vinyl groups into the PLA diol so that the resulting PLA diacrylate macromer could be used as a hydrophobic component to undergo cross-linking to form the hydrogel network. The PLA diol (Figure 3.1(2)) was dissolved in THF in an ice chilled round bottomed flask under a nitrogen purge. The calculated amounts of triethylamine (4:1molar ratio Et_3N /PLA diol) and acryloyl chloride (4:1molar ratio acryloyl chloride /PLA diol) were then added respectively. The mixture was stirred for three hours at $0^{\circ}C$ and then at room temperature for 18 hours. The triethylammonium hydrochloride by-product was removed by glass filtration. The PLA diacrylate macromer (Figure 3.1 (3)) was collected by pouring the filtrate into an excess of hexane. Purification of the macromer was carried out by dissolution and precipitation in THF and hexane respectively. The product was dried for 1 day under vacuum.

$$H-O-\overset{O}{\overset{\|}{C}}-\overset{CH_3}{\underset{|}{CH}}-O\left(\overset{O}{\overset{\|}{C}}-\overset{CH_3}{\underset{|}{CH}}-O\right)_n\overset{O}{\overset{\|}{C}}-\overset{CH_3}{\underset{|}{CH}}-OH$$

(1)

DCC/HOBT | 2- aminoethanol

$$HO-CH_2-CH_2-NH-\overset{O}{\overset{\|}{C}}-\overset{CH_3}{\underset{|}{CH}}-O\left(\overset{O}{\overset{\|}{C}}-\overset{CH_3}{\underset{|}{CH}}-O\right)_n\overset{O}{\overset{\|}{C}}-\overset{CH_3}{\underset{|}{CH}}-OH$$

(2)

acryloyl chloride   triethylamine

$$H_2C=CH-\overset{O}{\overset{\|}{C}}-O-CH_2-CH_2-NH-\overset{O}{\overset{\|}{C}}-\overset{CH_3}{\underset{|}{CH}}-O\left(\overset{O}{\overset{\|}{C}}-\overset{CH_3}{\underset{|}{CH}}-O\right)_n\overset{O}{\overset{\|}{C}}-\overset{CH_3}{\underset{|}{CH}}-O-\overset{O}{\overset{\|}{C}}-CH=CH_2$$

(3)
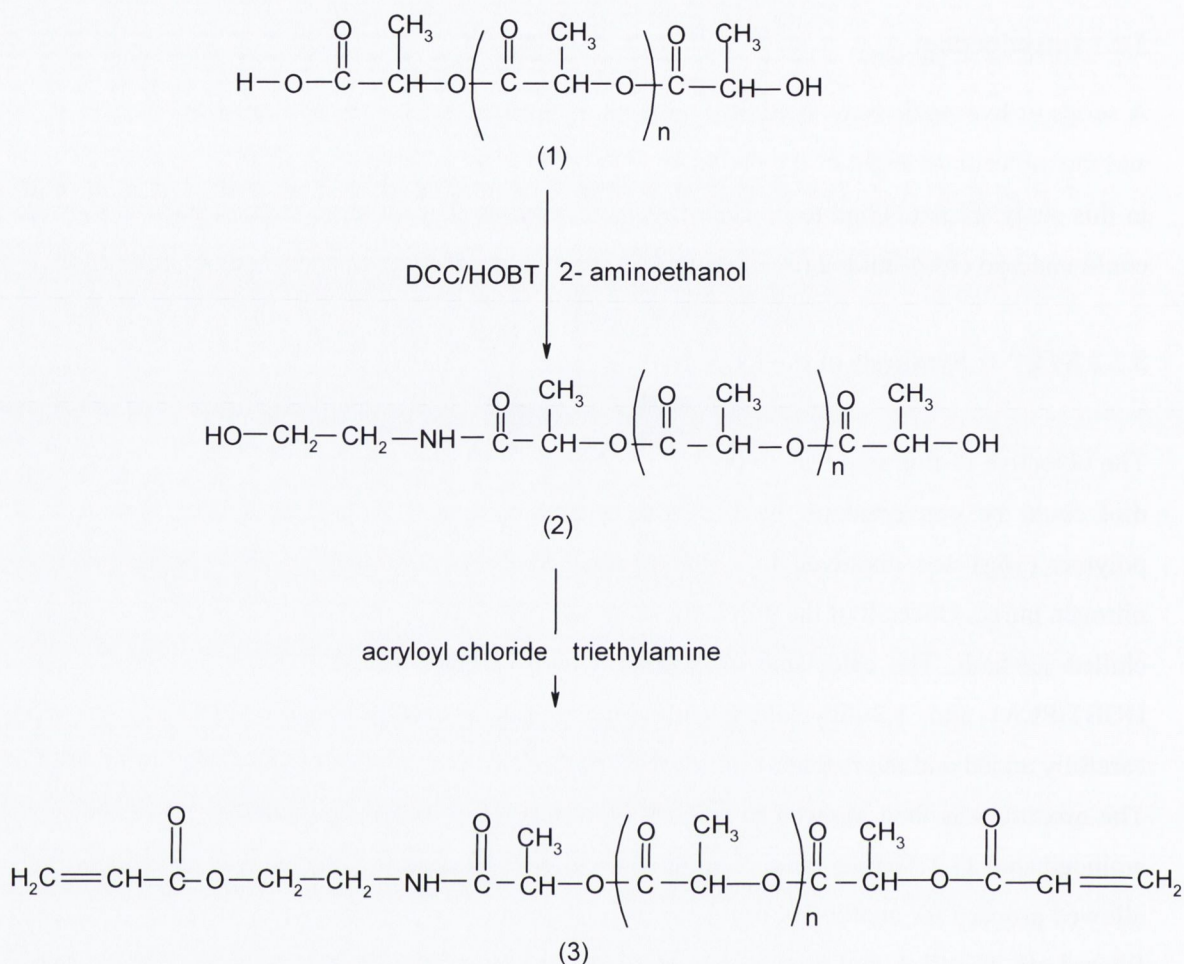
Figure 3.1: Synthesis of PLA diol (2) and PLA diacrylate macromer (PLAM) (3) from PLA (1)

3.2.4 STEP 3: Synthesis of the PNIPAAM-PLA hydrogels:

A series of PNIPAAM-PLA hydrogels were synthesised by varying the molar ratio of PNIPAAM to PLA (Figure 3.2). The hydrogels were synthesised in a cylindrical plastic tube (internal diameter 15mm) in DMF in the presence of a magnetic stirrer at $70^{\circ}C$ by solution polymerisation for 4 hours using AIBN (1% mol) as the initiator, N, N'-methylene bisacrylamide (4% mol) as the cross-linker and N, N, N, N'-tetramethylethylenediamine (9 % mol) as the accelerator (Appendix I).

The resulting hydrogels were first washed with DMF several times before a layer of water was added to obtain hard gels suitable for cutting into cylindrical discs of 15 mm diameter. The prepared hydrogels were washed repeatedly by swelling in a mixture of water and ethanol (50-

50 v/v) and dried in a vacuum oven at 50°C for 48 hrs. The dried discs had a diameter of 10-12mm.
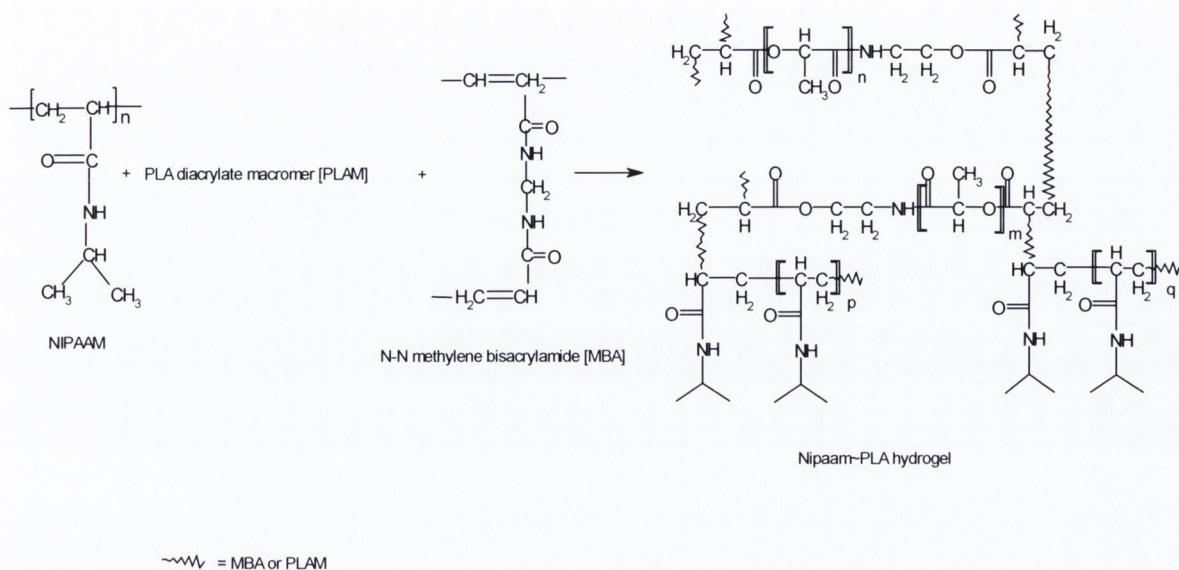
Figure 3.2: Schematic diagram of reaction forming the cross-linked hydrogel networks, where ⁓ᴡᴡᴠ symbolizes the crosslinking agent, PLAM (Figure 3.1 (3)) or MBA in the hydrogel networks.

3.2.5 Linear polymers

Linear polymers were synthesised in a similar manner to the hydrogels but without the cross-linker. After the solution polymerisation process, the polymer was collected by precipitation in dichloromethane. The polymer was collected by filtration washed in hot water and then dissolved in cold water. This process was repeated several times to purify the polymer. The collected polymer was dried in a vacuum oven at 50°C for 48hours.

3.3 METHODS OF CHARACTERISATION

3.3.1 Nuclear Magnetic Resonance (NMR)

The chemical structures of the polymers were determined by NMR. ^{1}H-NMR and ^{13}C-NMR spectra were recorded on a Varian Unity spectrophotometer at 400.130 MHz. The ^{1}H-NMR acquisitions were performed under the following parameter settings: SW 20.5524 ppm, TD 32,768 and TE 300.0 K. The sample concentration in the deuterated chloroform was ~25% (w/v). All chemical shifts were reported in parts per million (ppm). The central chloroform-d$_1$ resonance was set at 77.23 ppm in the 13C-NMR analysis. The peak of chloroform-d$_1$ at 7.27 ppm in the ^{1}H-NMR analysis was used as the reference line.

3.3.2 Fourier Transform Infrared (FTIR)

FTIR spectra were recorded on a Nicolet Magna-IR 560 spectrometer. Spectra were obtained by averaging 64 scans in the spectral range 4000-400cm^{-1}. PLA, PLA diol and PLA macromer were prepared by grinding a calculated amount of the sample (2 mg) with 220 mg of KBr in a mortar and pestle followed by compression in a 13 mm diameter punch and die set under 10 tonnes of pressure for 5 minutes (Zhang et al., 2000).

FTIR spectra of the linear polymers were obtained by casting a thin film on Zinc Selenide (ZnSe) salt discs from a THF solution (1% w/v) and further dried in a vacuum oven for 24 hours at room temperature to remove any residual solvent (Huang et al., 2004(a)).

FTIR spectra of the contents of the degradation medium after swelling studies were obtained using Zinc Selenide (ZNSE) salt plates (Specac Limited U.K.). A sample of 0.1 ml of the media was applied to the plates. Plates were then dried under vacuum at room temperature for 24 hrs.

3.3.3 Gel Permeation Chromatography (GPC)

The molecular weights of the linear polymer systems were determined by gel permeation chromatography. Samples were evaluated against a series of polystyrene standards (Aldrich). Solutions of the polymers were prepared in DMF and 50µl was injected into the system consisting of a Waters Styragel® HR column, a Waters 510 pump and a Waters 410 Differential Refractometer (elution rate 1ml/min). Millennium® 2010 software was employed to integrate the peaks. Samples were injected in triplicate and elution time compared with the calibration curve given in Appendix II.

3.3.4 Acid- Base Titrations

Acid base titrations were conducted on the linear polymers to confirm all of lactic acid monomer had been chemically incorporated into the backbone of the hydrogel. Sodium hydroxide solution (0.025M) was placed in a burette and titrated against a concentration of polymer solution dissolved in deionised water. Phenolphthalein was used as an indicator to determine the equilivence point during the titration. Similarly acid base titrations were preformed on the degradation medium following swelling studies to calculate the amount of LA present (Caulfield et al., 2003, Chiellini et al., 2002).

3.3.5 Glass transition temperature (Tg)

All differential scanning calorimetry (DSC) analysis was preformed using a Mettler Toledo 820^e DSC. Temperature calibration was preformed using an indium sample standard.

The glass transition temperature of the freshly made linear polymers and hydrogels systems were determined using 6-9 mg of dried samples. The samples encased in sealed aluminium crucibles were analysed under a N_2 atmosphere with three pierced vent holes in the lid. All samples were initially heated to 180°C at 10°C/min, cooled to 25°C at 20°C/min followed by heating to 260°C at 10°C/min. The role of the first heating cycle was to remove all residual moisture/ solvent and to erase the effect of previous thermal history. Results were analysed using $STAR^e$ software. Each sample was analysed in duplicate and the glass transition temperature was taken as the midpoint of inflection.

3.3.6 Phase Transition temperature (LCST)

3.3.6.1 DSC (LCST$_d$)

The LCST of the linear polymers (0.5% w/v) was determined using an aqueous sample (30-40 mg by weight). The samples were run in a sealed aluminium crucible under a nitrogen purge at 2°C/min unless otherwise stated. Samples were analysed in the range of 20°C to 50°C. The transition temperature has been defined in previous studies as either the temperature of onset (Otake et al., 1990) or the peak temperature (Eeckman et al., 2001). In the current work the phase transition temperature was defined as the maximum of the endothermic transition peak (average of the two measurements).

The hydrogel networks were similarly analysed using a solid sample (30-40mg by weight).

3.3.6.2 Transmittance measurements (LCST$_i$)

The LCST of the linear polymer was measured by determining turbidity of polymer solution as a function of temperature (Eeckman et al., 2001). The transmittance of 0.5% w/v of the PNIPAAM/PLA polymer solutions in PB was measured at 500 nm with the temperature controlled by a single cell peltier temperature controller (Thermo Electron Corporation, U.K.). The % transmittance of each solution was determined at specified temperature intervals at a heating rate of 2°C/min. Various authors have defined the LCST differently, usually as a percent of transmittance of the polymer solution during the heating process. Tachibana et al., (2003) defined the LCST as 90% transmittance. In the present study the LCST is defined as 50% transmittance of the polymer solution during the heating process (Wang et al., 2002).

3.3.7 Drug solubility studies

Solubility studies were carried out either at 20°C or 37°C in a jacketed water vessel containing phosphate buffer PB7.4 (isotonic) (PB) (Pharmaceutical handbook, 1980). Excess drug was added and solutions were agitated using an overhead stirrer at 300rpm. The solution was then assayed in triplicate at appropriate time intervals until equilibrium solubility was reached.

3.3.8 Swelling studies

All swelling studies were preformed in phosphate buffer 7.4 (isotonic) (PB). To determine the swelling ratio the dry disc was placed into an excess of the swelling medium at a specific temperature and the disc was allowed to swell to equilibrium. Swelling studies over time were preformed in a similar manner. The swollen hydrogel was briefly removed from the medium at specific time intervals and blotted with filter paper to remove any excess of surface moisture before weighing. This procedure was preformed in triplicate in each case. At the end of all swelling studies (2 months) gels were removed and dried under vacuum before reweighing. The fraction mass loss was determined as percent of the original freshly made dry sample.

The swelling behaviour of the two different types of PLA (MW 2000, MW 12000) discs, 13mm in diameter were prepared by compressing 200 mg of sample under 5 tonnes of pressure for 5 minutes in a 13mm punch and die set and these were immersed in 50ml of phosphate buffer pH 7.4. The specimens were incubated at both 20°C and 37°C. At appropriate intervals the pre-

56

weighed tablets were removed, gently blotted to remove surface moisture and reweighed. The degree of swelling was calculated using EQN 2.22 below similar to studies under taken by Andreopoulous et at., 2001;

$$\frac{M_t}{M_\infty} = kt^{0.5}$$
Equation 2.22

The phase transition temperature ($LCST_s$) of the hydrogel systems were determined by decreasing the temperature of the media daily to allow equilibrium swelling at that particular temperature. The LCST was defined as the temperature at which the hydrogel showed a significant increase in swelling from the baseline value.

In other experiments the pH of the medium was monitored (Olewnik et al., 2007). A decrease in pH was taken to signify degradation of the PLA component.

The swelling of the hydrogels and was then examined using the swelling ratio equation:

$$S.R. = \frac{W_s - W_d}{W_d}$$
Equation 2.27

Where,

Ws= weight of hydrogel at time t

W_d=weight of dry disc

3.3.9 Calculation of solubility parameter

The square root of cohesive energy density is called solubility parameter and it is a measure of the interatomic/molecular interactions. Hansen's basic assumption (Van Krevelen, 1990) of the partial solubility parameter stated:

$$\delta^2 = \delta^2{}_d + \delta^2{}_p + \delta^2{}_h \qquad\qquad \text{Equation 3.1}$$

Where δ is the total solubility parameter and δ_d, δ_h, δ_p are the contributions from the dispersive forces, hydrogen forces and polar forces components respectively. The solubility components may be predicted from group contributions using the following equations:

$$\delta_d = \frac{\sum F_d}{V} \qquad\qquad \text{Equation 3.2a}$$

$$\delta_p = \frac{\sqrt{\sum F^2{}_p}}{V} \qquad\qquad \text{Equation 3.2b}$$

$$\delta_h = \sqrt{\frac{\sum E_h}{V}} \qquad\qquad \text{Equation 3.2c}$$

Where F_d, F_p and E_h refer to the functional group contributions to the dispersion, polar and hydrogen components respectively and V is total molar volume (Van Krevelen, 1990). The values calculated for F_d, F_p and E_h for the functional groups were obtained from values compiled by Van Krevelen and the total molar volume from values compiled by Fredors (Van Krevelen, 1990).

3.3.10 Scanning Electron Microscopy

The freshly polymerised hydrogels were allowed to equilibrate for 48 hrs at specified temperature (20 °C and 37°C) in an excess of PB before flash freezing using liquid nitrogen. SEM was also carried out on the hydrogel systems to investigate the morphological effect of degradation over time. The swollen hydrogels, after 2 months incubation in PB at 20°C and 37°C were removed from the media and immediately frozen in liquid nitrogen to retain the swollen structure. All frozen hydrogel samples were subsequently dried for 2 days in Virtis Bench Top Freeze Dryer under vacuum at a temperature of –80°C. Samples were fractured, mounted on aluminium stubs and sputter coated with gold for examination using SEM Hitachi S-35500.

Approximate pore size in the SEM scans were obtained using Imagetool for windows ® version 3.0. Twenty measurements were obtained at random on n = 3 SEM images (magnification x 1500)(PNP-PLA-$_2$ systems), x 500 (PNP-PLA-$_{12}$ systems).

3.3.11 Determination of hydrogel structural parameters; Mc and Px

In order to characterise the hydrogels, the polymer volume fraction in the swollen state (V_{2s}), the polymer volume fraction in the relaxed state (V_{2r}), the molecular weight between cross-links, M_c and the cross-linking density, P_x were calculated. The pathway followed to calculate these parameters was explained in Section 2.2. To determine these parameters it was necessary to experimentally measure V_{2s} (Caykara et al., 2006) which was calculated as follows:

$$V_{2s} = \left[1 + \frac{\left(\dfrac{m_s}{m_d} - 1 \right)\rho_2}{\rho_1} \right]^{-1}$$

Equation 2.6 (a)

Where m_s the mass of the swollen hydrogel, m_d is the mass of the dry gel and ρ_2 and ρ_1 are densities of the polymer network and solvent respectively. The density of the polymer network was determined by a pycnometer (Section 3.3.13).

The polymer volume fraction in the relaxed state (V_{2r}) was calculated from the knowledge of the initial monomer concentration Co as defined by equation 3.5;

$$V_{2r} = Co\overline{V}r \qquad\qquad\qquad\qquad \text{Equation 2.7}$$

Where,

$\overline{V}r$ is the molar volume of monomer (ml/mol^{-1}).

Having determined the polymer volume fractions, the molecular weight between cross-links, Mc, could be determined. Initially, an equation to predict the Mc for highly swollen membranes, developed by Peppas and Merrill, (1977) was used.

$$\frac{1}{\overline{Mc}} = \frac{2}{\overline{Mn}} - \frac{\dfrac{\overline{v}}{V}\left[\ln(1 - v_{2s}) + V_{2s} + \chi V^2{}_{2s}\right]}{V_{2r}\left[\left(\dfrac{V_{2s}}{V_{2r}}\right)^{1/3} - \dfrac{1}{2}\left(\dfrac{V_{2s}}{V_{2r}}\right)\right]} \qquad\qquad \text{Equation 2.4}$$

Where,

$\overline{v}$ is the specific volume,

Mn is the molecular weight of the polymer (Mn) (GPC section 3.3.3)

The Flory interaction parameter χ, was determined from the Hildebrand solubility parameters (δa and δb) (section 3.3.9) where:

$$\chi = V\left(\frac{(\delta a - \delta b)^2}{RT}\right) \qquad \text{(Flory, 1953)} \qquad \text{Equation 3.3}$$

Where

R is the gas constant,

T is the temperature

V is the molar volume of the solvent (18molcm^{-1} for water)

δa is the solubility parameter of the polymer and δb is the solubility parameter of the solvent.

60

3.3.12 Solute Exclusion Technique

The pore size distributions of the hydrogels synthesised were characterised by the solute exclusion technique using a range of molecular probes (Wu et al., 1992). The initially weighed dry gels obtained by drying the hydrogel discs under vacuum overnight were first equilibrated at either 20 or 37°C for 72 hours and then weighed.

After equilibration the gels were placed into solutions (5 ml) of known concentrations of a molecular probe (DH 0.025µg/ml, Dextran fractions; (0.01µg/ml). The gels were left for exhaustive extraction for a week. The concentrations of FITC dextrans and DH solutions after equilibration, (C_o)(mg/ml) and after exhaustive extraction, C_e (mg/ml) were determined. The volume of pores accessible to each molecular probe (V,ml) was estimated by the equation:

$$V = 5\left(\frac{C_e}{C_o}\right)$$

Equation 3.5

Where C_o is the initial concentration of drug present (expressed in mg/ml) after equilibration of the gels and C_e is the drug concentration (mg/ml) after exhaustive extraction (Wu et al., 1992). The volume fraction of pores (VF) with sizes larger than the probing molecule is expressed by

$$VF = \frac{V}{V_t}$$

Equation 3.6

Where V_t is the total volume of medium in the gels determined gravimetrically.

3.3.13 Density determination

The density of the powdered model drugs and the linear co-polymers were determined using a Helium pycnometer (Micromeritics AccuPyc 1300). Powdered samples were dried overnight in a vacuum oven.

3.3.14 Melting point determination

The melting points of the various crystalline drugs and the pre-polymers, (PLA, the PLA diol and the PLA macromer of various molecular weights) were determined by DSC in an open pan. 5-10mg of sample was heated at a rate of 10°C/min from 25°C to a suitable temperature above the melting point. The melting point was taken to be the average onset of melting of three sample runs.

3.4 Drug loading and release studies:

3.4.1 Drug loading technique

The dried hydrogel discs were loaded with model drugs by sorption of a drug solution of known concentration and volume. This was followed by solvent evaporation in a dessicator at room temperature to entrap the compounds within the hydrogel meshwork. Loading of each crystalline drug was 10%w/w based on each dried hydrogel disc. These loading contents were controlled by complete sorption of a known aqueous or ethanolic drug solution for 48 hrs in suitable glass vial before drying out.

3.4.2 Controlled drug release studies

Controlled drug release experiments were conducted in triplicate for each hydrogel systems. Each hydrogel was placed in 900 ml PB at 20°C or 37°C in a USP paddle method dissolution bath (Sotax AT7, 50 r.p.m.). In the case of pulsatile drug release, the discs were transferred between identical baths maintained at 20°C and 37°C. Samples (5ml) were manually withdrawn periodically at appropriate intervals from the same position in the dissolution bath. Each sample was replaced with an equal volume of fresh media, which was maintained at the same temperature as the bulk media. The periodic removal of the release medium was carried out until the change in the concentration of the released drug was negligible or had reached equilibrium. Samples were filtered through 0.5μm filter and analysed.

Results were plotted as the cumulative amount release or fraction released against time. Calculations were based on the amount of drug released at each time interval divided by the total amount released for that sample. The profiles are the average of the three determinations with error bars indicating the standard deviation of these values.

3.4.3   Drug assays Methods

A Shimadzu UV was used to calculate the amount of each of the smaller molecular weight drugs present during release studies. The working wavelength range for analysis of each compound was determined by their individual absorption bands. Indomethacin and salicylic acid were detected at 318 nm and 296 nm respectively. Diltiazem HCl and its base were detected at 238nm. Calibration curves were prepared using five known concentrations of each model drug and plotted against absorbance (Appendix II).

The dextrans were assayed by detection of a dextran probe (FITC-Dextran) incorporated within the bulk dextran. The concentration of FTIC-dextran released was measured at room temperature using a Turner Quantech Digital filter Fluorometer at an excitation wavelength 490 nm and emission wavelength of 520 nm (Dong et al, 1994). A calibration curve was established for each of the fluorescent probes in the range of 0-0.025mg/ml (Appendix II).

3.4.4   Dissolution studies on pure drug discs

Pure drug discs were prepared by compressing 100 mg of drug under 5 tonnes of pressure for 5 minutes in a 8mm punch and die set. The rate of dissolution was determined in 900 ml PB at $20^{\circ}C$ and $37^{\circ}C$ in a USP paddle method dissolution bath (Sotax AT7, 50 r.p.m.) using an identical method to that described in previous section (3.4.2)(Appendix III).

3.4.5   Statistical significance testing

Statistical significance between two parameters was evaluated by an independent 2-sample t-test (0.05 probability level) using Minitab® statistical software version 13.32.

CHAPTER 4:

POLYMER, HYDROGEL AND DRUG

CHARACTERISATION

4.1 INTRODUCTION

The objective of this study was to synthesise a new series of biodegradable polymer network hydrogels. A series of multi-functional thermoresposive-co-biodegradable polymer networks were synthesised composed of PNIPAAM and PLA. To prepare the hydrogels, PLA had to be chemically modified so that it had unsaturated functional groups to undergo cross-linking as described in Section 3.2.

The PLA, its diol and macromer of different molecular weights in the present study were characterised in Section 4.2. Characterisation of the linear PNIPAAM based polymers is described in Section 4.3. In addition, the PNIPAAM based hydrogels used in the present study are characterised in Section 4.4 in relation to their swelling properties, thermal properties and pore size distribution. The model drugs are also described in Section 4.5.

4.2 Pre-Polymer Characterisation

To confirm the success of the syntheses, the chemical structures of PLA, the diol and its macromer were characterised by studying their infrared absorption bands as described in Section 3.3.2. In addition the chemical shifts of PLA, the PLA diol and its macromer were analysed using proton nuclear magnetic resonance (^{1}H-NMR) and carbon nuclear magnetic resonance (^{13}C-NMR). DSC as described in Section 3.3.5 measured thermal properties and polymer molecular weights were determined by GPC (Section 3.3.3).

4.2.1 Fourier Transform Infrared (FTIR) Spectroscopy

The absorption band spectrum of PLA was classified into five regions, which correspond to the following bands: -CH- stretch (2995 cm^{-1}, 2944cm^{-1}), -C=O- carbonyl (1759cm^{-1}), -CH- deformation including both symmetric and asymmetric bends (1453 cm^{-1}, 1382 cm^{-1}, 1362 cm^{-1}), -C-O- stretch (1268 cm^{-1}, 1194 cm^{-1}, 1130 cm^{-1}, 1093 cm^{-1}, 1047 cm^{-1}) and the -C-C- stretch (868 cm^{-1})(Kister et al., 1998). These peaks assignments and corresponding positions are shown in Figure 4.1 (a) for PLA with a molecular weight of 2000 daltons. The spectrum of PLA 12000 was similar only with higher intensity of the absorption bands were visible due to the increase in molecular weight.

The PLA diol was synthesised by coupling of 2-aminoethanol onto the PLA in the presence of a powerful dehydrating agent (DCC) and an auxiliary nucleophile (HOBT) to improve reaction rates and suppress any side reactions (Figure 3.1).

A.
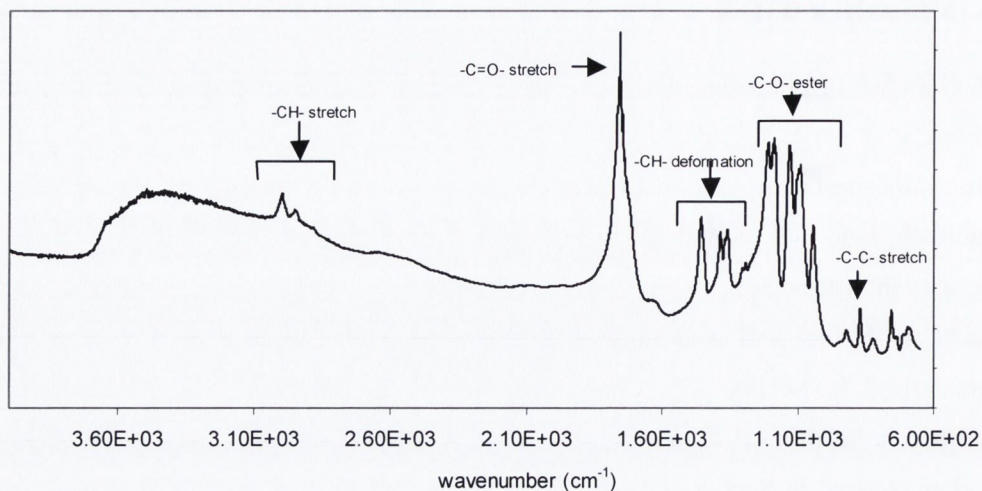
B.
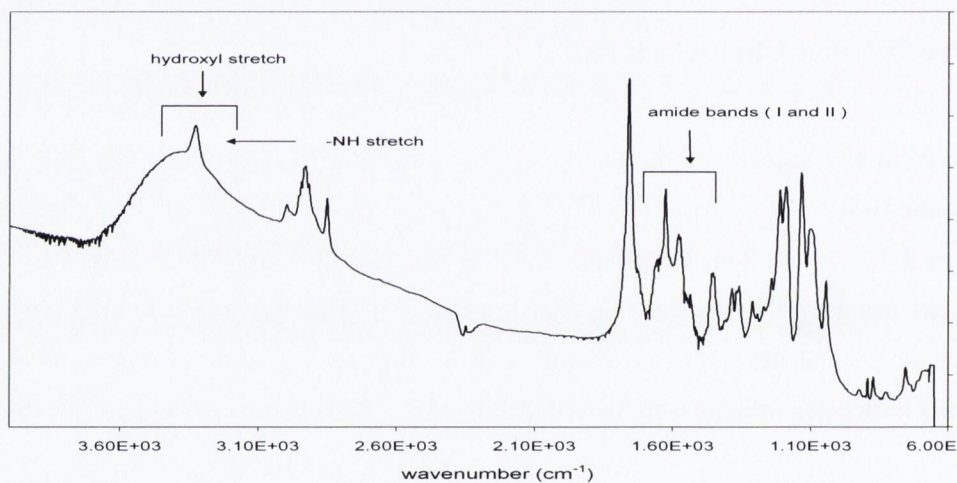
C.
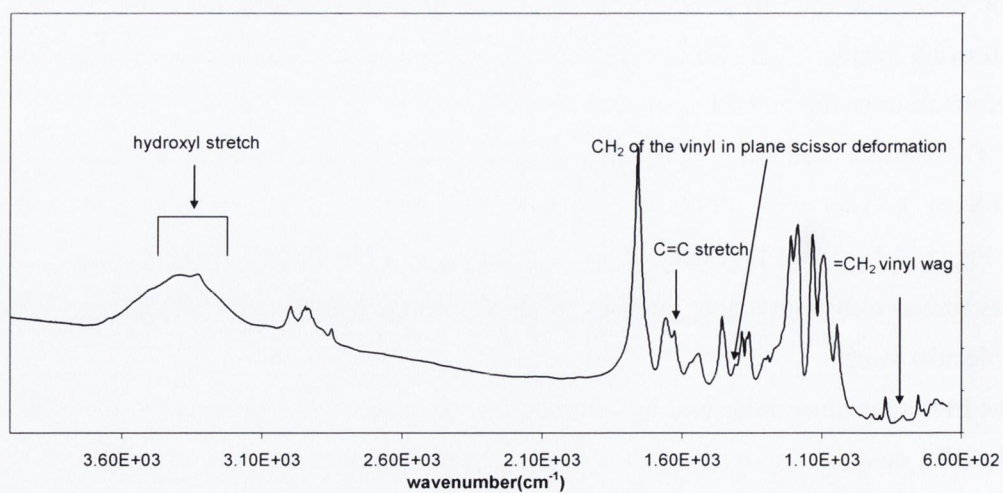
Figure 4.1(A) FTIR spectrum of PLA (MW 2000), (B): PLA diol (MW 2000) and (C) PLA
acrylate macromer (MW2000).

The FTIR spectrum of the PLA diol demonstrated the successful incorporation of the 2-aminoethanol into the carboxylic chain end of PLA (Figure 4.1(b)). A comparison of both the PLA and the PLA diol absorption spectra clearly showed the addition of the two-amide bands at 1670 cm^{-1} and 1540 cm^{-1} respectively. The -NH- stretch band was observed at 3300cm^{-1}. A broad stretch vibration of the hydroxyl chain end group is also seen at 3400cm^{-1}. The –OH peak intensity of the PLA diol increased compared to the original PLA diol due to the addition of another hydroxyl end group.

The FTIR spectrum of the PLA diacrylate macromer is shown in Figure 4.1(c). Compared to the PLA absorption band, the PLA diacrylate macromer showed the addition of five new peaks; 1670, 1640, 1540, 1420 and 810cm^{-1} due to the characteristic absorption bands of the amide 1(-C=0 stretching), C=C stretching band, the amide 2 absorption band (N-H bending), =CH_2 of the vinyl in-plane scissor deformation and the =CH_2 of the vinyl wag respectively. The presence of these additional peaks indicates the successful modification of PLA to the diacrylate macromer.

All peak assignments and positions in the spectra were similar for PLA of both molecular weights, however the effect of the molecular weight on the extent of the conversion of the –COOH chain end group to the –OH group and the –OH group to –CH=CH_2 was apparent in the FTIR spectra (Table 4.1).

In the case of the PLA diol the amide band at 1670cm^{-1} in the FTIR spectra can be used to represent the amount of the –OH end group introduced onto the PLA chain via coupling of 2-aminoethanol onto the polymer. The carbonyl band represents the repeating unit of the PLA backbone. Since no additional carbonyl group was introduced into the PLA diol, the ratio of the peak intensity of the amide 1 band and the carbonyl band can be used to indicate the extent of the conversion of the –COOH chain end group to the –OH group (Zhang et al., 2000).

In the case of the diacrylate macromer, the FTIR peak intensity at 3400cm^{-1} can be related to the intensity of the remaining –OH end-group after the reaction. Since no additional methylene (-CH_2-) or methyl (-CH_3) groups were introduced in this step except for the acrylate group (CH_2=CH-), the peak intensity in the region of 2880-2995cm^{-1} (relating to the –CH_2 and –CH_3 absorption band) was used as the reference of the PLA backbone. Both peak intensity ratios at 1638 cm^{-1} (CH_2=CH-) to 3400 (-OH) and 1638 to 2880-2995 cm^{-1} (-CH_2- and –CH_3) were calculated to estimate the number of –OH end groups of the diol which were converted to –CH=CH_2 representative of the PLA acrylate macromer (Zhang et al., 2000). These results are presented in Table 4.1 and will be discussed in Section 4.2.3 in relation to the MW of each precursor unit.

4.2.2 Nuclear Magnetic Resonance (NMR)

^{1}H-NMR and the ^{13}C-NMR spectra shown in Figure 4.2 (a) and 4.2 (b) further confirmed the success of each step from the PLA to the PLA diacrylate macromer. The assignment of ^{1}H-NMR and [13]-CNMR were as follows:

PLA (MW 2000):

^{1}H-NMR (CDCl$_3$) :
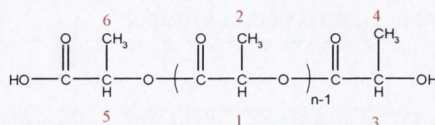
δ 5.19 (m, H1 and H5) δ 4.3 (m, H3), δ 1.5 (d, H2 and H6) and δ 1.4 (d, H4).

^{13}C-NMR (CDCl$_3$):
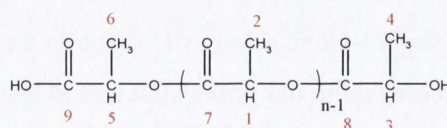
δ169.18 (-C=O, C7, C8 and C9), δ68.55 (-CH, C1 and C5), δ68.30 (-CH, C3), δ20.05 (-CH$_3$, C4), δ16.19 (-CH$_3$, C2 and C6).

The most intense signals of the PLA were those located at δ 5.19 (-CH groups) and δ 1.5ppm (–CH$_3$ groups) in the ^{1}H-NMR spectrum, which correspond to the central protons in the backbone of the polymer. The methine proton and methyl group at δ 5.19 and δ 1.4 respectively represent the chain end group of the polymer.

PLA diol (MW 2000):

^{1}H-NMR (CDCl$_3$):
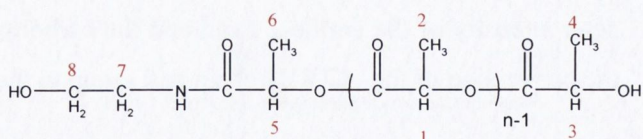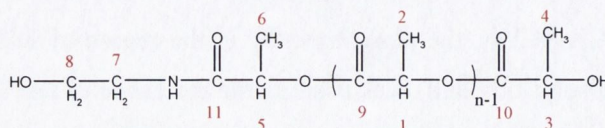
δ 5.19 (m, H1 and H5) δ 4.3 (m, H3), δ 3.7 (m, H8) δ 3.4 (m, H7), δ 1.5 (d, H2 and H6) and δ 1.4 (d, H4).

^{13}C-NMR (CDCl$_3$):

δ 169.18(-C=O , C7, C8 and C9), δ68.55(-CH, C1 and C5), δ68.30(-CH, C3), δ62.3 (-CH$_2$ CH8),δ42.6 (-CH$_2$, CH7) δ20.05 (-CH$_3$, C4), δ16.19 (-CH$_3$, C2 and C6).

A)
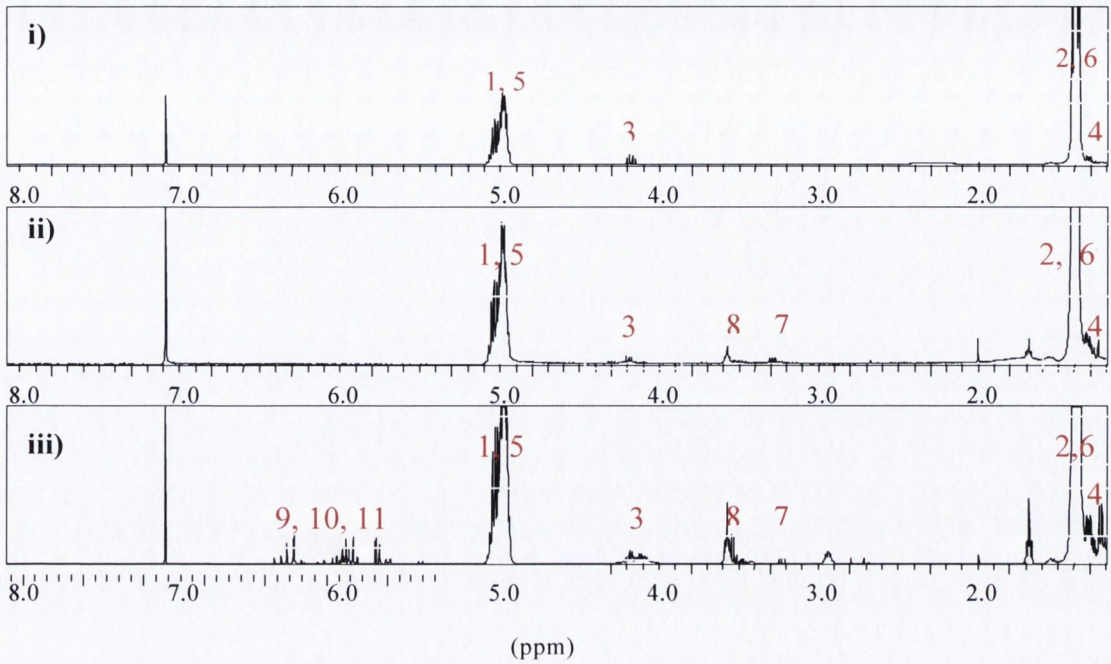
B)
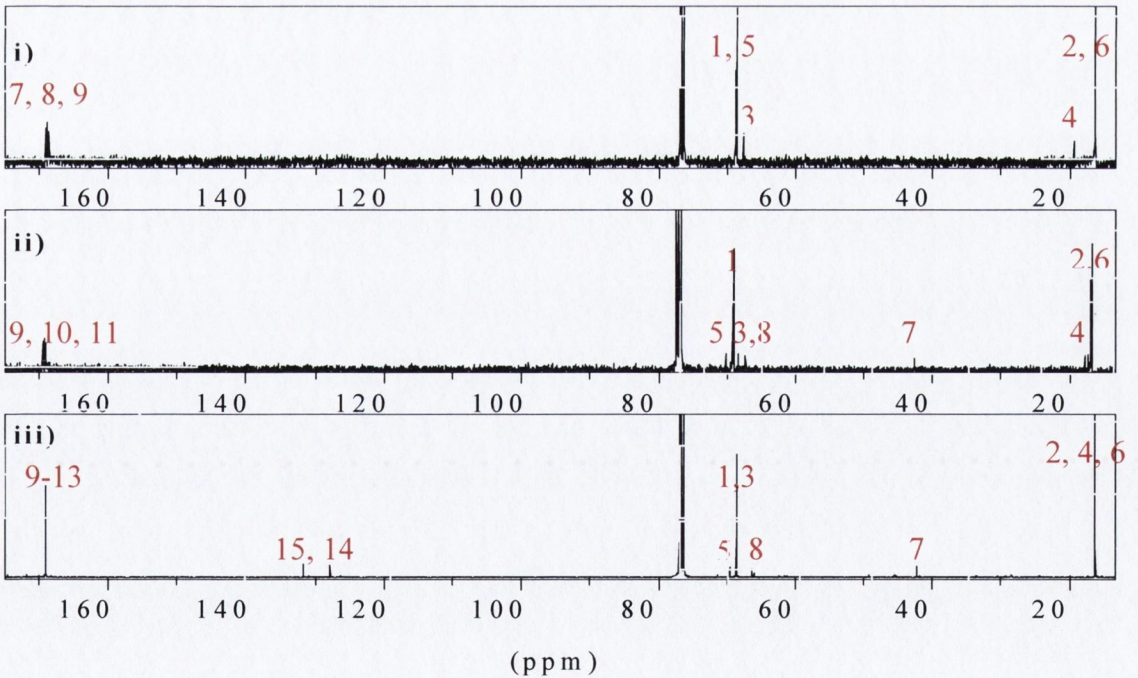
Figure 4.2(a) ^{1}H-nmr Spectra of PLA MW 2000 (i) and its corresponding PLA diol (ii)
and PLA macromer (iii) and 4.2 (b) ^{13}C-NMR of PLA MW 2000 (i),and its corresponding PLA
diol (ii) and PLA macromer(iii)

The PLA diol in the ^{1}H-NMR showed a new peak at $\delta 3.79$ ppm in the PLA diol, which was attributed to the protons of CH_2 next to the OH end group of the 2-aminoethanol segment, and the peak at $\delta 3.39$ was due to the protons of CH_2 next to the NH group of the 2 amino segment. The ^{13}C-NMR spectrum of the PLA diol shows the additional chemical shifts at $\delta 42.6$ ppm and δ 62.3 ppm; these were assigned to the carbon atoms of CH_2-NH and CH_2-OH of the 2aminoethanol respectively. These peaks were absent from PLA spectrum.

PLA acrylate macromer (MW2000):

^{1}H-NMR (CDCl$_3$):
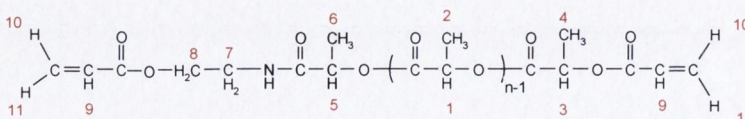
δ 6.70- 5.75 (m, H9, H10and H11) δ 5.19 (m, H1 and H5) δ 4.3 (m, H3), δ 3.7 (m, H8) δ 3.4 (m, H7), δ 1.5 (d, H2, H4and H6).

^{13}C-NMR (CDCl$_3$):
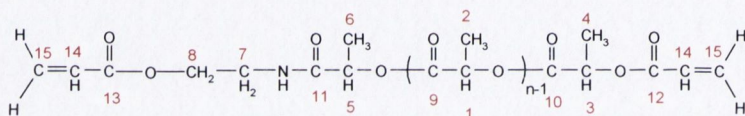
δ 132.2 and 127.6 (CH=CH$_2$, C14 and C15 respectively) δ 169.18(-C=O, C9-C13), δ68.55 (-CH, C1 and C5), δ68.30(-CH, C3), δ62.3 (-CH$_2$ CH8),δ42.6 (-CH$_2$, CH7) , δ16.19 (-CH$_3$, C2 ,C4 and C6).

The ^{1}H-NMR of the PLA diacrylate macromer shows small peaks for the protons of the acrylate group in the region of δ5.75 to 6.70ppm that are not found in the diol indicating successful incorporation of the acrylate groups into the PLA acrylate macromer. In addition the ^{13}C-NMR (Figure 4.2 (b)) displayed chemical shifts at δ127.6 ppm and δ 132.2 ppm, which are characteristic of two carbon atoms of a double bond.

The use of ^{1}H-NMR in calculating the molecular weight has been reported by others [*Han et al., 1997*]. Theoretical molecular weights were estimated using ^{1}H-NMR and compared to that of the GPC results for each polymer. The results are listed in Table 4.1. The modified structure of PLA MW 12000 had similar results to PLA 2000.

4.2.3 Molecular Weight

The molar ratio of the reactants was identical for both PLA units (MW 2000, MW 12000) in all reactions as well as the duration allowed for the completion of the reaction. The molecular weights of the PLA, PLA diol and PLA macromer of each batch was determined by gel permeation chromatography (GPC), the extent of conversion measured by FTIR peak intensities as well as their thermal properties are shown in Table 4.1. Crystallinity of PLA (MW 2000) was confirmed by XRD (Appendix V).

Table 4.1 Comparison of properties of PLA precursors.

MW 2000	Glass transition temperature $(Tg)(^{o}C)$	Melting point $(Mp)(^{o}C)$	(Mn) (g/mol;GPC)	Mn (g/mol;^{1}HNMR)	FTIR Peak intensity Ratio	
PLA	88	149	1900	1818	-----------------	
PLAdiol	57	143	1300	1092	$1670cm^{-1}/1750cm^{-1}$	0.67
PLAmac	54	148	1600	1308	$1638cm^{-1}/2994cm^{-1}$	0.79
					$1638cm^{-1}/3400cm^{-1}$	0.60
MW 12000						
PLA	100	55.7	12200	9642	--------------------	
PLAdiol	85	55.0	10200	8197	$1670cm^{-1}/1750cm^{-1}$	0.46
PLAmac	83	63.3	6000	3895	$1638cm^{-1}/2994cm^{-1}$	0.57
					$1638cm^{-1}/3400cm^{-1}$	0.50

On examination of Table 4.1, the effects of employing different molecular weight PLA on the conversion of –COOH to -OH groups was significant. The FTIR peak intensity ratio of the amide 1 band to the carbonyl had a value of 0.67 for PLA MW 2000 and 0.46 for MW 12000. Previous studies undertaken by Zhang et al., (1999) showed that the optimal reaction conditions for the synthesis of the diol was the use of small amounts of reactants and a short reaction time to achieve high conversion without the expenses of molecular weight reduction. However in the present study the effect of employing a larger molecular weight lactic acid significantly reduced the rate of conversion. This is also pronounced in the reduced molecular weight indicating chain fragmentation during the reactions whereby chain cleavage increased the –CH end group.

The conversion of the diol to the macromer was similarly estimated by the FTIR peak intensity ratio of the introduced double bond ($1638cm^{-1}$) on the polymer to the remaining –OH end group ($3400\ cm^{-1}$) and the backbone of the polymer (-CH_2 and –CH_3 groups, $2994\ cm^{-1}$) after the reaction. A significant decrease in the peak intensitiy ratios was observed in comparison to the lower molecular weight PLA. If all the hydroxyl groups were converted to the acrylate group without cleavage of the polymer chain the MW should not decrease. A significant decrease was seen in the case of the larger MW diacrylate macromer. This was also observed in the ^{1}H-NMR spectrum where the peak area at 4.26ppm increased as more of the –CH- end group appeared leading to a reduced molecular weight (Figure 4.2 (a) (iii)).

Generally the glass transition signifies the beginning of chain mobility. Therefore if interactions between chains were strong a higher temperature would be needed to promote this chain mobility. From the data above the glass transition temperature for the polymers were in agreement with the molecular weight. Since an observed decrease in MW was a result of chain scission within the method of synthesis, a resulting lower Tg would be expected due to a decrease in chain entanglements and therefore increase in chain mobility (Sousa et al., 1998).

4.3 LINEAR POLYMER CHARACTERISATION

In the present work, biodegradable polymers from chemically modified poly lactic acid (PLA) and N-isopropylacrylamide (NIPAAM) were prepared by polymerisation based on a method by *Lowe et al., (2003).* The aim of the work was to determine the effect of incorporating polylactic acid of different molecular weights and composition ratios on the chemical/physical properties of the polymers. Firstly, the chemical structure of the biodegradable NIPAAM-PLA polymers were analysed by FTIR and NMR to demonstrate the successful incorporation of the poly lactic acid into the backbone of the polymer by the introduction of unsaturated vinyl groups. The characteristics of the linear batches of PNP-L to PNP-L3$_{-2}$ (Table 4.2) were examined for comparison with the hydrogels. The prepared batches were characterised by molecular weight and analysis of the phase transition temperature.

4.3.1 Fourier Transform Infrared (FTIR) Spectroscopy

Seven linear polymers were synthesised by varying the molar ratio of N-isopropylacrylamide (NIPAAM) and PLA as well as the molecular weight of the hydrogel component, PLA. Their compositions are summarised in Table 4.2. The FTIR spectra confirmed the chemical structure of the polymers (linear poly (N-isopropylacrylamide) (PNP-L), linear 93-7 molar ratio PNIPAAM co-PLA (PNP-L1$_{-2}$), linear 86-14 molar ratio PNIPAAM co-PLA (PNP-L2$_{-2}$) and linear 72-28 molar ratio PNIPAAM co-PLA (PNP-L3$_{-2}$) are shown in Figure 4.3.
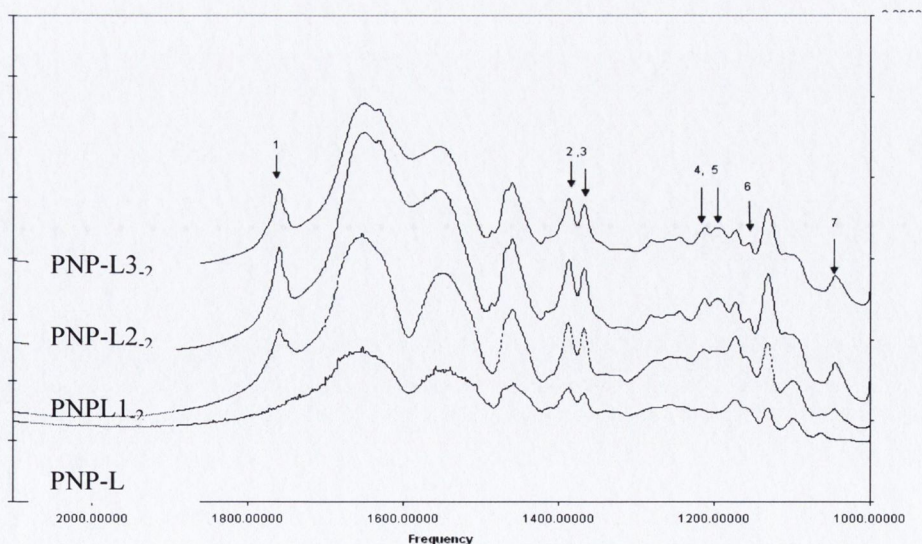
Figure 4.3: FTIR spectra of the polymer systems with PLA (MW2000): PNP-L, PNP-L1$_{-2}$, PNP-L2$_{-2}$, and PNP-L3$_{-2}$

PNIPAAM was observed in the IR spectra (Figure 4.3) of all the polymers represented by two absorption bands of the symmetric –CH $(CH_3)_2$ group at 1388 and 1370 cm^{-1}(peak 2, 3). In the co-polymeric systems additional absorption bands were present at 1760 (C=O stretching, peak 1) 1215 (C-O-C asymmetric stretching, peak 4), 1200 (O-CO stretching, peak 5), 1117 $[CH(CH_3)=O$ stretching, peak 6] and 1050cm^{-1} (C-OCO stretching, peak 7) indicating successful incorporation of PLA into the backbone of the polymer systems. The higher the calculated amount of PLA incorporated into the backbone of the polymers, the stronger the intensities of the observed peaks. Similar results were observed for PLA MW12000 and its corresponding diol and macromer.

The FTIR spectra of PNP-L2$_{-2}$ and a physical mixture of PNIPAAM and PLA macromer manufactured by solvent evaporation were also examined (Figure 4.4). The decrease of the C=C bands at 1638 (peak 1), 1407 (peak 2) and 810 (Peak 3) cm^{-1} in PNP 2$_{-2}$ after polymerisation of PLA and NIPAAM, demonstrates the crosslinkable double bonds available in the diacrylate macromer to form the three dimensional polymer network. In the physical mixture, the double bonds are still present indicating PLA was not incorporated into the backbone of the hydrogel by chemical means.
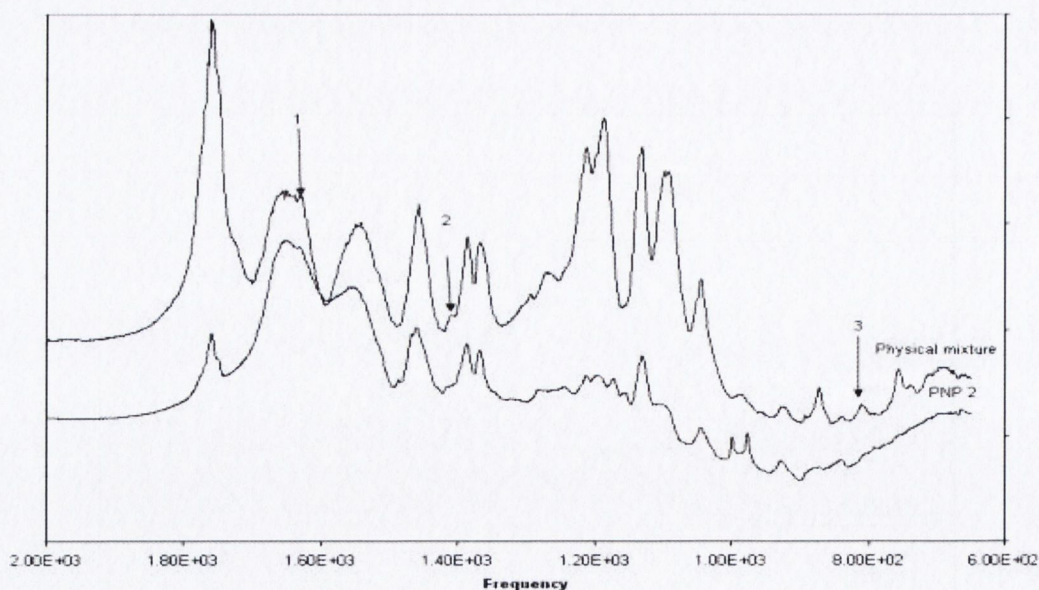
Figure 4.4: FTIR spectra of the co-polymer PNP-L2$_{-2}$ and a physical mixture of PNIPAAM and PLA.

4.3.2 Nuclear Magnetic Resonance (NMR)

NMR spectra were obtained of PNP and the co-polymer systems to further confirm the chemical composition and structure of the networks. Samples were dissolved in CDCl3 and the chemical shifts were expressed in ppm with respect to the CDCl3 signals at δ 7.28ppm in the proton spectrum and at δ 78ppm in the carbon spectrum respectively. The ^{1}H-NMR spectrum of the homopolymer, (PNP-L) and the co-polymer PNP-L2$_{-2}$ are shown in Figure 4.5 and 4.6. The respective peak assignments are listed below for the PNIPAAM and the co-polymer, PNP-L2$_{-2}$.

PNP-L (CDCl$_3$):

^{1}H-NMR (CDCl$_3$) :

δ1.14 (H1, methyl proton of the isopropyl group), δ1.64 (H2, methylene proton), δ1.81 (H3, methyne proton), δ3.1 (H4, proton of NH), δ4.00 (H5, -lone proton of the isopropyl group).

^{13}C-NMR (CDCl$_3$):

δ22.1 (C1, methyl carbon), δ36 (C2, methylene carbon), δ41 (C3, methyne carbons in the polymer backbone and the isopropyl group), δ 173 (C4, carboxyl carbon).
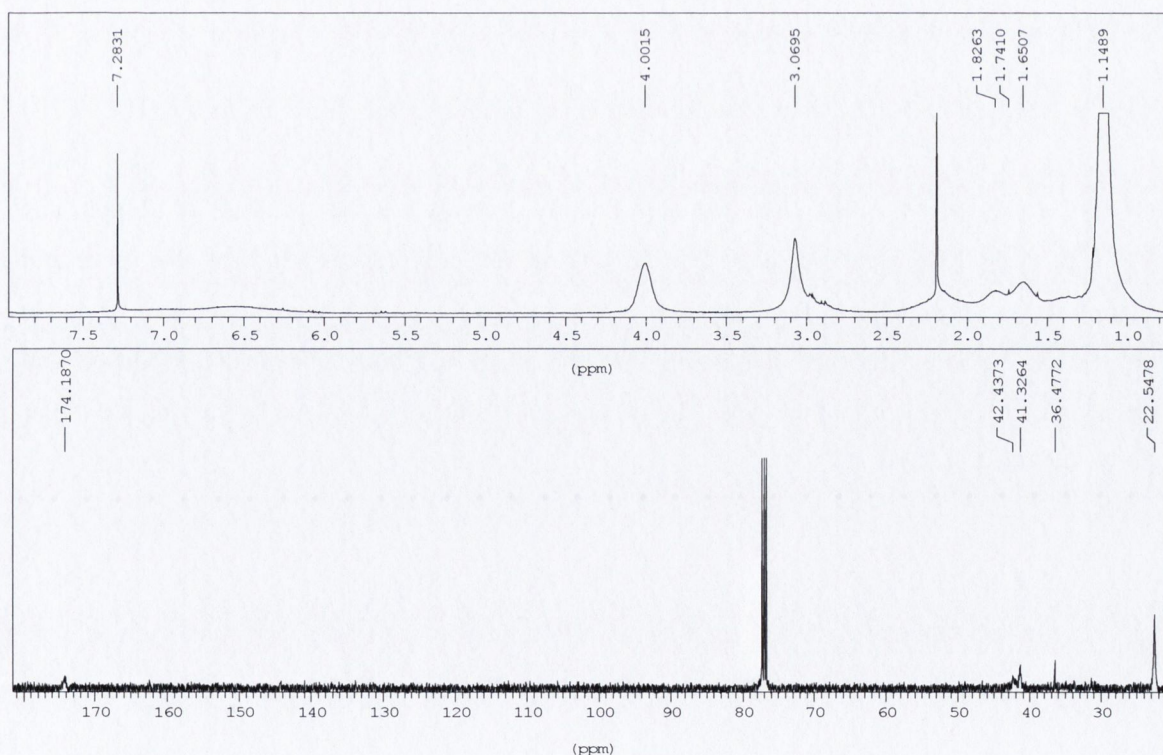
Figure 4.5: ^{1}H-NMR (top) and the ^{13}C-NMR (bottom) spectra of PNP.

The ^{1}H-NMR revealed two broad signals for the methylene proton and one for the methyne proton in the vicinity of the strong methyl signal at $\delta 1.14$ppm. This broadening of ^{1}H signals can be attributed to a distribution of PNIPAAM chain conformations, which are somewhat fixed due to the lack of mobility. The ^{13}C-NMR spectrum showed a multiplet at $\delta 41$ representive of methyne carbon resonance. This could be due to both the different tacticities of the side chain onto the backbone methyne carbon and environment change around the methyne with increasing temperature (Tokuhiro et al., 1991).

PNP-L2$_{-2}$ (CDCl$_3$):

^{1}H-NMR (CDCl$_3$) :

$\delta 1.14$ (CH$_3$ on isopropyl group of PNIPAAM), $\delta 1.50$ (CH$_2$ on PNIPAAM) $\delta 1.58$ (CH$_3$ on PLA) $\delta 1.91$(-CH on PNIPAAM), $\delta 3.97$ (NH on PNIPAAM), $\delta 5.16$ (-CH on PLA).

^{13}C-NMR (CDCl$_3$):

$\delta 16.12$ (CH3 on PLLA), $\delta 22.5$ (methyl carbon on the isopropyl group of PNIPAAM), $\delta 68$ (methylene carbon of PLA). $\delta 169$ (carboxyl carbon).

The ^{1}H-NMR of PNP-L2$_{-2}$ showed a decrease in the proton signals from 5.6 to 6.2 (H$_2$C=CH-) indicative of the integration of PLA into the backbone of the polymer. The double bonds (H$_2$C=CH-) in the ^{13}C-NMR were also significantly decreased in the spectrum at 125ppm and 130ppm. Acid base titrations were carried out on the polymers to confirm the successful incorporation of PLA in to the backbone of the hydrogels as described in section 3.3.4. No colour change was observed indicating that the PLA had been chemically modified and chemically incorporated into the gels. The various gel systems synthesized by varying the molar ratios are listed in Table 4.2.

(A)
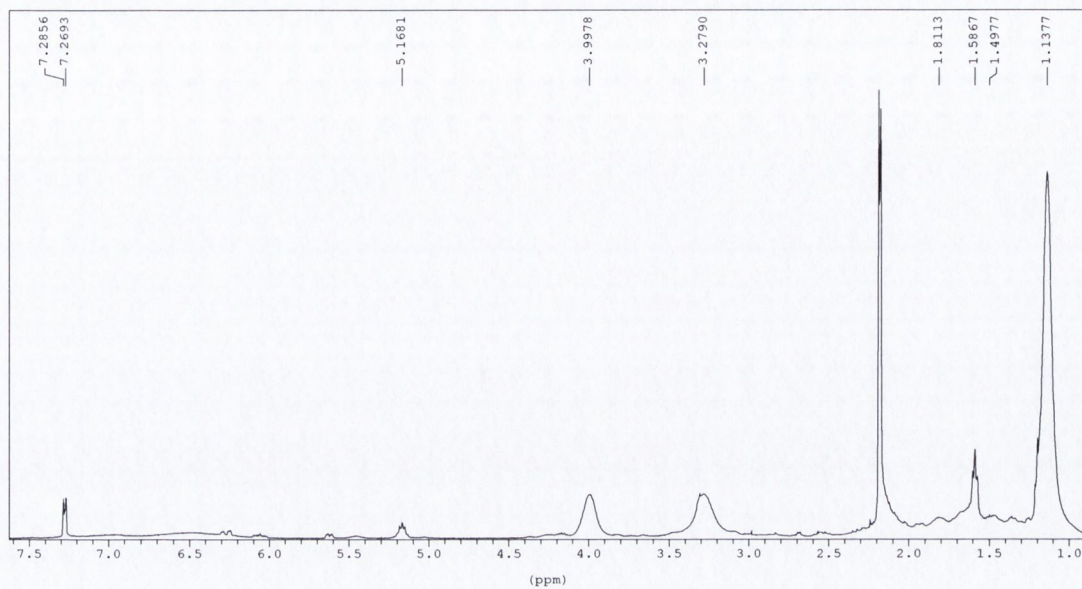
(B)
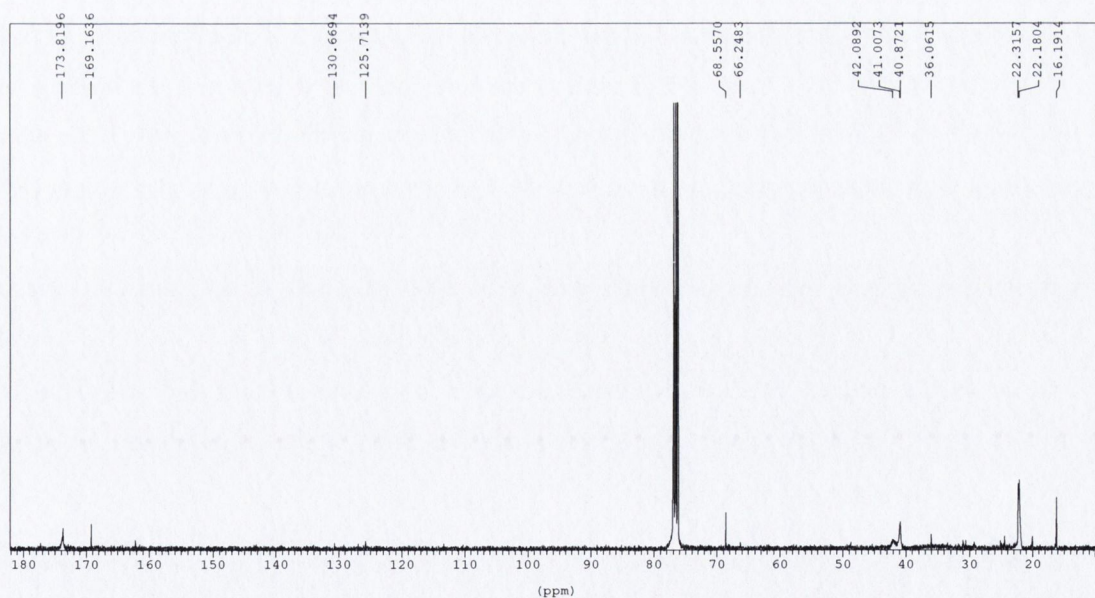
Figure 4.6: (a) ^{1}H-NMR and (b) ^{13}C-NMR spectra of PNP-L2$_{-2}$.

4.3.3 Molecular weight

Seven batches of linear polymers were synthesised (PNP-L, PNP-L1$_{-2}$, PNP-L2$_{-2}$, PNP-L3$_{-2}$, PNP-L1$_{-12}$, PNP-L2$_{-12}$ and PNP-L3$_{-12}$) and their molecular weights determined by gel permeation chromatography (GPC) as described in Section 3.3. The results are shown in Table 4.2 below.

Table 4.2: Comparison of properties of PNIPAAM based linear polymers

transition	Molar ratio PNP/PLA	(%w/w) ratio	Molecular weight($\times 10^4$)	Glass transition temperature (^{o}C)	Phase temperature
PNP (100)	100	100-0	2.01	110.92	28.4
PNP-L1$_{-2}$	93-7	84-16	1.52	107	28.5
PNP-L2$_{-2}$	86-14	76-24	1.09	90.59	29.5
PNP-L3$_{-2}$	72-28	56-44	0.87	86.95	32.5
PNP-L1$_{-12}$	93-7	84-16	2.0	112.16	29.2
PNP-L2$_{-12}$	86-14	76-24	1.50	106.75	33.4
PNP-L3$_{-12}$	72-28	56-44	1.42	102.92	34.2

Altering the molar ratio of reactants and the molecular weight of the precursor unit, PLA, led to a significant difference ($p<0.05$) between the molar weight of the batches of polymers. There was an observed decrease in molecular weight as the amount of PLA increased. Increasing the molecular weight of the pre-precursor PLA increased the overall molecular weight of the co-polymers, however a noted decrease in the molecular weight was still observed as the percent of PLA increased. The glass transition of each of the polymers was determined at a heating rate of 10°C/min. The Tg obtained for the linear poly (N-isopropylacrylamide) was 100.92^{o}C, which is consistent with values reported in literature as 85-130°C dependent on molecular weight (Rosen, 1993). The molecular weights and Tgs tabulated above were plotted against one another and an increasing trend was seen for the series with MW 2000 PLA ($R^2=0.911$) and the series with MW 12000 PLA ($R^2=0.905$) (Figure 4.7 (b)). From the data above it is evident that overall an increase in the percent of PLA decreases the glass transition (Figure 4.7 (a)). This is not surprising, since aliphatic spacers bring side chain flexibility to the co-polymers, lowering the Tg (Salgado-Rodriguez et al., (2004)).

In addition, as the molecular weight of the linear polymers increases, it's expected that the Tgs for the polymers become closer to one another, due to the fact that the chain entanglements which increase with molecular weight diminishes dramatically their mobility. That is, a higher temperature is needed to promote chain mobility, characterizing the glass transition. Figure 4.7 (a) shows the plotted results of the Tg against the amount PLA in the co-polymer systems.

(a)

(b)
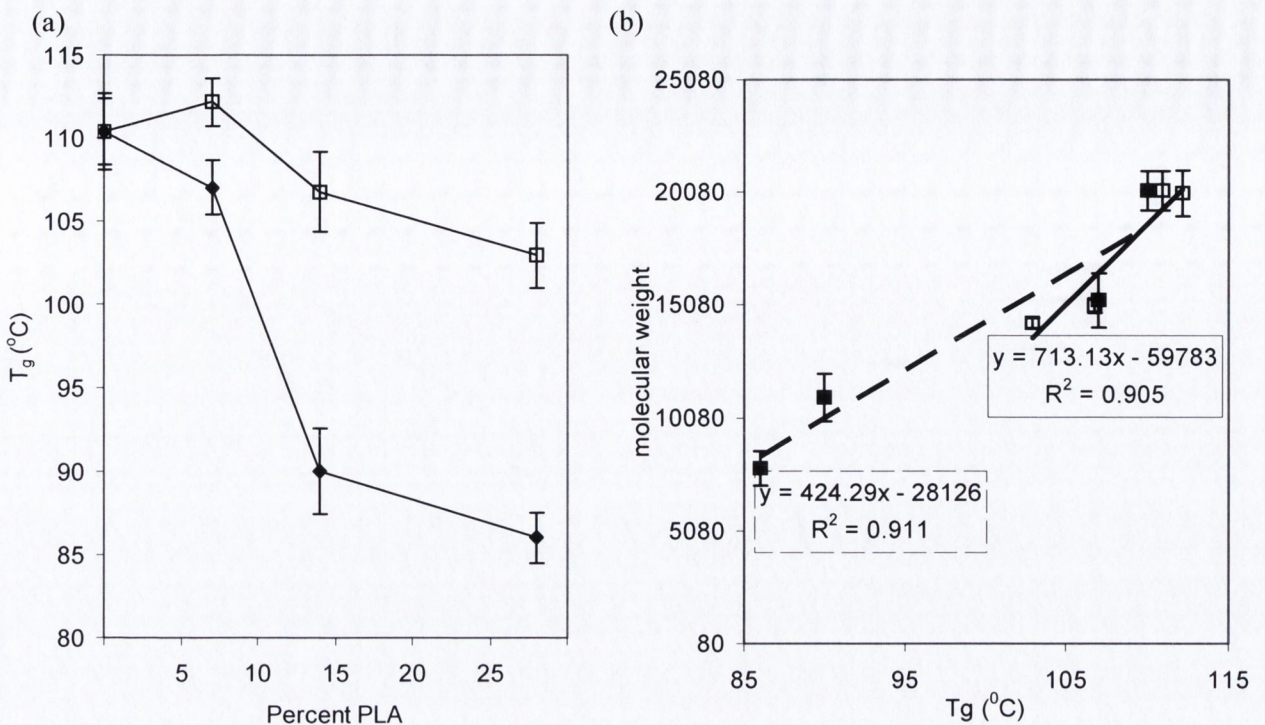
Fig 4.7 (a): Relationship between PLA content and the Glass transition temperature (Tg) (^{o}C) for polymers MW2000 (■) and polymers MW 12000 (□) and (b): the relationship between the glass transition temperature and the molecular weight for polymers MW2000 (■) and polymers MW 12000 (□).

4.3.4   LOWER CRITICAL SOLUTION TEMPERATURE

The lower critical solution temperature in PB of the synthesised polymers was determined by differential scanning calorimetry (DSC) and by measuring the transmittance of a polymer solution at various temperatures as described in Section 3.3.6.

4.3.4.1 Differential Scanning calorimetry (DSC)

DSC analysis of the linear polymer solutions resulted in a distinct endotherm at the lower critical solution temperature due the precipitation of the polymer at that temperature (Figure 4.8 (a)).
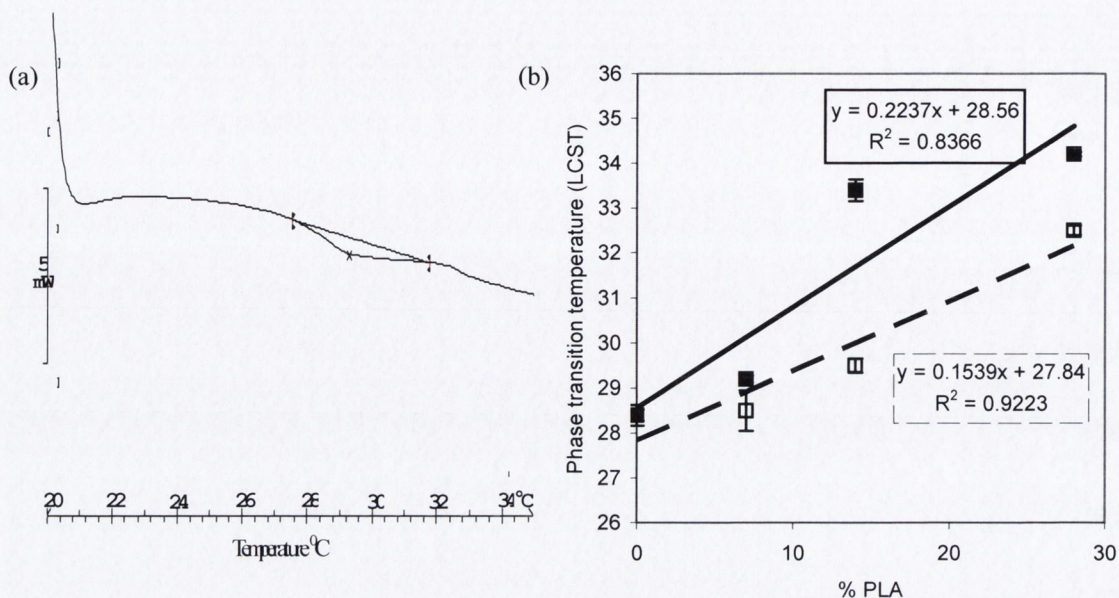
Figure 4.8:(a) DSC thermogram of a 0.5% w/v solution of PNP-L2$_{-2}$ in PB at a heating rate of 2°C/min. (b) relationship between the hydrogel composition and the LCST where (■) signifies PLA MW 12000 and (□) signifies PLA MW 2000 incorporated into the hydrogel.

There was a significant increase ($p < 0.05$) in the phase transition temperature on increasing PLA content. The increase in peak position, on increasing PLA content, would suggest that PLA increased the overall hydrophilicity of the systems also shown by an increase in the LCSTs (Table 4.2). In the case of the PLA co-monomers having free acid groups, a more hydrophobic co-monomer structure was expected. Schild, (1992) in his review on NIPAAM polymers discussed whether it is hydrogen bonding or hydrophobic effects that influence the LCST. Based on the current work; an increase in the LCST could be explained in terms of hydrogen bonding since ester groups along the PLA chain are polar or weakly charged. This would lead to additional polymer-water interactions as opposed to polymer-polymer interactions leading to a reduced driving force for a phase transition. This leads to an increase in the LCST, since the hydrophobic interactions, which increase with temperature, are compensated for up to a higher temperature due to increased polymer-water interactions. Therefore the phase transition temperature is determined by relative hydrophilicity of the polymer, whereby the polar ester groups are increasing the hydrophilicity; (Feil et al., 1992; Beltran et al., 1991; Peppas and Khare, 1993). An upward trend existed between the percent of PLA in the hydrogel system and the LCST with an R^2 value of 0.9223 and 0.8366 for the hydrogel series with PLA MW 2000 and 12000 respectively (Figure 4.8 (b)).

4.3.4.2 TRANSMITTANCE

The phase transition temperature of the linear polymer systems were also examined by measuring the transmittance of the polymer solution at 500nm at different temperatures. At temperatures below the LCST the solution remained clear, while at a certain temperature (cloud point, LCST) the polymer precipitated out of solution and the transmittance decreased dramatically (Figure 4.9). The LCST was defined as 50% transmittance of the polymer solution during the heating process.
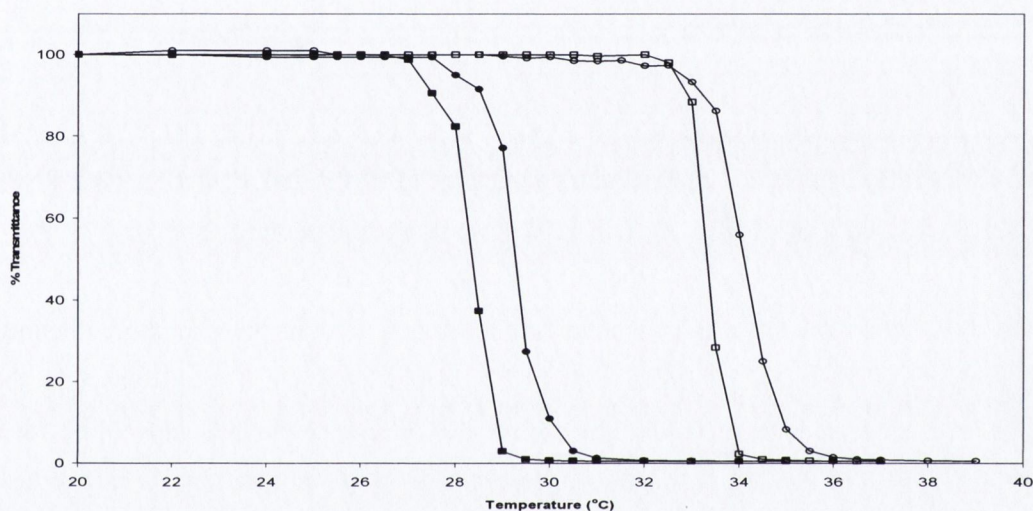
Fig 4.9: Percentage transmittance of PNP in water □ and PB■ and PNP-L2$_{-2}$ in water (○) and PB (●) at various temperatures.

The effect of buffer on the LCST as well as incorporating PLA into the polymer network was examined and can be seen in Figure 4.9. The effect of the buffer salts was to decrease the phase transition temperature of both polymer systems. The phase transition decreased from 33.3 to 28.4 and 34.1 to 29.5 for PNP and PNP2$_{-2}$ respectively. Saito et al., (1992) and Eeckman et al., (2001) showed a similar decrease in the LCST of thermoresponsive polymers with various salt types. This was attributed to the ability of the salt anions to break the hydrogen layer around the polymer chains.

It can be noted that the homo-polymer PNIPAAM had a sharp decrease in transmittance once the LCST was reached (Figure 4.10). The higher the amount of PLA incorporated into the backbone of the hydrogel the slower and more gradual the decline in transmittance. On increasing the molecular weight of PLA this effect was less pronounced. A linear correlation existed between the percent of PLA in the hydrogel system and the LCST with an R^2 value of 0.9136 and 0.9743 for the hydrogel series with MW 2000 and 12000 respectively (Figure 4.11).
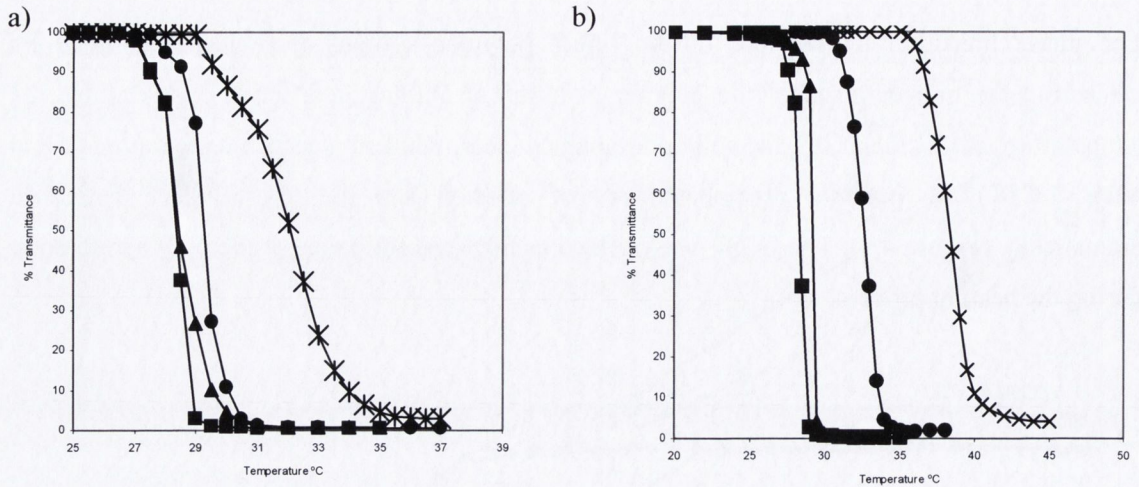
Figure 4.10: a) Percent transmittance of PNP-L (■), PNP-L1$_{-2}$ (▲), PNP-L2$_{-2}$ (●), PNP-L3$_{-2}$ (x) in PB at various temperatures and b) Percent transmittance of PNP-L (■), PNP-L1$_{-12}$ (▲), PNP-L2$_{-12}$ (●), PNP-L3$_{-12}$ (x) in PB at various temperatures.

The values obtained for the lower critical solution temperature were higher than those obtained by DSC particularly for linear polymers with PNP3 system hydrogel. The difference in the results obtained between both methods may reflect the differences in heating/cooling rates (*Otake et al., 1990*). The use of transmittance measurements is complicated by the rate of heat transfer in the larger volumes used as well as variations in precipitated aggregates, sizes and settling of precipitates (*Schild and Tirrell, 1990*).
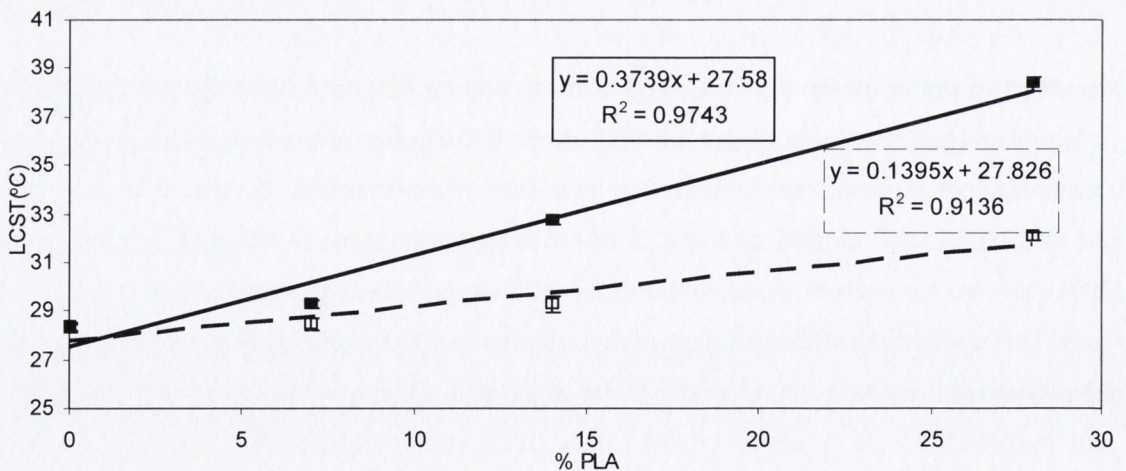
Figure 4.11: Relationship between the LCST and hydrogel composition where the hydrogels composed of MW 12000 PLA are represented by the closed symbol (■) and MW 2000 PLA by the open symbol (□).

4.4 HYDROGEL CHARACTERISATION

A series of poly (N-isopropylacrylamide) and poly L-lactic acid (PLA) based hydrogels were synthesised, each with a different percent of the hydrophobic lactic acid and a fixed amount of cross-linker as described in Section 3.2. The effect of the molecular weight of the PLA component and molar ratio was examined and the measured glass transition temperature (T_g) of the systems are listed below.

Table 4.3: Percent PLA incorporated into the gels and glass transition temperature of PNIPAAM-PLA based hydrogels.

Hydrogel	%PLA	PNIPAAM-PLA (w/w)	$T_g(^{\circ}C)$
PNIPAAM	0	100-0	122.00
PNP1$_{-2}$	7	86-14	116.59
PNP2$_{-2}$	14	74-26	111.28
PNP3$_{-2}$	28	56-44	103.23
PNP1$_{-12}$	7	86-14	148.00
PNP2$_{-12}$	14	74-26	148.00
PNP3$_{-12}$	28	56-44	141.14

The glass transition temperature obtained for the homopolymer PNIPAAM was 122.84°C, which is higher than the one obtained for the linear polymer. As reported in literature linear poly (N-isopropylacrylamide) has a glass transition temperature in the region of 85-130°C probably depending on molecular weight. This increase can be understood as a result of cross-linking, which significantly lowers the mobility of the chains and thus a higher temperature is needed to promote mobility, characterizing the glass transition (Sousa et al., 1998). By analyzing the results summarized in Table 4.3, it can be noted that similarly to the linear polymers, the co-polymers (PNP-co-PLA) exhibit lower T_g on increasing the percent PLA in the gel. There was a direct linear relationship (R^2=0.9909) between the glass transition temperature and the percent PLA in the gel for the systems with PLA MW2000. The mechanical strength of the hydrogel can also be improved by increasing the degree of cross-linking (Johnson et al., 2004) or by co-polymerization with PLA. The resultant gels synthesized after polymerization with PLA present were easier to handle and fairly robust while PNP was fragile (Figure 4.16). The effect of PLA on the crosslinking density will be discussed in Section 4.4.5.

4.4.1 Equilibrium swelling studies

The swelling of the hydrogels were characterised using the swelling ratio (EQN. 2.7). In the case of the hydrogels with PLA MW 2000, the equilibrium-swelling ratio of each system was examined over a range of temperatures in PB (Figure 4.12). The phase transition based on the swelling data (LCST$_s$) was defined as the temperature at which the hydrogel showed a significant increase in swelling from the baseline.

The thermoresponsive study demonstrated that the swelling ratios of all hydrogels systems were dependent on the co-polymer composition. The phase transition temperature of the co-polymer networks increased on increasing the PLA content. However the degree of change in the equilibrium-swelling ratio with temperature change became less sharp as the molar portion of PNIPAAM decreased and that of the PLA increased. PNP1$_{-2}$ showed a phase transition of 29^0C. In literature the phase transition in water is reported within the range (32^0C -34^0C) (Schild 1992). Other authors have noted a marked decrease in the phase transition temperature of the hydrogel due to the effect of buffer salts (salting out effect). Similar observations were observed on the linear systems, described using transmittance measurements (Section 4.3.4).
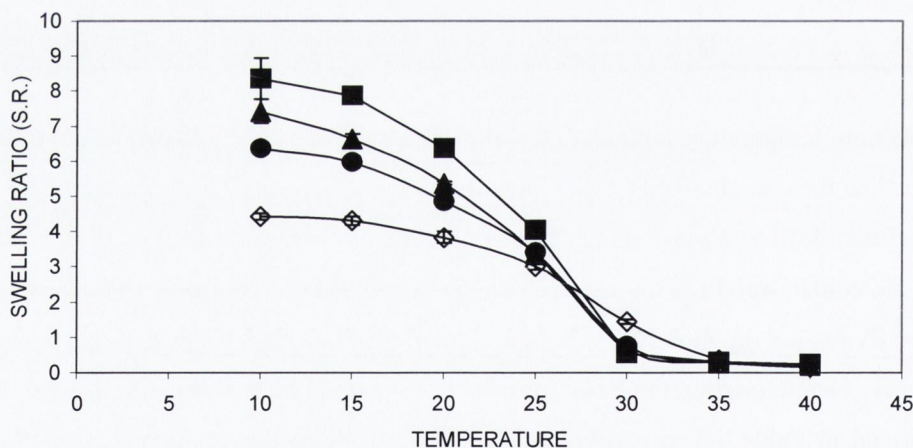
Figure 4.12: Equilibrium swelling ratio of PNP based hydrogels (PNP (■), PNP1$_{-2}$ (▲), PNP2$_{-2}$ (●) and PNP3$_{-2}$ (◊)) in PB at various temperatures with PLA MW 2000 incorporated into hydrogel networks.

The equilibrium swelling of the above hydrogel systems were dependent on their composition both above (37°C) and below (20°C) the phase transition temperature. The equilibrium-swelling ratio of the hydrogel systems with PLA MW 2000 incorporated into the backbone is shown below and above the LCST at 20°C and 37°C respectively in Figure 4.13(a). The swelling ratio below the LCST (20°C) of the PNP-PLA$_{-2}$ hydrogels depended on the hydrophobicity of the

PLA component. The hydrogels expanded from 5.8 to 8 times their volume depending on the amount of PLA incorporated into the backbone of the polymer network. As the PLA component increased, a more significant (p<0.05) suppression in the swelling ratio was observed leading to a more compact structure. A trend emerged (R^2= 0.923) between the amount of hydrophobic PLA and the swelling ratio (Figure4.13 (b)).

Above the LCST (37°C), due to the hydrophobic nature of PNIPAAM, the equilibrium-swelling ratio was significantly smaller than at 20°C. There was no statistical difference (p>0.05) between PNP2$_{-2}$ and PNP3$_{-2}$ swelling levels at this temperature. The magnitude of swelling change between the two temperatures decreased with increasing the percent of PLA. The incorporation of PLA therefore influenced the equilibrium swelling at both temperatures. An upward trend was seen in the swelling ratio with increasing PLA content.

(a)   (b)
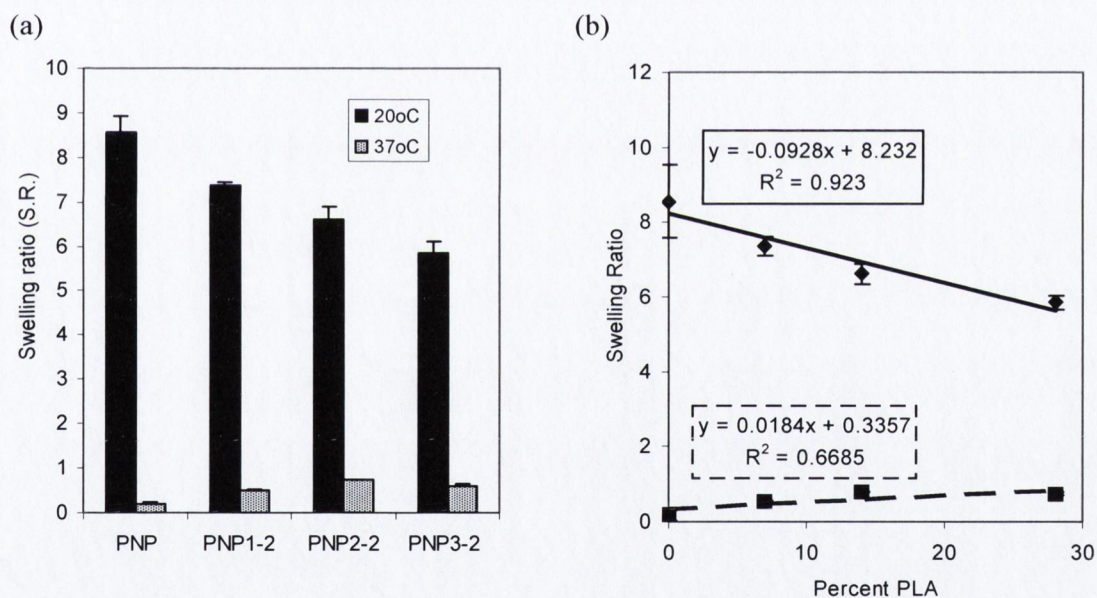
Figure 4.13 (a) Equilibrium swelling ratio of the hydrogels at 20°C and 37°C in PB (b) relationship between equilibrium swelling ratio at 20°C (♦) and 37°C (■) and % PLA (MW2000) present in the network systems.

In this study, we observed that the effect of the equilibrium-swelling ratio of the PNIPAAM-PLA based hydrogels was affected by the molar ratio of constituents. The extent of the swelling was also dependent on the MW of PLA incorporated into the backbone of the hydrogel. Increasing the molecular weight of PLA resulted in a significant increase (p<0.05) in the swelling ratio both below and above the phase transition temperature (Figure 4.14(a)).

At 20°C an increase in the MW of PLA (from 2000 to 12000) resulted in 34%, 55% and 65% increase in the swelling ratios of 93-7, 86-14 and 72-28 NIPAAM-PLA respectively. Since the cross-linking sites are at the two chain ends of PLA macromolecule an increase in the MW of PLA would reduce the overall total number of end groups available for cross-linking leading to a lower cross-linking density. Thus, a lower degree of cross-linking should lead to a more open and less compact 3D network structure and hence a higher swelling ratio. The MW effect was composition dependent whereby an increase in PLA appeared to increase the equilibrium-swelling ratio.

Above the LCST a significant increase of 20%, 55% and 85% were observed in the swelling ratios of 93-7, 86-14 and 72-28 PNP-PLA$_{-12}$ co-polymers respectively. An increasing trend was seen between the PLA content and the equilibrium-swelling ratio both below and above the LCST (Figure 4.14(b)).

(a)   (b)
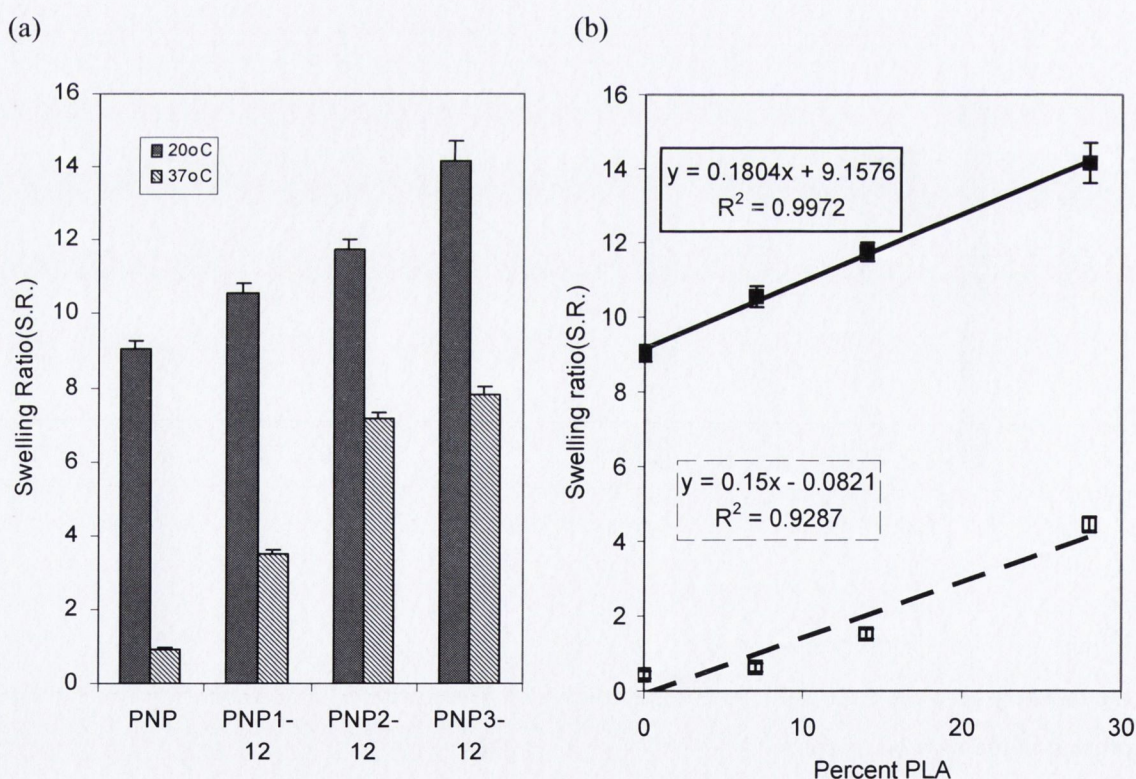
Figure 4.14: (a) Equilibrium swelling ratio of the hydrogels (PNP-PLA$_{-12}$) at 20°C and 37°C in PB. (b) Relationship between equilibrium swelling ratio at 20°C (■) and 37°C (□) and % PLA (MW12000) present in the network systems.

4.4.2 Phase transition temperature

The phase transition temperature of the PNIPAAM-co-PLA gels, which were determined in phosphate buffer 7.4 by DSC analysis are shown in Table 4.4. In the case of the hydrogels, a sample of the swollen hydrogel (20°C) was scanned at 2°C/min in a sealed pan.

In the case of both PNIPAAM-co-PLA gels with PLA MW 2000 (R^2=0.9841) and PLA MW 12000 (R^2=0.9377), there was a linear increase in the endotherm peak position as the % of PLA increased. Adjusting the relative hydrophobicity controlled the LCST of the thermoresponsive gels. PLA has an effect of raising the LCST and the effect became more prominent the higher the molar feed ratio of PLA. This conclusive pattern is also evident with the onset of the endotherm where similarly a linear correlation was observed between the LCST and the amount of PLA incorporated into each hydrogel system for both polymeric systems containing PLA MW 2000 (R^2=0.985) and PLA MW 12000 (R^2=0.9621). The increase in the peak positions indicated that the chemical nature of PLA had a hydrophilic effect on the phase transition temperature as similarly seen in Section 4.3.4 with the linear polymers. An increase in the peak position of the order 0.7-3.11°C and 0.96-4.56°C was seen for PNP-co-PLA$_{-2}$ (PLA MW 2000) and PNP-co-PLA$_{-12}$ (PLA MW12000) respectively.

Table 4.4 Phase transition temperature (n=3) of PNIPAAM-co-PLA systems in PB

DSC- PB 7.4					
MW 2000	Onset (°C)	Peak (°C) (LCST$_d$)	Integral (J/g gel)	Integral (kJ/mol)	Swelling * (LCST$_s$)(°C)
PNP	27.00	28.41	0.83	1500	32
PNP-1$_{-2}$	27.39	29.11	1.32	880	33
PNP-2$_{-2}$	28.44	30.33	0.59	450	34.5
PNP-3$_{-2}$	29.89	31.52	0.60	350	36
DSC- PB 7.4					
MW 12000	Onset (°C)	Peak (°C) (LCST$_d$)	Integral (J/g gel)	Integral (kJ/mol)	Swelling * (LCST$_s$) (°C)
PNP	27.00	28.43	0.83	1500	32
PNP-1$_{-12}$	29.29	31.94	1.50	640	ND
PNP-2$_{-12}$	31.94	34.17	2.47	1200	ND
PNP-3$_{-12}$	34.56	36.69	3.94	2000	ND

* LCST as defined in Section 3.36
*ND not determined

4.4.3 Swelling kinetics

The presence of the different percentages and molecular weights of PLA not only influenced equilibrium swelling at a particular temperature, but also affected the rate of swelling at that temperature. The swelling rates of the hydrogel discs, initially in a dried out state, were examined over time at 20°C and 37°C (Figure 4.15).

At 20°C (Figure 4.15 (a)), the swelling profiles were found to be approximately proportional to the square root of time (EQN. 2.22,) (Table 4.5).

Equilibrium swelling was reached after 48hrs for PNP, however in the case of the co-polymers, a slow sluggish increase in the swelling ratio over time was seen, which may be due to degradation. A better fit was obtained in each case when the diffusional exponent (n) was allowed to vary (Table 4.5).

Table 4.5: Swelling rate constant (k_s) (Higuchi, 1961) at 20°C and 37°C with the associated coefficient of determination (CD) for polymers with molecular weight 2000 PLA incorporated into the backbone of the hydrogel. Diffusional exponent, (n) and the swelling rate constant (k_p) were estimated using EQN 2.25(Peppas, 1985).

	$M=k_s t^{0.5}$		$M=k_p t^n$		
20°C	k_{s20} x 10^2(min$^{-0.5}$)	CD	k_{p20} x 10^2 (min^{-1})	n	CD
PNP	17.44±0.0028	0.9893	9.72±0.348	0.6015±0.0060	0.9997
PNP1$_{-2}$	19.15±0.0038	0.9843	10.39±1.54	0.6062±0.0253	0.9957
PNP2$_{-2}$	14.90±0.0023	0.9899	10.05±1.53	0.5658±0.0256	0.9950
PNP3$_{-2}$	14.51±0.0032	0.9815	6.52±0.217	0.6389±0.0055	0.9998
37°C	k_{s37} x 10^2 (min$^{-0.5}$)	CD	k_{p37} x 10^2 (min^{-1})	n	CD
PNP	1.34±0.0005	0.9840	2.90±0.183	0.3407±0.0394	0.9997
PNP1$_{-2}$	1.88±0.0004	0.9843	3.32±0.356	0.3967±0.0200	0.9974
PNP2$_{-2}$	2.52±0.0005	0.9779	4.90±0.409	0.3816±0.0126	0.9979
PNP3$_{-2}$	3.47±0.0009	0.9922	5.57±1.140	0.4030±0.0424	0.9978
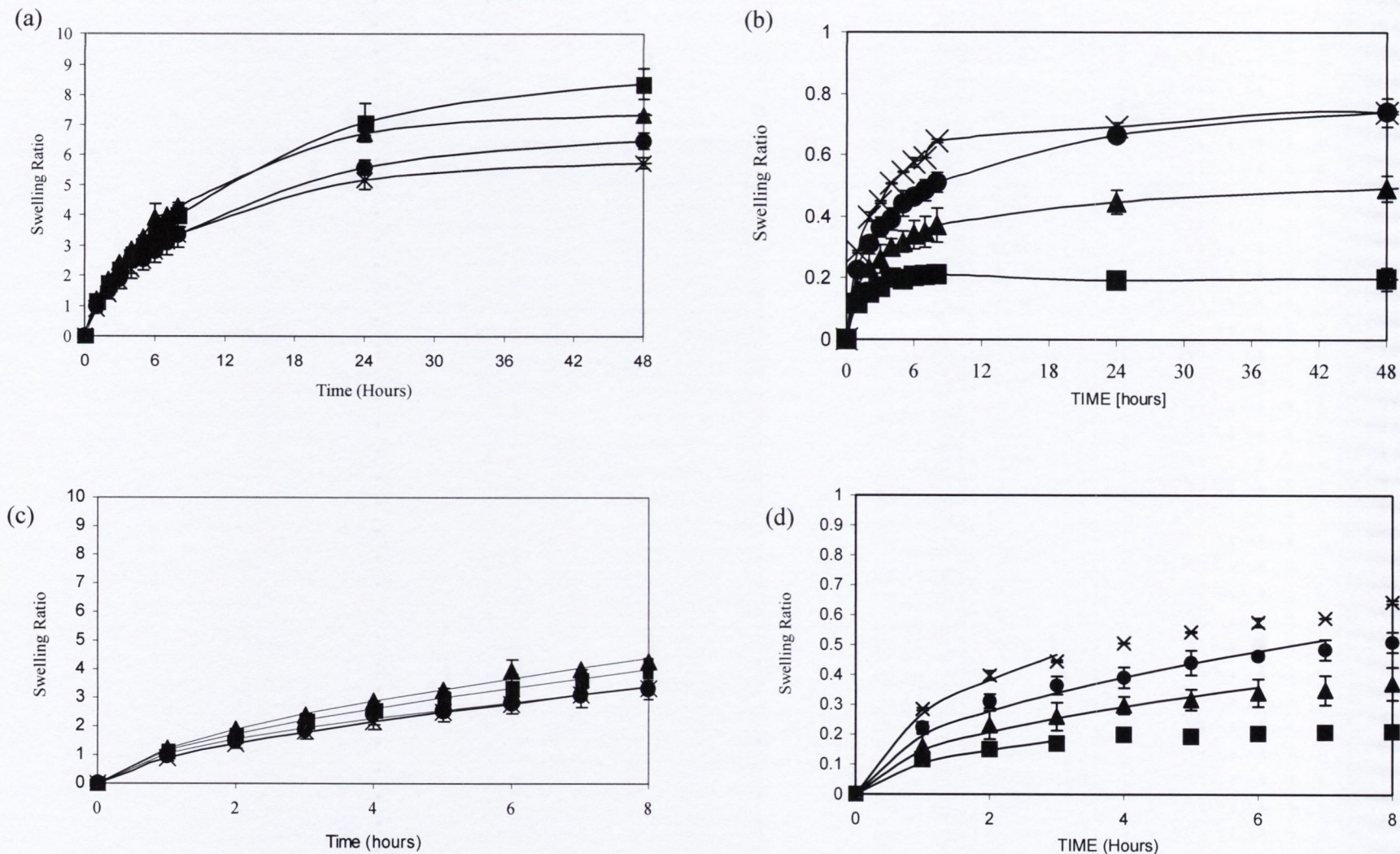
Figure 4.15: Swelling kinetics of PNP (■), PNP1-2 (▲), PNP2-2 (●) and PNP3-2 (x) over time at (a) 20°C and (b) 37°C in PB. Also shown are the early time periods (S.R.<60% of equilibrium) at (c) 20°C and (d) 37°C fitted to the square root of time (EQN. 2.22, Higuchi, 1961).

In the case of the gels with PLA MW 2000 a decrease in the swelling rate at 20°C with an increase in the incorporation of the PLA moiety would be expected since PLA is hydrophobic; the equilibrium swelling capacity of the hydrogels would be expected to decrease as the percent of PLA increased. However, in the early time (up to 60% swelling), the swelling rate constant of PNP1$_{-2}$ appeared to deviate from the trend. However late time swelling showed a significant decrease in the swelling kinetics for the co-polymer systems ($p<0.05$) with an increase in the hydrophobic monomer content. Similarly Xue et al., (2002) synthesised PNIPAAM gels with hydrophobic co-monomers ranging in chain length. The increased hydrophobicity led to a decrease in the rate of water uptake and swelling ratio.

From Photographs in Figure 4.16 it can be clearly noted that as the PLA concentration increased the swelling decreased as the hydrophobic moiety makes it more difficult for water to penetrate the gel. This is reflected in the values estimated for the rate of water uptake at 20°C, which ranged from 19.15×10^{2} (min$^{-0.5}$) to 14.51×10^{2} (min$^{-0.5}$).
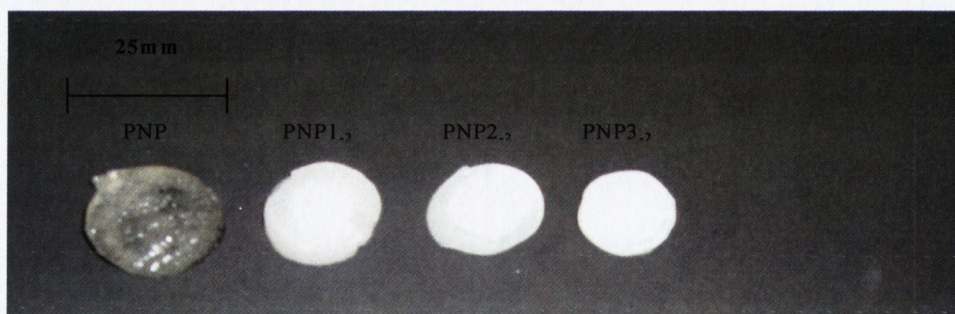
Fig 4.16:Photographs of PNP, PNP1$_{-2}$, PNP2$_{-2}$ and PNP3$_{-2}$ at equilibrium swelling at 20°C

Above the LCST, there was a linear relationship between the swelling rate constant and the percent of PLA (MW 2000) present in the hydrogel (Figure 4.17). The extent of swelling was considerably less in comparison to swelling studies undertaken at 20°C. However a significant increase ($p<0.05$) was observed in the rate of swelling as PLA content increased with $R^{2}=0.9957$.
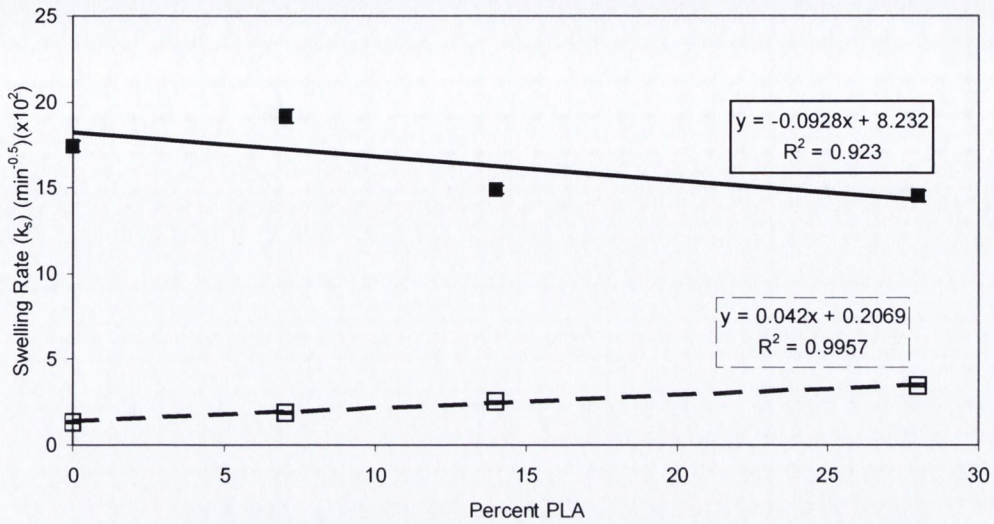
Figure 4.17: Plot of swelling rate constant at 20°C (■) and 37°C (□) and the percent of PLA (MW 2000) present in the hydrogel series PNP-PLA$_{-2}$.

The effect of the composition of the hydrogels played an important role, on the diffusional exponents and the surface area of the hydrogels, which in turn influenced the rate of swelling and the equilibrium-swelling ratio. Table 4.6 displays the swelling rate constants at 20°C and 37°C with the associated coefficient of determination (CD) for polymers with PLA MW 12000 incorporated in the backbone of the hydrogel.

Table 4.6: Swelling rate constant (k_s) (Higuchi, 1961) at 20°C and 37°C with the associated coefficient of determination (CD) for polymers with PLA molecular weight 12000 incorporated in the backbone of the hydrogel. Also the diffusional exponents, (n) and swelling rate constant (k_p) were estimated using Equation 2.25 (Peppas, 1985).

	$M = k_s t^{0.5}$		$M = k_p t^n$		
20°C	$k_{s20} \times 10^2$ (min$^{-0.5}$)	CD	$k_{p20} \times 10^2$ (min^{-1})	n	CD
PNP1$_{-12}$	29.30±0.0037	0.9942	21.41±0.896	0.5146±0.0275	0.9945
PNP2$_{-12}$	42.17±0.0032	0.9986	37.22±3.170	0.5234±0.0165	0.9991
PNP3$_{-12}$	55.49±0.0074	0.9971	41.80±4.040	0.5552±0.0186	0.9992
37°C	$k_{s37} \times 10^2$ (min$^{-0.5}$)	CD	$k_{p37} \times 10^2$ (min^{-1})	n	CD
PNP1$_{-12}$	3.68±0.0032	0.9085	22.08±0.76	0.1356±0.0149	0.9994
PNP2$_{-12}$	7.75±0.0045	0.9602	25.17±4.95	0.2575±0.0408	0.9976
PNP3$_{-12}$	19.88±0.0011	0.9996	20.03±1.82	0.4983±0.0182	0.9996

The effect of the MW of PLA component on the rate of swelling had the reverse effect to that of the smaller MW. A significant increase ($p<0.05$) in the rate of swelling was seen as the molar ratio of PLA increased. The composition dependant MW effect on the swelling kinetics can be attributed to cross-linking density and the hydrophobicity/hydrophilicility balance of the gels (Section 4.4.5). For example an increase in MW of PLA resulted in a 17% reduction or 46% increase in the swelling ratios of PNP3$_{-2}$ and PNP3$_{-12}$ in comparison to PNP. Such a swelling behaviour came from the density of the cross-linkable groups, which decreased as the MW increased. These results can be noted in Figure 4.18 where an increase in the swelling is observed on increasing the PLA content. This is reflected in the values estimated for the rate of water uptake at 20°C, which ranged from 29.30 x 10^{-2} (min$^{-0.5}$) to 55.49 x 10^{-2} (min$^{-0.5}$).
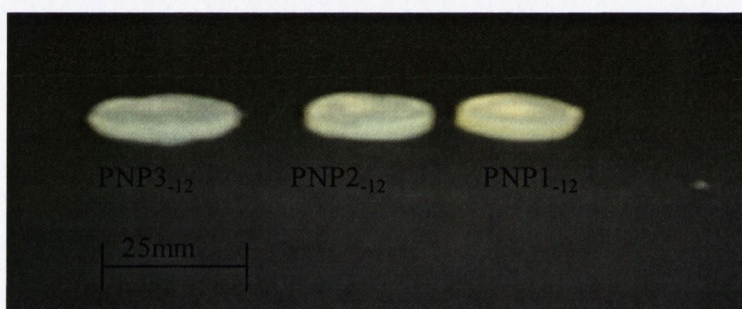
Figure 4.18: Photographs of PNP1$_{-12}$, PNP2$_{-12}$ and PNP3$_{-12}$ at equilibrium swelling at 20°C.

Cruise et al., (1998) prepared hydrogels from poly (ethylene glycol) (PEG) diacrylate precursor with different MW. They observed an increase in pore size with an increase in MW. This result is consistent with present findings; a more open gel structure could be obtained from a higher MW precursor having cross-linkable group at chain ends. Inoue et al, (1997) grafted oligomers of methyl methacrylate(OMMA) onto the backbone of the grafted PAAc hydrogels. They found that the rate of swelling of the gels was directly related to the MW of OMMA, the hydrophobic segment. Figure 4.19 (a-d) displays the swelling profiles at 20°C and 37°C for gel series with MW 12000 PLA incorporated into the gel. All systems gave a reasonable fit to the Higuchi (1961) equation. A linear correlation existed between the percent of PLA and the swelling rate constant both below and above the LCST (Figure 4.20).

92
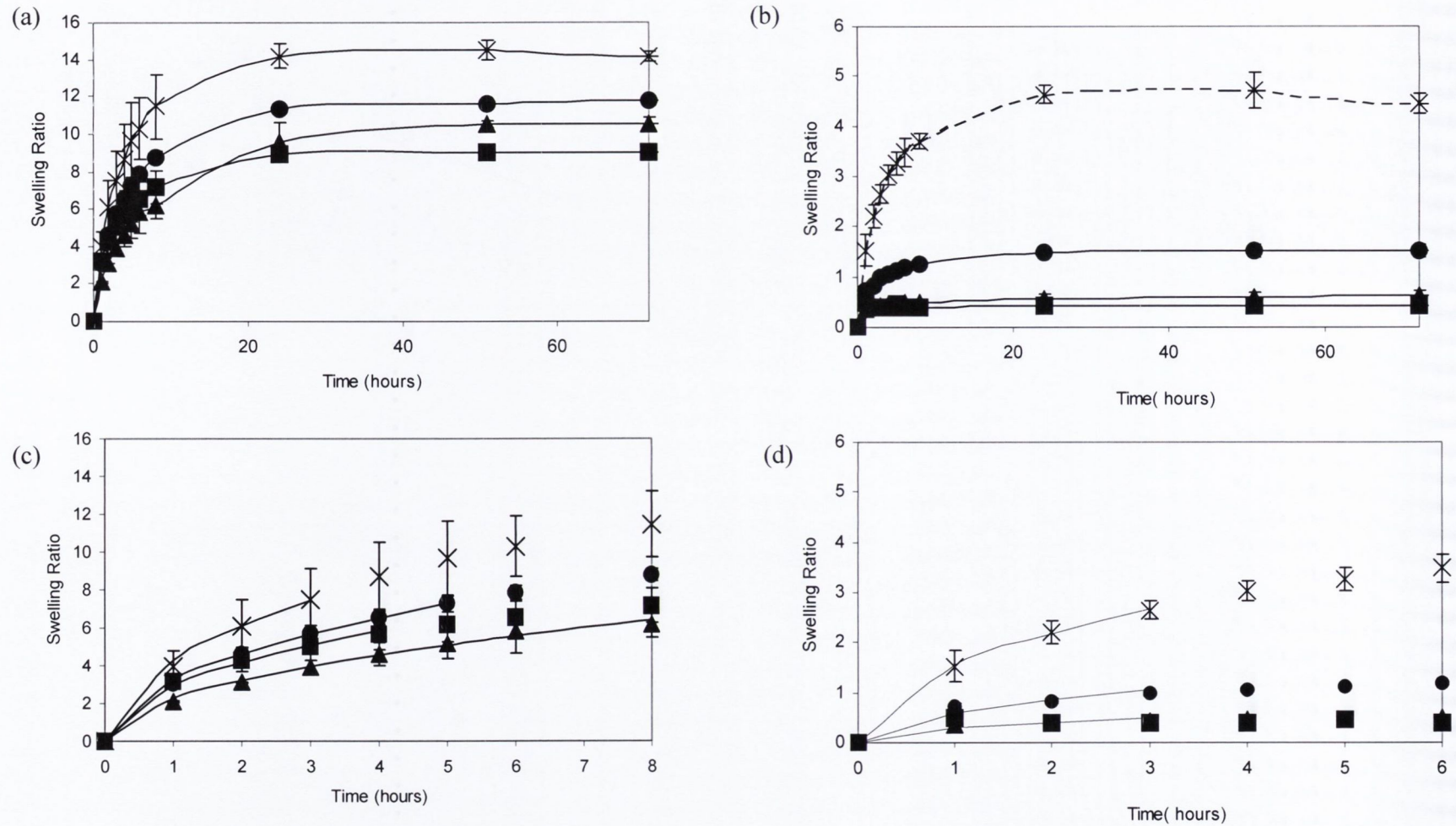
Figure 4.19: Swelling profiles of the hydrogel series with PLA MW 12000 at (a) 20 and (b) 37°C. Also shown are early time periods fitted to the square root of time (Equation 2.22 Higuchi, 1961) at (c) 20°C and (d) 37°C where (■) is PNP (▲) is PNP1$_{-12}$ (●) is PNP2$_{-12}$ and (x) is PNP3$_{-12..}$
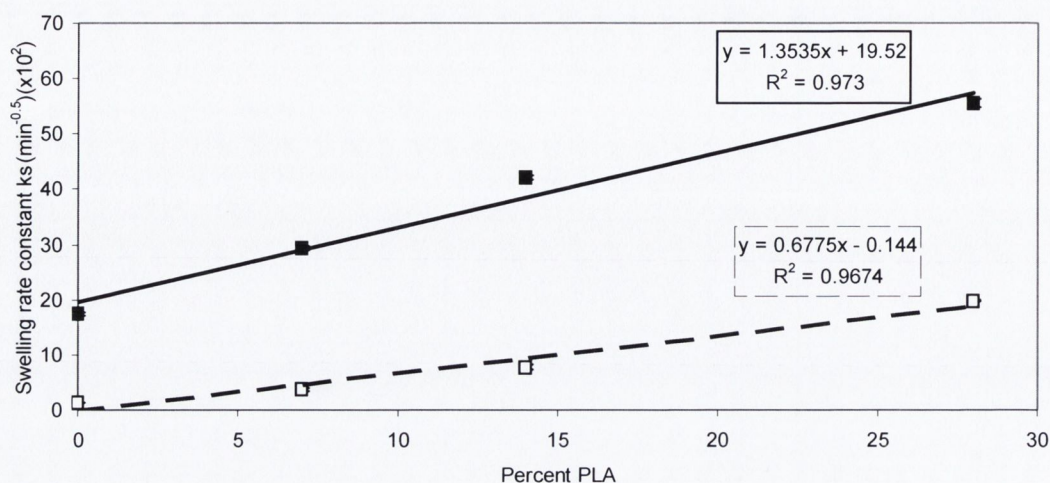
Figure 4.20: Relationship between PLA content and the swelling rate constant (k_s) for the hydrogels synthesised with MW 12000 PLA at (■) 20°C and (□) 37°C.

For all systems examined, a decrease was observed in the surface area the higher the PLA content which would be expected as a result of the relative hydrophobicity of PLA to that of PNIPAAM (Figure 4.21(a)). Incorporating the higher MW PLA further increased the surface area (Figure 4.21(a) as result of a lower crosslinking density. These results in turn influenced the swelling rate of medium into the gel and a trend was visible for all hydrogels examined (Figure 4.21(b)).
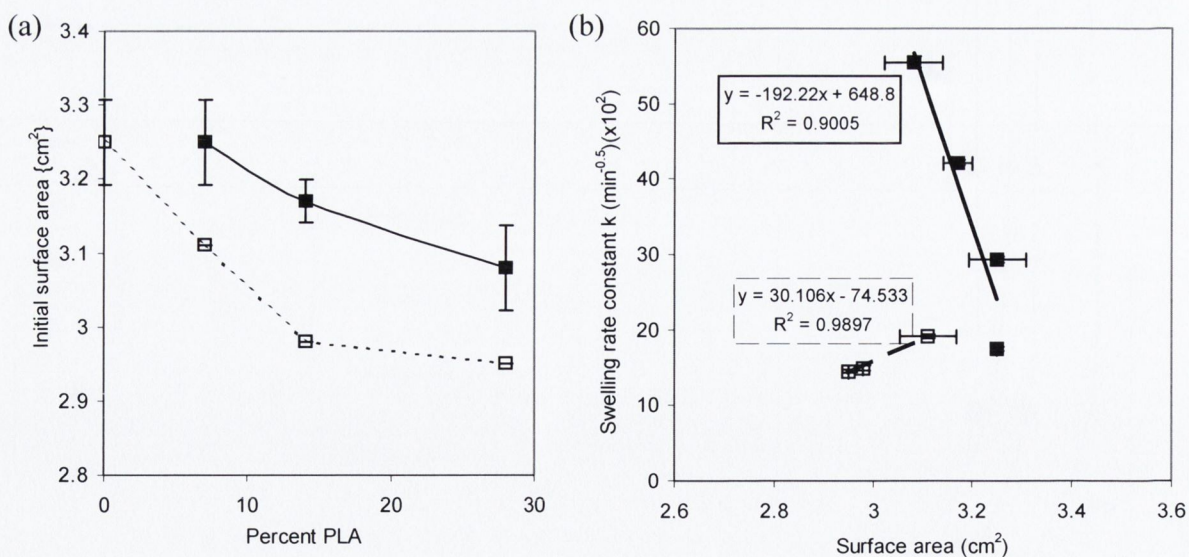
Figure 4.21: (a) relationship between polymer composition and the surface area of the hydrogels for PNP-PLA$_{-2}$ (□) and PNP-PLA$_{-12}$ series (■).(b): Relationship between the swelling rate and the surface area for the gels with PLA MW 12000 (■) and MW 2000 (□).

At 37°C for the gels with PLA MW 12000 the diffusional exponents in the series were <0.5 although reasonable fits were still obtained when plotted against the square root of time. There was a dramatic decrease in the rate of swelling as well as the extent of swelling for all hydrogel in comparison to the swelling kinetics at 20°C. The equilibrium level of swelling at 37°C, defined as the "equilibrium residual volume", was reached within 4 hours for the homopolymer PNP but took 48 hour for the co-polymeric systems after which a slow sluggish increase continued which may be due to degradation.

4.4.4 Swelling/deswelling kinetics with hydrogel systems with PLA MW 2000 incorporated into the backbone

Figure 4.22 shows the swelling / deswelling contraction patterns of the unloaded hydrogel discs [MW2000] (in PB) on switching the temperature between $20^{\circ}C$ and $37^{\circ}C$.

The swelling was found to be proportional to the square root of time during the first hour of swelling (k_{s1}) for each system (Table 4.7). However during the second swelling period (4-7 hrs), k_{s2} did not obey Fickian diffusion. However, a linear decrease ($R^2=0.9225$) was observed in the diffusional co-efficient with an increase in the amount of PLA present.

Table 4.7: Swelling rate constants (k_s, based on swelling ratio) and maximum contraction rates (k_{MC}) for the two swelling-contraction cycles (Figure 4.22 (a)). Also given are the diffusional exponents calculated using the power law equation (Peppas, 1985) and their associated coefficients of determination.

Hydrogel	$M=k_s t^{0.5}$		$M=k_p t^n$		
	$k_{S1}(min^{-0.5})(x10^2)$	CD	$n\pm s.d$	CD	$k_{MC1}(min^{-1})(x10^2)$
PNIPAAM	15.25±0.287	0.9938	0.4670±0.0281	0.9956	14.02
PNP1$_{-2}$	13.87±0.330	0.9857	0.4280±0.0222	0.9952	13.72
PNP2$_{-2}$	10.10±0.411	0.9538	0.3616±0.0227	0.9938	8.50
PNP3$_{-2}$	6.36±0.218	0.9679	0.3768±0.0083	0.9991	3.12
	$k_{S2}(min^{-0.5})(x10^2)$	CD	$n\pm s.d$	CD	$k_{MC2}(min^{-1})(x10^2)$
PNIPAAM	19.04±1.250	0.8020	0.3399±0.0510	0.9530	19.43
PNP1$_{-2}$	19.50±1.320	0.7774	0.3244±0.0458	0.9158	19.79
PNP2$_{-2}$	13.53±0.930	0.7709	0.3188±0.0447	0.9189	13.15
PNP3$_{-2}$	10.31±1.060	0.1836	0.2411±0.0616	0.7119	4.905

A temperature switch above the LCST of the polymer caused a rapid and sharp deswelling or contraction of the hydrogel with expulsion of the absorbed medium. The maximum contraction rate (K_{MC}, indicated in Figure 4.22 (b)) (Coughlan et al., 2004) was dependant on the polymer composition as well as the duration of the swelling phase. The k_{MC} of the hydrogel systems was thus greater after the second (3 hour) period of swelling (k_{MC2}) than it was after the first period (1 hour, k_{MC1}) and a linear relationship ($R^2=0.9893$) was established.

(a)

(b)
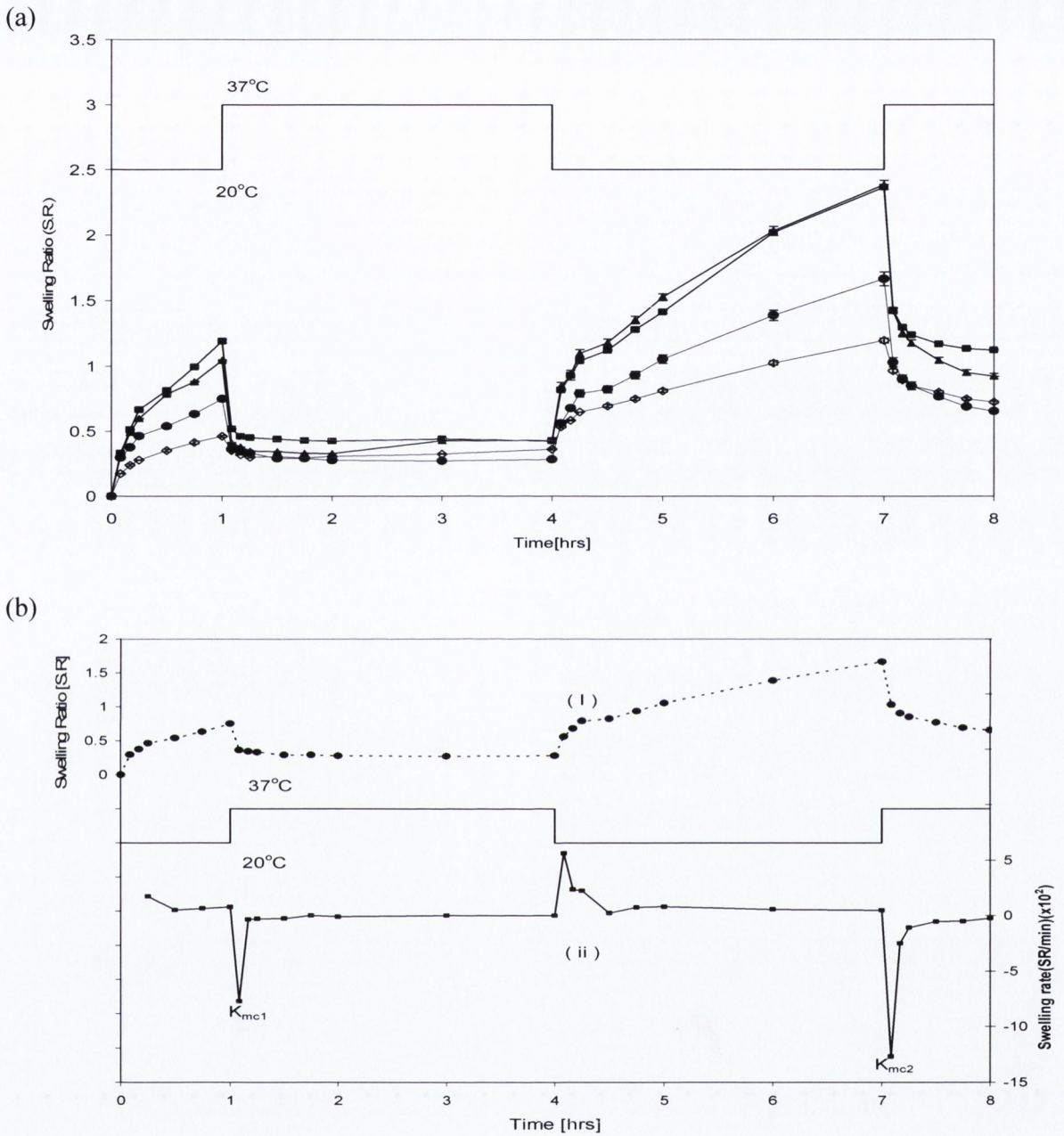
Figure 4.22: Swelling contraction cycle

(a)   of PNP (■) PNP1$_{-2}$(▲), PNP2$_{-2}$ (●) and PNP3$_{-2}$ (♦) on temperature switch between 20°C
        and 37°C.

(b)   of PNP2$_{-2}$ (i, ●) and corresponding contraction rate (ii) on temperature switch between 20°C
        and 37°C. Also shown are K$_{mc1}$ and K$_{mc2}$ along with first hour of swelling fitted to Equation
        2.22

Temperature switch indicated by solid line.

Following contraction, a residual volume was reached at 37°C. This residual volume had its own equilibrium value, shown in Figure 4.13 (a) for the various hydrogel systems. The equilibrium residual volume was not reached after the first swelling period for any of the systems. Following the second contraction equilibrium volume was not reached for any of the hydrogel systems indicating that the presence of PLA causes a skin dense layer, which prevents the medium being expelled from the gel on temperature switch.

A statistical difference was observed ($p<0.05$) between the k_{MC} of all the hydrogels and the resulting magnitude of contraction and a linear correlation ($R^2 = 0.9887$) (Figure. 4.23(a)). The magnitude of contraction also proved to be significantly dependent on the polymer composition ($p<0.05$) (Figure 4.23(b)).

(a)   (b)
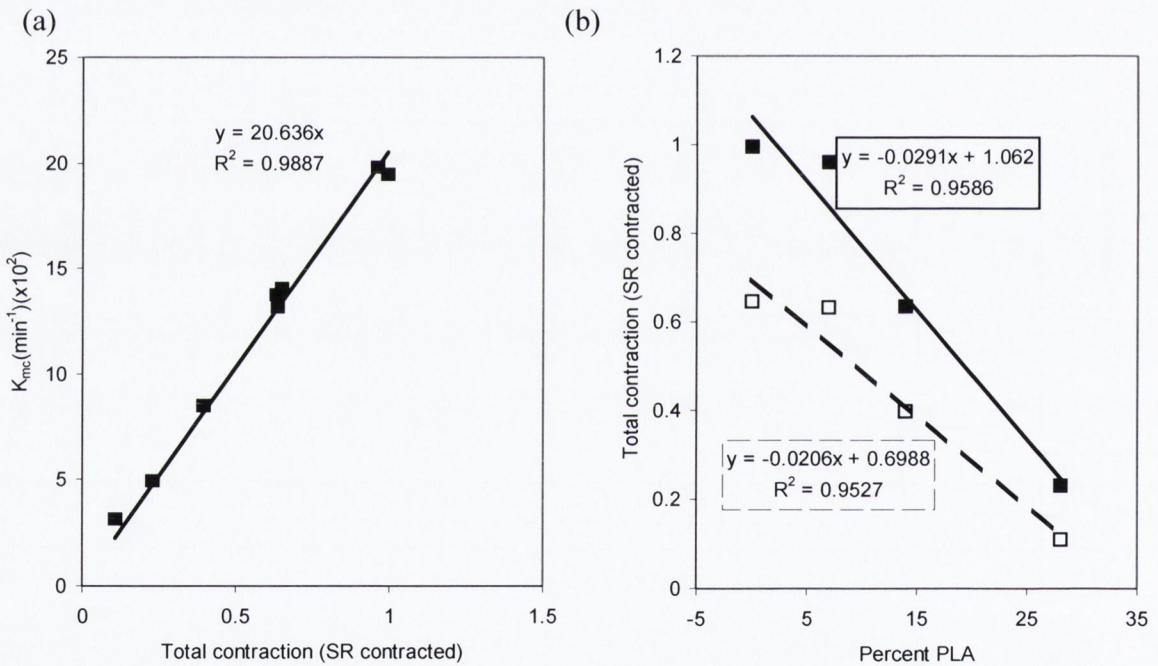
Figure 4.23 :(a) Relationship between magnitude of contraction and the K_{mc} and (b) the polymer composition and magnitude of contraction.

4.4.5 Hydrogel structural parameters

Three important parameters can define the structure of biomedical hydrogels; the polymer fraction volume in the swollen state, v_{2s}, the number average molecular weight between cross-links, M_c, and the correlation length, ξ, also known as the network mesh or pore size [*Peppas et al., 2000*]. These parameters were determined for the various hydrogel morphologies using the equilibrium swelling theory as described in Section 2.2. In this way it is possible to establish which polymer network has the largest space available for diffusion and thereby lead to a greater rate of degradation. In addition to the use of theoretical studies to estimate the pore size, experimental techniques such as size exclusion or to examine the hydrogel in the solid state using scanning electron microscopy (SEM) can be undertaken.

4.4.5.1 Theoretical evaluation of hydrogel structural parameters.

The important structural parameter for characterising cross-linking in polymers, Mc, which is directly related to the cross-linking density [EQN 2.7] was calculated for the synthesised PNP and PNP-co-PLA hydrogels. Because of network variations, only average values for the cross-linking density and the molar mass between cross-links can be determined. For the determination of the polymer volume fraction in the swollen state (V_{2s}), it was necessary to experimentally measure the equilibrium-swelling ratio in PB 7.4 at 20°C. These measurements were preformed as outlined in Section 3.3.11. As defined in equation (2.1), the reciprocal of the polymer volume fraction in the swollen state (V_{2s}) is the volumetric swelling ratio. The results obtained for V_{2s}, V_{2r}, as well as the volumetric swelling ratio (Q) are given in Table 4.8. From the parameters mentioned above, the degree of cross-linking of the network was estimated through the determination of the molecular weight between two adjacent cross-links. The Peppas and Merrill (1977) model was employed to calculate the Mc. The various parameters necessary to perform all the calculations are presented in Appendix IV.

Table 4.8: Calculated results of the structure analysis of the cross-linked equilibrium swollen hydrogel series at 20°C.

Gel	V_{2r}	V_{2s}	M_c(cal)	M_c(theor)	P_x	<C>
PNP	0.2308	0.1036	1149	1451.62	0.0164	0.885
PNP1$_{-2}$	0.2516	0.1139	937.21	4806.00	0.0200	0.877
PNP2$_{-2}$	0.2752	0.1219	874.03	4627.00	0.0217	0.840
PNP3$_{-2}$	0.3206	0.1352	764.79	4279.00	0.0249	0.825
PNP1$_{-12}$	0.2422	0.0786	1939.77	4738.00	0.0103	0.806
PNP2$_{-12}$	0.2596	0.0707	2265.75	4502.26	0.0090	0.700
PNP3$_{-12}$	0.2879	0.0564	3123.17	4020.20	0.0065	0.605

A molar cross-linking ratio of 0.04 of the initial monomers to BIS was employed in all hydrogel systems (Appendix I). The corresponding data for hydrogels prepared by varying the molar ratio of PNIPAAM to PLA are listed in Table 4.8. The experimentally measured volume fraction of polymer, V_{2s}, in each hydrogel system at equilibrium (20°C) was plotted against the percent of PLA incorporated into the gel. A trend was evident with a R^2=0.989 and R^2=0.8913 for the series of gels with PLA MW 2000 and PLA MW 12000 respectively. As defined in equation (2.1), the reciprocal of the polymer volume fraction in the swollen state (V_{2s}) is the volumetric swelling ratio. These results are in agreement with the studies undertaken in Section 4.4.1.

The values of the molecular weight between cross-links and the cross linking density for the synthesized gels are displayed in Table 4.8. In the case of the gel series consisting of PLA MW 2000, the M_c values show a decrease with increasing PLA content in the gels (Figure 4.24(a)). In addition, it is also evident that the ratio of PLA repeating units in the gel has a significant effect on the cross-linking density. On closer examination of the difference between the theoretical and calculated M_C values, a large difference in the estimated values ($p<0.05$) in the co-polymer systems indicate the PLA monomer has a tendency to self-cross-link leading to a more tightly meshed network the higher the PLA content. The dependence of the molecular weight between cross-links on other structural parameters was also investigated. The effect of the parameter Mn on the value of M_c calculated for the hydrogels is illustrated in Figure 4.24(b). It can be seen that an upward trend is apparent between Mn and M_C with a R^2 value of 0.9627.
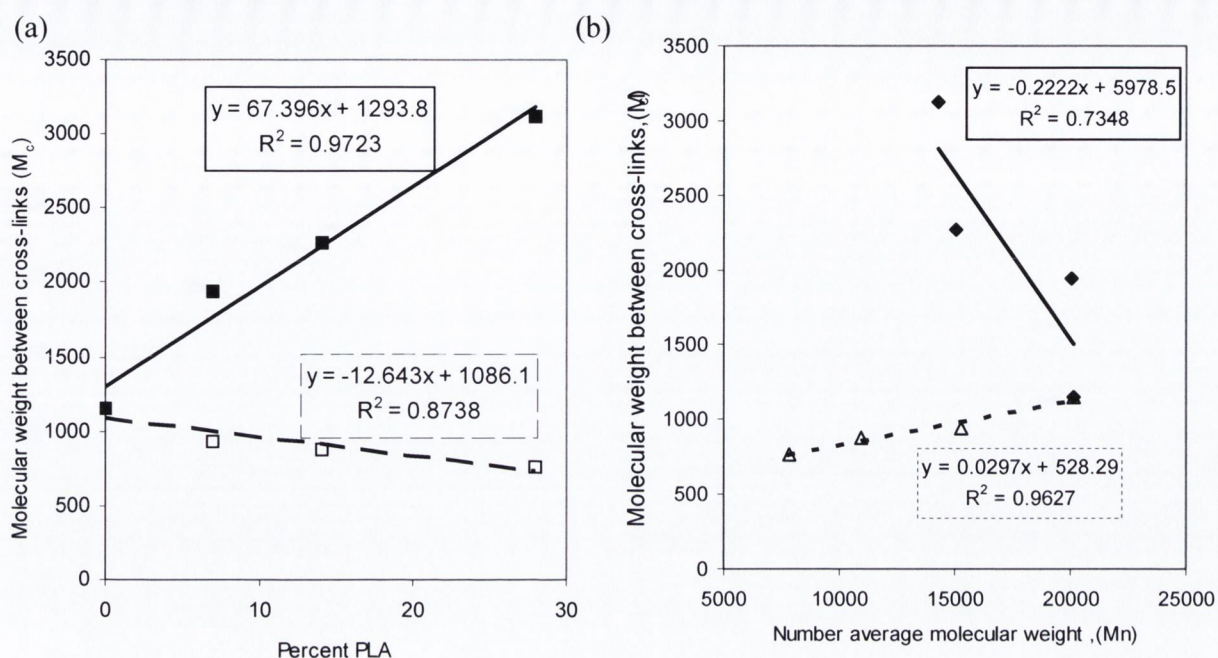
Figure 4.24: Relationship between (a) polymer compositions for hydrogel series with PLA 200($\square$) and PLA 12000 ($\blacksquare$) and the Mc and (b) number average molecular weight (Mn) for the hydrogel series with PLA 2000 ($\lozenge$) and PLA 12000 ($\blacklozenge$) and the Mc.

On the other hand, the experimental values of M_c for the hydrogel series containing PLA MW 12000 appeared to decrease the effective cross-linking density which in turn leads to an increase in the molecular weight between cross-links the higher the present of PLA present in the gel. A plot of the amount of PLA present against the Mc values revealed a linear correlation with a R^2 value of 0.9723.This can be explained by a larger molecular weight of PLA reducing the cross linking density. This result is also reflected in Figure 4.24 (b) where an increase in the Mn leads to a smaller Mc value. In addition the correction factor <C> for the network imperfections as a result of chain ends appeared to decrease with increasing the content of PLA indicating a lower cross-linking density.

For all the systems examined, a relationship (R^2=0.9293) existed between the polymer volume fraction, V_{2s} and the molecular weight between cross-links, M_C (Figure 4.25 (a)). The higher the swelling level attained, the smaller the cross-linking density as predetermined by the amount and MW of PLA present. The data indicates that as the cross-linking ratio decreased in the hydrogels, the mesh size increased and a trend was observed with a R^2 value of 0.8931(Figure 4.25 (b)).

101
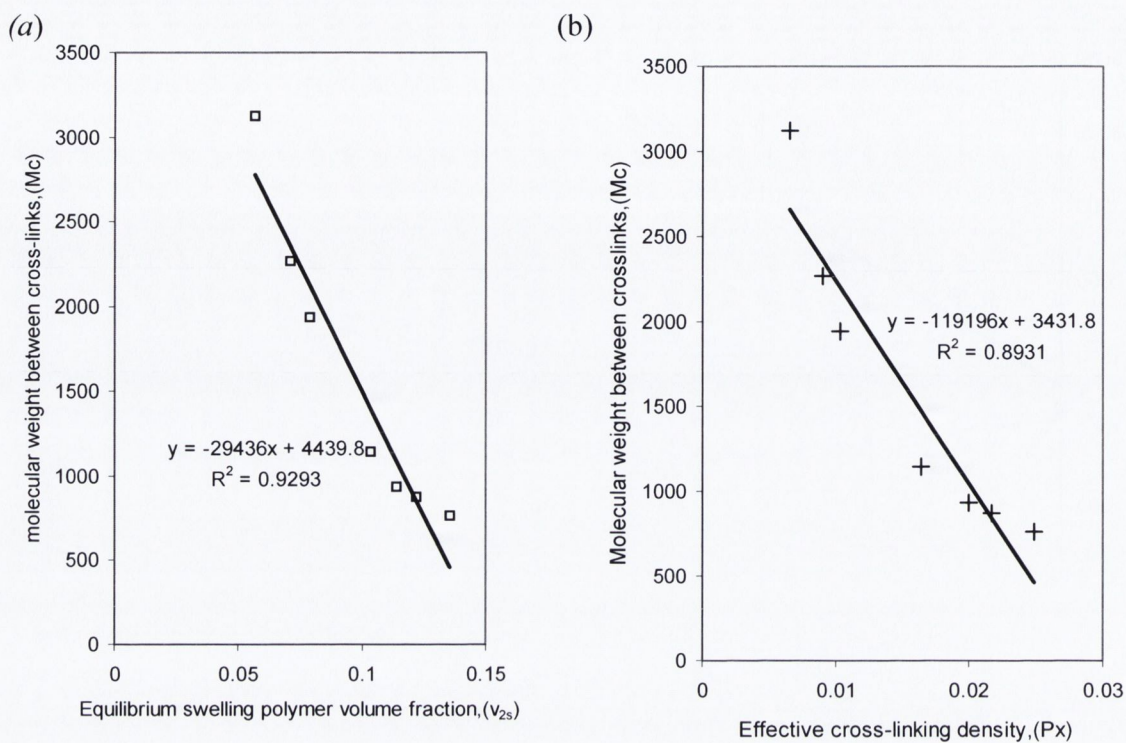
Figure 4.25: Relationship between (a) equilibrium polymer volume fraction, V_{2s} and Mc and (b) the effective cross-linking density and Mc for synthesised hydrogels.

4.4.6 Solute exclusion technique

The pore size/mesh size was also characterised by solute exclusion technique using a series of model probes of various sizes as described in Section 3.3.12. This technique involves the measurement of the ability of a probe molecule to permeate from the bulk media into the equilibrated hydrogel at a given temperature.

A plot of the pore volume inaccessible to a given molecular probe as a function of molecular probe size gives the cumulative pore volume curve. The plateau of the curve is called the fiber saturation point, which corresponds to the volume of water, which is inaccessible to polymer molecules having a size too large to fit the pores containing the water. The principle of the solute exclusion technique for the characterisation of the pore size distribution of the hydrogels is illustrated in Figure 4.26.
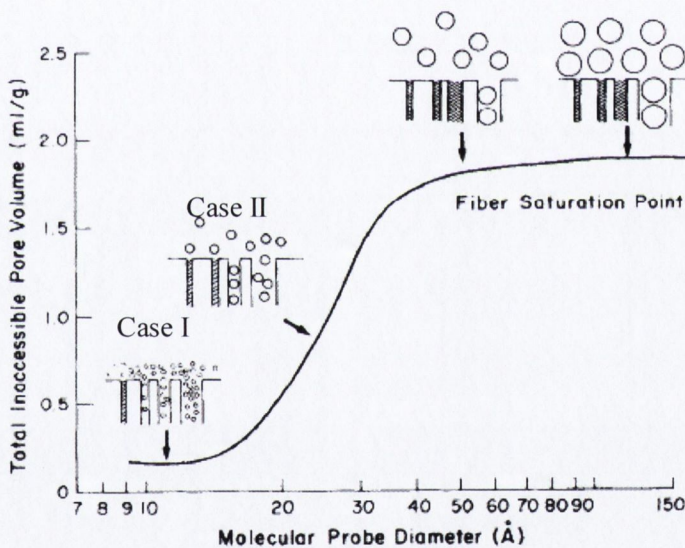
Figure 4.26: Schematic illustration of correspondence of pore distribution curve to solute excluded from pores (Wu et al., 1992).

A hydrogel swollen in water to an equilibrium state is immersed in a volume of a known solution containing a molecular probe. If it is assumed that all the water originally associated with the hydrogel is accessible to the molecular probe, it will equilibrate and dilute the solution as shown in case I (Figure 4.26). Alternatively a solution of larger molecules as shown in case II will lead the smaller pores inaccessible to the probe molecule. Therefore the medium is unavailable for dilution and a mixed solution will be somewhat less diluted than in case 1.This difference in concentration is the basis of a simple calculation to give the amount of water inaccessible to the probe. In the present

studies the permeation kinetics of the chosen probe molecules through the pores of the homopolymer PNP and co-polymer PNP2$_{-2}$ were studied.

Figure 4.27 shows the volume fraction, which is accessible to each probe molecule for the two hydrogels, studied at both 20 and 37°C. The values were lower at 37°C due to the hydrogels being in a collapsed state, resulting in smaller pore size and less media present. Comparing PNP and PNP2$_{-2}$ at 37°C, no statistical difference (p>0.05) was observed in the volume fraction of probe molecules accessible to the hydrogel pores. Below the LCST a larger volume of pores are available due to the hydrophilic nature of PNIPAAM. When these volumes of accessible pores were taken into account, the examination of the volume fraction of pores with sizes larger than the probing molecule were considered (Figure. 4.28)
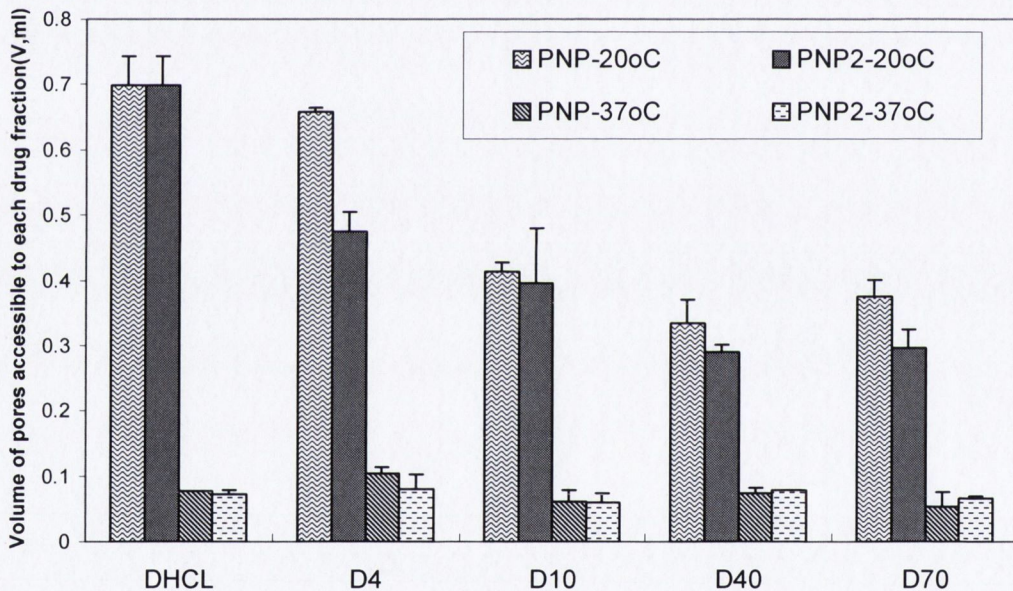
Figure 4.27: Bar chart displaying the volume of pores of both PNP and PNP2 accessible to each drug fraction at 20 °C and 37 °C.

In the case of the molecular probe molecule DHCl (8.19Å) (Coughlan and Corrigan, 2004), the value of VF is approximately 1 indicating the probe molecule is small enough to access all hydrogel pores. This was observed for both polymeric systems at 20°C. At 37°C, when the hydrogel was in the collapsed state, DHCl could access 90% and 75% of the available pores of PNP2$_{-2}$ and PNP respectively. As seen in Section 4.4.3, above the LCST, PNP2$_{-2}$ swells to a greater degree than PNP leading to a larger pore size. This result is pronounced in Figure 4.28 whereby a larger number of

pores with sizes larger than the probe molecule are seen for the co-polymer in comparison to the of the homopolymer PNP. The difference in the pore volume between the two hydrogels at 37°C can be explained in terms of thermosensitivity of the co-polymer. A marked decrease in the molar ratio of PNIPAAM is incorporated into the gel on increasing the PLA content, affecting both the thermosensitivity and the degree of swelling.
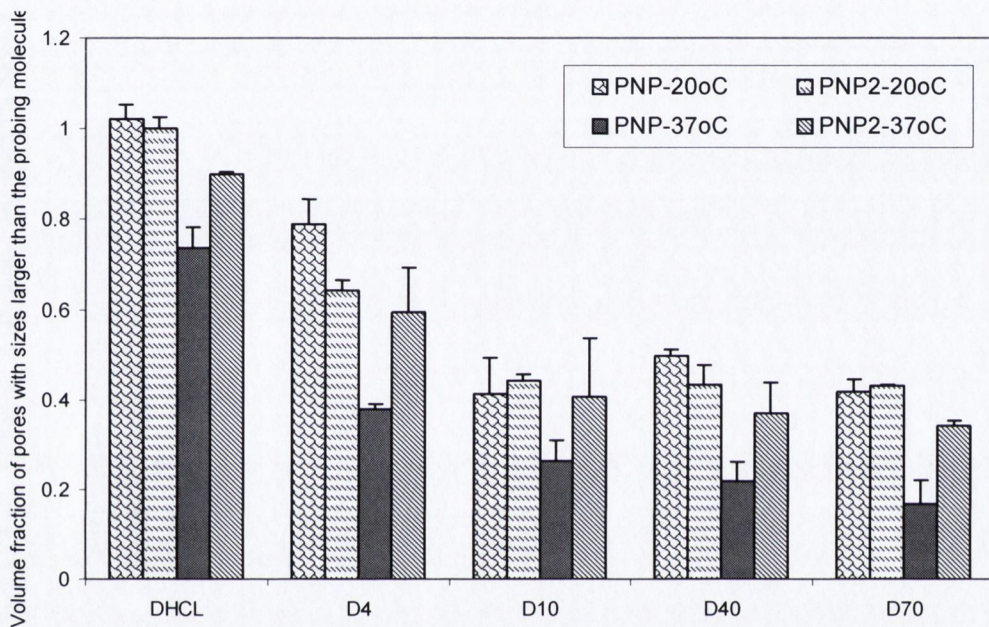
Figure 4.28: volume fraction of pores with sizes larger than the probing molecule.

In the case of the dextran fractions, the greater the molecular diameter, the more difficulty the probing molecule had in accessing the pores within the hydrogel network. Figure 4.29 displays the relationship of the molecular probe size (Å) and the fraction of pores oversized to accommodate the model probe molecule. At 20°C PNP, which swelled to a greatest degree in a given medium, could accommodate a larger fraction of the probing molecule followed by PNP2-2. For the dextran series D4 (25Å) and D10 (38 Å) the volume of pores in PNP, which could access the probing molecule, was 78% and 50% respectively. In the case of PNP2-2 with the hydrophobic unit PLA present, 64%, and 44% of the pore volume was accessible to the probe molecule. The larger dextrans could access ~40% of the pores in PNP2-2 assuming no polymer drug interactions.
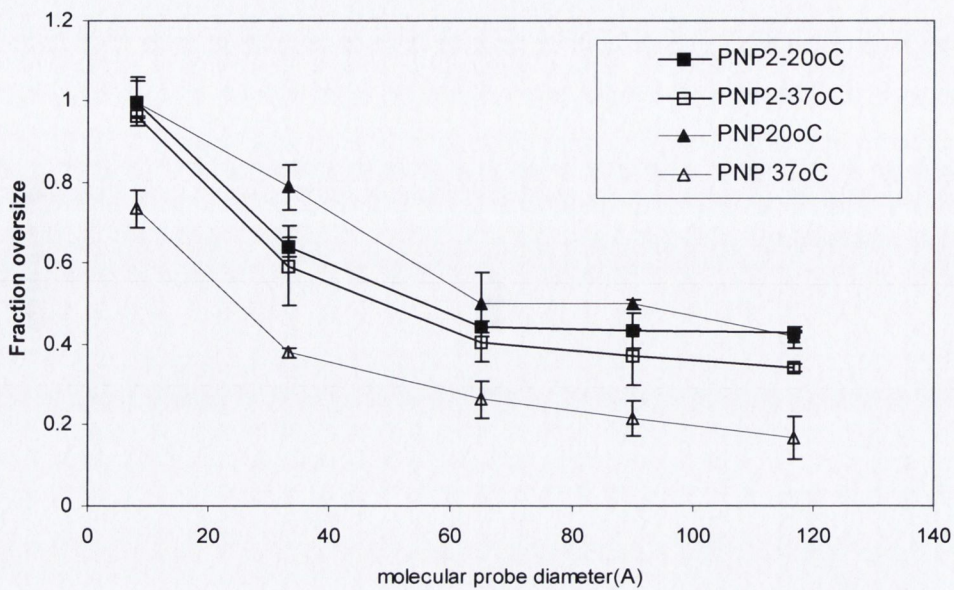
Figure 4.29: volume fraction of pores with sizes larger than the probing molecule.

These results were successful in determining the ability of the probe molecule to permeate the pores of a hydroglels with different swelling capacities. In addition the effect of the hydrogel structure at a given temperature on the permeation of the probe molecules could be examined. The results were conclusive and in agreement with the swelling studies. At 37°C the smallest probe molecule DH was inaccessible to a volume of pores indicating that the average mesh size was below 8Å. Below the LCST all pores were accessible to DH indicating that the pore size was above (8Å). Peppas and Merrill model showed a decrease in M_C value the higher the PLA content (MW 2000), which is directly related to the crosslinking density. In the following section the effect of temperature and composition will be examined in relation to the pore size calculated using SEM.

4.4.7 Scanning electron microscopy

SEM is a solid-state method of examining the interior morphology of hydrogels. The hydrogels equilibrated in a medium at their respective temperatures are usually freeze-dried to retain their swollen structure. Previous studies undertaken by Lee et al., (2005) examined porous structures of hydrophobic modified hydrogels. The results indicated that the pore size became smaller as the content of the hydrophobic monomer increased. Zhang and Peppas (2002) studied the interior morphology of hydrogel composed of PNIPAAM-poly (methacrylic acid) IPNs. A general decrease in pore size of their gels was observed on decreasing the pH and/or increasing the temperature in these studies.

In the present studies freshly synthesised gels swollen at respective temperatures (i.e. $20^{\circ}C$ and $37^{\circ}C$) were freeze dried to retain their swollen structure and sputter coated with gold prior to examination using SEM.

The influence of the hydrophobic PLA (MW 2000) below the LCST on the pore size can be seen in the SEMs in Figure 4.30 (a). Under the same magnification (x 1,500), the morphological changes induced by PLA were significantly different. A trend towards a decrease in pore size with increasing the percent of PLA could be observed characteristic of the hydrophobic monomer. PNP swelled to a greater extent at this temperature than all other hydrogels (Figure 4.13) resulting in a greater pore size.

On examination of the effect under magnification (x 500) of the MW of PLA on the morphological changes in the co-polymeric networks, an increase in the MW of PLA resulted in larger sized porous structures (Figure 4.30(b)). Increasing the molar ratio of PLA pronounced this effect. In addition a comparison of the hydrogels with the same composition ratio but different molecular weight PLA showed that the structural integrity increased as a result of the increase in MW.

107

(a)
(b)

(c)
(d)
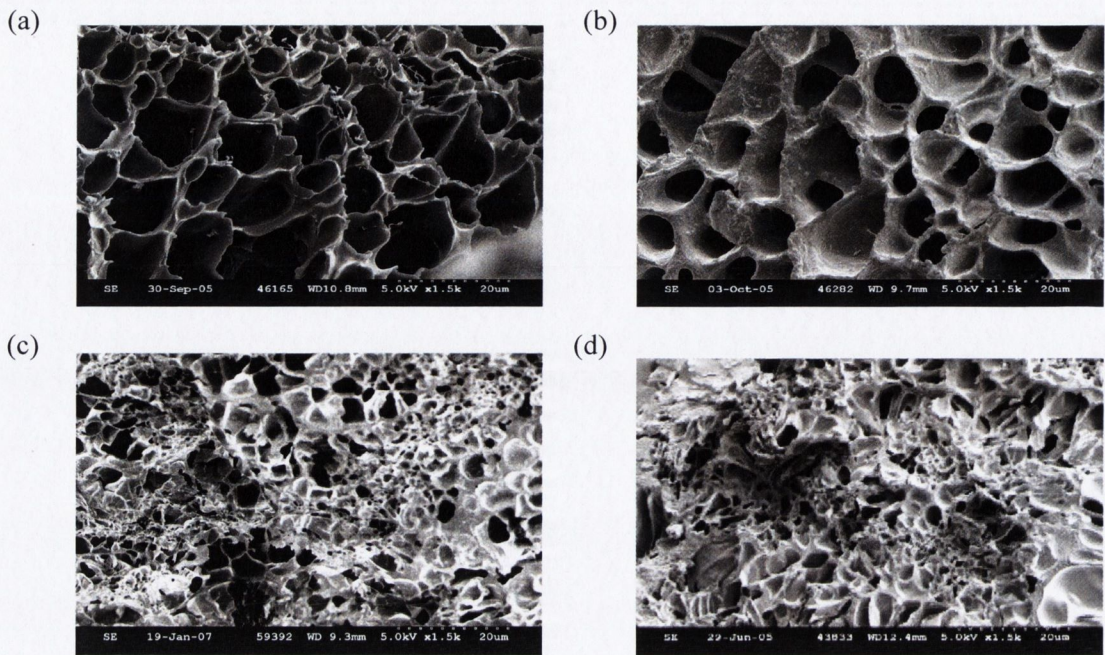
Figure 4.30 (a): SEM images (magnification X 1500) of (a) PNP, (b) PNP1$_{-2}$ (c) PNP2$_{-2}$ and (d) PNP3$_{-2}$

at 20°C.

(a)
(b)

(c)
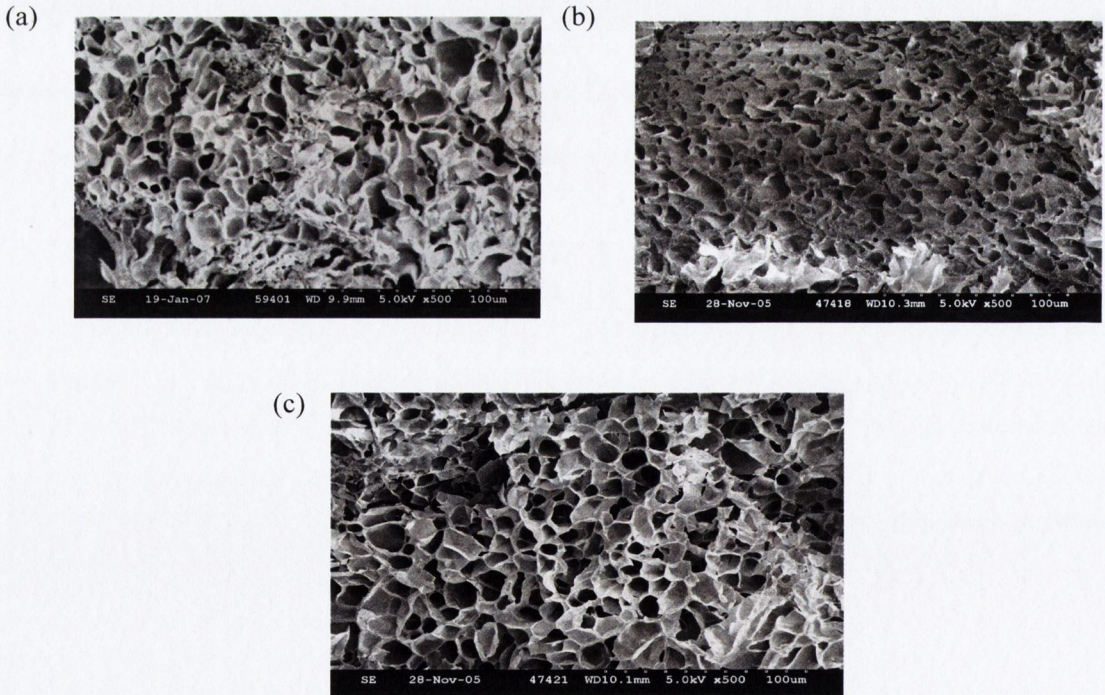
Figure 4.30(b): SEM images (magnification x500) of (a) PNP1$_{-12}$ (b) PNP2$_{-12}$ and (c) PNP3$_{-12}$

at 20°C.

108

(a)

(b)

(c)

(d)
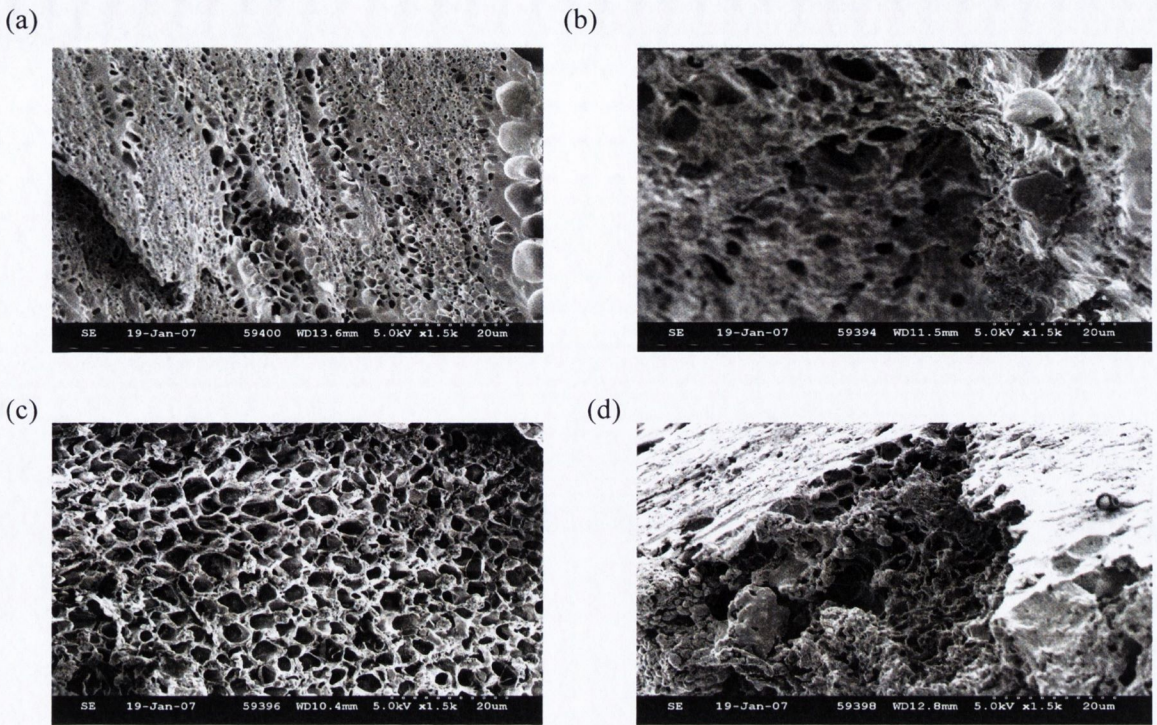
Figure 4.31(a): SEM images (magnification x1500) of (a) PNP, (b) PNP1$_{-2}$ (c) PNP2$_{-2}$ and (d) PNP3$_{-2}$ at 37°C.

(a)

(b)

(c)
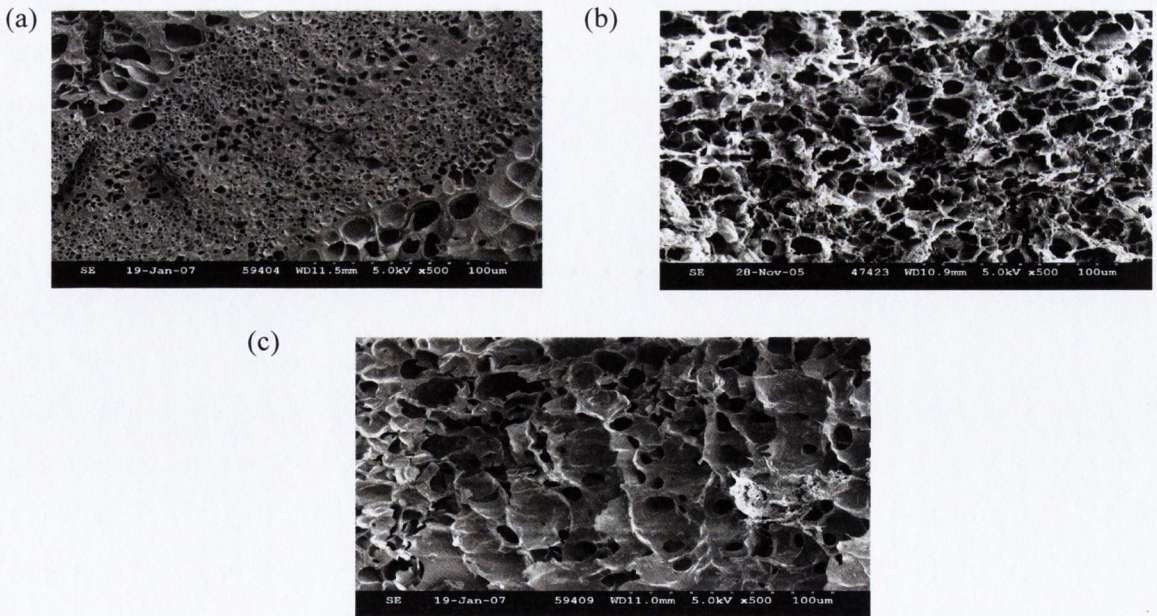
Figure 4.31(b): SEM images (magnification x500) of (a) PNP1$_{-12}$ (b) PNP2$_{-12}$ and (c) PNP3$_{-12}$ at 37°C.

In an attempt to quantify the size of the pores seen visually by SEM, approximates pore sizes were estimated using a computer software program (Imagetool for windows ® Version 3.00).

Table 4.9: Hydrogel macropore size (mean ± s.d) as determined by SEM. Also shown is the equilibrium swelling ratios for each hydrogel network.

Hydrogel	Molar-Ratio PLA(%)	20°C		37°C	
		Equilibrium swelling (S.R)	Observed pore size (μm)	Equilibrium swelling (S.R)	Observed pore size (μm)
PNP	0	8.53	8.52 ± 1.70	0.1957	0.89 ± 0.560
PNP1$_{-2}$	7	7.30	5.79 ± 1.01	0.5236	2.09 ± 0.610
PNP2$_{-2}$	14	6.61	3.94 ± 0.65	0.7842	2.13 ± 0.720
PNP3$_{-2}$	28	5.85	2.82 ± 1.00	0.7400	2.57 ± 0.720
PNP1$_{-12}$	7	10.54	10.61 ± 0.29	0.6212	3.50 ± 0.123
PNP2$_{-12}$	14	11.74	11.06 ± 2.40	1.5190	7.18 ± 0.386
PNP3$_{-12}$	28	14.14	11.96 ± 3.00	4.4500	7.82 ± 3.330

The SEM data was successful in examining the nature and pore size of the polymeric systems in their swollen state. A trend towards a decrease in the mean pore size was observed for the co-polymeric systems containing PLA MW 2000. Lee et al., (2005) when introducing hydrophobic monomers into thermoresponsive gels observed similar trends. Comparing the methods employed to calculate the pore size, at 20°C Peppas and Merill model also showed a decrease in the value of Mc as the molar ratio of PLA increased. In addition PLA appeared to be self cross-linking leading to a higher cross-linking density as the Percent of PLA increased. Previous studies undertaken by Peppas and Lustig, (1985), Ende et al., (1995) observed a similar trend whereby the mean pore size decreased with increasing percentage crosslinker.

The effect of increasing the MW PLA led to larger pores, the effect magnified the higher the molar ratio of PLA. These results are also pronounced with the equilibrium-swelling ratio (Table 4.9). Similarly a smaller distribution of pores could be seen the higher the molecular weight. These results are in agreement with a section 4.4.5 whereby nearly a two-fold decrease in the cross-linking density was noted as a result of larger molecular weight between cross-links.

At 37°C, all hydrogel systems increased in the mean pore size as the percent of PLA increased. Size exclusion technique was used to compare the homopolymer PNP and PNP2$_{-2.}$ At 37°C there were pores, which were inaccessible to even the smallest molecular probe for both gels, however it could

be deduced that a lager volume fraction of pores was accessible to PNP2$_{-2}$. The non-thermoresponsive nature of PLA therefore acted in increasing the pore size above the LCST as also shown by the swelling studies. These results are in good agreement with the calculated SEM pore sizes where 0.89µm to 2.12µm were the experimentally calculated values for the pore sizes of PNP and PNP2$_{-2}$ respectively.

4.4.8 Conclusions:

In the present chapter novel biodegradable hydrogels were synthesised by varying molar ratios of PNIPAAM to PLA. The swelling studies presented at 20°C have shown a decrease in swelling rate with increasing PLA content for PNIPAAM-co-PLA$_{-2}$ gels. In addition on increasing the amount of PLA macromer in the hydrogel, a noted decrease in the molecular weight between cross-links was observed and the cross-linking density increased. At 37°C, faster swelling rates and a higher equilibrium swelling ratio was observed above the LCST for PNP3$_{-2}$ than for the other hydrogels, leading to a greater effective pore size as shown by SEM. The increase in the effective pore size can be attributed to the reduced thermoresponsive unit PNIPAAM above the LCST.

The extent of swelling as well as the equilibrium-swelling ratio of the hydrogels was strongly influenced by the amount and the MW of PLA incorporated into the three dimensional polymer networks. An increase of 20-85% in the swelling ratios were observed on increasing the MW of PLA from 2000 to 12000 with the results influenced strongly by the polymer composition and temperature. These results were reflected in the pore size of the gel estimated using SEM. The differences in the pore sizes on changing the MW of PLA were attributed to the crosslinking density as shown by the Peppas and Merrill (1977) model.

On comparing the methods used to determine the pore size, a plot of the molecular weight between cross-links against the pore size and the equilibrium polymer volume fraction against the pore size as determined by SEM is shown in Figure 4.32. A linear correlation is seen between Mc and ξ (Figure 4.32(a)) and V$_{2s}$ and ξ (Figure 4.32(b)) for both hydrogel series. In the following chapters a closer look at the effect of the mesh size, volume fraction of swollen polymer and interior network structural parameters of these gels will be examined in relation to their influence on degradation and diffusional properties of model drugs from these matrices.
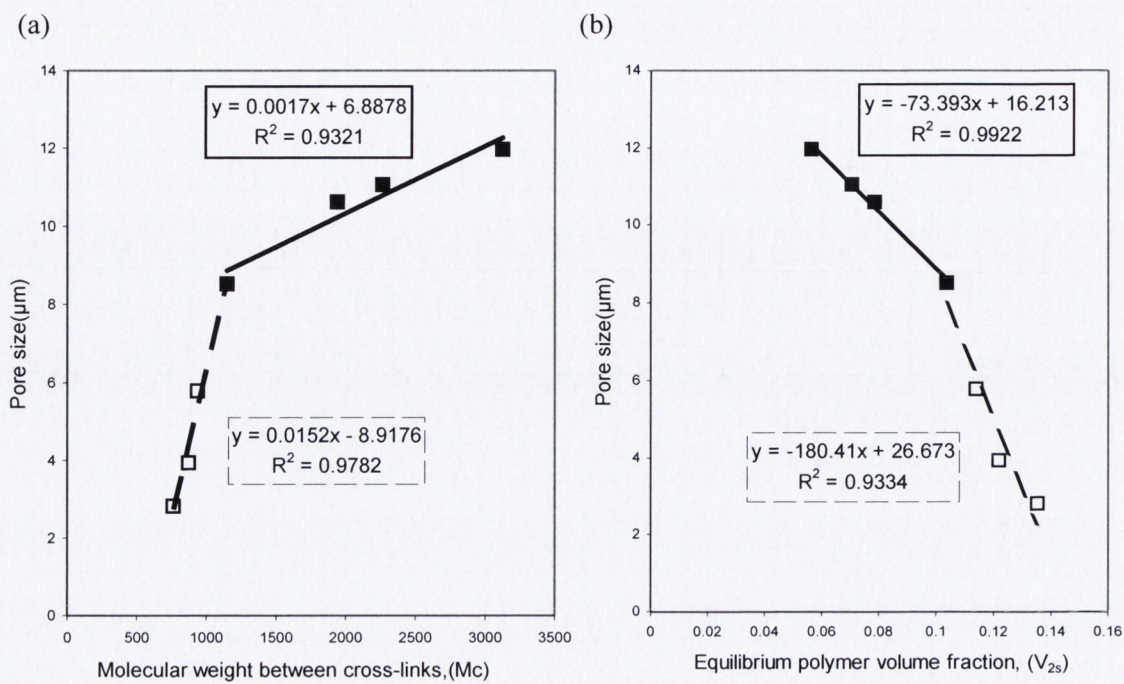
Figure 4.32: (a) Correlation length of the mesh size as a function of the number average molecular weight cross-links, Mc and (b) the relationship between the equilibrium polymer volume fraction and the pore size,ξ.

4.5 Model drug characterisation

The monomer composition of a co-polymer can be manipulated to influence drug permeation and diffusion characteristics. Through this manipulation, hydrogels can be synthesised to accommodate a variety of drugs including charged, hydrophilic, hydrophobic, neutral small molecules and macromolecules. In this section a variety of model drugs were chosen with different physicochemical properties. The model drugs are shown in Figure 4.33 along with their physicochemical properties in Table 4.10.
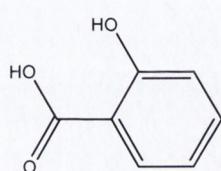
salicylic acid

(SA) 138.12
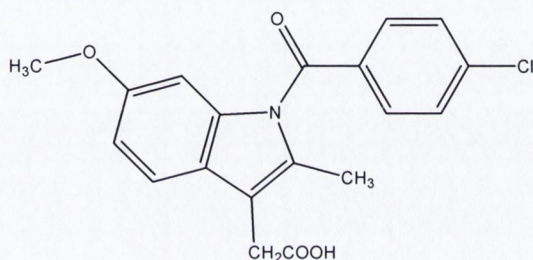
Indomethacin

(IDM) 357.79
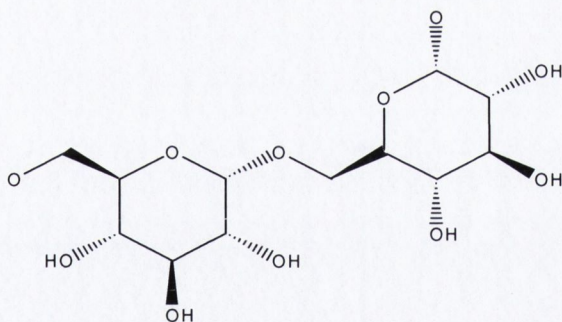
Dextran(1,6 linkage)
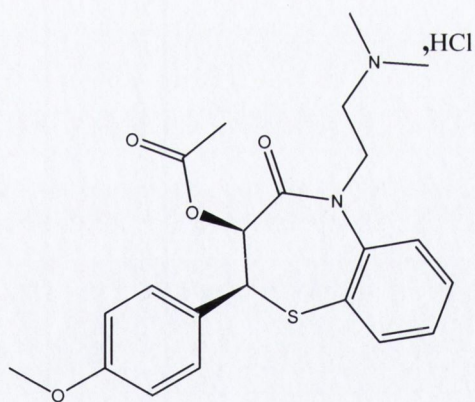
Diltiazem

Diltiazem Base (DB)   414
Diltiazem HCl (DH)   451

Figure 4.33: Structure and molecular weight of drugs used.

Table 4.10: Physiochemical properties of model drugs

Model drug	Molecular weight	Solubility in PB (isotonic) at 20°C (g/L)	Solubility in PB (isotonic) at 37°C(g/L)	pKa	FITC label (mol/mol glucose)
Diltiazem HCl	451.0	434.99	549.34	7.7	------------------
Diltiazem Base	414.5	1.99	3.43		------------------
Salicylic acid	138	2.0	8.18	2.97	----------------
indomethacin	357	0.56	1.16	4.5	----------------
Dextran MW 4000	4300 (a)	Very soluble (b)	Very soluble (b)	----------	4.0
Dextran MW 10000	10200(a)	Very soluble (b)	Very soluble (b)	----------	0.5
Dextran MW 40000	43000(a)	Very soluble (b)	Very soluble (b)	-----------	0.5
Dextran MW 70000	68800(a)	Very soluble (b)	Very soluble (b)	----------	0.65

a) Molecular weight of bulk dextran as stated by Sigma-Aldrich

b) Martindale 1996

Diltiazem base and its hydrochloric salt were used as model acidic and basic drugs respectively. Diltiazem, Indomethacin and salicylic acid were also used as model acidic drugs to give a drug series with decreasing acidity respectively. The drugs were divided into a hydrophobic and hydrophilic series, the former reflecting solubility less than 10mg/ml i.e. "slightly soluble" according to the U.S.P. definition of solubility (United States Pharmacopoeia, 2000). A range of Dextrans (MW4000 to MW70000) was used as larger model drugs. These compounds along with DH made up the hydrophilic drug series while SA, IDM and DB made up the hydrophobic series. The model drugs used thus provided a series of probe molecules with different physiochemical properties, namely, solubility, size and chemical nature.

4.5.1 Fourier transform infrared spectroscopy

The FTIR spectra of the model compounds were obtained as described in Section 3.3.2. The FTIR spectra of Diltiazem base and its hydrochloric salt are given in Figure 4.34.
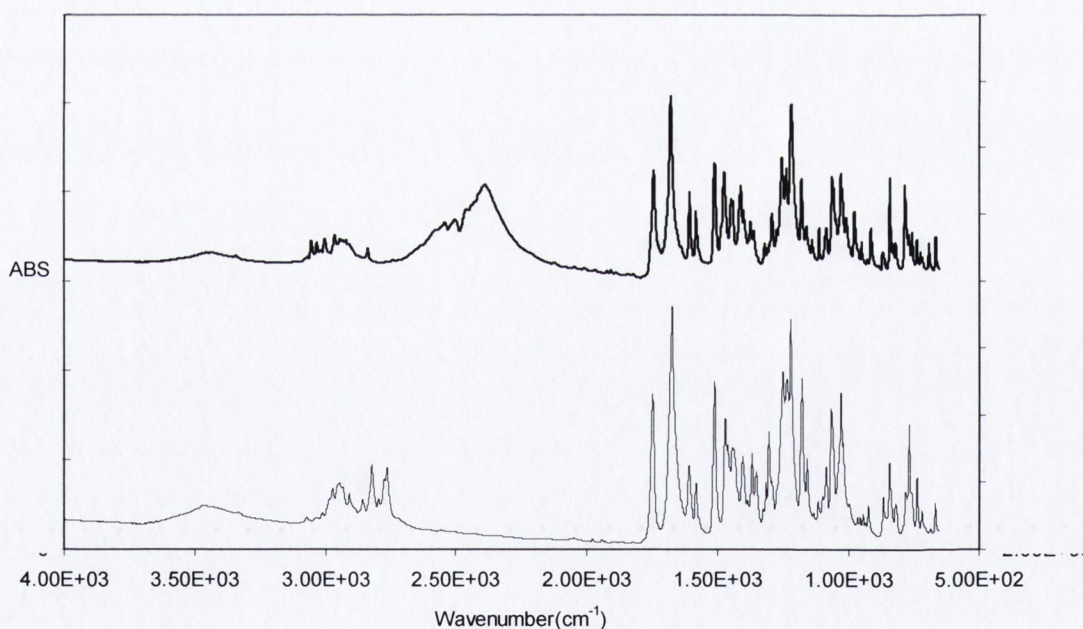
Figure 4.34: FTIR spectra of diltazem hydrochloride (top) and diltiazem base (bottom).

The bands associated with the carbonyl stretching appeared at $1747cm^{-1}/1647cm^{-1}$ for DB and 1743 cm^{-1} /1679 cm^{-1} for DH (Kugita et al., 1971; Tanaka et al., 1992). The peaks around 3000 cm^{-1} can be assigned to the aliphatic and aromatic C-H stretching.
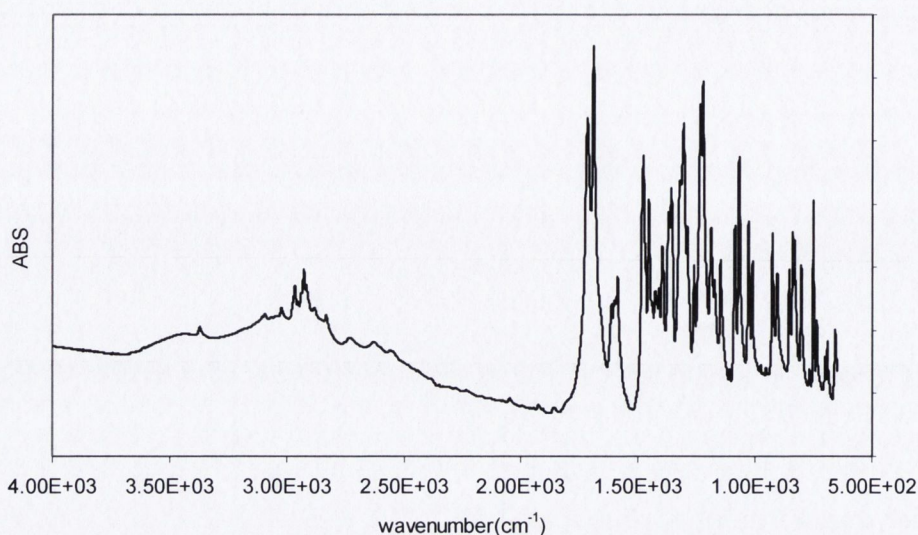
Figure 4.35: FTIR spectrum of indomethacin.

The FTIR spectrum of indomethacin is given in Figure 4.35. The band at $1717cm^{-1}$ can be ascribed to the v(C=O) mode of the carboxylic group, while that for the amide group is recorded at $1690cm^{-1}$(Del Arco et al., 2004). The bands between 1625-1575 and $1479cm^{-1}$ are due to the V (C-C) stretching modes of the aromatic rings; those due to the V (C-O) of the ether group are recorded at $1270-1225cm^{-1}$. The absorption bands below $1000cm^{-1}$ are characteristic of the V (C-H) deformation modes and the V (C-Cl) stretching mode is recorded below $740cm^{-1}$. The high wavenumber ranges between $4000-2500cm^{-1}$ contains the bands due to V (OH), V (NH) and V (CH).

The FTIR spectrum of salicylic acid is shown in Figure 4.36. The pair of bands seen at $1580 cm^{-1}$ and $1609 cm^{-1}$ in the IR spectrum are assigned to the C=C stretching vibrations of the aromatic ring. The C=O stretching is clearly observed at $1657 cm^{-1}$ in the spectrum. At higher frequencies of $3062cm^{-1}$ and $3235 cm^{-1}$ the C-H and O-H stretches respectively were visible. The out of plane C-H and O-H bends were prominent in the middle and lower frequency range of the spectrum (Goulet et al., 2004).

116
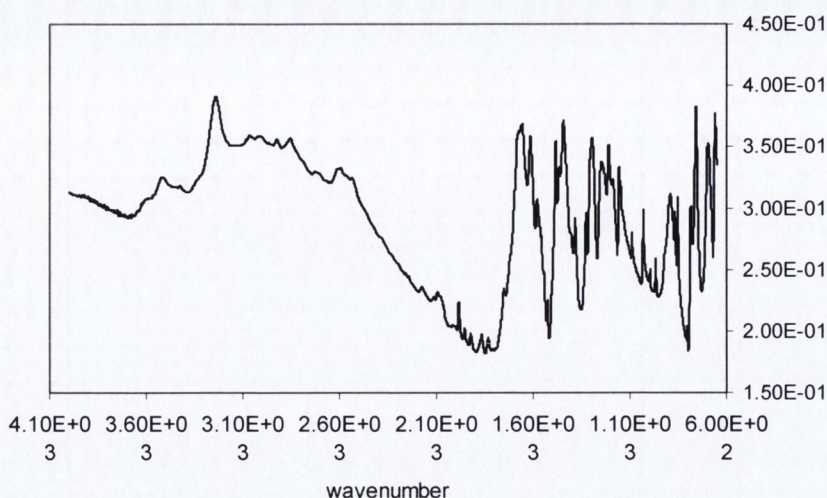
Figure 4.36: FTIR spectrum of salicylic acid.

The FTIR spectrum of dextran is shown in Figure 4.37 below. The typical asymmetrical C-O-C stretching of the ring at 1150-1085cm^{-1} was evident (Barbani et al., 2005). The characteristic C=C stretching band was prominent in the spectra at 1660cm^{-1}. At the upper end of the frequency the CH stretching was seen at 2942cm^{-1}. The hydroxyl stretch dominated the FTIR spectra of the dextrans with maximum absorption bands in the region of 3400-3430cm^{-1} and 1012-1018cm[-1](Wang et al., 2002). The broad –OH band at ~3400cm-1 shifted to a higher wavenumber with increasing molecular weight. A linear correlation between the position of the –OH band and the glass transition temperature (R^2=0.933) of the dextran series was seen (Table 4.4). A similar study by Wolkers et al., (2004) showed that a range of carbohydrates of various sizes exhibit a positive linear correlation with the Tg. The observation was attributed to an increase in the average length of the hydrogen bonds with increasing Tg.
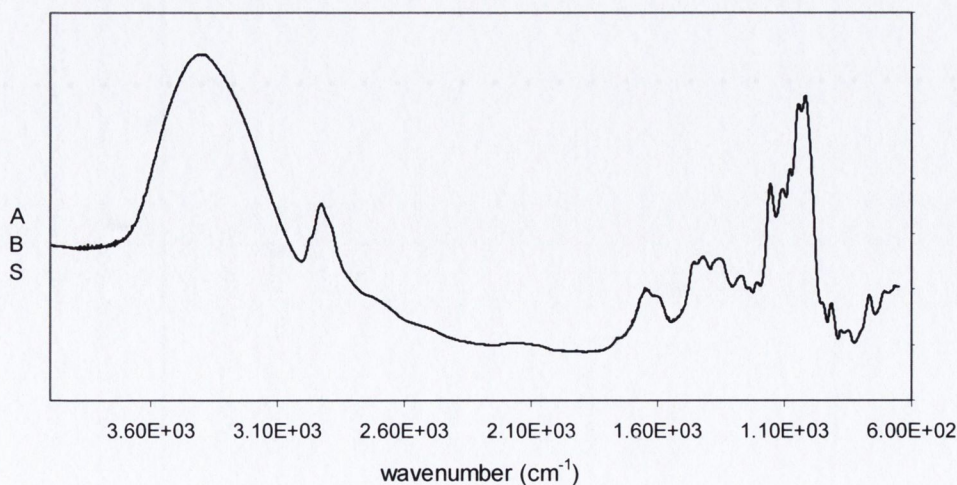
Figure: 4.37: FTIR spectra for Dextran (D4).

117

Table 4.11: Properties of linear polymers PNP, PNP2 and PLA with various model compounds.

	Melting temperature Tm (°C)	Glass transition temperature Tg (°C)	Tg/Tm	Density (gcm^{-3})	Partial solubility parameters (MPa)$^{1/2}$[a]			
					δ	δ_d	δ_p	δ_H
PLA$_{-2}$	149	88	0.59	-------	29.63	20.80	18.42	10.30
PNP-L	----	110.92	-----	1.104	20.96	17.84	8.27	7.27
PNP2-L	----	90.59	------	1.075	22.54	19.63	6.58	8.91
Diltiazem HCl	212.48	102.38	0.48	0.890	-------	--------	------	------
Diltiazem Base	87.17	28.17	0.32	0.966	22.27	20.44	4.86	7.39
Salicylic acid	159.60	36.04	0.22	1.419	28.74	21.40	7.0	17.87
Indomethacin	161.56	47.6	0.29	1.389	20.77	18.5	4.61	8.24
Dextran MW 4000[b]	---	177.74	-----	0.851	46.24	26.00	17.92	33.82
Dextran MW 10000[b]	----	209.22	----	0.732	46.24	26.00	17.92	33.82
Dextran MW 40000[b]	----	218.99	----	0.716	46.24	26.00	17.92	33.82
Dextran MW 70000[b]	----	221.40	----	0.732	46.24	26.00	17.92	33.82

(a) The calculated partial solubility parameters were estimated using Hoftzymer/Van Krevelen method and the molar volumes of Fredors (Van Krevelon, 1990) (Section 3.3.9).

(b) Coughlan et al., 2005

Drug solubility was determined in phosphate buffer as described in Section 3.3.7. The rise in temperature increased the solubility of each model drug. This would be expected since a rise in heat facilitates the dissolving reaction by providing energy to break bonds in the solid. Table 4.11 further displays the melting point, glass transition temperature, density and estimated partial parameters of each compound.

The partial solubility parameters of each of the model drugs and the linear polymers were determined by a method of Hoftyzer-Van Krevelen (Van Krevelen, 1990). This technique is a useful tool to determine the compatibility or miscibility of drugs/excipients and polymers [Hancock et al., 1997]. According to the concept, the solubility parameter is a measure of the specific intermolecular interactions which is separated into three different types of partial solubility parameters: dispersion, polar and hydrogen bonds. When the solubility parameters of two materials are similar, they will be mutually and thermally soluble (Hancock et al., 1997). Greenhalgh et al., (1999) categorised excipients based on differences between solubility parameters of excipients and drugs ($\Delta\delta$). It was concluded that substances with $\Delta\delta<7.0MPa^{1/2}$ were likely to be miscible, whereas those with $\Delta\delta>10MPa^{1/2}$ were likely to be immiscible.

The estimated solubility parameters given in Table 4.11 for the smaller molecular weight drugs were likely to be miscible with PNP, PNP2 and PLA although in the case of SA, the partial solubility parameters revealed significant differences in the hydrogen forces and each of the polymer systems. The total partial solubility parameters of the dextrans were estimated using one repeating monomer unit of glucose. These values predicted immiscibility between the dextrans and the polymer systems. The estimated solubility parameters were also calculated for the hydrogels using one repeating monomer unit [Appendix IV]. These values predicated immiscibility or solubility of the gel in water as described in Section 3.3.9.

CHAPTER 5:

AN INVESTIGATION INTO THE DEGRADATION AND RELEASE KINETICS FROM A SERIES OF GELS SYNTHESISED BY VARYING THE MOLAR RATIO OF PNIPAAM TO PLA (MW 2000).

5.1 INTRODUCTION:

The present chapter investigates the influence of both structural (polymer composition, mesh size) and environmental parameters (temperature) on the degradation behaviour of the gels. The properties of these polymers and their susceptibility to degradation were investigated at two different temperatures by swelling, Scanning Electron Microscopy (SEM), Fourier Transform Infrared Spectroscopy (FTIR), pH studies and acid–base titrations. For comparisons, the hydrolytic degradation of low molecular weight linear PLA (MW2000) tablets immersed in PB 7.4 at both 20°C and 37°C were studied as described in Section 3.8. The engineered delivery systems will be examined in relation to controlled and sustained release of model drugs at both 20°C and 37°C. The effect of the hydrolytic degradation of the gels on the versatility of the drug release will also be examined.

5.2.1: SWELLING AND HYDROLYTIC DEGRADATION OF PNIPAAM-CO-POLY (LACTIC ACID) (MW2000) BASED HYDROGELS

An integral aspect of hydrogel properties is their swelling behaviour in water. Temperature can affect degradable hydrogels in a complex manner: directly through degradation kinetics and indirectly through the swelling behaviour. Previously in chapter 4 the swelling kinetics and equilibrium-swelling ratio during the initial stages of immersion in PB (up to 3 days) for the hydrogels series were discussed. Figure 5.1(a) shows the continuation of the experiment over a two-month time frame, with the swelling ratio (S.R.) plotted as a function of time at 20°C.

In the case of PNIPAAM water diffuses into the network, pushing the chains apart causing swelling. When the water diffusing into the gel is balanced, the stretching equilibrium of the chains is reached and no further swelling occurs. However after 2 months a decline in mass was observed. Previous studies by Torchilin et al., (1977) noted degradation of poly (vinylpyrrolidone) (PVP) hydrogels slowly by hydrolysis of the crosslinker (BIS) and degradation was sensitive to the concentration of BIS employed.

(a)   (b)
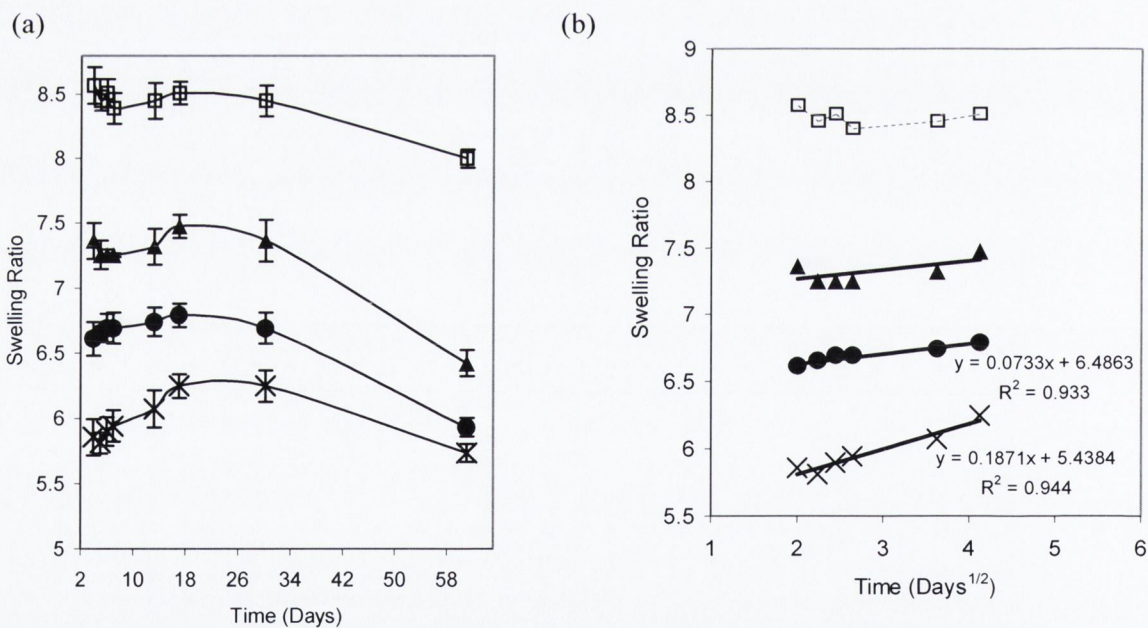
Figure 5.1(a) Swelling ratio plotted against time for the hydrogel series: PNP (□), PNP1-2 (▲), PNP2-2 (●), PNP3-2 (X) at 20°C (b) The swelling ratio plotted against the square root of time for PNP (□), PNP1-2 (▲), PNP2-2 (●), PNP3-2 (X) hydrogel systems.

The swelling ratios as a function of time for the co-polymers are displayed in Figure 5.1(a). In contrast to the pure PNP system, in the early stages of the experiment, a continual uptake in water is seen (15 days) for the co-polymeric systems. Since the main influence on the swelling

ratio (S.R.) is the molecular weight between crosslinks; as degradation occurs lactide ester linkages are cleaved throughout the gel and the ongoing cleavage of these crosslinks within the gel systematically decreases the crosslinking density of the overall network thereby increasing the swelling ratio. After a period of 1-2 months the network cannot sustain itself and a significant decline in the swelling ratio is observed.

The initial swelling ratio (≤15 days) is plotted as a function of the square root of time in Figure 5.1(b). PNP showed no statistical differences in the S.R. In the case of the co-polymers the data was fitted to equation 2.22 (Higuchi, 1961) in order to compare degradation kinetics. The higher the PLA content the more significant the increase in the swelling ratio in the first 2 weeks indicative of the rate of degradation.

Variations in temperature as previously seen will affect the Flory-Huggins interaction parameter (Flory 1953) (Equation 3.3), which was shown to reduce the swelling of the hydrogels with increasing temperature. Reductions in swelling are likely to affect the rate of degradation of the hydrogels. Figure 5.2 displays the continuation of the swelling experiments conducted in chapter 4 (Section 4.4.3) over a two-month time frame, with the swelling ratio (S.R.) plotted as a function of time at 37°C. In the initial phase (~9 days) a continual uptake of medium is seen for the co-polymeric systems. This can be attributed to the mass uptake of medium replacing the slow degradation of PLA at this temperature. As the duration of immersion of the co-polymeric systems in PB increases, a decline in the swelling ratio is observed. In contrast the homopolymer, PNP, remains constant as a function of time. On comparing the results with swelling studies undertaken at 20°C (Figure 5.1), a more significant decrease is seen in the S.R. below the LCST indicating that degradation is faster at 20°C. This can be attributed to the hydrophilic state of the polymer below the LCST.
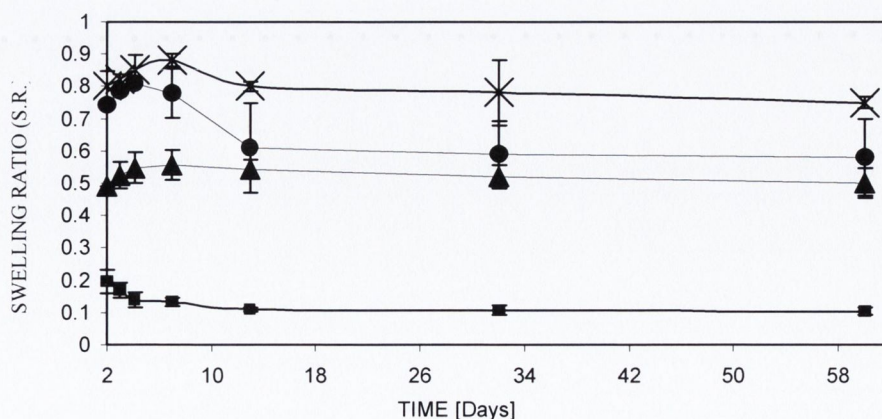
Figure 5.2: Swelling ratio as a function of time for the hydrogel series PNP (■), PNP1-2 (▲), PNP2-2 (●) and PNP3-2 (x) at 37°C.

At the end of the swelling studies (60 days), the gels were removed, reweighed and dried under vacuum. Mass losses of 21.5%, 30.38% and 40.00 % (w/w) was observed for PNP1$_{-2}$, PNP2$_{-2}$ and PNP3$_{-2}$ respectively at 20°C. At 37°C a slower rate of degradation led to a mass loss of 13.34%, 25.59% and 33.05% (w/w) for PNP1$_{-2}$, PNP2$_{-2}$ and PNP3$_{-2}$ gels respectively. The molar ratios (weight) used to synthesise the gels are presented in Table 4.2 (PNP1$_{-2}$ (84-16 w/w), PNP2$_{-2}$ (76-24 w/w), and PNP3$_{-2}$ (56-44 w/w)). A greater mass loss was observed below the LCST than the weight of PLA present in PNP1$_{-2}$ and PNP2$_{-2}$ systems indicating that PNIPAAM chains are also being cleaved in the degradation process.

5.2.2 FTIR Analysis of degradation media of the hydrogel systems

FTIR analysis was also conducted on the degradation medium of the hydrogel systems in order to detect the possible presence of PLA and/or PNIPAAM fragments in the swelling medium reflecting hydrolysis of the co-polymers (Section 3.3). At 20°C, Evidence for the presence of PNIPAAM was detected in all PB media solutions by the presence of the amide 1 and 2 bands at 1670 cm^{-1} and 1540 cm^{-1} respectively (Figure 5.3). Similarly the peaks at 1388 cm^{-1} and 1371cm^{-1} are characteristic of the isopropyl groups. Thus it is possible that PLA undergoes hydrolysis, leading to scission of NIPAAM units in the co-polymeric systems and their release into the PBS solution. PNP also revealed PNIPAAM fragments in the degradation medium, which could be the result of the crosslinker degrading (Torchilin et al., 1977) (Appendix VI).
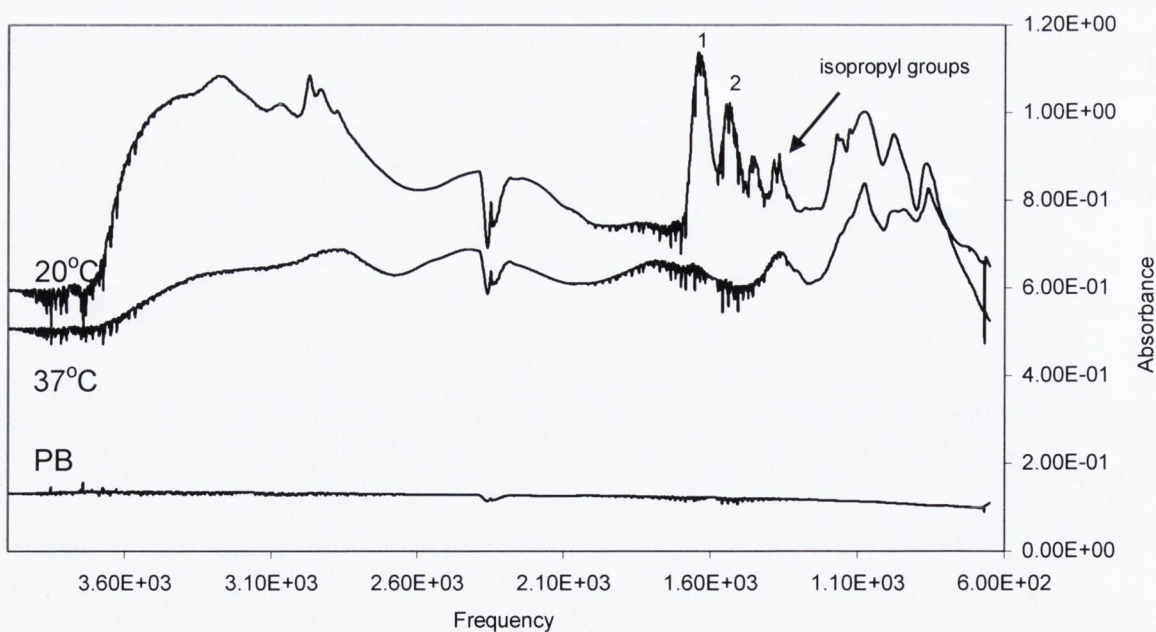
Figure 5.3: FTIR analysis of degradation medium from the swelling studies at 20°C and 37°C for the co-polymer PNP3$_{-2}$ (where 1 and 2 represents the amide bands of PNIPAAM) and the buffer medium used before studies was undertaken.

For the two component hydrogels, PNP1$_{-2}$, PNP2$_{-2}$ and PNP3$_{-2}$, the C=O stretching band at 1720 cm^{-1} was detected for all systems suggesting the presence of the carboxylic acid in the aqueous medium and indicative of hydrolytic cleavage of the ester bond of the PLA component in the three dimensional hydrogel systems. As the percent of PLA incorporated into the hydrogel backbone increased the peak intensity became stronger at 1720cm^{-1}. Similarly IR peaks at 1638 cm^{-1} and 1411cm^{-1} were attributed to the C-O asymmetric stretching and C-O symmetric stretching of the carboxylate respectively. They were stronger in intensity as the ratio of PLA incorporated into the backbone increased. The IR peak 1160 cm^{-1} (O-CO stretching) was weakly present in the 85-15 NIPAAM-PLA system and increased in intensity the more PLA present. An extra peak at 1117cm^{-1} (CH (CH$_3$)=O stretching) also was apparent in the media of the polymeric systems with higher amounts of PLA present. The increase in absorption was noted in all systems of the gels at 20°C suggesting degradation occurs faster below the LCST. These results were in agreement with the mass loss observed in Section 5.2.1.

At 37°C, the presence of PNIPAAM within the degradation media was not clearly visible, however overlapping of PLA and PNIPAAM is possible in the lower region of the spectrum (1100-600 cm^{-1}). The spectra showed three strong absorption bands at 1080, 988, and 863 cm^{-1} which can be assigned to the -CO- stretch, the -C-C- stretch and the -C-COO- stretching of PLA respectively. The collapsed hydrophobic state of the gel at this temperature may lead to physical entrapment of PNIPAAM within the hydrogel once the bonds have been cleaved. The absorption spectrum of the swelling medium is characteristic of that of PLA (Figure 5.12) with the -CH- deformation bands visible in the region of 1450-1350cm^{-1} and the carboxylic group in the region of 1800-1700cm^{-1}.

5.2.3. pH studies indicative of degradation of the hydrogel systems

The pH of the medium was monitored during swelling studies of the gels at 20°C. PLA polymers degrade in aqueous media to acidic oligomers and ultimately lactic acid. Figure 5.4 shows the change in pH of each of the hydrogel systems as a function of time, the decrease in pH is consistent with degradation of PLA. The higher the percent of PLA, the greater the drop in pH over time. Simultaneously swelling increased as the pH decreased (Figure 5.1) indicating disruption to the porous network, leading to a higher degree of porosity (See section 5.2.5).
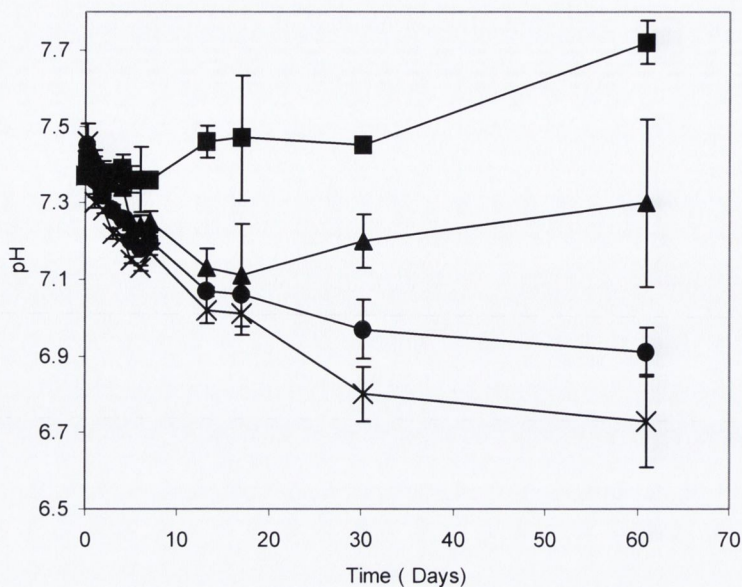
Figure 5.4: Degradation behaviour of hydrogels series: PNP (■), PNP1-2 (▲), PNP2-2 (●), and PNP3-2 (x) as a function of pH at 20°C.

The concentration of acid in the aqueous medium was calculated as a function of time by employing Equation 5.1

$$pH = -\log[H^+]$$

EQN. 5.1

Where;

pH= measured pH of degradation medium over time

$[H^+]$= concentration of acid in degradation medium

Figure 5.5 illustrates early time release of LA into the swelling media indicative of the increase in degradation over time. An increasing trend is seen whereby the larger amount of PLA incorporated in to the backbone of the gel the greater the rate of degradation. The rate of degradation of each system characteristic of zero order kinetics gave reasonable fit with R^2 values of 0.9577, 0.9482 and 0.9011 for PNP1-2, PNP2-2 and PNP3-2 respectively. It is well known that degradation is accelerated by an autocatalytic action of carboxylic acid end groups in poly lactic acid (Olewnik et al., 2007). The ester bonds in the backbone of the polymer can break randomly to generate carboxyl groups. Consequently the decrease in molecular weight packing density accelerates the penetration of water molecules between molecular chains resulting in a higher degradability.
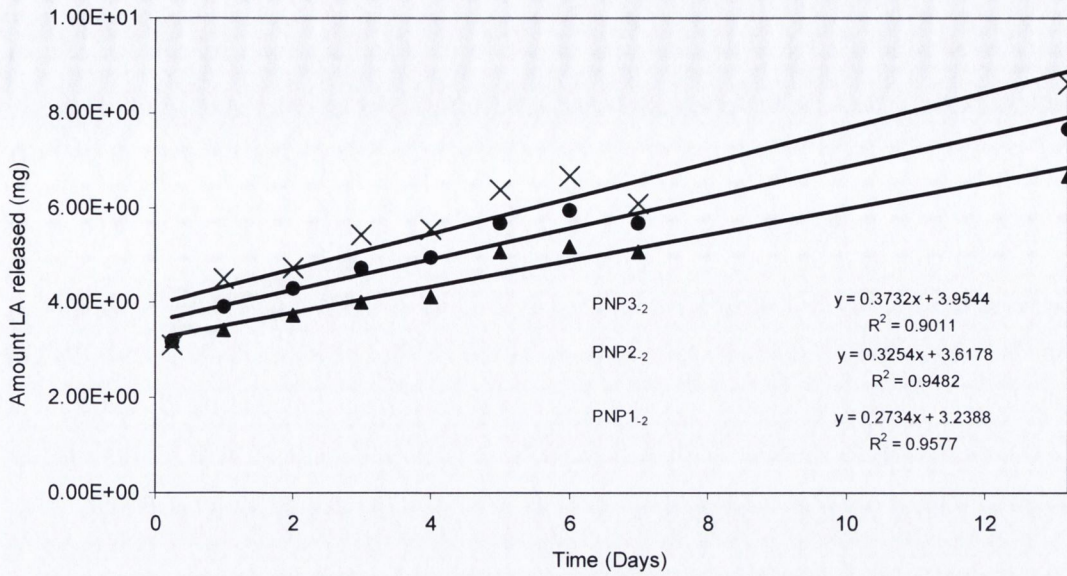
Figure 5.5: The concentration of LA within degradation media as a function of time for PNP1$_{-2}$ (▲), PNP2$_{-2}$ (●) and PNP3$_{-2}$ (x) hydrogel systems at 20°C.

Figure 5.6 shows the degradation rate constant plotted against the hydrogel composition. A trend emerged whereby the higher the amount of PLA incorporated into the hydrogel system, the larger the zero order degradation rate constant. The decrease in molecular packing density as a result of degradation would lead to an increase in water uptake; this could attribute to a higher rate of degradation the higher the amount of PLA incorporated in to polymer network.
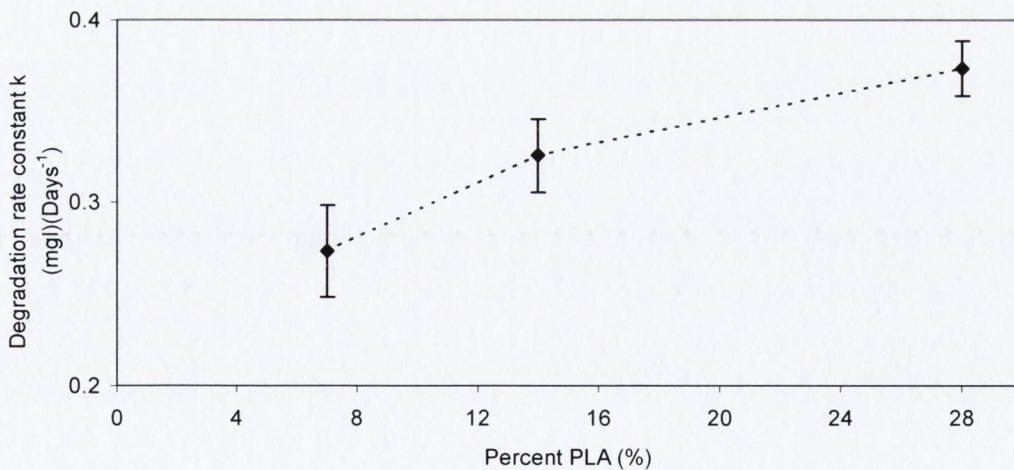
Figure 5.6: Relationship between the hydrogel composition and the degradation rate constant of the hydrogel systems.

5.2.4 Acid-Base Titrations of degradation media

Previously in Section 5.2.1 temperature was shown to play an important role in the rate of degradation. After 2 months acid base titrations were preformed on the degradation media to calculate the concentration of lactic acid present (Figure 5.7). The higher the percent of PLA incorporated into the gel, the faster degradation occurred. Also degradation was faster below the LCST due to the hydrophilic state of the polymer. The effect of the temperature on the rate of hydrolysis can be seen in Figure 5.7 where a 2.9, 2.0 and 1.7 fold increase in the amount of PLA in the degradation medium was present at 20°C for PNP1$_{-2}$, PNP2$_{-2}$ and PNP3$_{-2}$ respectively. At 37°C, a combined effect of a larger swelling ratio and increasing PLAM content in the gel led to a greater amount of PLA being released into the media. These results suggest both temperature and water absorption are important in controlling degradation behaviour.
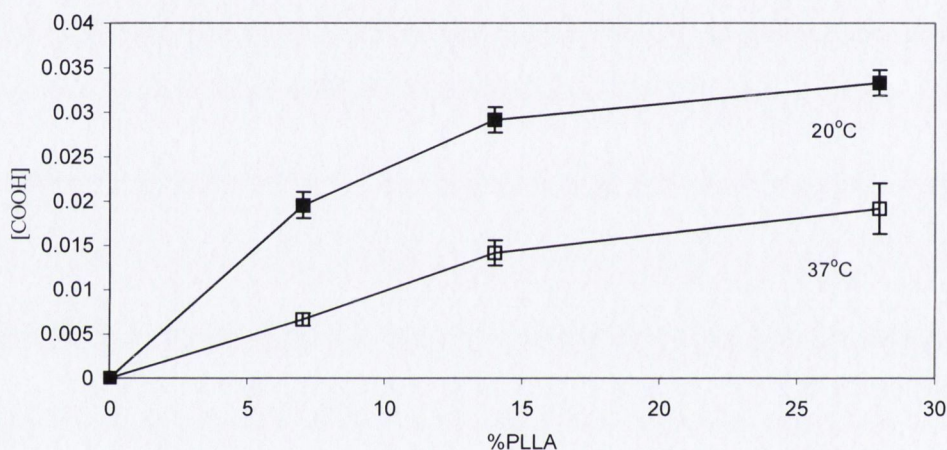
Figure 5.7: Relationship between the % PLA in the hydrogel systems and the [COOH] in the degradation medium at 20°C (■) and 37°C (□).

The molar concentration of LA released into the swelling medium was used to determine the amount of LA degraded from each hydrogel system. At 20°C a total of 88 mg, 138 mg and 148mg LA were present after 2 months for PNP1$_{-2}$, PNP2$_{-2}$ and PNP3$_{-2}$ respectively. At 37°C a slower rate of degradation led to 30 mg, 66 mg and 86mg LA present in the medium after 2 months for PNP1$_2$, PNP2$_{-2}$ and PNP3$_{-2}$ respectively. The overall weight loss was determined relative to that of the initial weight of the dry hydrogel discs and an 18%, 26% and 34% weight loss was observed below the LCST while only 6% 12.4% and 19.77 % weight loss was observed above the LCST.

5.2.5 Scanning electron microscopy (SEM)

The effect of incorporating PLA into the hydrogel systems on the morphology of the polymeric networks after two months in the release medium at 20°C is shown in Figure 5.8. Also freshly polymerised systems are shown for comparison relative to that of the degraded systems. The higher the amount of PLA present, the greater the porosity and loss in the structural integrity within the hydrogel, consistent with hydrolytic degradation of PLA resulting in larger pore size. Similarly a greater difference is seen between the systems of higher PLA content when comparing SEMs performed before and after degradation, indicating the hydrolytic cleavage of PLA.

The results of Imagetool were employed in an attempt to quantify pore sizes after degradation to compare with those calculated for freshly synthesised systems (Section 4.4.7). Table 5.1 summaries the hydrogel macropore sizes determined by SEM.

Table 5.1: Calculated pore size (average diameter) before and after degradation.

Hydrogel	Molar ratio PLA (%)	Observed pore size (μm) before degradation	Observed pore size (μm) after 60 days	Change in pore size due to degradation
PNP	0	8.52 ± 1.70	9.80 ± 1.05	1.28
PNP1$_{-2}$	7	5.79 ± 1.01	7.71 ± 1.58	1.92
PNP2$_{-2}$	14	3.94 ± 0.98	6.19 ± 1.16	2.25
PNP3$_{-2}$	28	2.82 ± 0.68	8.91 ± 2.46	6.09

A trend is evident whereby the higher the content PLA the larger the increase in the pore size as a result of hydrolytic degradation (Table 5.1). The results are in rank order with the degradation rate constants calculated in section 5.2.3 (Figure 5.9 (a)). An exponential increase in the pore size after degradation was observed the greater the amount of PLA incorporated into the hydrogel systems (Figure 5.9(b)).

(a i)

(b i)

(a ii)

(b ii)

(c i)

(d i)

(c ii)

(d ii)
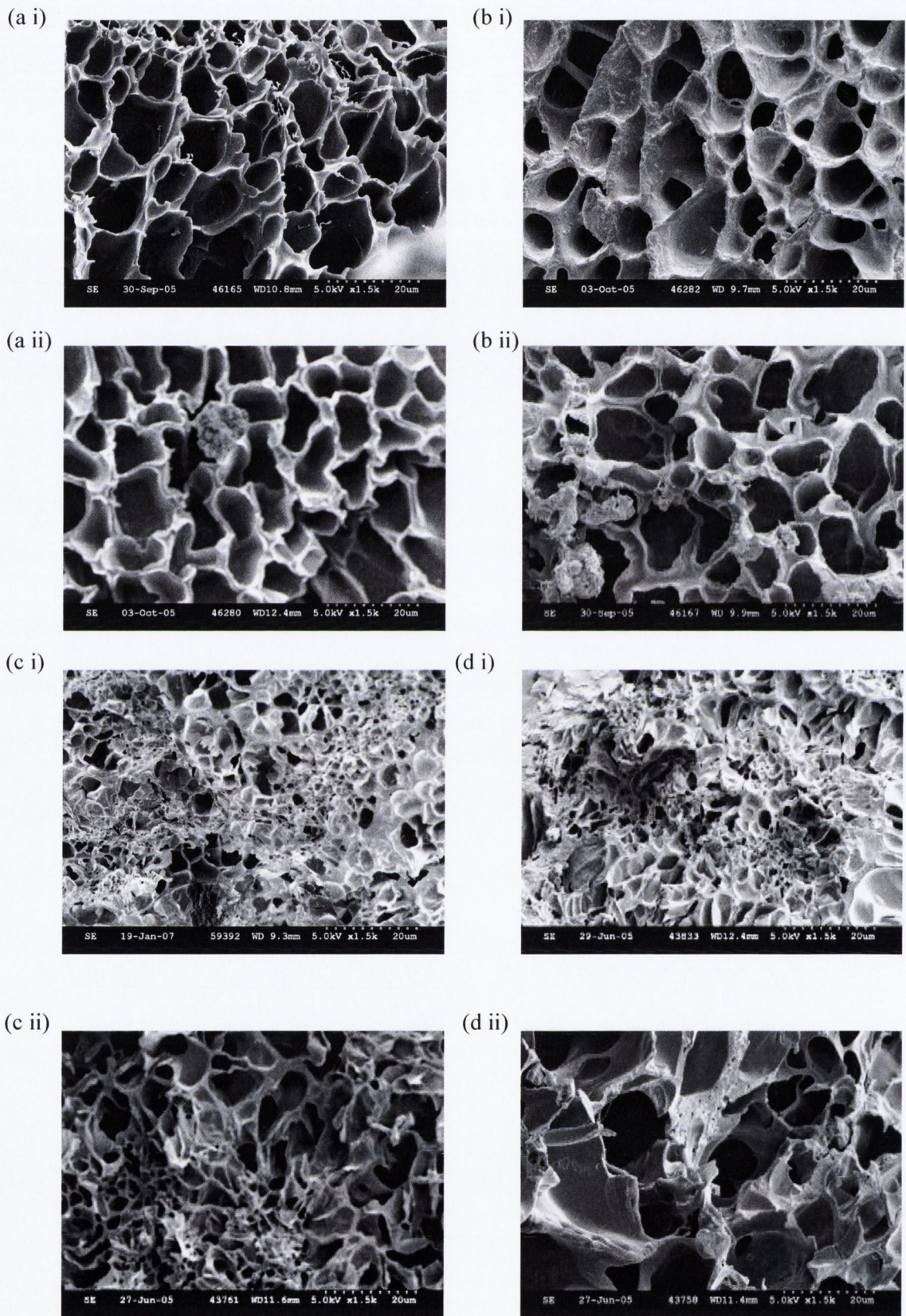
Figure 5.8: SEM images (x500) of (a) PNP, (b) PNP1$_{-2}$ (c) PNP2$_{-2}$ and (d) PNP3$_{-2}$ before (i) and after (ii) degradation studies undertaken at 20°C.

(a)

(b)

$y = 1.2336e^{0.0546x}$

$R^2 = 0.9724$
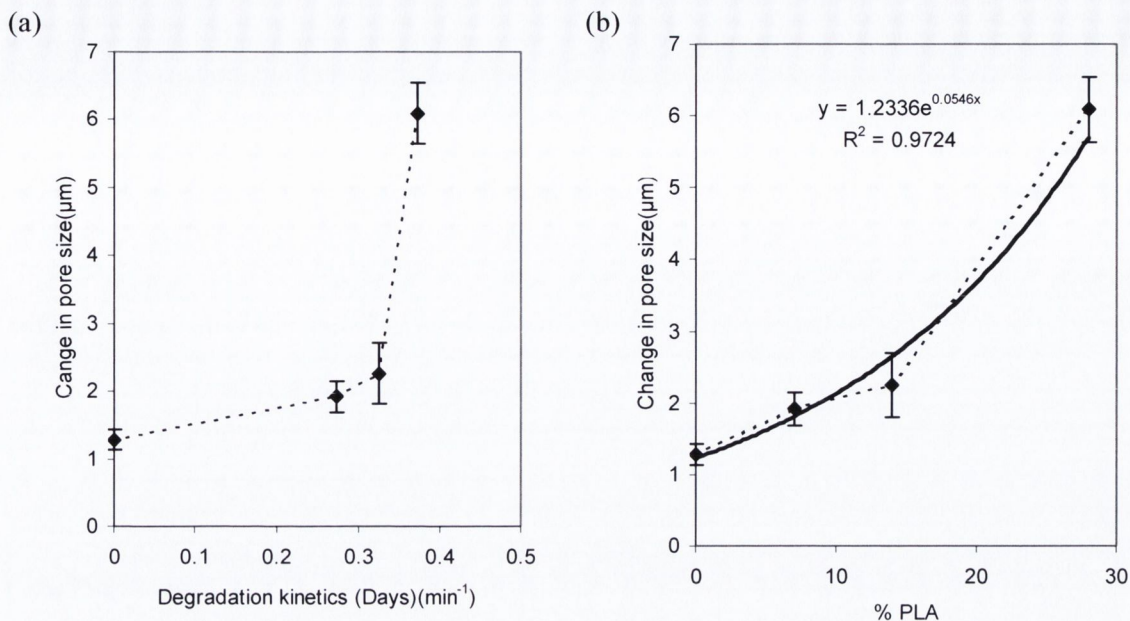
Figure 5.9: (a) Relationship between the degradation kinetics and change in pore size

(b) Relationship between hydrogel composition and the change in pore size

In Section 5.2 the ester concentration and the number of intact crosslinks within the network degraded resulted in a continuous mass increase until the network could not sustain itself. A relationship existed between the swelling ratio and the [COOH] detected in the swelling media at 20^0C (R^2=0.9874) and 37^oC (R^2=0.9974) suggesting that the degree of swelling plays an important role in the degradation behaviour.

SEM images revealed a higher degree of porosity after degradation reflective of degradation of crosslinks within the network. FTIR was successful as a qualitative method in identifying PNIPAAM and PLA in the degradation medium. pH studies and acid base titration were successful as a quantitative method in determining the amount of PLA present within the swelling media. Both the degradation rate constants and the extent of degradation of the gels were dependant on the temperature, composition and chemical nature of the gels.

5.2.6 Hydrolytic degradation of poly (Lactic acid) (MW2000)

In the following section the degradation of PLA will be examined for comparisons with that of the co-polymeric hydrogel systems.

5.2.6.1 Swelling and hydrolytic degradation of poly (Lactic acid) (MW2000) in aqueous solution

The swelling of PLA$_{-2}$ tablets in terms of buffer uptake at 20°C is illustrated in Figure 5.10 (a) as well as the sorption in terms of Mt/M∞ versus the square root of time (Figure 5.10 (b)). This expression was selected in order to examine the applicability of Fick's law (EQN 2.22).
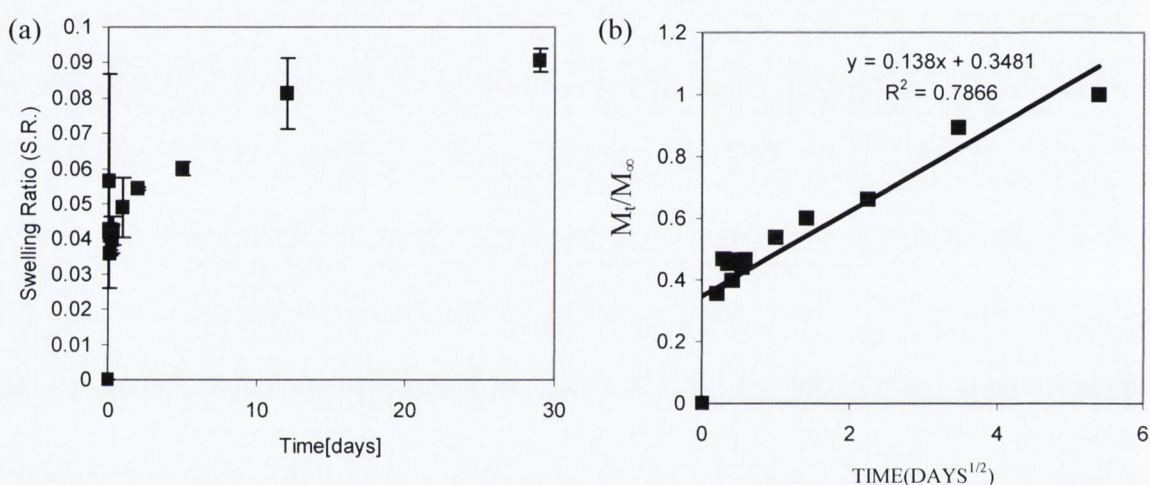
Figure 5.10: (a) Swelling behaviour of PLA$_{-2}$ as a function of time at 20°C (b) Fraction swelling of PLA$_{-2}$ against the square root of time.

In Figure 5.10(b) poor linearity is evident even in the first stages of sorption (R^2=0.7866). This behaviour can be attributed to some degradation of low molecular weight material, which will greatly influence the water transport procedure. Also changes in average molecular weight and molecular weight distribution are likely to strongly affect the value of the diffusion co-efficient. As a result increased weight reflects an increase in water uptake reflective of degradation.

In the case of PLA, the reaction rate for hydrolysis is usually temperature dependent (Andrepoulous et al., 2001), the rate increasing with an increase in temperature. From the curve in Figure 5.11 (a) it is clear that sorption reaches a maximum and a weight decrease is recorded leading to a value even lower than the original dry PLA samples. This is due to the degradation of the polymer at 37°C. A poor fit was seen when fraction swelling was plotted against the square root of time (Figure 5.11 (b)). At both temperatures swelling kinetics of PLA was not adequately described by Fickian diffusion.

132

Since equilibrium is not reached by this material the stability of weight found after a few days could simply suggest that the rate of sorption and degradation become equal at that time (Andreopoulous et al., 2001).

(a) (b)
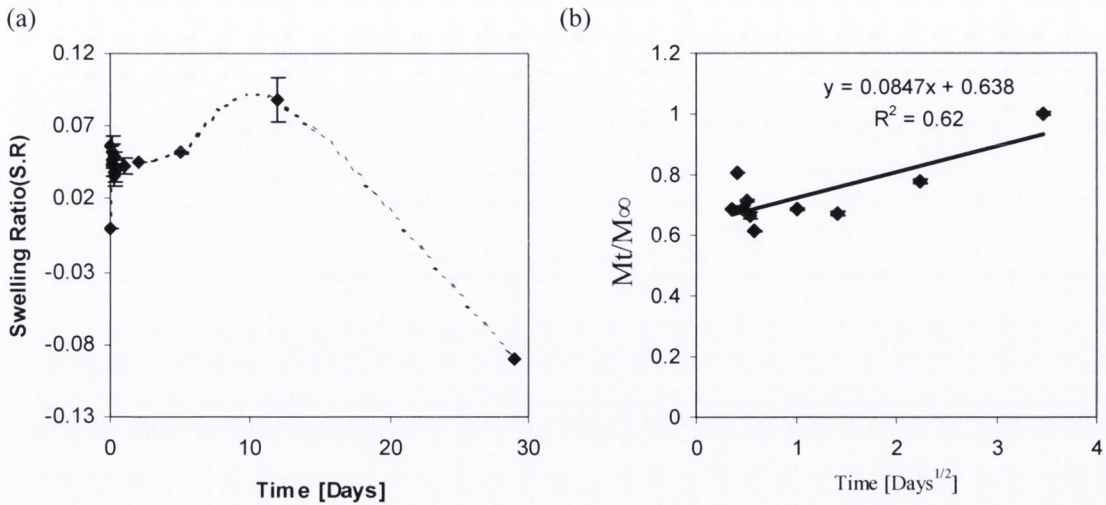
Figure 5.11: (a) Swelling behaviour of PLA (MW 2000) at 37°C

(b) Swelling Behaviour fitted to the square root of time (Higuchi, 1961).

5.2.6.2 FTIR analysis of degradation medium

The hydrogel degradation study was also investigated using ATR-FTIR technique (Section 3.3.2). Figure 5.12 shows the IR spectra of the PB in which the PLA samples were immersed for 2 months at both 20°C and 37°C. IR analysis for PLA was previously examined at five regions as outlined in Figure 4.1.
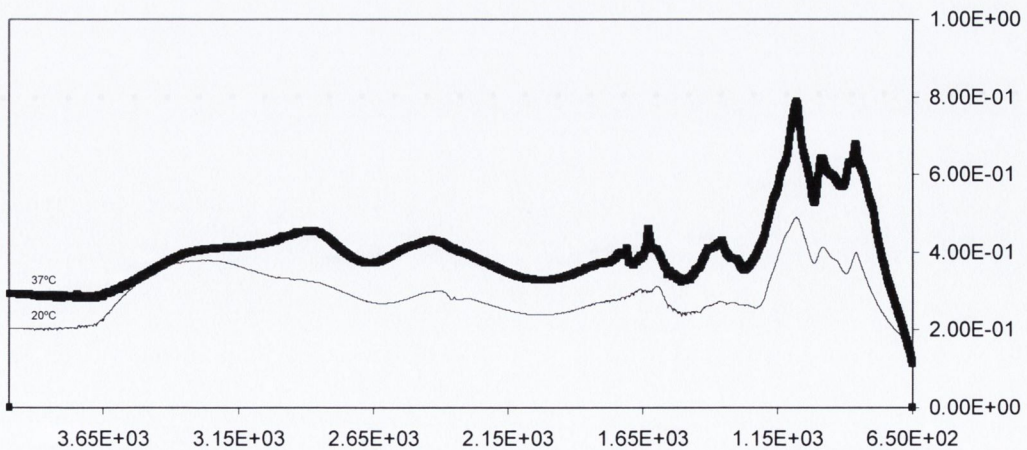
Figure 5.12: FTIR spectra of degradation media after immersion of PLA discs in PB at 20°C and 37°C for 2 months.

133

The spectral evaluation in the region of the carbonyl stretching vibrations between $1800cm^{-1}$ and $1600cm^{-1}$ revealed some characteristics of ester bands. In addition formation of new bands at near frequencies i.e.$\pm10cm^{-1}$ is apparent. Acetaldehyde has been identified as a reaction intermediate for the hydrolysis of lactic acid (Li et al., 1999). It is well known that C=O stretching vibrations of aldehydes are observed at lower frequencies (1750-1700 cm^{-1}) than ester bands. Therefore the new band could be attributed to the formation of the aldehyde group. An additional band is located at $1640cm^{-1}$, which is characteristic of the bending vibration of water. It can be observed that the absorbance of the band at 1640 cm^{-1} is relatively larger than that at 1740 cm^{-1} indicating that water held a large portion of the active sites on PLA surface. This effect is more prominent in the degradation medium at 37^oC (Zhang et al., 2004).

The -CH- deformation bands were visible in the region of 1450-$1350cm^{-1}$. The original polymer has characteristic peaks at 1268 cm^{-1}, 1194 cm^{-1}, 1130 cm^{-1}, 1093 cm^{-1} and $1047,cm^{-1}$ for the -CO- ester linkage (Figure 4.1(a)). The -C-O- ester linkage, the site of hydrolysis was found to be significantly different from the original polymer after degradation. A significant increase in the intensities as well as the area under the curve (AUC) was observed. The spectra showed three strong absorption bands at 1080, 988, and $863cm^{-1}$ which can be assigned to the -CO- stretch, the -C-C- stretch and the -C-COO- stretching of PLA respectively (Kister, 1995). It has been reported that the –C-C- stretch is sensitive to the crystallinity of the polymer. Iannace et al., (2001) and Agarwal et al., (1998) observed an increase in the crystalline/amorphous phase of the polymer during hydrolysis of PLA, which was attributed to the erosion of the less thermodynamically stable crystals within the polymer. The significant increase in the AUC and intensities may be a result of a change in the degree of crystallinity of the polymer, as hydrolyic cleavage of the ester bonds occurs.

5.2.6.3 Acid-Base Titrations of PLA swelling medium

The concentration of PLA detected within the swelling media was quantified employing acid-base titration's using phenolphthalein as an indicator. The concentration [COOH] at 20 and 37^oC detected within the media was 0.015625 and 0.04 mol/L respectively. These results were used to calculate the mass LA present within the degradation medium giving values of $0.07g$ (35%) and $0.18g$ (90%) respectively indicating that ~2.5-fold increase was seen on increasing the temperature in the rate of degradation.

5.2.7 Conclusions:

From the present study it can be concluded that degradation of hydrogel series can be manipulated by controlling monomer molar ratios of the reactants and temperature at which degradation studies are conducted. At both 20°C and 37°C, a higher rate of degradation was observed for PNP3$_{-2}$.

As expected, the linear PLA appeared to degrade faster at 37°C, which is reflected in the amount of LA detected within the swelling media of the PLA discs. However on comparison with that of the co-polymers degradation was faster below the LCST on co-polymerisation with NIPAAM due to increase in the water uptake leading to hydrolysis. This is reflected in [COOH] detected within the degradation media after swelling studies. In contrast pure PLA degrades faster than the co-polymers at 37°C which is seen by comparing the [COOH] in the swelling media. Therefore a reversal in the role of temperature on the rate of degradation was seen by the introduction of the thermoresponsive unit, NIPAAM.

5.3 Model Drug release

In this study PNP2-2 was chosen to examine the release of model compounds at 20°C and 37°C. The effect of the temperature on the rate of dissolution of pure drug discs was compared to release profiles of the model compounds from the degradable hydrogel both above and below the LCST. The release profiles were also examined in relation to hydrogel pore size (Mc, chapter 4).

5.3.1 Effect of temperature on drug dissolution:

Solubility of the model drugs was examined at both 20°C and 37°C. The influence of the temperature on the rate of dissolution of the pure drug substances was investigated. Pure drug discs (100mg) (8mm) were prepared as described in Section 3.3.8 and dissolution studies were carried out in 900ml PB at 20°C and 37°C. The dissolution profiles obtained are shown in Appendix III. The dissolutions profiles obtained were fitted to the Hixon-Crowell cube root law (EQN 2.14) to give the dissolution rate constants shown in Table 5.2. An estimate of the ratio of the dissolution rate constant at 37°C and 20°C is also given in Table 5.2.

Table 5.2: Cube root dissolution rate constants (k_c, equation 2.14) at 20°C and 37°C and associated co-efficient of determination (CD).

	20°C			37°C			$k_{c37}:k_{c20}$
	Solubility in PB (mg/ml)	k_{c20} $(min^{-1})(x10^2)$	C.D	Solubility in PB (mg/ml)	k_{c37} $(min^{-1})(x10^2)$	C.D.	
DH	422 ± 6.45	20.98 ± 0.0080	0.9976	562 ± 32.61	25.57 ± 0.013	0.9947	1.21:1
DB	1.99 ± 0.03	0.029 ± 0.0024	0.9067	3.43 ± 0.12	0.131 ± 0.018	0.8817	4.51:1
SA	2.00 ± 0.09	0.861 ± 0.0056	0.9996	8.18 ± 0.42	1.141 ± 0.014	0.9982	1.32:1
IDM	0.56 ± 0.10	0.015 ± 0.0014	0.8409	1.16 ± 0.06	0.068 ± 0.003	0.9394	4.53:1
D4	*very soluble	**5.022 ± 1.908	0.9971	*very soluble	**4.178 ± 0.891	0.9942	0.8:1
D10	*very soluble	**1.477 ± 0.1373	0.9931	*very soluble	**2.435 ± 0.099	0.9975	1.6:1
D40	*very soluble	**0.744 ± 0.0320	0.9910	*very soluble	**1.128 ± 0.127	0.9937	1.5:1
D70	*very soluble	**0.691 ± 0.0092	0.9225	*very soluble	**0.883 ± 0.011	0.9922	1.3:1

*Martindale 1996

**Coughlan 2005

For the hydrophobic series of drugs, the solubility increased in the order IDM, DB, SA and the dissolution rate constants (k_c) exhibited a linear dependence on solubility at 37°C (Table 5.2). In addition a linear relationship existed for the dissolution rate constants k_{c37} and k_{c20}. A 1.3 to 4.5–fold increase in the dissolution rate was obtained for the hydrophobic drugs on increasing the temperature (Table 5.2).

The dissolution rate of the hydrophilic drugs was more rapid than for the hydrophobic series as expected due to their higher aqueous solubility. DH had the highest aqueous solubility at both temperatures. Studies undertaken by Coughlan et al., (2004) showed a significant decrease in the dissolution rate with increasing molecular weight of the dextran series at both temperatures (Table 5.2). This would be expected since a smaller diffusional co-efficient on increasing molecular weight would lead to a slower rate of dissolution.

5.3.2 Release of smaller molecular weight compounds from PNP2.₂

The release of various model drugs from PNP2.₂ was examined at both 20°C and 37°C in 900ml PB. The fraction released over 8 hours for DH, SA and IDM at 20°C and 37°C are shown in Figure 5.13. The complete release profiles (72 hours) are shown in Appendix VII. The fraction released at both temperatures was plotted against the square root of time (Higuchi, 1961) to give the release rate constant k_{dh20} and k_{dh37} (Table 5.3).

(a)

(b)
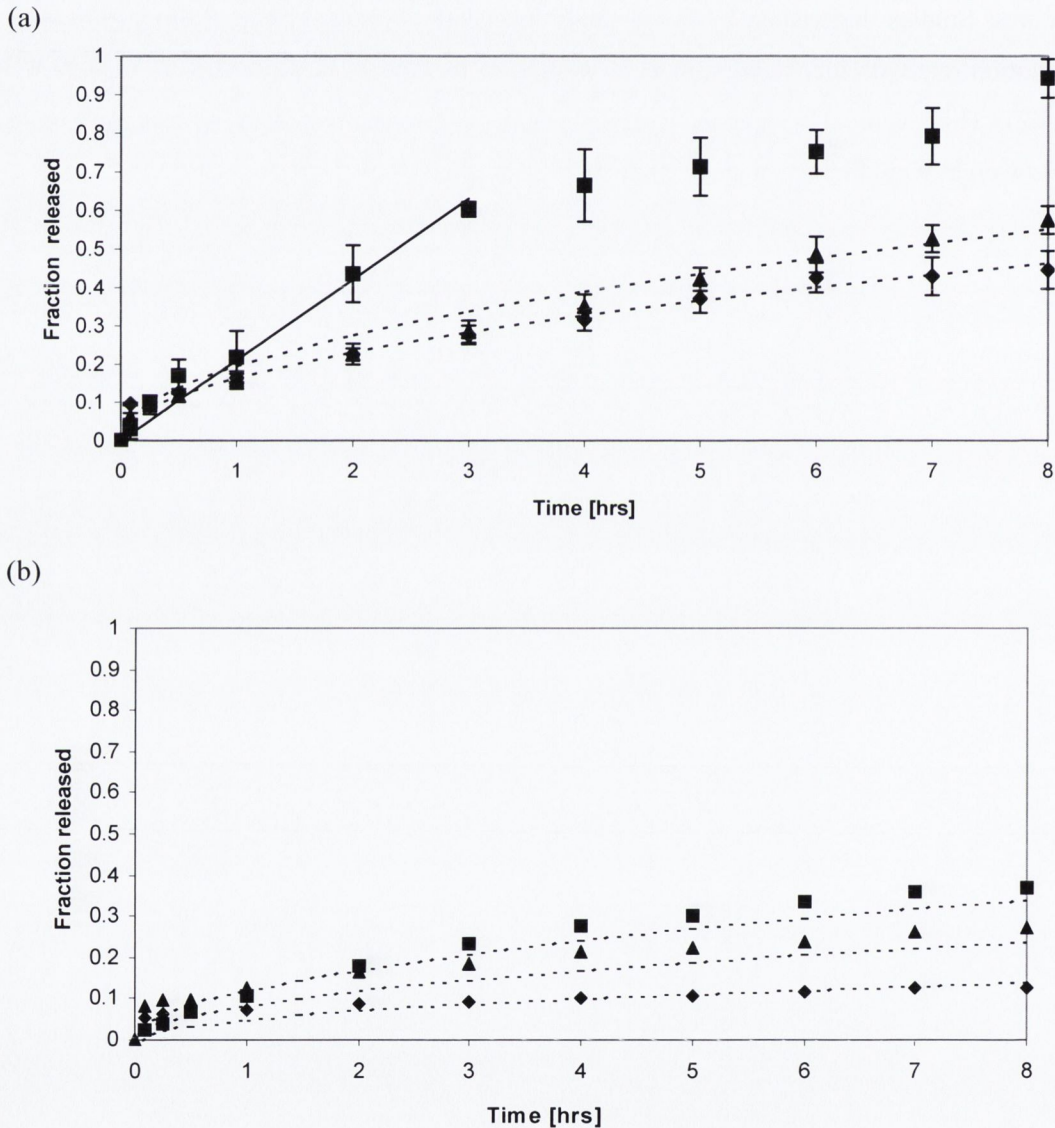
Figure 5.13: Plot of the fraction DH (■), SA (▲) and IDM (♦) released over time in PB at (a) 20°C and (b) 37°C. DH was fitted to zero order kinetics (solid line) at 20°C. Dashed line represents the data fitted to the square root of time (Higuchi, 1961).

138

Table 5.3: Release rate constants (k_{dh}) at 20°C and 37°C calculated using equation 2.22(Higuchi, 1961) along with their associated coefficients of determination (CD). Also shown are the diffusional exponents (n) and release rate constants (k_{dp}) calculated using the power law equation 2.25(Peppas, 1985).

20°C	k_{dh20}(min$^{0.5}$)(x10^2)	CD	k_{dp20}(min^{-1})(x10^2)	n ±s.d.	C.D	k_{dh37}:k_{dh20}
DH	3.889 ± 0.292	0.9282	1.00 ± 0.241	0.7867± 0.0548	0.9930	0.34:1
IDM	2.112 ± 0.400	0.9851	2.65 ± 0.406	0.4597± 0.0283	0.9875	0.24:1
SA	2.830 ± 0.075	0.9803	1.75 ± 0.366	0.5880± 0.0379	0.9882	0.46:1
37°C	k_{dh37}(min$^{0.5}$)(x10^2)		k_{dp37}(min^{-1})(x10^2)			
DH	1.3415 ± 0.059	0.9236	2.60 ± 0.488	0.4051± 0.0283	0.9671	
IDM	0.5080 ± 0.041	0.5881	2.31 ± 0.261	0.2792± 0.0165	0.9714	
SA	1.3290 ± 0.054	0.9064	3.85 ± 0.303	0.3099± 0.0130	0.9898	

Sustained release of the drugs was achieved at both temperatures with a lack of swelling at 37°C significantly slowing the release (p<0.05) of the model drugs relative to that at 20°C. The release rate constants increased as the solubility of the model drugs increased at both temperatures. The ratios between k_{dh37} and k_{dh20} are also shown in Table 5.3 indicative of the ability of the gel to thermally control the release of drug.

The drug release from the semi-biodegradable hydrogel at 20°C and 37°C was also examined using the power law equation (Equation 2.25, Peppas 1985), where the diffusional exponent was estimated. This equation gave a better fit to the data compared with equation 2.22, (Higuchi, 1961) and it reflects the contribution of swelling to the release mechanism. At 20°C, there was an increase in the diffusional exponent towards unity as the solubility of the drugs increased. At 37°C an increase in the diffusional exponent also occurred with increasing solubility. The diffusional exponents were higher at 20°C than 37°C due to the greater contribution of the swelling process on the rate of release (Figure 5.14 (a)).
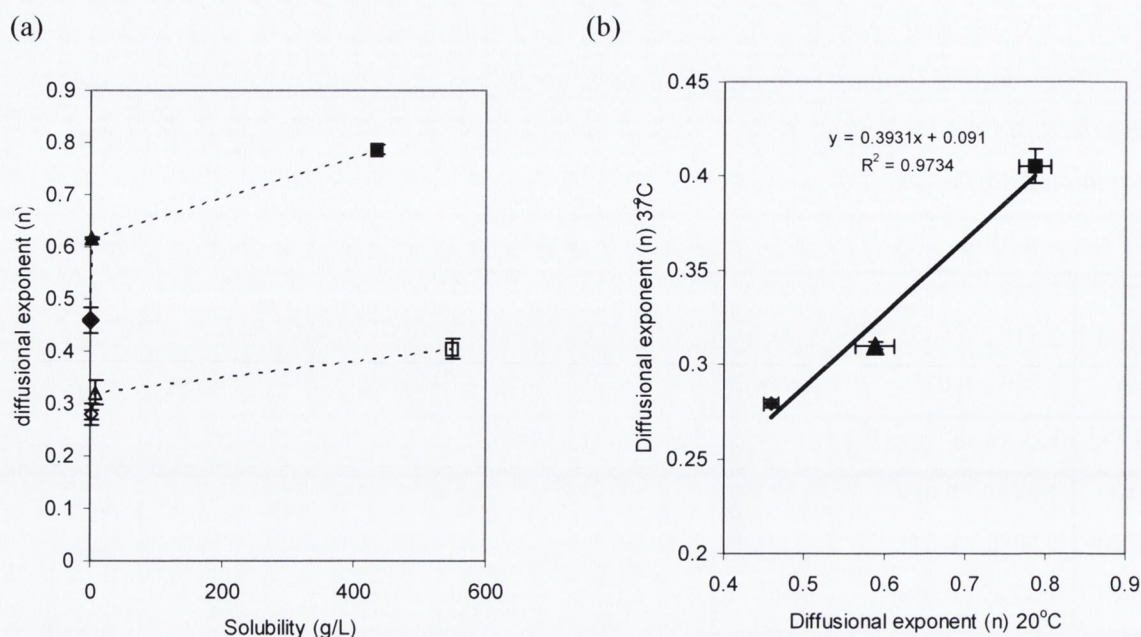
Figure 5.14: (a) Plot of diffusional exponent (n) at 20°C (closed symbols) and 37°C (open symbols) against drug solubility for IDM (♦), SA (▲) and DH (■). (b) Relationship between diffusional exponent (n) at 20°C and 37°C for IDM (♦), SA (▲), DH (■).

At 37°C, the drug release rate was less significant than at 20°C due to the low swelling rate and the residual level of swelling reached by the hydrogel at that temperature. Over a longer time frame, IDM had a slow sluggish release, which started to level off once 20% of the loading was released. A similar effect was observed with SA once ~70% release was achieved (Appendix VII). Both model drugs had a dramatic effect in the suppression of the S.R. and the rate of swelling compared to unloaded gels (chapter 7). It is likely that a drug-polymer interaction is reducing the release of the drug. The estimated time taken for 50% release was calculated using the release rate constants obtained in Table 5.3 and compared to the time taken for 50% dissolution of the model compounds. An effective 3.5 (IDM) to 8-fold (DH) reversal of thermal control of drug diffusion (decrease in drug dissolution) was achieved. The extent of the control was solubility dependant with least control of IDM.

At 20°C, the release mechanism varied from Fickian diffusion for IDM to anomalous diffusion for SA and DH. As the solubility of the model compounds increased the diffusion exponent increased towards unity indicative of zero order kinetics. Due to the hydrophilic state of the gel, the total drug release occurred much quicker compared to release profiles at 37°C ranging from 24hrs to 72 hrs for DH and IDM respectively. After 24 hrs the release rate of SA levelled off with only 80% of the loading released and no subsequent release was seen. The acid dissociation constant (Table 4.10) of each model compound appeared to play a role in determining the time of total drug release at both temperatures. During the timescale studied

(96hrs) SA did not reach total drug release at either temperature. Controlled drug release of SA has been studied using different types of formulations, such as PLA tablets and poly (ethylene oxide) (PEO) hydrogels (Andreopolous et al., 2001, Savas et al., 2001). The release rate from PLA tablets of various molecular weights was investigated. This also found that increasing the SA loading increased the rate of release however the total delivery time was the same for all samples studied. This was attributed to interactions of SA with the polymeric matrix PLA, where hydrolysis was likely to be promoted by the presence of an acidic substance. Savas et al., (2001) similarly noted that release of various model compounds from PEO hydrogels depended on the strength of association between PEO and the active substances. The formation of hydrogen bond was attributed to the interaction between H donor and acceptor functional groups. In addition Coughlan and Corrigan (2004) noted binding between model compounds (benzoates) and PNIPAAM. The effect of the binding on the hydrogel was clarified in relation to LCST and swelling kinetics. Drug release rates were shown to be dependent on the drug binding properties.

The ability to thermally control the release of drug from biodegradable matrix was most successful with IDM, followed by DH and SA. The drug-polymer interactions played an important role in determining the extent of drug release at both temperatures. SA-polymer interactions prevented total release of the loaded drug at either temperature. The possibility of the surrounding environment changing due to the acidic nature of the degrading hydrogel networks may also reduce the drugs solubility leading to a reduced affinity for the external medium. This resulted in temperature having a less significant effect on release. Thermal control of the release rate of IDM was most successful. This could be attributed to the entrapment of IDM at 37°C within the hydrophobic PLA domains.

5.3.3 Dextran release from PNP2_{-2}:

The fractions released over time of the dextrans are shown in Figure 5.15. A much greater release was observed at 20°C for all dextran fractions in comparison to release at 37°C. The release profiles all gave poor fits when plotted against the square root of time. Examination of the release profiles reveals no trend or molecular weight gradient dependency (p>0.05) on the rate of release. When the diffusional exponent, n, was allowed to vary better fits resulted (Table 5.4).

Table 5.4: Release rate constants (k_h) at 20°C calculated using equation 2.22 along with their associated coefficients of determination (CD). Also shown are the diffusional exponents (n) and release rate constants (k_p) calculated using the power law equation 2.25 (Peppas, 1985).

20°C	$k_{h20}(min^{-0.5})(x10^2)$	CD	$k_{p20}(min)(x10^2)$	n ± s.d	CD
D4	3.45 ± 0.037	0.4790	19.07 ± 1.40	0.1974 ± 0.163	0.9847
D10	7.17 ± 0.731	0.7530	17.25 ± 4.05	0.2845 ± 0.060	0.9263
D40	3.48 ± 0.145	0.9290	07.93 ± 0.57	0.3451 ± 0.138	0.9938
D70	5.64 ± 0.641	0.5457	20.79 ± 1.71	0.2095 ± 0.019	0.9937

A trend was observed for the first three dextran fractions of the series ($\leq$ 40,000Daltons) and the rate of release. The higher molecular weight dextrans would be expected to give slower release rate than D4 as a result of a slower diffusional co-efficient and a greater hindrance of release. In the present study the release rate increased the smaller the MW dextran with the exception of D70.

In chapter 4 it was observed that the greater the molecular diameter of the dextrans fractions the more difficulty they had with accessing the pores within the hydrogel network (~40Å). This may explain the higher release rate of D70 (98 Å) where a large portion of the pores where not accessible to the molecular probe, leading to drug on the surface of the matrix. In addition drug-polymer interactions between the dextrans and the polymer may cause the reduction in the release rate. The duration taken for complete drug dissolution was dependent on MW with the smaller MW taking the least time (Figure 5.15 (a)). The diffusional exponents were all significantly less then 0.5 indicative of potential drug–polymer interactions. Furthermore in chapter 7 the effect of loading dextran in the hydrogel system led to a significant impact on the swelling kinetics, which could in turn be influencing the release rates.

At 37°C, a sharp burst release of the dextran fractions were observed in the early time period (<0.5hrs) (Figure 5.15 (b)). This can be attributed to drug present on the surface of the matrix.

There was no further release after the burst effect due to the hydrogel pore size (~9Å) being smaller than the molecular diameter of the dextrans (25Å to 98Å) (Coughlan and Corrigan, 2004). Therefore the effect of the higher temperature was to stop the release of the relatively larger soluble dextrans.
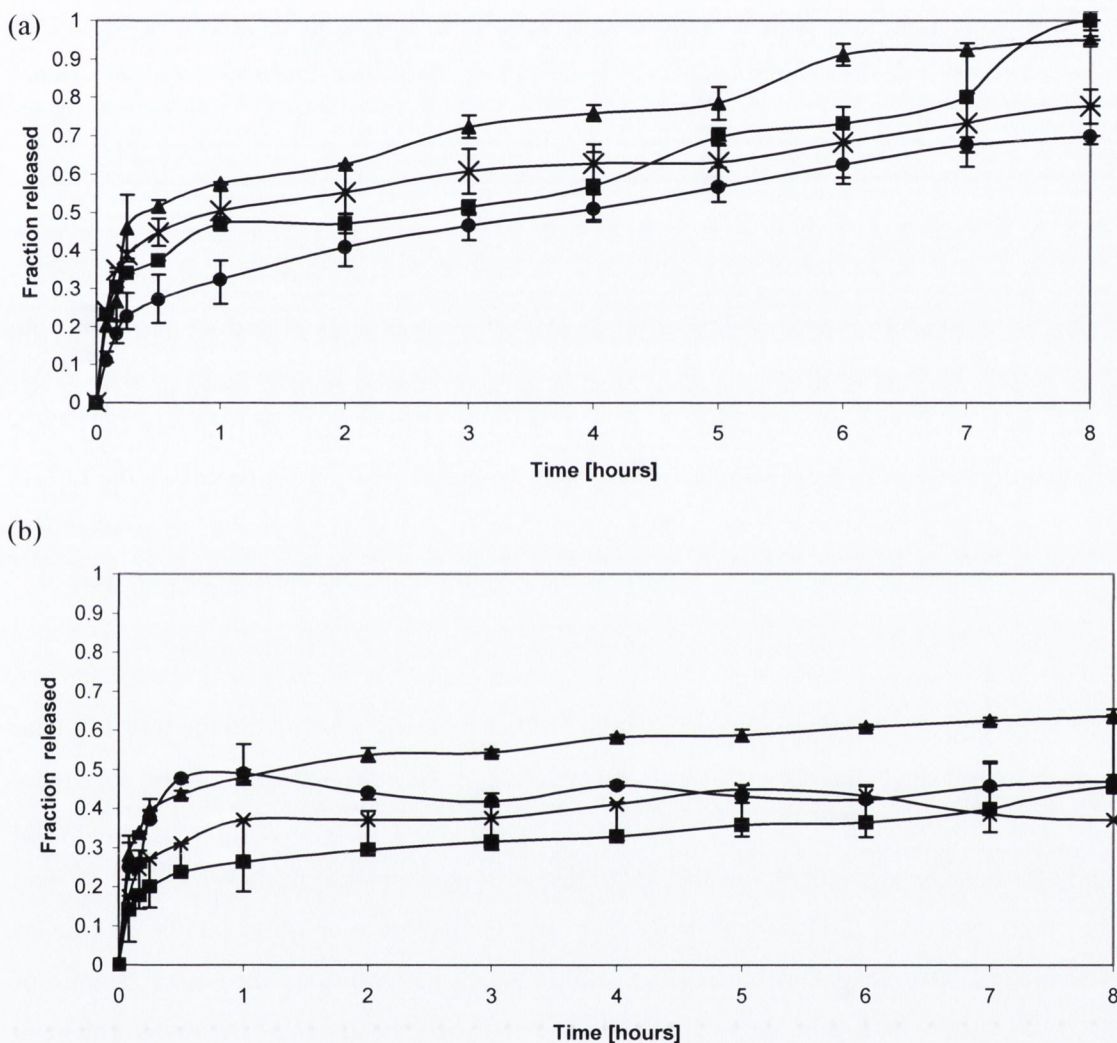
Figure 5.15: (a) Plot of dextran fraction released over time at 20°C (b) fraction dextran released over time at 37°C. [D4 (■), D10 (▲), D40 (●), D70 (x)].

The present study showed that the drug release rate from a thermoresponsive-co-biodegradable hydrogel depended on the temperature and the nature and size of the model drug used. From these experiments predictions of the release rate as well as the ability to control the extent of drug release can be made at both temperatures with potential to predict the pattern of pulsatile release.

Increasing the temperature increased both the solubility and intrinsic dissolution rate of the model drugs as expected. In contrast, increasing the temperature decreased the ability of the hydrogel to swell and decreased the rate of diffusion as well as the diffusional exponent of the drug from the system. In thermoresponsive systems these two temperature effects counteract one another and an effective reversal of thermal control resulted. The magnitude of this reversal was particularly dependent on drug size, where drugs with molecular diameter >20Å (dextrans) were not released at the higher temperatures during the timescale studied. However the incorporation of large drugs into a tightly crosslinked network such that the molecules cannot pass through the network pores will result in degradation controlled release if surface/bulk erosion occurs and the network size will increase allowing the drug to diffuse into the medium.

The smaller MW compounds (molecular diameter ≤8 Å) were small enough to permeate through the matrix however solubility and polymer–drug interactions played an important role in determining the extent of release. DH was diffusion controlled. However after 3 days IDM, SA and DH reached 20, 50 and 80% release respectively. The diffusional exponents (n) were n<0.5 is reflective of the entrapment or interactions formed within the matrix above the LCST. A levelling off of the drug release rate in both SA and IDM suggest the physiochemical properties of the drugs could be controlling the degree of swelling and the degradation rate.

At 20°C, the dextran series showed no obvious trend during early time release probably due to a molecular size gradient formation during loading. After the early time period the larger bulkier dextran fractions displayed slower release rates as would be expected. In spite of the highly swollen gel (~4μm) at 20°C the mechanism and duration of release for the smaller molecular weight drugs were dependent on the solubility of the series as well as degree of acid dissociation. Release of IDM was diffusion controlled in contrast to non-Fickian release kinetics of SA and DH. The release of SA levelled off at 80% of the total drug release. In the case of acidic drugs one can expect faster hydrolysis of the ester bonds in PLA based polymers (Tarvainen et al., 2006).

5.4 AN INVE5TIGATION INTO THE EFFECT OF PLA CONTENT ON THE RELEASE KINETICS FROM PNIPAAM-*CO*-PLA HYDROGELS.

The drug release studies presented in Section 5.3 were preformed using PNIPAAM-co-PLA (86-14 molar ratio respectively) hydrogel with PLA MW 2000. Three other hydrogel systems were also synthesised by varying the molar ratios of PNIPAAM to PLA; the homopolymer PNP PNP1$_{-2}$ (93-7), and PNP3$_{-2}$ (72-28).

Studies by Peppas et al., (1985) have shown the importance of crosslinking in controlling the mesh size and therefore the rate of drug release from swellable devices. Generally the release of solutes from non-degradable hydrogels follows first order kinetics (Van Dijkhuizen-Radersma et al, 2005). However increasing the crosslinking density decreases the mesh size at a molecular level leading to a smaller volume available for solute transport. Omidian et al., (1998) and Kabiri et al., (2003) have shown changes in the swelling kinetics of hydrogels due to increased crosslinking density.

For degradable polymers, other release profiles may be obtained such as zero order kinetics or delayed release (Dijkhuizen-Radersma et al, 2005). Degradation of the matrix may increase the mesh size, which will increase the diffusion co-efficient. In addition release rate may be altered due to erosion and/or pore formation. In chapter 4, the swelling studies at 20°C showed a decrease in the swelling rate on increasing the PLA content. At 37°C, a reverse trend was seen whereby a greater effective pore size was observed in PNP3$_{-2}$ at equilibrium swelling. In addition Section 5.2 revealed the rate of degradation of the hydrogel series was shown to be faster at 20°C with degradation of the polymer at both temperatures significantly greater the higher the PLA content.

Co-polymerisation of PLA with PNIPAAM resulted in a significant increase in the rate of degradation at 20°C due to the increased hydrophilicity of the matrix relative to that of linear PLA (Section 5.2). The present section examines the release patterns from a series of thermoresoponsive-co-biodegradable hydrogels at 20°C and 37°C.

145

5.4.1 Drug release of smaller molecular weight compounds from the hydrogel series

The release of DH, SA and IDM from the four hydrogels was examined at 20°C and 37°C.

5.4.1.1 DH release from a range of hydrogel systems:

The fraction released of DH over time at both 20°C and 37°C is shown in Figure 5.16. The fraction released was fitted to Equation 2.25 (Peppas, 1985) (Table 5.5) and there was an increase in the diffusional exponent (n) with increasing the amount of PLA at 37°C and 20°C. At 20°C increasing the amount of PLA resulted in an anomalous release pattern, deviating from Fickian diffusion behaviour and resulting in a near zero order release pattern. In order to compare the release rates, the release exponents were fixed as unity and reasonable fits were obtained as shown in Table 5.5.

A plot of the release rate constant of DH against the percent of PLA in the hydrogel systems is displayed in Figure 5.17 both above and below the LCST. There was a significant decrease (R^2=0.9883) in the rate of release with increasing the percent of PLA for the co-polymeric systems. In the early time release the presence of PLA appeared to assist the release DH however after 72hrs PNP3$_{-2}$ had only reached 83% of the total release while PNP and PNP1$_{-2}$ and PNP2$_{-2}$ had 100% of the total loading released (Appendix VIII). Increasing the PLA content within the hydrogel network appears to lead to a stronger interaction between the polymer and drug reducing the drug release rate. The pore size at equilibrium swelling was shown by SEM to decrease as the percent of PLA incorporated into the gel increased. The reduced release rate may be due to a slower swelling rate and a reduced pore size with a higher level of PLA.

At 37°C, above the LCST, release was much slower than at 20°C and increases with increased PLA content, as did polymer swelling (Figure 4.13). In contrast below the LCST, where polymer swelling was much greater, drug release was also faster, but tended to decrease with increased PLA content. This trend was also in line with the change in swelling at 20°C, which decreased with increasing PLA. At 37°C, the diffusional exponents were classified as Fickian behaviour suggesting that the rate of release was significantly slower than that of the polymer relaxation at this temperature. A greater effective pore size with increasing PLA content was observed by SEM suggesting a greater free volume or diffusional space for transport. This was reflected in the release rate constants of DH where a linear dependence on composition was seen with an R^2 value of 0.9403 (Figure 5.17). Only 30–60% release was achieved after 48 hours depending on hydrogel composition. The higher level of PLA may be acting in these systems to prevent complete hydrophobic collapse of the thermoresponsive polymer resulting in a greater effective pore size as the PLA content increased.

Table 5.5: *Release rate constants (k_{dh}) of DH, SA and IDM from various hydrogels at 20 and 37°C calculated using Equation 2.22 (Higuchi, 1961) along with their co-efficient of determination (CD). Also shown is the diffusional exponent (n) and release rate constants (k_{dp}) estimated using equation 2.25 (Peppas, 1985). DH was also fitted to zero order kinetics and release rate constants (k_d) are presented in Table 5.5 below.*

	$F=k_{dh}^{0.5}$		$F=k_{dp}t^n$			$F=k_d t$		
	k_{dh} (min$^{-0.5}$)(x10)	CD	k_{dp}(min^{-n})(X10)	n±s.d.	C.D	k_d(min^{-1})(X10^2)	C.D.	K_{dh37}:k_{dh20}
20°C	k_{dh20}		k_{dp20}					
PNP (DH)	2.43±0.800	0.9572	1.394±0.439	0.5994±0.0604	0.9700	0.135±0.009	0.8539	0.3584:1
PNP1$_{-2}$(DH)	4.16±0.320	0.9269	1.556±0.256	0.7296±0.0686	0.9956	0.457±0.030	0.9393	0.2401:1
PNP2$_{-2}$(DH)	3.88±0.003	0.9107	1.005±0.256	0.7867±0.0126	0.9913	0.350±0.010	0.9670	0.3453:1
PNP3$_{-2}$(DH)	2.96±0.002	0.9310	0.750±0.212	0.7531±0.0698	0.9893	0.188±0.011	0.9589	0.5262:1
PNP (SA)	2.48±0.072	0.9545	2.991±0.776	0.4671±0.0456	0.9565			0.2705:1
PNP1$_{-2}$(SA)	2.52 ±0.040	0.9930	1.851±0.156	0.5545±0.0147	0.9973			0.3170:1
PNP2$_{-2}$(SA)	2.51±0.040	0.9903	1.300±0.232	0.6165±0.0638	0.9906			0.3968:1
PNP3$_{-2}$(SA)	1.45±0.051	0.9311	3.063±0.200	0.3508±0.0106	0.9941			0.6910:1
PNP (IDM)	1.36±0.120	0.6693	0.946±0.025	0.6008±0.0046	0.9997			0.2000:1
PNP1$_2$(IDM)	2.53±0.043	0.9742	1.602±0.221	0.5806±0.0647	0.9935			0.1201:1
PNP2$_2$(IDM)	2.11±0.050	0.9515	2.653±0.428	0.4597±0.0551	0.9920			0.3044:1
PNP3$_2$(IDM)	1.39±0.150	0.7594	0.868±0.047	0.5747±0.0368	0.9984			0.6561:1
37°C	k_{dh37}	CD	k_{dp37}	n±s.d.	C.D	k(min^{-1})(X10^2)	C.D.	
PNP (DH)	0.871±0.040	0.9087	1.498±0.377	0.4358±0.0326	0.9483			
PNP1$_{-2}$(DH)	0.999±0.020	0.8325	2.594±0.897	0.3655±0.0561	0.9078			
PNP2$_{-2}$(DH)	1.340±0.030	0.9236	2.602±0.510	0.4081±0.0284	0.9623			
PNP3$_{-2}$(DH)	1.544±0.020	0.9646	1.769±0.398	0.4784±0.0337	0.9660			
PNP (SA)	0.671±0.060	0.9973	0.860±0.210	0.4996±0.0087	0.9597			
PNP1$_{-2}$(SA)	0.799±0.040	0.8313	2.809±0.228	0.3315±0.0245	0.9889			
PNP2$_{-2}$(SA)	0.996±0.730	0.8650	3.208±0.220	0.3435±0.0241	0.9926			
PNP3$_{-2}$(SA)	1.002±0.019	0.8805	2.915±0.358	0.3572±0.0168	0.9785			
PNP (IDM)	0.272±0.059	0.4724	0.005±.0002	0.8965±0.2440	0.9913			
PNP1$_2$(IDM)	0.304±0.040	0.8155	1.091±0.269	0.3532±0.0903	0.9571			
PNP2$_2$(IDM)	0.408±0.075	0.5968	2.115±0.251	0.2781±0.0167	0.9815			
PNP3$_2$(IDM)	0.912±0.030	0.9375	2.161±0.166	0.3850±0.0104	0.9967			
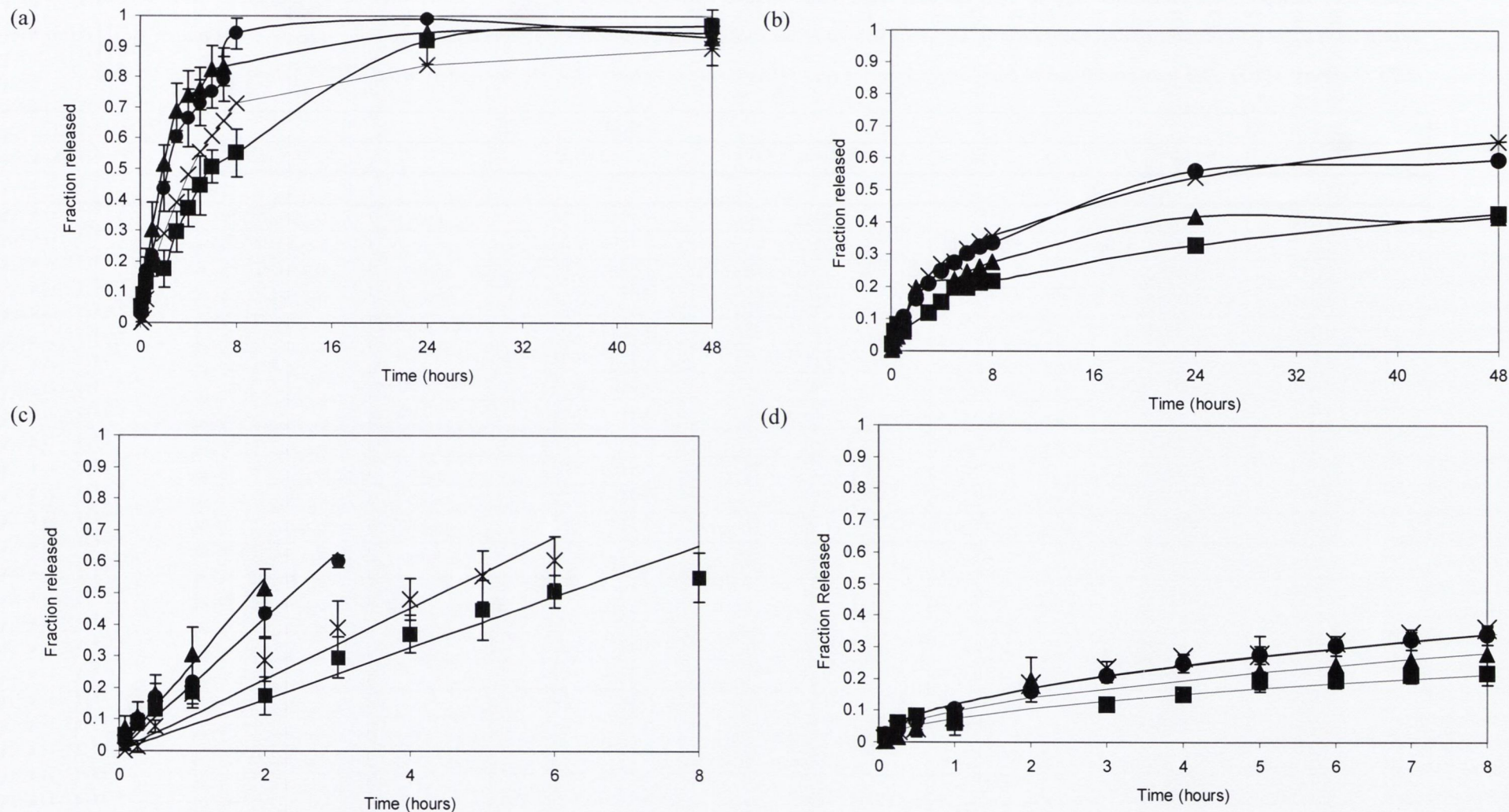
Figure 5.16: The fraction of DH release over time at both (a) 20°C and (b) 37°C from the hydrogel series: PNP (■), PNP1$_{-2}$ (▲), PNP2$_{-2}$ (●) and PNP3$_{-2}$ (x). The fraction released was also fitted to (c) zero order release kinetics at 20°C and (d) Fickian diffusion at 37°C.
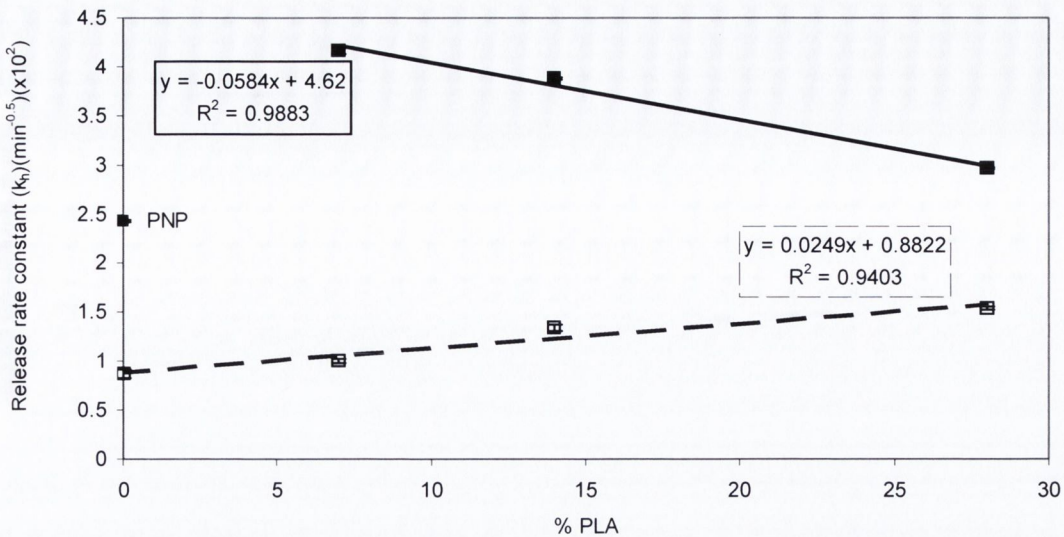
Figure 5.17: Plot of the relationship between hydrogel composition and release rate constant of DH from the hydrogel series at 20 (■) and 37°C (□).

Figure 5.18 displays the relationship between the pore size and the release rate constant. At both temperatures an increase was observed in the release rate with increasing the PLA unit in the gel. At 20°C, a trend was seen whereby the greater the pore size the faster the release rate for the co-polymer systems. At 37°C the lack of dependency on the pore size may be due to the collapsed state of the pores as well as increased polymer drug interactions at this temperature (Figure 5.18). Similar studies carried out on the release of DH from PNIPAAM-co-MAA at 37°C showed release behaviour depends strongly on co-polymer composition (Diez-Pena et al., 2003). Swelling behaviour, polymer–drug interactions as well as drug-solvent interactions play an important role in the release behaviour. This is supported by the slower release rate from PNP in comparison to that of the co-polymers at 20°C (Figure 5.18).
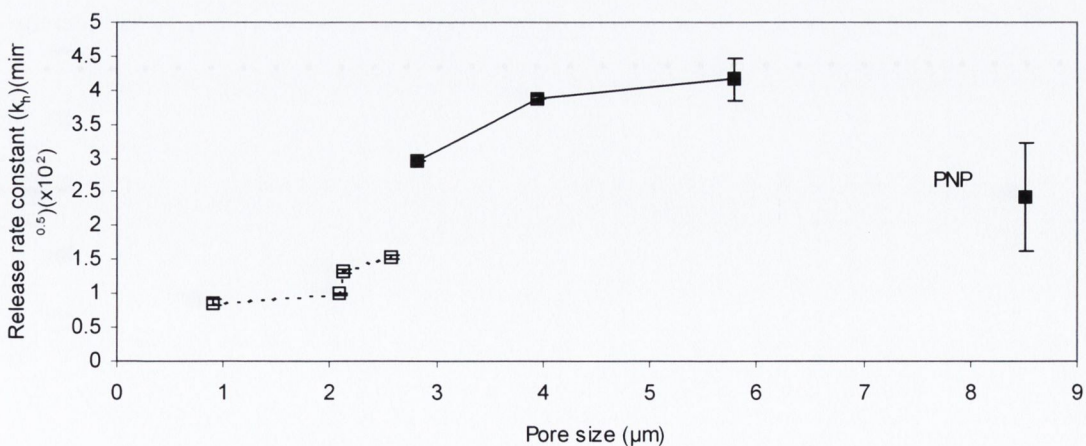
Figure 5.18: Relationship between the pore size and the release rate constant (k_{dh}) of DH at 20°C (■) and 37°C (□).

149

The data in chapter 4 showed that PLA reduced the thermosensitivity of the system, the effect being more pronounced with a higher content of PLA (Table 4.4). The swelling kinetics as well as the equilibrium-swelling ratio further demonstrated the decrease in thermosensitivity at 37°C. The ability to thermally control the release of active substances therefore decreased as the molar ratio of PNIPAAM to PLA decreased. This is reflected by the ratio of the rate constants (k_{dh37}; k_{dh20}) at both temperatures (Table 5.5). The ratio of the release rate constant varied from 0.24 to 0.5 indicative of a significant reduction in the release of the active compounds on increasing the temperature.

The ability to control the release rate constant of the small highly soluble DH from the hydrogel series was achieved by varying the molar ratio of PNIPAAM to PLA. The release profiles were dependent on the monomer content as well as the temperature the experiment was conducted. Above the LCST, both swelling and drug release were diffusion controlled whereas below the LCST, the swelling displayed non-Fickian behaviour and release exponent approached zero order kinetics on increasing PLA content.

5.4.3 SA release from a range of hydrogel systems:

The release profiles of SA at 20°C and 37°C are displayed in Figure 5.19. SA release from the homopolymer PNP was the fastest of all the hydrogels studied at both temperatures. The relatively slower release of SA from the co-polymers was probably due to the entrapment of SA within the hydrophobic PLA domains and drug polymer interactions. In addition, in chapter 4 a slower swelling rate was seen for the hydrogels on increasing temperature to 37°C. Also at 20°C incorporating a higher amount of PLA into the hydrogel network led to a slower rate of water uptake and smaller equilibrium-swelling ratio. These swelling kinetics would be expected to lead to smaller size pores and a slower rate of formation of pores within the network thereby hindering the release of the drug molecules.

(a)

(b)
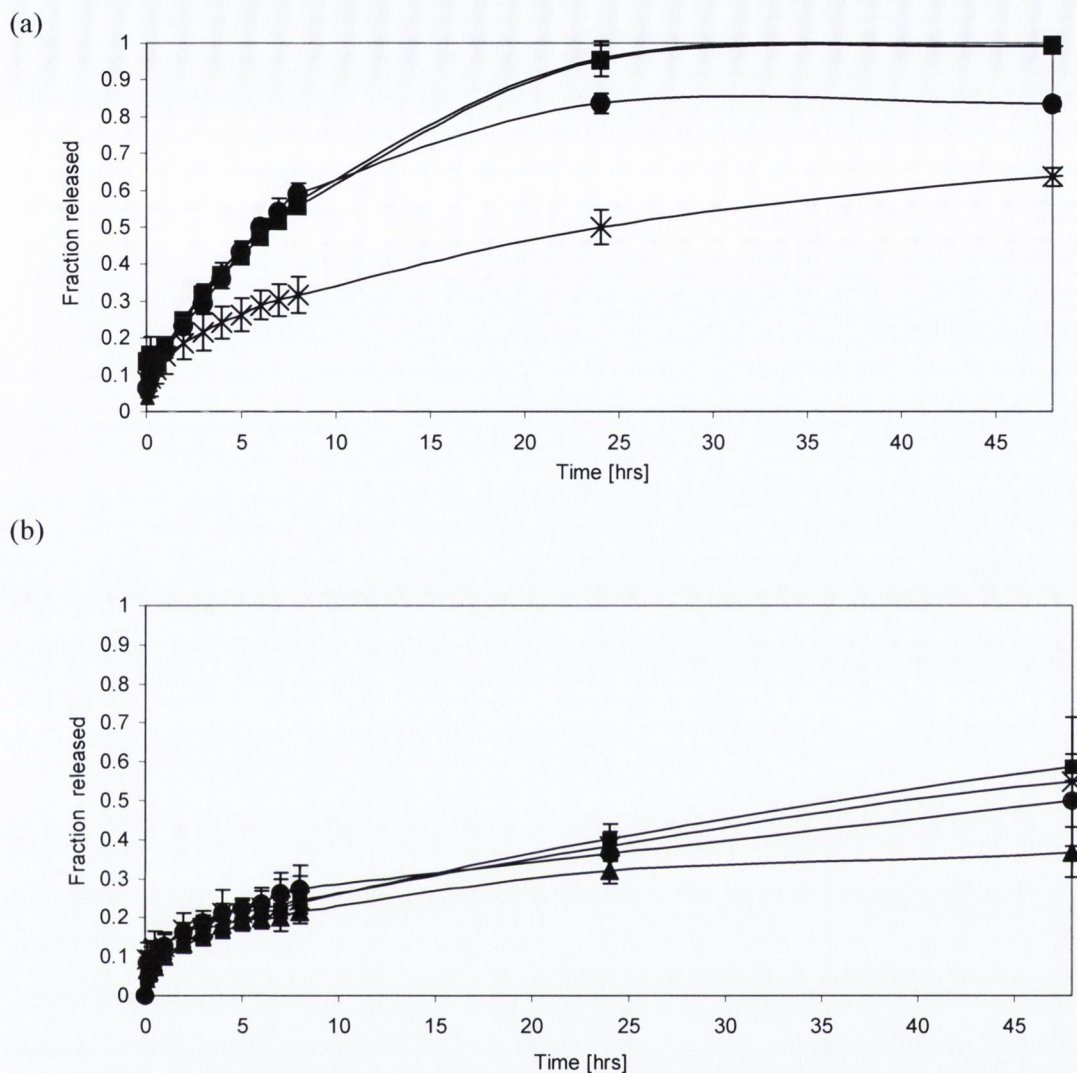
Figure 5.19: Fraction released of SA from the hydrogel series PNP (■), PNP1$_{-2}$ (▲), PNP2$_{-2}$ (●) and PNP3$_{-2}$ (x) at (a) 20°C and (b) 37°C.

At 20°C, the release behaviour displayed non-Fickian release with the diffusional exponent increasing towards unity for the first three hydrogels of the series (PNP-PNP2$_{-2}$) (Figure 5.20(b)). PNP3$_{-2}$ showed a significant decrease in the release exponent. In chapter 4 swelling kinetics of PNP3$_{-2}$ were characteristic of an anomalous swelling pattern. This suggests drug release was considerably slower in comparison to the rate of medium uptake (Figure 5.20(b)). There was no apparent differences in the release rate (p>0.05) between SA loaded hydrogels for the first three of the series (Figure 5.20 (a)). A significant decrease in both the release exponent and release rate (p<0.05) was observed for PNP3$_{-2}$ (Figure 5.20 (b)). The present results suggest pore size was not important in controlling release of SA below the LCST and that polymer-drug interactions play a more dominant role in the release patterns.

151
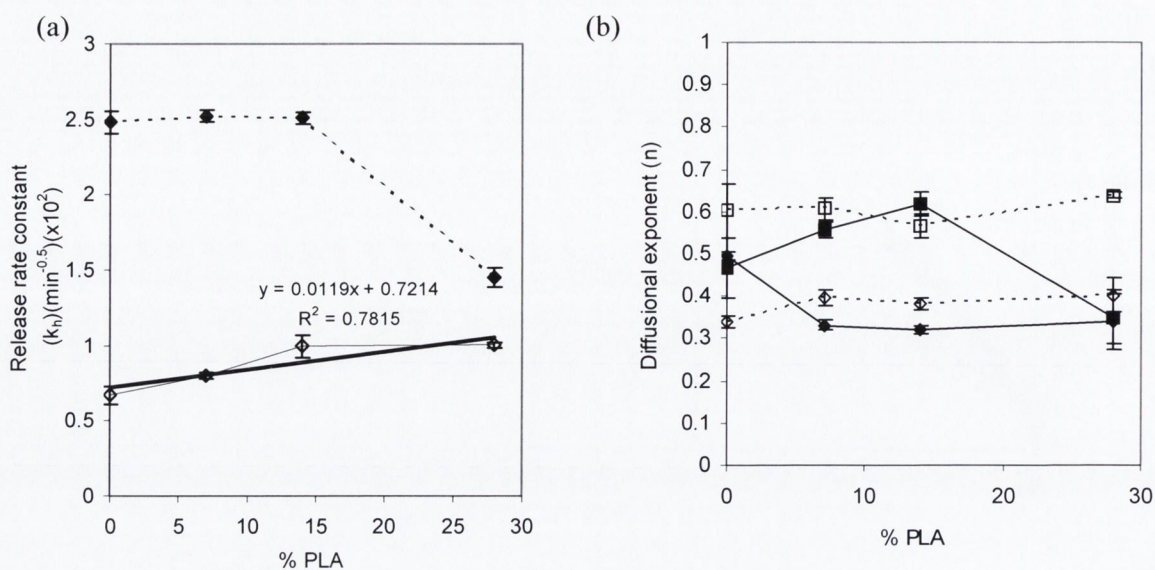
Figure 5.20: (a) the relationship between the PLA content and the release rate constants of SA at both 20 (closed symbol) and 37°C (open symbol) from the hydrogel series (b) the swelling exponents (open symbol) from the gel series and release exponents of SA (closed symbol) at 20(□) and 37°C (◊) from the gel series.

At 37°C, PNP3$_{-2}$ was shown to have higher swelling rate and greater effective pore size by SEM relative to the other gels studied. However the release kinetics were significantly influenced by the hydrogel composition. The swelling of the hydrogel series was characteristic of Fickian diffusion for all systems studied. In addition, the rate of release of SA was controlled by Fickian diffusion. Figure 5.20 (b) displays the swelling exponent and release exponents of SA for each hydrogel system. A marked decrease is observed in the release exponent indicating that the swelling front advanced faster than the drug could diffuse out. This result is in agreement with the loading of SA significantly reducing the rate of swelling and size of the pores in the gel and/or drug-polymer interactions (chapter 7).

As reflected in the parameters obtained when the release data was fitted to equation 2.22 (Higuchi, 1961), an increase in the release rate constant of SA was observed as the percent of PLA increased (Table 5.5). Over longer time periods the release rate of SA from the co-polymer systems effectively stopped between 70 and 90% depending on the hydrogel composition (Figure 5.19).

152

The mechanism of release or release rate of SA from the gels does not appear to be predominately controlled by the pore size from the biodegradable gels at either temperature (Figure 5.21).
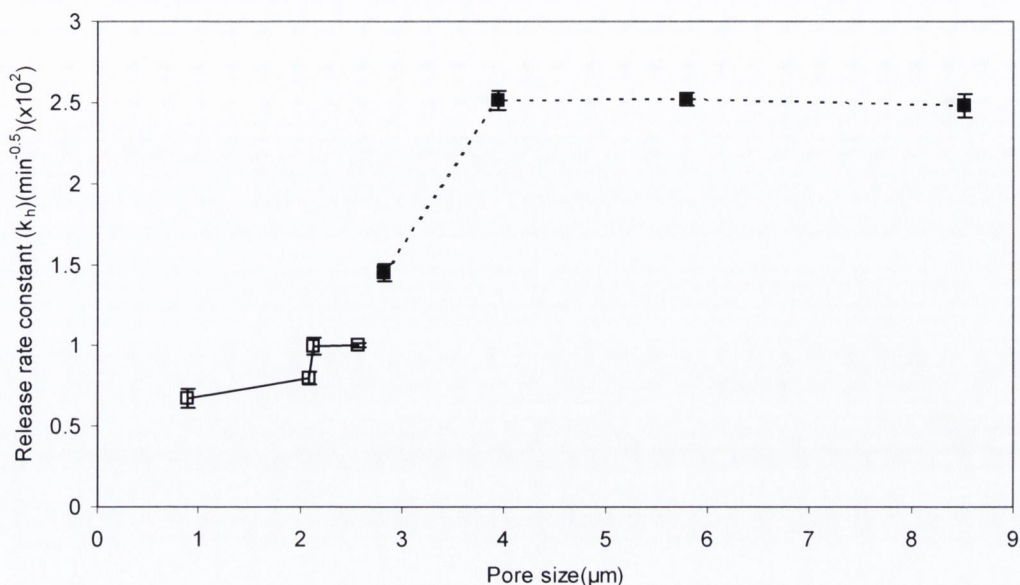
Figure 5.21: A plot of the release rate constants of SA against the pore size of the hydrogel series at $20^{\circ}C$ ($\blacksquare$) and $37^{\circ}C$ ($\square$).

At $20^{\circ}C$ the release mechanisms varied from Fickian to anomlolous diffusion depending on the composition of the polymer matrix. By tailoring the hydrogel composition (increasing PLA content) a delay in the duration of release was achieved with a levelling off of 83 and 69% of the total drug delivered from $PNP2_{-2}$ and $PNP3_{-2}$ respectively after 3 days (Appendix VIII). In contrast at $37^{\circ}C$ the diffusion exponent (n) was <0.5 indicative of polymer-drug interactions or entrapment of the drug within the polymer. After 3 days the release profile levelled of with only 46%, 52% and 56 % delivered from $PNP1_{-2}$, $PNP2_{-2}$ and $PNP3_{-2}$ respectively. The ability to thermally control the release rate of SA from the hydrogel series decreased on increasing PLA content as shown by the ratio of rate constants at both temperatures, which varied from 0.27 to 0.69 (Table 5.5). This can be attributed to the stronger affinity SA has for the polymer matrix on increasing PLA content and the smaller net differences between swelling rates on increasing PLA content.

5.4.4 IDM release from a range of hydrogel systems:

The release profiles of IDM at both temperatures from the hydrogel series are shown in Figure 5.22.

(a)

(b)
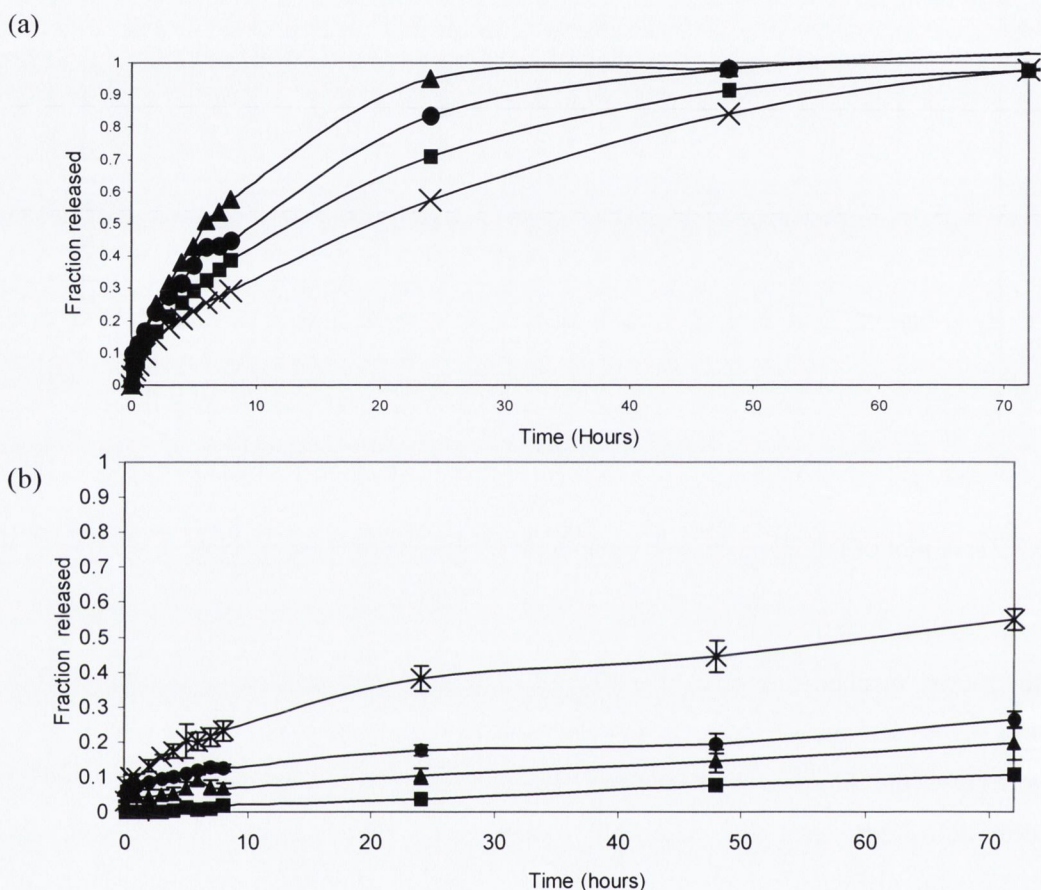
Figure 5.22: Fraction released over time of IDM from hydrogels containing various percentage of PLA at (a) 20°C and (b) 37°C [PNP (■), PNP1₋₂ (▲), PNP2₋₂ (●) and PNP3₋₂ (x)].

At 37°C, the release rate of IDM from the hydrogels corresponded with the pattern of swelling above the LCST, with an increase in the rate of release as the percent of PLA increased. The release kinetics of IDM from the hydrogel series was also dependent on hydrogel composition. A significant decrease in the diffusional exponent was observed for the co-polymer systems with $n < 0.5$. The tightness of the hydrogel network structure upon swelling as well as hydrophobic interactions previously seen in section 5.3.2 could be delaying the release of IDM. PNP3₋₂ had released ~50% after 3 days which can be attributed to the faster and more extensive formation of a loose 3D- network structure in the PNP-co-PLA₋₂ gel. The extent of IDM release could be expected to depend upon the degradation rate of the hydrogels. The more the hydrogel degraded the easier the IDM could diffuse from the hydrogel.

154

At 20°C, below the LCST, a similar release pattern was observed to that of DH whereby the presence of PLA appeared to assist the release of IDM. In the case of the co-polymers, the higher the amount of PLA incorporated into the gel, the greater the decrease in the rate of release of IDM. When the fraction released was fitted to Equation 2.25 (Peppas), Fickian diffusion was observed for the co-polymeric systems. A trend emerged at both temperatures between the release rate constant and the hydrogel composition. At 20°C, increasing the amount of PLA in the hydrogel led to a decrease in the rate of release of IDM. In contrast at 37°C an increase in the release rate was observed on increasing PLA content with a R^2 value of 0.9037 (Figure 5.23 (a)).
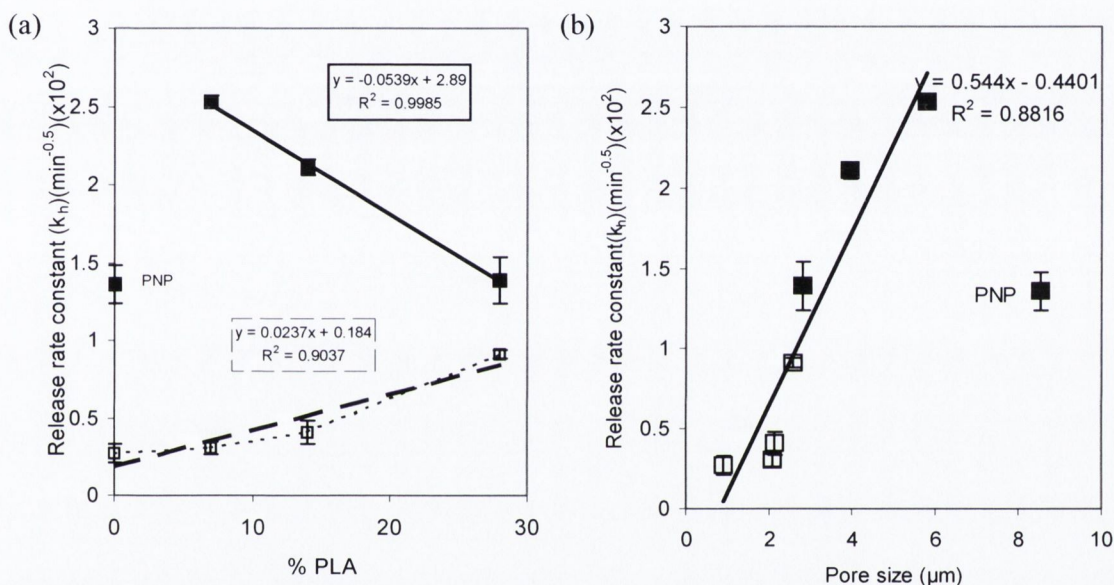
Figure 5.23: (a) Relationship between the release rate constants of IDM and hydrogel composition at 20°C (■) and 37°C (□) (b) Relationship between the release rate constants of IDM at 20°C (■) and 37°C (□) and pore size.

A plot of the relationship between the pore size and release rate from the hydrogel series are given in Figure 5.23 (b). A higher swelling results in a larger mesh size, which facilitates a faster drug release rate. At 20°C, PNP deviated from the trend with a slower release rate than the co-polymer systems. PNP was shown to have a greater effective pore size than any of the other hydrogel systems below the LCST however the presence of PLA appears to assist the release of IDM in the early stages of drug release (Figure 5.23(a)).

The ability to thermally control the release of IDM decreased as the percent of PLA increased. The ratio of the release rate constants at 37°C and 20°C (k_{37}:k_{20}) ranged from 0.20, 0.12, 0.19 and 0.65 for PNP, PNP1$_{-2}$, PNP2$_{-2}$ and PNP3$_{-2}$ respectively (Table 5.5). The limited ability to

thermally control the release of IDM from PNP3$_{-2}$ can be attributed to a smaller net difference in the swelling kinetics between both temperatures.

The effect of increasing the PLA content may result in strong interactions between the drug and PLA, which can either be strong hydrophobic binding between PLA and the drug or formation of reversible polymer-drug linkages such as hydrogen bonds. This may lead to a tighter packing in the core. Hence, drug release takes place as a result of two factors; overcoming the polymer-drug interactions and diffusion of the drug through the tightly meshed polymer matrix. In addition, a possible method of overcoming the drug release is hydrolytic degradation of PLA leading to scission of polymer chains. This would lead to a greater mesh size, an increase in solute diffusion which in turn would lead to a reduction in polymer-drug interactions.

5.4.5 Release of the Dextran fractions from hydrogel series containing PLA$_{-2}$

The release of the dextran fractions from the 4 different hydrogels was investigated at 20°C and 37°C. The release of the dextran fractions at 20°C from PNP2$_{-2}$ was previously presented in section 5.3.3. In Figure 5.24 the dextran release profiles at 20°C from the PNP, PNP1$_{-2}$ and PNP3$_{-2}$ are displayed. A biphasic release pattern is observed in all profiles with a rapid initial release rate (burst) followed by a gradual increase with time.

(a)
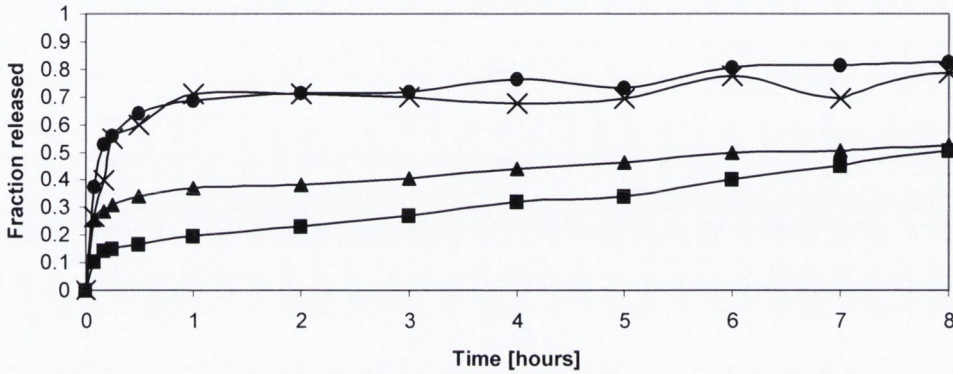
(b)
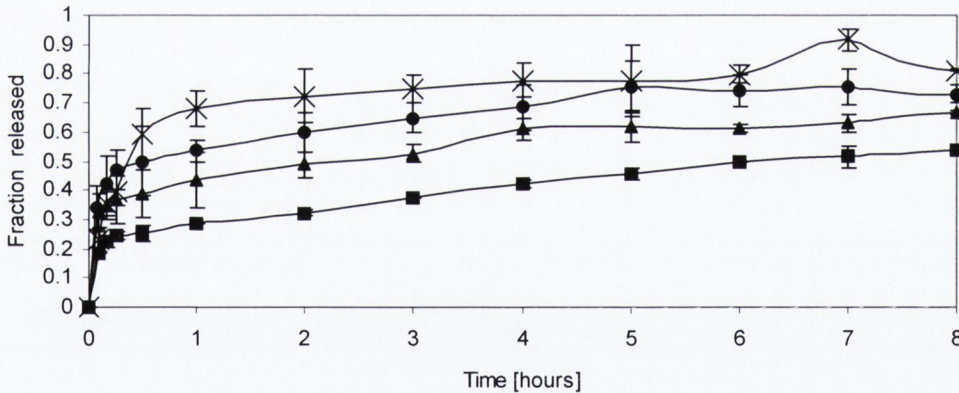
(c)

Figure 5.24: (a) Release of the dextran fractions D4 (■), D10 (▲), D40 (●) and D70 (x) from (a) PNP (b) PNP1$_{-2}$ and (c) PNP3$_{-2}$ at 20°C.

Table 5.6: Release rate constants (k_{dh}) of the dextran series from various hydrogels at $20^{\circ}C$ calculated using equation 2.22(Higuchi, 1961). The diffusional exponent and release rate constants (k_{dp}) were also estimated using equation 2.25(Peppas, 1985). Also shown are the associated co-efficients of determination.

| 20°C | $F=k_h^{.0.5}$ | | $F=kt^n$ | | |
	k_{dh} (min$^{-0.5}$)(x10^2)	CD	k_{dp} (min^1)(x10^2)	Diffusional exponent (n)	CD
PNP (D4)	2.19±0.083	0.9278	4.29±0.921	0.3803±0.0382	0.9547
PNP1₋₂ (D4)	2.72±0.169	0.7354	11.18±1.06	0.2475±0.0175	0.9547
PNP2₋₂ (D4)	4.44±0.480	0.4779	19.07±1.40	0.1907±0.0163	0.9847
PNP3₋₂ (D4)	1.02±0.090	0.6847	1.679±1.25	0.4125±0.102	0.6913
PNP (D10)	2.84±0.269	0.1814	19.92±0.86	0.1526±0.0091	0.9896
PNP1₂ (D10)	4.63±0.569	0.2762	23.61±1.54	0.1598±0.0148	0.9845
PNP2₂ (D10)	5.39±0.560	0.6685	16.66±2.92	0.2497±0.0600	0.9443
PNP3₂ (D10)	2.66±0.078	0.9668	3.51±0.820	0.4499±0.1037	0.9704
PNP (D40)	15.58±0.65	0.9802	21.95±0.38	0.3560±0.0481	0.9931
PNP1₂ (D40)	7.22±1.030	0.3483	29.09±1.75	0.1528±0.0164	0.9909
PNP2₂ (D40)	3.55±0.174	0.7987	8.25±0.571	0.3350±0.0366	0.9940
PNP3₂ (D40)	3.51±0.300	0.6934	14.15±1.13	0.2283±0.0682	0.9887
PNP (D70)	12.07±0.65	0.9558	15.69±4.05	0.4091±0.0892	0.9674
PNP1₂ (D70)	10.71±0.172	0.9962	10.43±0.989	0.5088±0.0318	0.9963
PNP2₂ (D70)	6.48±0.750	0.6099	20.35±2.05	0.2168±0.0197	0.9803
PNP3₂ (D70)	3.02±0.320	0.4410	16.58±1.52	0.1653±0.0241	0.9778

The release profiles in Figure 5.24 at $20^{\circ}C$ were fitted to equation 2.22 (Higuchi, 1961) and the model does not adequately account for the early-time period release (burst) (Table 5.6). D4, the smallest of the dextran fractions, revealed a slower release rate than any of the larger fractions examined. The higher molecular weight dextrans may expect to have slower release rates than D4 from the hydrogel series due to a lower diffusion co-efficient and greater hindrance of release. In addition a lag phase may have been expected to be observed in the release profile of a molecule larger then the available mesh size (Am Ende et al., 1995). As described in chapter 4, the higher molecular weight dextrans were not accessible to all pores at $20^{\circ}C$ (Section 4.4.6). At $20^{\circ}C$ this effect would be more pronounced on increasing the amount of lactide within the hydrogel system. Therefore a molecular size gradient appears to have formed during the loading process, particularly with the larger dextrans.

In the case of the homopolymer, PNP (Figure 5.24 (a)), the average pore size was larger than D4, D10 and D40 however a molecular size dependent gradient still appears to have formed during the drug loading process. Previous studies undertaken by Coughlan and Corrigan (2004) observed a similar molecular size dependent pattern in the release profiles of dextrans from PNP. They found that the drying process also contributed to the molecular size dependent drug pulse whereby larger molecules appear to become preferentially entangled in the outer sections of the hydrogel during loading and particularly drying leading to this moleceular size dependent gradient. Similarly variations in the pore size at the surface of the gel could be accountable for the observed release.

When the release profiles were fitted to Peppas equation (2.25), better results were obtained (Table 5.6). The time needed for complete drug release was dependent on the gel composition, where a longer time was needed the higher the amount of PLA incorporated into the hydrogel. Possible reasons may be entrapment of the dextran fraction within the matrix. The dextran-loaded gels were yellow in appearance and these matrices remained yellow throughout the release experiment indicative of entrapment of the drug within the hydrogel system. In chapter 7 it will be seen that loading of the dextrans suppressed the rate of swelling of the co-polymers, the effect significantly increased the higher the MW of the dextran. A slower rate of swelling and pore formation would be expected to lead to lead to a slower rate drug release. Also Coughlan and Corrigan (2004) observed an increase in swelling kinetics for dextran loaded PNP gels where the magnitude of acceleration was dependent on MW of the dextran. Therefore it is also likely that a secondary drug-polymer interaction between PLA and dextran is reducing the drug affinity for the buffer medium.

In the case of PNP3$_{-2}$ the mesh size characterised by SEM was 2.82µm (chapter 4). D4 was the only fraction small enough to diffuse through the gel during loading. This is reflected in the prolonged release of the dextran fraction (D4), whereas an initial rapid release was apparent for the higher MW fractions (Figure 5.24(c)). PNP3$_{-2}$ displayed a slow rate of hydration during swelling studies, which would lead to a slower formation of pores large enough to accommodate drug diffusion (chapter 4).

On examination of the dextran release in relation to the various pore sizes, the higher MW dextran revealed a pattern whereby the smaller the pores size the slower the rate and duration needed for complete release. Due to the entrapment of the dextran n (diffusional exponent) values were <0.5. The drug release profiles from PNP3$_{-2}$ were the slowest for all dextran fractions, attributable to the smaller mesh size. In addition the mechanism of release varied from Fickian diffusion for the smaller Dextran fractions to values of n<0.5 for larger dextran fractions

reflecting the free space available for diffusion for smaller molecules and the greater hindrance of the larger MW dextran.

(a)

(b)

(c)
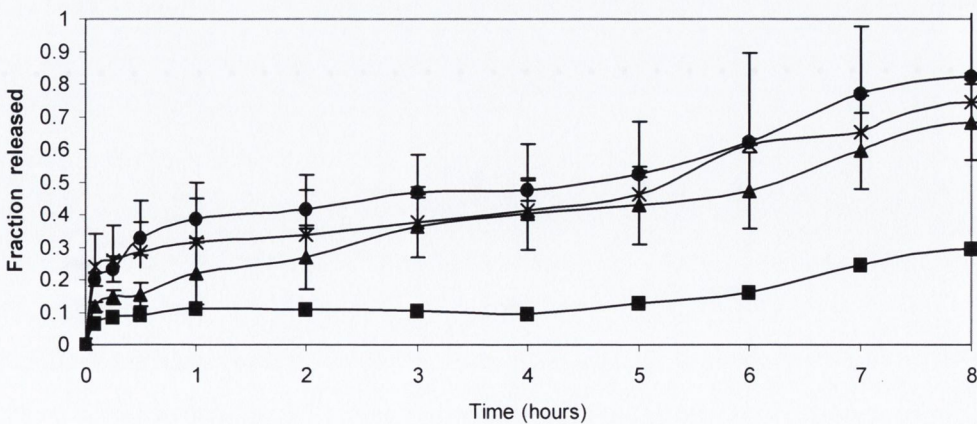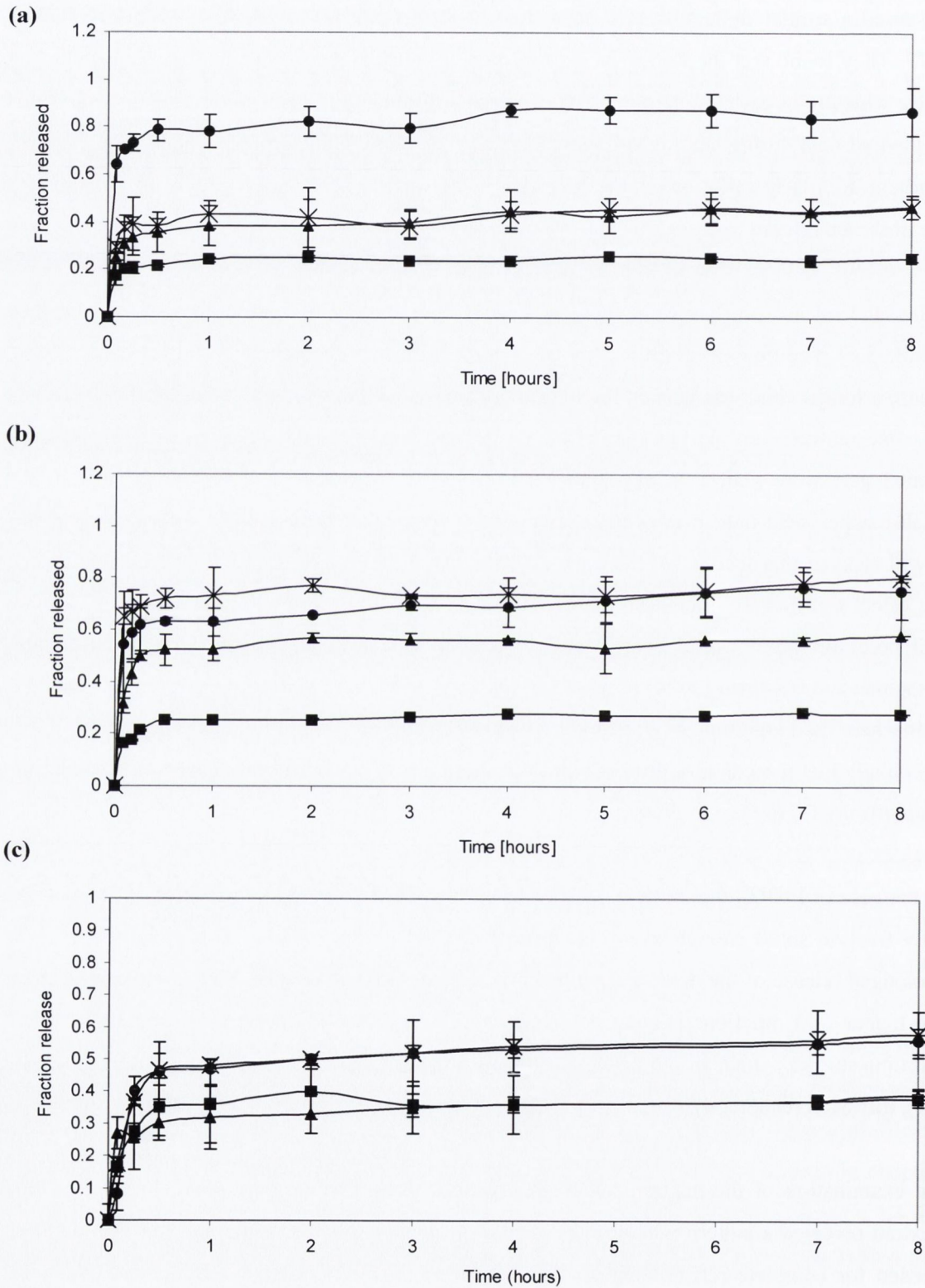

Figure 5.25: (a) Release of the dextran fractions D4 (■), D10 (▲), D40 (●) and D70 (x) from (a) PNIPAAM (b) PNP1$_{-2}$ and (c) PNP3$_{-2}$ at 37°C.

At 37°C, the release of D40 and D70 from PNP3$_{-2}$ occurred gradually due the surface bound drug (Figure 5.25). However once the initial surface bound drug was released no further release of the dextrans was observed due the hydrogel pore sizes being smaller than that of the dextran fractions. The increase in temperature was to effectively stop the diffusion rate once the surface dextran was released.

5.5 Conclusions:

The degradation behaviour of these cross-linked hydrogel networks were very different from degradable linear system PLA. Co-polymerisation of PNIPAAM and PLA led to a significant increase in the rate of degradation below the LCST. The results demonstrated the strong coupling of the network microstructure to the degradation rate and swelling ratio. In addition the network structure was formed during polymerisation and can therefore be altered by changing the molar ratio of monomers. Increasing the PLA content led to networks with lower characteristic Mc and pore sizes and hydrogels with lower slower swelling ratios. The chemistry of the polymer also played an important role in determining the degradation properties. Co-polymerisation of PNIPAAM and PLA led to an increase in the mechanical strength and increase in the degradation rate, the higher the PLA content. Overall by tailoring the network structure the desired hydrogel properties and degradation behaviour could be designed to meet specific criteria.

The purpose of the study was also to determine if a range of different drugs could successfully be released from PNP-co-PLA hydrogels and if the release could be controlled and predicted. The release kinetics were dependent on the temperature at which they were conducted with a higher rate of release below the LCST. The smaller MW compounds revealed a trend towards zero order kinetics as the PLA content increased. Drug physicochemical properties played an important role in the release behaviour influencing both the rate and mechanism of release. The larger macromolecules showed a MW gradient upon loading.

At 37°C, due to the entrapment of the higher MW model compounds, degradation controlled release could be obtained. Network swelling and polymer-drug interactions controlled release profiles of the model compounds at this temperature. Depending on the drug physiochemical properties degradation controlled release could be obtained.

CHAPTER 6:

AN INVESTIGATION INTO THE DEGRADATION AND RELEASE KINETICS FROM A SERIES OF GELS SYNTHESISED BY VARYING THE MOLAR RATIOS OF PNIPAAM TO PLA (MW 12000).

6.1 Introduction:

The degradation behaviour of PNIPAAM-co-PLA gels (MW 2000) was studied in chapter 5 revealing a strong correlation between degradation and pore size. The mechanism of drug release and release profiles were dictated by hydrogel composition, drug physiochemical properties, and polymer-drug interactions.

The objective of this study was to examine the effect of increasing the molecular weight of the hydrogel component PLA on the degradation behaviour and drug release profiles from a range of polymer networks. A series of biodegradable hydrogels by varying the molar ratio of PNIPAAM to PLA (MW 12000) were synthesised as previously outlined in chapter 3. Degradation behaviour was investigated above and below the LCST. The effect of temperature on the rate of drug release as well as the influence of gel structural properties on the release profiles were also investigated.

6.2.1: SWELLING AND HYDROLYTIC DEGRADATION OF PNIPAAM-CO-POLY (LACTIC ACID) (MW12000) BASED HYDROGELS

Previously in Chapter 4 the swelling kinetics and equilibrium-swelling ratio during the initial stages of immersion in PB (up to 3 days) for the hydrogel series were discussed. Figure 6.1 shows the continuation of the experiment over a two-month time frame both below and above the LCST. Below the LCST (Figure 6.1 (a)) no statistical difference was observed in the degree of swelling over time. Previously, in Chapter 5 a continual increase in weight was observed until the network could not sustain itself, which was attributed to hydrolytic degradation of the polymers. By increasing the MW of PLA it would be expected to take longer for hydrolytic degradation to occur. A larger pore size was observed for the gels composed of PLA MW 12000 facilitating a larger space for solute diffusion. A possible explanation for the steady mass is a continual uptake of water counterbalancing the loss of degraded material. Above the LCST a noted decrease in the swelling ratio was observed after 3 weeks with the effect more pronounced the higher the amount of PLA incorporated into the gel (Figure 6.1 (b)). This can be explained by combined effect of a larger porosity capacity for solute diffusion and higher temperature leading to degradation or autocatalysis of lactic acid within the gel.
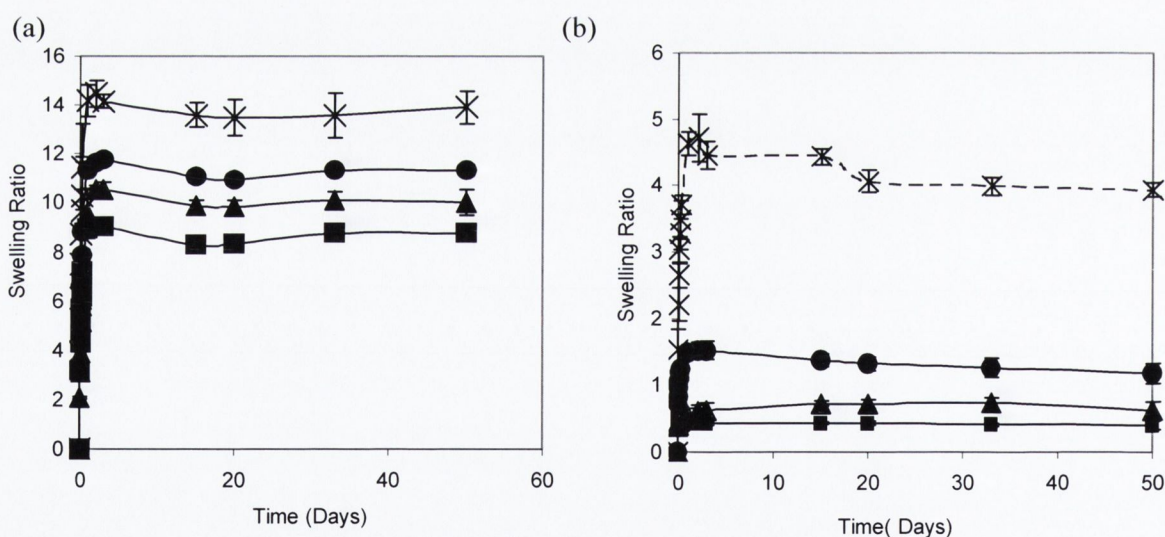
Figure 6.1: Swelling ratio of the hydrogel series PNP ($\blacksquare$), PNP1$_{-12}$, ($\blacktriangle$) PNP2$_{-12}$, ($\bullet$) and PNP3$_{-12}$ (x) as a function of time at (a) 20°C and (b) 37°C.

At the end of the experiment the hydrogel discs were removed and dried under vacuum before being reweighed and compared to that of their original dry mass. A mass loss of 36.5%, 17.5%, and 31.5% was obtained for PNP1$_{-12}$, PNP2$_{-12}$, PNP3$_{-12}$ gels respectively after ~2 months below the LCST in comparison to 24%, 24.5%, 51% above the LCST after the same time period. Mass loss results are indicative of degradation with an overall higher rate of degradation observed

above the LCST. As previously discussed in chapter 5, the molar ratios (weight) used to synthesise the gels were presented in Table 4.2 (PNP1$_{-2}$ (84-16 w/w), PNP2$_{-2}$ (76-24 w/w), and PNP3$_{-2}$ (56-44 w/w)). These results suggest scission and release of PNIPAAM bonds into the external media as a higher mass loss is observed relative to PLA component.

6.2.2 FTIR analysis of the degradation media

Once the swelling studies were conducted and the gels removed, FTIR spectroscopy was conducted on the degradation medium as previously described (Section 3.3.2) to detect the presence of lactic acid or PNIPAAM fragments within the swelling media. The FTIR spectra of PNP3$_{-12}$ swelling media at both 20°C and 37°C are shown in Figure 6.2. The presence of PLA was evident in the co-polymeric systems as a broad absorption band between 1850cm^{-1} and 1600cm^{-1} characteristic of the carboxylic group and hydrolytic altered ester bond of the PLA backbone chain. Also a strong presence of PNIPAAM is seen at 1372cm^{-1} characteristic of the isopropyl group. At 37°C a weak peak at 1670cm^{-1} representing the amide of PNIPAAM is seen over shadowed by lactic acid ester bonds. The lower end of the spectrum revealed four absorption bands in the range of 1088-864cm^{-1}. These bands are associated with C-O stretching groups,-C-C stretch and the –C-COO stretch which are most likely a mixed contribution of both PLA and PNIPAAM. The absorbance intensities revealed a trend whereby a higher absorption was apparent at the upper temperature (37°C). It is worth mentioning that mass loss studies after swelling were in good agreement with absorption intensities indicative that degradation was faster overall above the LCST.
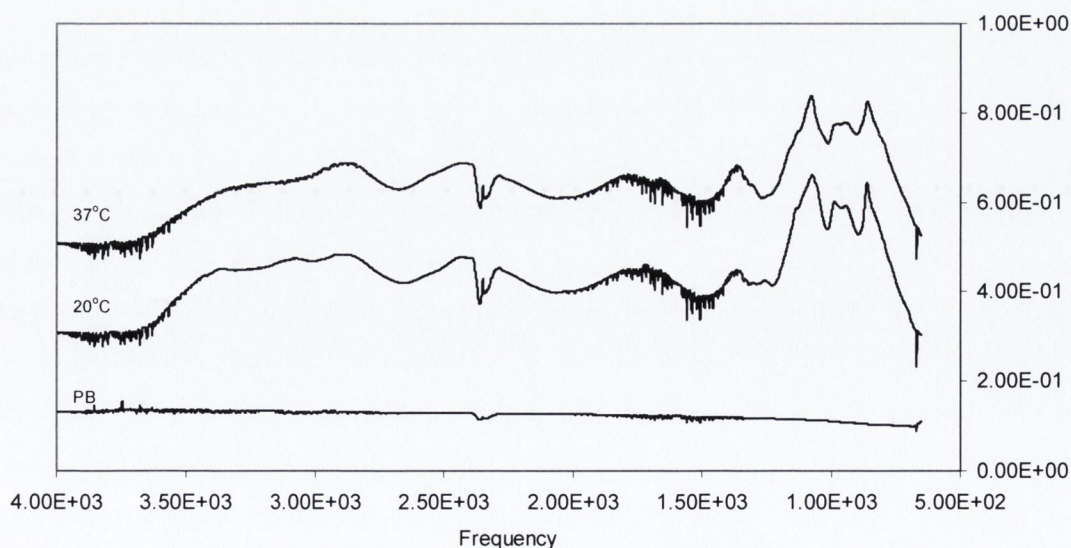
Figure 6.2: FTIR absorption spectra of the degradation medium of PNP3$_{-12}$ at 20°C and 37°C. Also shown is the buffer medium (PB) in which experiments were conducted.

6.2.3 Acid-Base Titrations of degradation media

The swelling medium was also analysed after 2 months by acid–base titrations in order to obtain the calculated amount of degraded material, LA, within the swelling media. Table 6.1 displays the relationship between hydrogel composition and the molar concentration of LA degraded during swelling studies. At 20°C the calculated amount of lactic acid within the swelling medium ranged from 0.0075M/L to 0.0158M/L and did not appear to follow a trend (Table 6.1). This could be attributed to random polymerisation defects within the system in question (PNP1-12) as well as the possibility of the crosslinker degrading thereby leading to the formation of acidic by-products. These results were in agreement with the pore size estimation observed using SEM images of the degraded hydrogel systems removed from the swelling medium (Table 6.2) (Figure 6.3 and 6.4).

Table 6.1: The concentration of LA present in the external medium after a 2-month period at 20°C and 37°C. Also shown are the ratios of the increase in amount of LA present on increasing temperature.

Gel	[COOH] in external media (20°C)(M/L)	[COOH] in external media (37°C) (M/L)	[COOH] $_{37}$:[COOH]$_{20}$
PNP1-12	0.0158	0.001	0.063
PNP2-12	0.0075	0.0125	1.666
PNP3-12	0.0108	0.0216	2.000

* Original dry disc ~ 0.2g

At 37°C a relationship was observed whereby the higher the amount of poly (LA macrmomer) incorporated into the gel the higher the amount of LA seen in the swelling/degradation media. In Chapter 4, a higher rate of swelling and equilibrium swelling ratio was seen the higher the PLA content at this temperature. Therefore a larger space for solute diffusion would be expected to lead to faster rate of hydrolytic degradation. On increasing the MW of PLA, it should be noted that degradation behaviour appears to be faster at 37°C than 20°C. The effect of temperature on the rate of degradation can be seen where a 1.66 and 2-fold increase in the amount of PLA within the degradation medium was present at 37°C for PNP2-12 and PNP3-12 hydrogel systems respectively (Table 6.1). In Chapter 5 the reverse trend was seen on incorporating PLA MW 2000 into the hydrogel systems where degradation appeared to be faster below the LCST. The reversal in temperature control on the degradation behaviour can be attributed to a significantly increased pore size at 37°C for the PNP-PLA-12 gels relative to that of the PNP-PLA-2 gels (chapter 4).

At 20°C, the calculated amount of LA in the external media was 71mg, 33.75mg and 48.6mg for PNP1-2, PNP2 and PNP3 respectively. Above the LCST, 4.5mg, 56mg and 97mg of LA were present in the swelling media after 2 months. In addition the overall weight loss was determined relative to that of the dry discs revealing a 35%, 16.87% and 24.3% weight loss below the LCST while a 2.5%, 28% and 48% was seen above the LCST. Similar weight losses were observed in Section 6.1 after swelling studies. The small differences can attributed to the scission of PNIPAAAM fragments during degradation, would not be detected.

6.2.4 Scanning electron microscopy (SEM)

The effect of increasing the MW of PLA on the gels was seen to lead to a greater pore size and increase in structural integrity in Chapter 4. After incubation for 2 months the gels were freeze dried and examined using SEM to compare pore size before and after degradation. The results are tabulated below.

Table 6.2: Calculated pore size for hydrogel series before and after degradation at both 20°C and 37°C. Also shown is the difference in pore size deduced from data using image tool.

Hydrogel	PLA (%)(w/w)	Observed pore size (µm)	Observed pore size (µm) after 60 Days	Change in pore size due to degradation
20°C				
PNIPAAM	0	8.52 ± 1.70	09.80 ± 1.05	1.28
PNP1-12	7	10.61 ± 0.29	29.60 ± 4.05	18.99
PNP2-12	14	11.06 ± 2.40	23.74 ± 3.02	12.68
PNP3-12	28	11.96 ± 3.00	27.35 ± 4.56	15.39
37°C				
PNIPAAM	0	0.89 ± 0.56	0.950 ± 0.12	0.23
PNP1-12	7	3.50 ± 1.23	07.64 ± 2.15	4.14
PNP2-12	14	7.18 ± 0.38	12.70 ± 3.20	5.52
PNP3-12	28	7.82 ± 3.33	16.82 ± 1.74	9.00

The morphological change of the PNIPAAM/PLA gels as a function of composition ratio was attributed to the swelling induced as well as the hydrolytic–induced pore formation (Figure 6.3-6.4). Since a lower crosslinking density was observed with the higher PLA content, the swelling induced porous structure occurred more rapidly when immersed in PB. From the values calculated using image tool presented in Table 6.2 the size of the pores became larger with time of immersion due to hydrolysis. On comparing the SEM images of the same MW but different composition ratios all PNP3-12 gels showed thinner walls and larger pore sizes and channels due to hydrolytic degradation of PLA component.

(a i)

(a ii)

(b i)
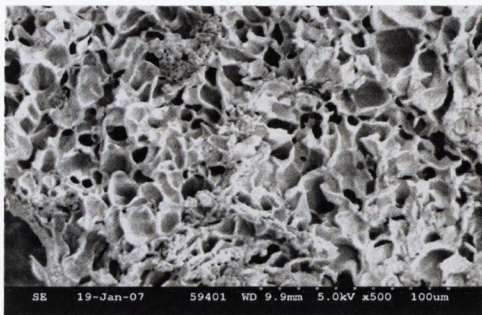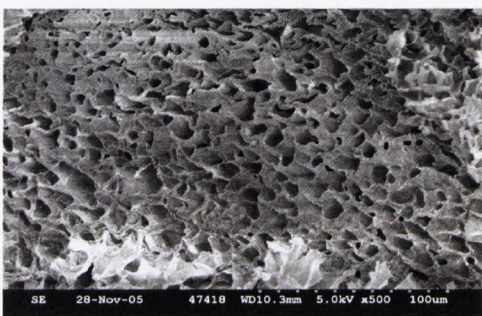
(b ii)
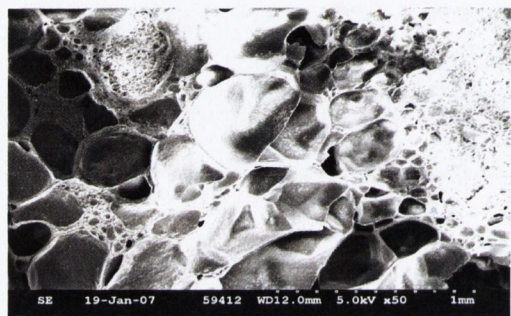
(c i)
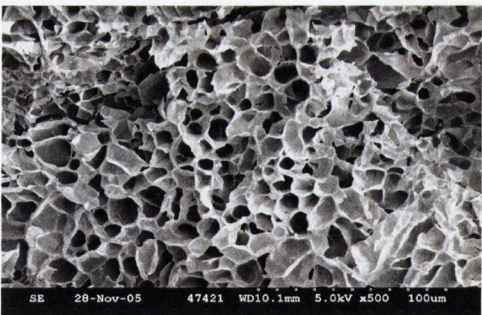
(c ii)
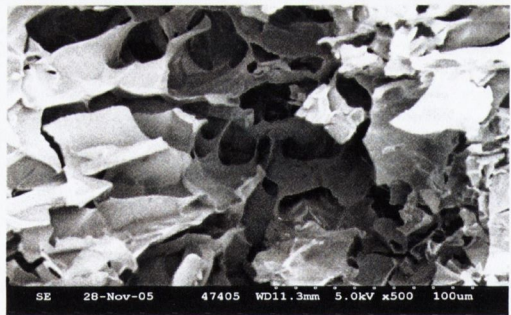
Figure 6.3: SEM images (x 500) of (a) PNP-1$_{-12}$, (b) PNP2$_{-12}$ (c) PNP3$_{-12}$ before (i) and after (ii) degradation at 20°C

(a i)   (a ii)

(b i)   (b ii)

(c i)   (c ii)
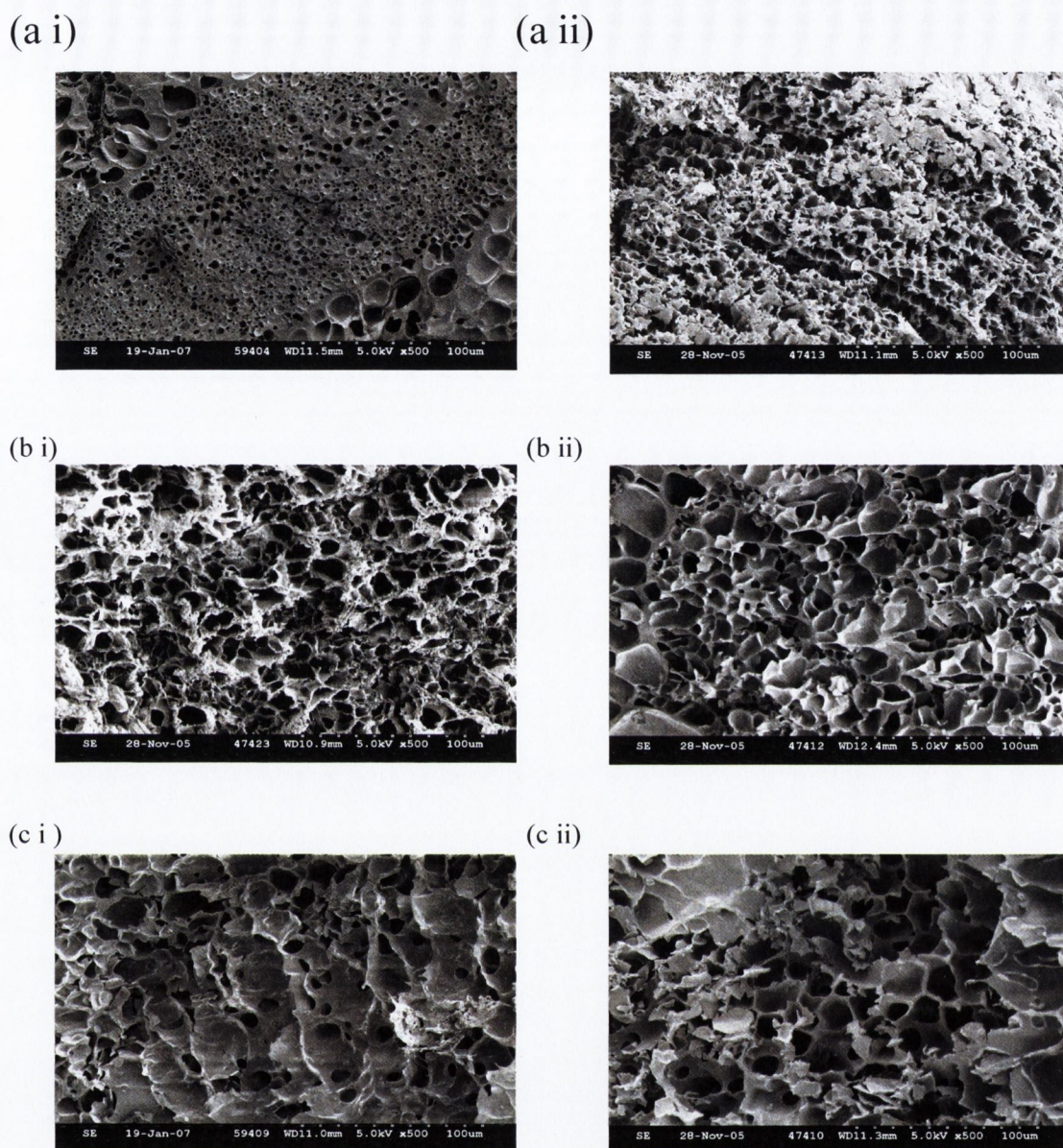
Figure 6.4: SEM images (x 500) of (a) PNP-1$_{-12}$, (b) PNP2$_{-12}$ (c) PNP3$_{-12}$ both before (i) after (ii) degradation at 37°C.

Above the LCST (37°C) a trend emerged whereby the higher the equilibrium-swelling ratio and percent PLA incorporated into the hydrogel the larger the increase in pore size after degradation. These results were in good agreement with [COOH] present within the swelling media. A trend emerged whereby the higher concentration of [COOH] detected in the swelling medium the larger the change in pore size observed after 2 months, as a result of hydrolytic degradation (Figure 6.5). Below the LCST, a linear relationship was apparent between the change in pore size and the [COOH] detected in the swelling media with a R^2 value of 0.9615 (Figure 6.5).
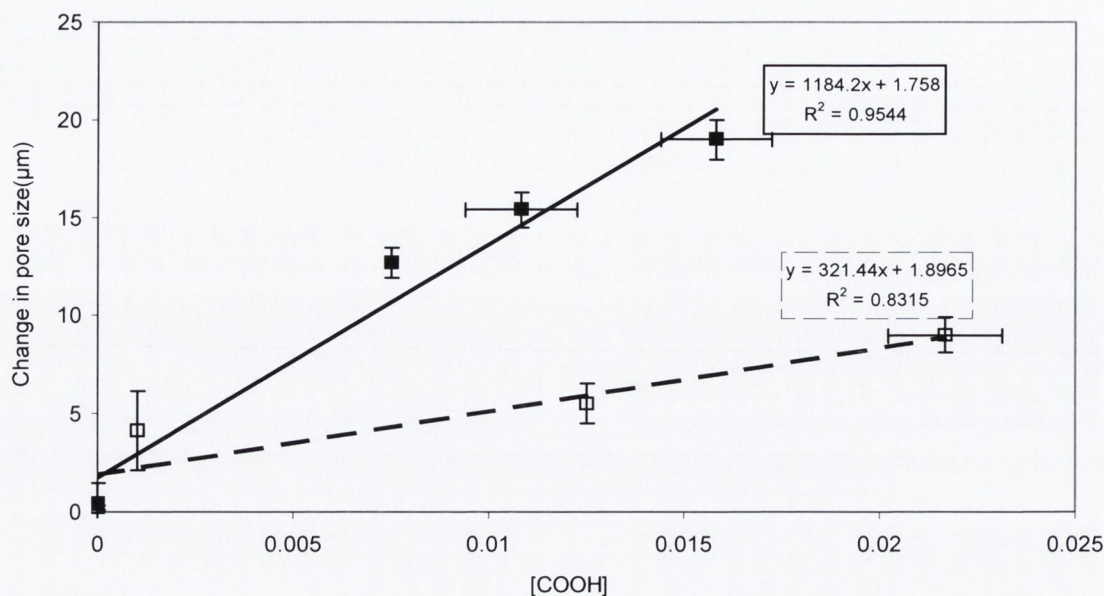
Figure 6.5 [COOH] and the change in the porosity of the gels after degradation studies at $20^{o}C$ (■) and $37^{o}C$ (□).

Overall it was apparent that by increasing the MW of PLA component a reversal in temperature control on the rate of degradation of these hydrogel systems was achieved. In order to analyse the impact of co-polymerisation of PLA with temperature sensitive polymers, pure PLA degradation kinetics were analysed in the following section.

6.2.5: Swelling and hydrolytic degradation of poly (Lactic acid) (MW12000) in aqueous solution:

6.2.5.1: Swelling and hydrolytic degradation of PLA:

The swelling of the PLA tablet (MW 12000) in PB is shown in Figure 6.6. At $20^{o}C$ the water sorption proceeds for the first 12 days at a rate much lower than that of the specimen with MW 2000. At this point it is possible that equilibrium is reached whereby the rate of swelling and degradation become equal during this period, so that no change in weight is observed. A second swelling stage emerged after this point where an increased rate of water uptake is recorded. This suggests that degradation of the higher MW PLA leads to a modified product that is more susceptible to swelling compared with the polymer of low MW (Andreopoulous et al., 1999).

170
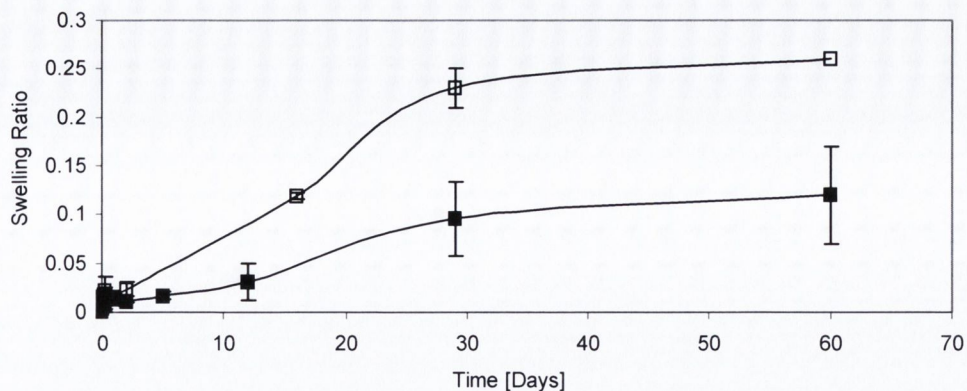
Figure 6.6: Swelling ratio of PLA (MW12000) as a function of time at 20°C (■) and 37°C (□).

Temperature was shown to have a significant impact on the rate of degradation of PLA in Section 5.2. From the curve in Figure 6.6 at 37°C it is clear the sorption of medium accelerates after 2 days and further increases after 5 days. At this time there is ~two-fold increase in the rate of water sorption relative to the results observed at 20°C. The increase in water uptake is consistent with degradation (Andreopoulous et al., 1999).

6.2.5.2: FTIR analysis of the degradation medium

FTIR spectra of the swelling media in which the PLA tablets were immersed are shown in Figure 6.7. The absorption intensities are higher at 37°C than at 20°C also indicative that degradation occurs faster at the upper temperature. The spectral evaluation of the stretching vibrations corresponded with that of PLA MW 2000. Carbonyl stretching vibration between 1800cm^{-1} and 1600cm^{-1} was seen characteristic of ester bond. The presence of water was seen on active sites of PLA similar to that of PLA MW 2000. However absorbance intensities were significantly larger due to a larger number of repeating units. The lower end of the spectra revealed 3 strong absorption bands at 1080, 988 and 863 which were assigned to the –CO-stretch, -C-C- stretch and the –C-COO- stretching of PLA (Section 5.1). Increasing the molecular weight resulted in stronger intensities as would be expected due to a larger number of repeating units. This was also reflected in the amount of water bound to the PLA active sites at 1600cm^{-1}.
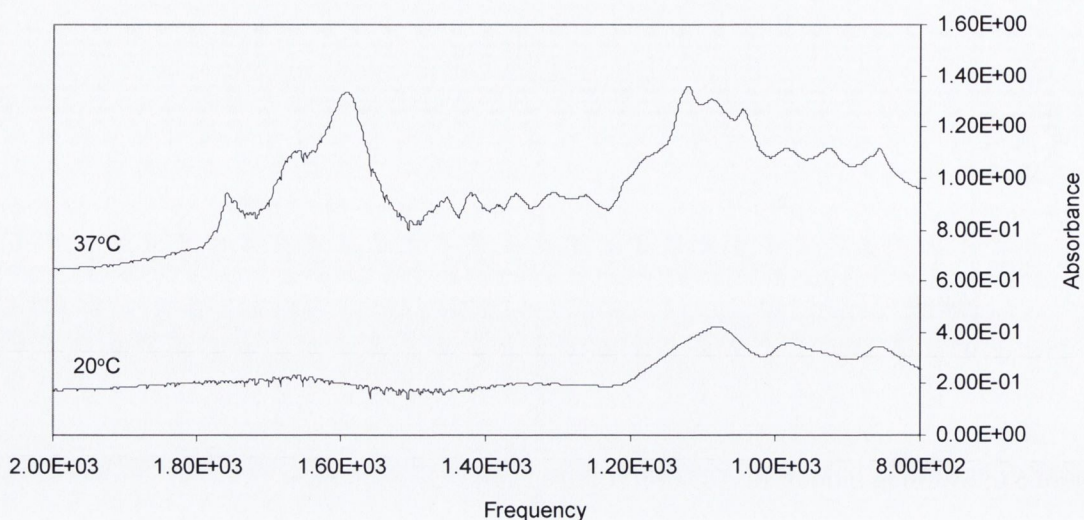
Figure 6.7: FTIR spectra of PLA (MW 12000) swelling media after degradation studies at 20°C and 37°C.

6.2.5.3: Acid-base titrations of swelling media

The concentration of PLA detected within the swelling media was quantified employing acid-base titrations using phenolphthalein as an indicator. The concentration [COOH] at 20°C and 37°C detected within the media was 0.014167M/L and 0.0325M/L respectively. These results were used to calculate the mass of LA present within the degradation medium and gave values of 0.06g (30%) and 0.146g (73%) respectively indicative more than a ~2.4-fold increase was seen on increasing the temperature. On comparing these results with the smaller MW PLA (MW 2000) a slower degradation is observed which would be expected.

6.2.6 Conclusions

In the case of Linear PLA, all analytical techniques were in good agreement displaying an increase in degradation at higher temperature. This was evident in swelling studies in addition to quantitative and qualitative methods employed in identifying and calculating the degree of degradation. Higher absorption intensities were seen in FTIR at 37°C as well as over a two-fold increase in the amount of LA seen in the swelling medium after degradation on increasing temperature. Furthermore on comparing these results with co-polymeric systems, it is evident that changing environmental and structural parameters of the polymers can alter the degradation behaviour. Hydrogels offer a more open network susceptible to hydrolytic degradation. By altering the monomer ratios, hydrophobicity, hydrophilicity and the crosslinking density, the degradation of the three dimensional networks can be modified for specific criteria.

6.3. Model drug release:

As previously seen in chapter 5 the rate of swelling, size of the polymer network and the physicochemical properties of the drug molecule influence the drug release profiles or the mechanism of release. In chapter 4 a noted increase in the pore size and swelling trend was observed for the hydrogel series with PLA MW12000. In this section investigation of the model drugs from $PNP2_{-12}$ containing MW PLA 12000 was undertaken and the effect of hydrogel composition on their release profiles examined.

6.3.1 Release of Small molecular weight compounds from $PNP2_{-12}$

Release of the small molecular weight compounds from $PNP2_{-12}$ at both 20 and 37°C in 900ml PB over 48 hours was examined (Figure 6.8). The fraction released at both temperatures was plotted against the square root of time to give the release rate constants k_{h20} and k_{h37} (Table6.2.).

Table 6.2 Release rate constants (k_{dh}) of model compounds at 20°C and 37°C from $PNP2_{-12}$ calculated with equation 2.22 (Higuchi, 1961) along with their co-efficient of determination (CD). Also shown is the release rate constant (k_{dp}) are their diffusional exponents when n is allowed to vary (Peppas, 1985).

	$F=kt^{0.5}$		$F=kt^{n}$			
20°C	$k_{dh20}(min^{0.5})(x10^2)$	C.D	$k_{dp20}(min^1)(x10^2)$	$n \pm s.d$	C.D.	$k_{dh37}: k_{dh20}$
DH	3.841 ± 0.0036	0.8928	0.751 ± 0.1008	0.8451±0.027	0.9983	0.4186:1
SA	3.143 ± 0.0004	0.9929	2.287 ± 0.1614	0.5589±0.012	0.9982	0.4101:1
IDM	1.603 ± 0.0005	0.9515	1.859 ± 0.3378	0.5822±0.058	0.9599	0.6356:1
37°C	$k_{dh37}(min^{0.5})(x10^2)$	C.D.	$k_{dp37}(min^1)(x10^2)$	$n \pm s.d$	C.D.	$k_{dh37}:k_{dh20}$
DH	1.608 ± 0.0003	0.9848	1.859 ± 0.2512	0.4769±0.021	0.9864	
SA	1.289 ± 0.0073	0.9987	1.436 ± 0.03625	0.4835±0.003	0.9951	
IDM	1.019 ± 0.0075	0.9982	0.973 ± 0.0478	0.5066±0.006	0.9984	

The increase in pore size resulted in rapid drug diffusion at both temperatures with least thermal control observed by IDM. As previously seen in chapter 5, the release rate constants increased with increasing solubility at both temperatures. When the diffusional exponent was allowed to vary (EQN 2.25) the contribution of swelling to the release mechanism could be examined. At 37°C all systems were characteristic of Fickian diffusion. The ability to thermally control the rate of release was less successful using gel composed of a higher MW PLA. The ratios between k_{dh37} and k_{dh20} shown in Table 6.2 indicate poorer thermal control on increasing temperature relative to that of the systems composed of PLA MW 2000.
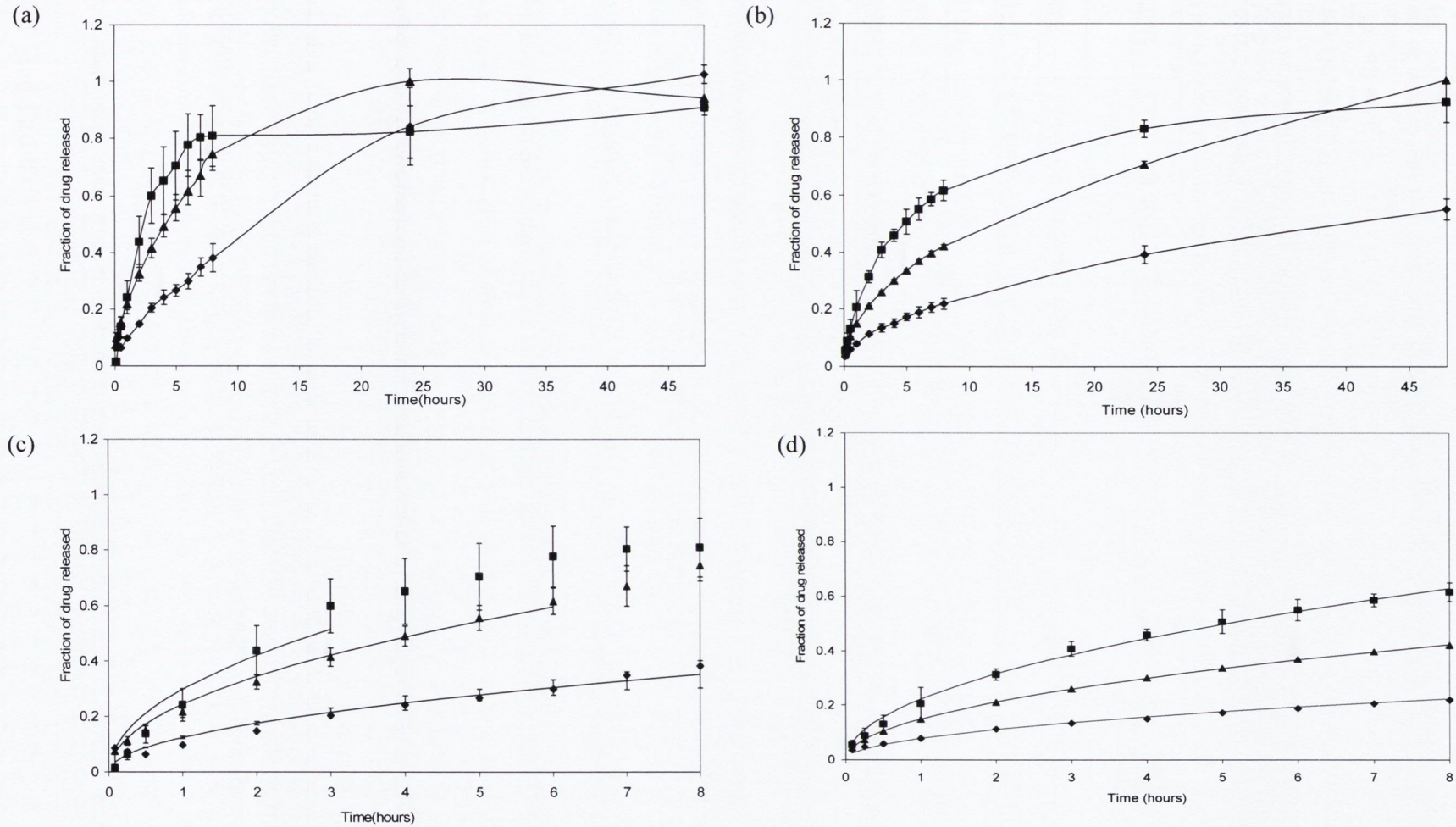
Figure 6.8: Plot of fraction of DH (■), SA (▲), and IDM (♦) released over time from PNP2$_{-12}$ in PB at a) 20°C and b) 37°C. Also shown the plot of the fraction of DH (■), SA (▲) and IDM (♦) fitted to the square root of time at (c) 20°C and (d) 37°C (Higuchi 1961).

174

At 37°C a noted increase in the diffusional exponent occurred as the solubility of the model drugs increased. After 48 hours DH and SA had reached 90% release whereas IDM had reached 50% release. However a 2.2 fold increase in the release of IDM was observed in comparison to that of the hydrogel system with PLA 2000 incorporated into the gel. This can be attributed to a significantly larger mesh size above the LCST on increasing the MW of the PLA co-monomer.

At 20°C the diffusional exponent was dependent on the drug physiochemical properties where n approached unity as the pKa increased. Increasing the molecular weight of PLA resulted in an increase in the overall rate of drug release and the mechanism of release was dependent on the PLA component. This is apparent in the lower diffusional exponent of SA in comparison with the release exponent from co-polymeric systems of lower MW PLA, indicative of polymer drug interactions.

The time needed for total drug release varied from 2 to 5 days, with DH taking 5 days and SA and IDM taking 2 days. The significantly larger mesh size on increasing the MW PLA did not significantly change the rate of DH release, however a noted increase in the diffusional exponent as well as the duration for total drug release was observed. The model compounds with poor solubility, IDM and SA, resulted in an increase in drug release relative to that of PLA MW 2000 systems, which can be attributed to a larger space for solute diffusion and dissolution.

6.4 AN INVESTIGATION INTO THE EFFECT OF THE PLA (MW 12000) ON THE RELEASE KINETICS FROM PNIPAAM-PLA HYDROGELS

The drug release studies presented in section 6.3 were preformed using PNIPAAM-co-PLA (86-14 molar ratio NIPAAM-PLA respectively) PNP2$_{-12}$ hydrogel. Three other hydrogel systems were also synthesised by varying the molar ratios of PNIPAAM to PLA (MW 12000); the homopolymer PNP, PNP1$_{-12}$ and PNP3$_{-12}$. As previously seen, degradation behaviour can be manipulated by introducing co-monomers. The aim of the present study was to evaluate the drug release from the hydrogel series with PLA MW 12000 incorporated into the backbone of the three dimensional network.

6.4.1 DH release from PNP-PLA$_{-12}$ hydrogel systems

The fraction of release of DH as a function of time at 20°C and 37°C from the various hydrogel systems is displayed in Figure 6.9. The release was greater at 20°C due to a greater contribution of swelling. The difference in the release profiles was reflective of the increase in the PLA content. The fraction of release was fitted to equation 2.25 (Peppas, 1985) (Table 6.3) and there was a significant increase in the release rate constant with increasing the amount of PLA incorporated into the gel.

(a)
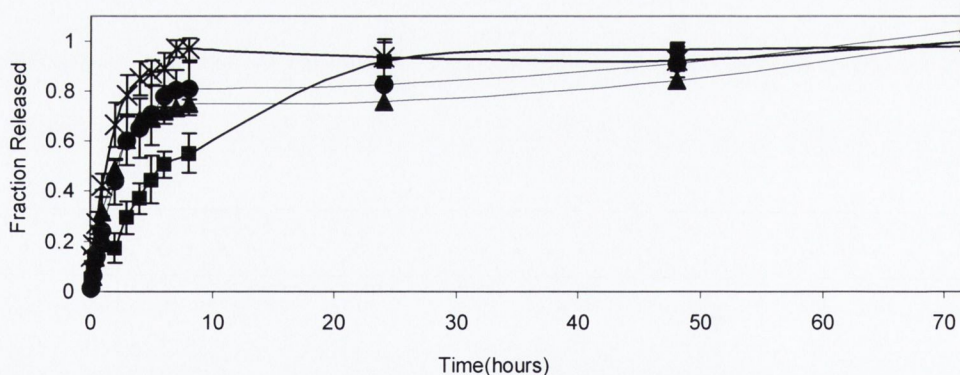
(b)
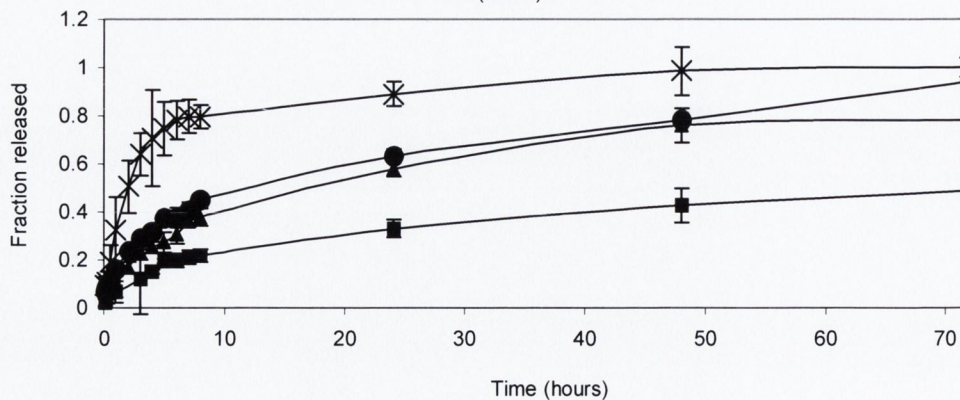
Figure 6.9: The fraction of DH released over time at both (a) 20°C and (b) 37°C from the hydrogels series PNP (■), PNP1$_{-12}$ (▲), PNP2$_{-12}$ (●) and PNP3$_{-12}$ (x).

176

Table 6.3: Release rate constants (k_{dh}) of DH, SA and IDM from PNP-PLA$_{-12}$ hydrogels at 20 and 37°C calculated using Equation 2.22 (Higuchi, 1961) along with their co-efficient of determination (CD). Also shown is diffusional exponent (n) and release rate constant (k_{dp}) estimated using 2.25 (Peppas, 1985).

20°C	$F=k_h^{0.5}$		$F=kt^n$			
	k_{dh20} $(min^{0.5})(x10^2)$	C.D.	k_{dp20} $(min^{-1})(x10^2)$	n ±s.d	C.D.	$k_{dh37}{:}k_{dh20}$
PNP (DH)	2.43±0.08	0.9572	1.132±0.38	0.5944±0.06	0.9710	0.3584:1
PNP1$_{12}$(DH)	3.84±0.03	0.9345	1.688±0.53	0.6953±0.06	0.9840	0.5208:1
PNP2$_{12}$(DH)	4.21±0.04	0.8928	0.751±0.10	0.8451±0.02	0.9983	0.3800:1
PNP3$_{12}$(DH)	5.26±0.02	0.9702	4.882±1.30	0.5207±0.08	0.9713	0.8041:1
PNP (SA)	2.48±0.07	0.9545	1.206±0.09	0.4671±0.04	0.9957	0.2700:1
PNP1$_{-12}$(SA)	2.72±0.04	0.9903	1.845±0.16	0.5702±0.01	0.9973	0.4705:1
PNP2$_{-12}$(SA)	3.14±0.04	0.9929	2.287±0.16	0.5589±0.01	0.9982	0.4076:1
PNP3$_{-12}$(SA)	3.31±0.06	0.9883	2.814±0.44	0.5314±0.03	0.9900	0.6737:1
PNP (IDM)	1.36±0.12	0.6693	0.946±0.02	0.6008±0.01	0.9997	0.2000:1
PNP1$_{12}$(IDM)	1.64±0.04	0.9742	0.711±0.06	0.6468±0.01	0.9977	0.2579:1
PNP2$_{12}$(IDM)	1.60±0.05	0.9515	1.859±0.33	0.5822±0.05	0.9599	0.6875:1
PNP3$_{12}$(IDM)	1.44±0.15	0.7594	0.011±0.01	1.3370±0.21	0.9258	1.1805:1
37°C	k_{dh37}	C.D.	k_{dp20}	n ±s.d	C.D.	$k_{dh37}{:}k_{dh20}$
PNP (DH)	0.871±0.04	0.9087	1.498±0.37	0.4358±0.03	0.9483	
PNP1$_{12}$(DH)	2.050±0.02	0.9913	2.466±0.25	0.4675±0.01	0.9934	
PNP2$_{12}$(DH)	1.600±0.03	0.9848	1.859±0.25	0.4769±0.02	0.9864	
PNP3$_{12}$(DH)	4.234±0.02	0.9439	2.112±0.55	0.6629±0.08	0.9854	
PNP (SA)	0.671±0.06	0.9973	0.703±0.99	0.4939±0.01	0.9974	
PNP1$_{-12}$(SA)	0.788±0.02	0.9545	1.572±0.19	0.4080±0.03	0.9856	
PNP2$_{-12}$(SA)	1.289±0.73	0.9987	1.436±0.03	0.4835±0.01	0.9951	
PNP3$_{-12}$(SA)	2.230±0.01	0.9983	1.897±0.05	0.5285±0.01	0.9996	
PNP (IDM)	0.272±0.05	0.4724	$2.69E^{10}±1.05E^9$	1.97±0.2440	0.9349	
PNP1$_{12}$(IDM)	0.423±0.04	0.6737	0.986±0.06	0.3964±0.08	0.6296	
PNP2$_{12}$(IDM)	1.109±0.07	0.9982	0.973±0.04	0.5066±0.01	0.9984	
PNP3$_{12}$(IDM)	1.709±0.03	0.9842	2.278±0.28	0.4493±0.02	0.9898	

At 20°C, introducing PLA resulted in non-Fickian release pattern (Peppas, EQN 2.25). In order to compare the release rates the diffusional exponent was fixed as 0.5 and reasonable fits were obtained as shown in Table 6.3. A plot of the release rate against the percent of PLA and the

pore size gave a linear relationship with R^2 values of 0.922 and 0.978 at 20°C respectively (Figure 6.10). PNP1$_{-12}$ and PNP2$_{-12}$ displayed a continuous release in drug after 24 hours whereas PNP3$_{-12}$ had levelled off with ~95% of the total drug released within 8 hours. After 3 days ~95% release was achieved from all systems.

(a)   (b)
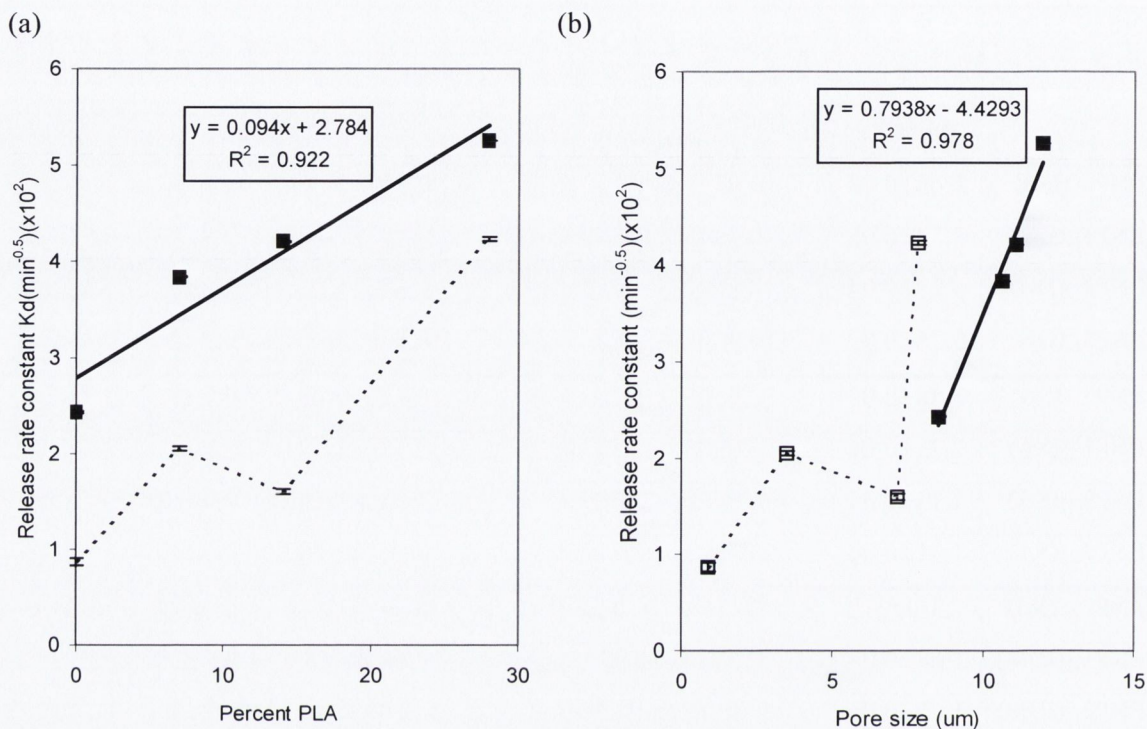
Figure 6.10 (a): Relationship between the hydrogel composition and release rate constant of DH at 20°C (■) and 37°C(□) (b): Relationship between the release rate constant of DH and pore size at 20°C (■) and 37°C(□).

At 37°C, release was much slower than at 20°C and increased with increasing PLA content, as did polymer swelling. The diffusional exponent increased as PLA content increased varying from Fickian to anomalous diffusion indicative that the mechanism of release above the LCST was composition dependent. After 3 days drug release levelled off with 95%, 80% and 60% of the total drug was released for PNP3$_{-12}$, PNP2$_{-12}$ and PNP1$_{-12}$ respectively. No further release was seen without decreasing the temperature. Above the LCST, an upward trend was seen between the pore size and release rate constant.

The thermal ability to control the rate of release decreased as the percent of PLA increased. This can be explained relative to the differences in the swelling kinetics as well as the equilibrium-swelling ratio. A significant reduction in the crosslinking density was seen using the Flory-Rehner theory (Section 4.4.5), on increasing MW of PLA in addition to the amount of PLA incorporated into the gel. This led to a higher swelling ratio of the gels at both temperatures the higher the PLA content. Similarly an increase in pore size was observed with increasing PLA

content using SEM. These results are illustrated by the ratio of the rate constants at both temperatures in Table 6.3 where the ratios varied dependent on composition.

6.4.2 SA release from PNP-PLA$_{-12}$ hydrogel systems

The release profiles of SA at 20°C and 37°C are displayed in Figure 6.11
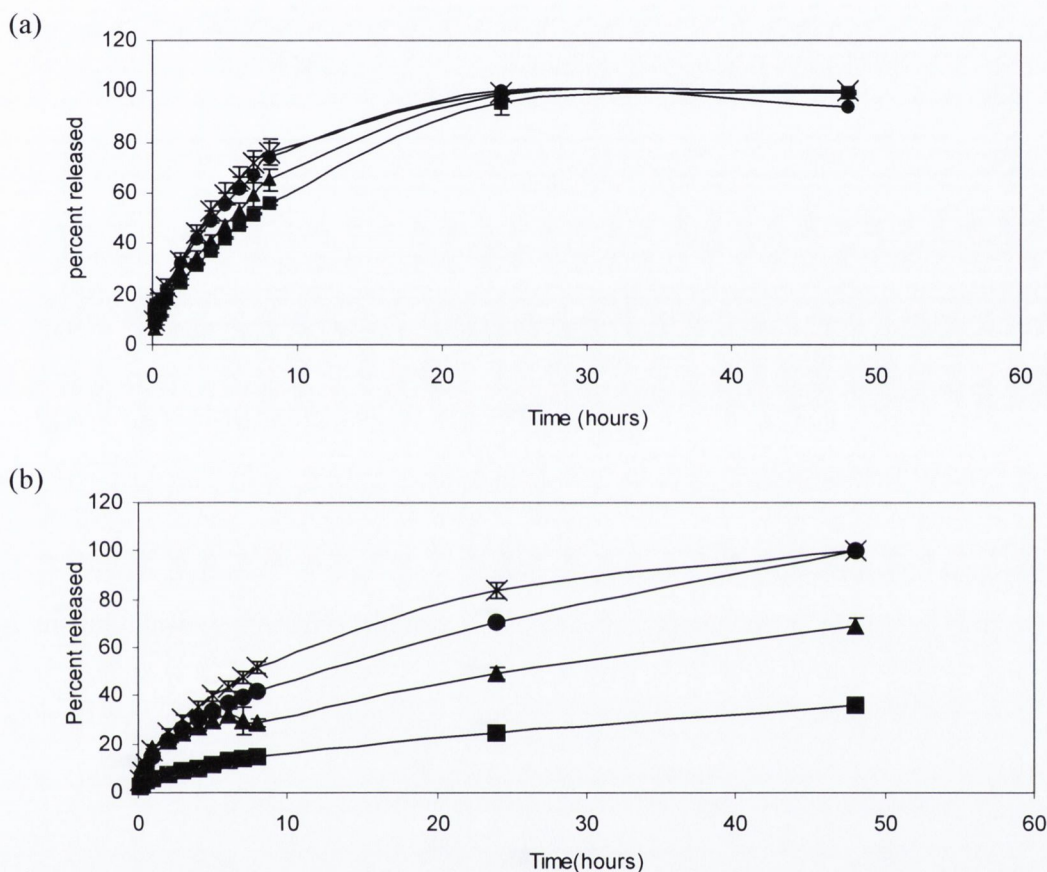
Figure 6.11: The fraction of SA release over time at both (a) 20°C and (b) 37°C from the hydrogels series PNP (■), PNP1$_{-12}$ (▲), PNP2$_{-12}$ (●) and PNP3$_{-12}$ (x).

PNP3$_{-12}$ gel had the fastest SA release rate of the all the gels at both temperatures, which in turn is reflective of the swelling kinetics. The release rate had a linear correlation with hydrogel composition at both temperatures with R^2 values of 0.984 and 0.9246 at 20°C and 37°C respectively. At 20°C the release behaviour for the co-polymeric systems was characteristic of non-Fickian behaviour. A levelling off of drug release was achieved within 24 hours for all systems.

At 37°C the rate and duration needed for total drug release were significantly influenced by hydrogel composition. This can be attributed to the collapsed state of the hydrogel network. The diffusional exponent increased as the percent of PLA increased. In addition the mechanism of

release and rate of release of SA from the hydrogel series was controlled by the pore size available for diffusion at both temperatures. A statistical difference ($p<0.05$) was observed between the pore size and rate of release at both temperatures (Figure 6.12) and a trend was established with a R^2 value of 0.9051.
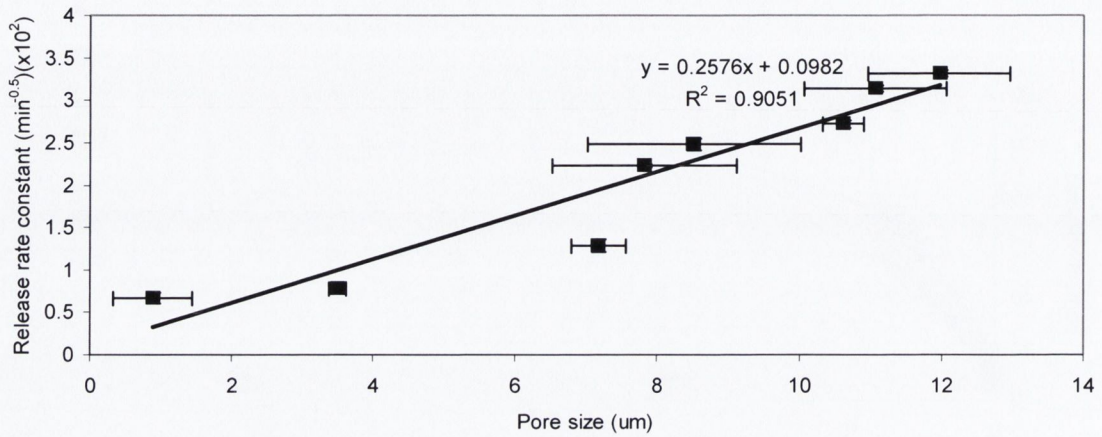
Figure 6.12 Relationship between the release rate constant of SA from the hydrogel series and the pore size of the hydrogel series.

6.4.3 IDM release from PNP-PLA$_{-12}$ hydrogel systems

The release profiles of IDM at both temperatures from the hydrogel series are shown in Figure 6.13.
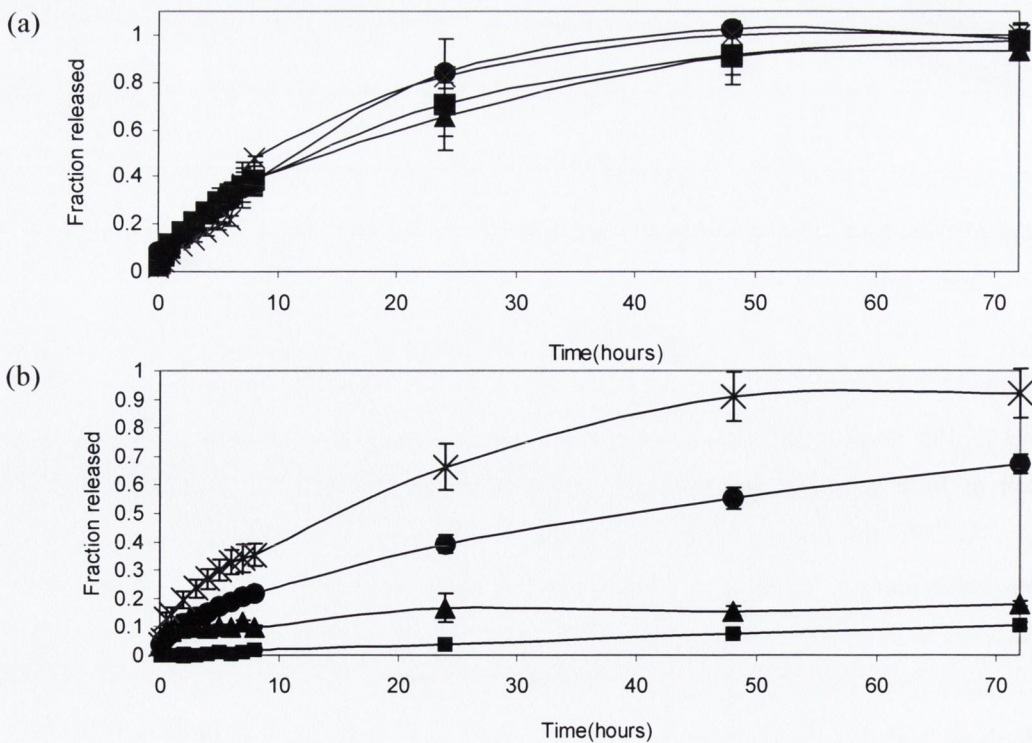
Figure 6.13: The fraction of IDM release over time at both a) 20°C and b) 37°C from the hydrogels series PNP (■), 93-7 (▲), 86-14(●) and 72-28(x).

At 37°C, the release rates from the hydrogels corresponded to the swelling pattern above the LCST with a linear correlation (R^2=0.9610) between the rate of IDM release and hydrogel composition (Figure 6.14 (a)). The release kinetics are characteristic of Fickian diffusion. A 2-fold increase was seen in the release of IDM on increasing the MW of PLA. This can be attributed to the lower crosslinking density of the three dimensional network leading to a more porous structure. As a result of a larger more open network the ability to thermally control the release of IDM significantly decreased ($p < 0.05$). After 3 days PNP3$_{-12}$ had successfully released the total amount of IDM loaded.
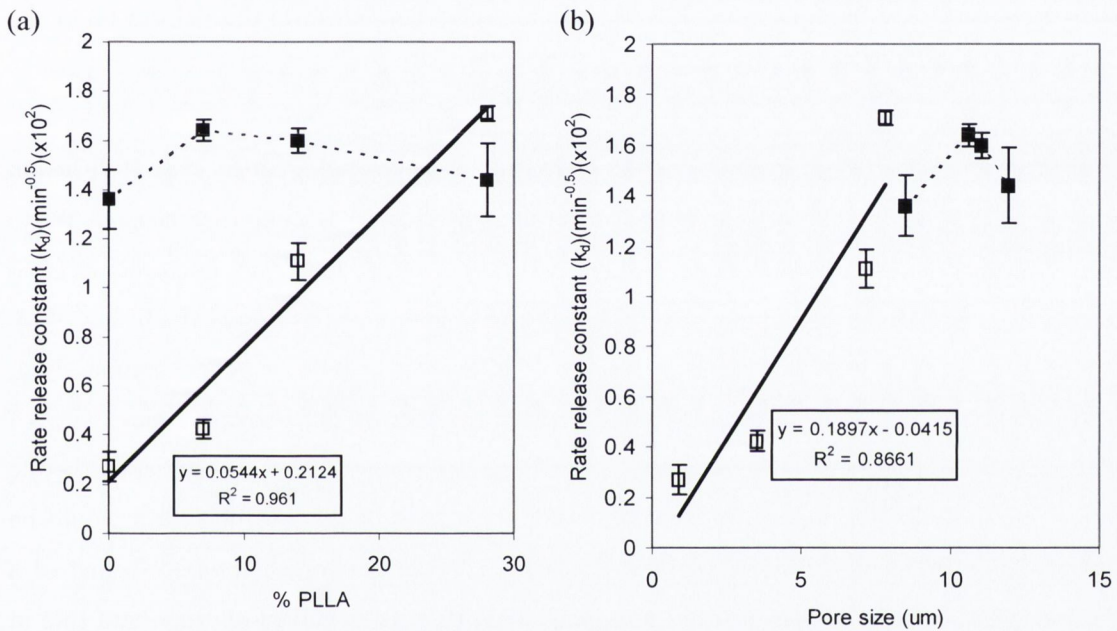
Figure: 6.14 (a): Relationship between hydrogel composition and release rate constants of IDM at 20°C (■) and 37°C(□) (b): Relationship between release rate constants of IDM and pore size of the hydrogel series at 20°C (■) and 37°C (□).

At 20°C, in the case of the co-polymers, drug release was faster, the greater the rate of swelling. Increasing the amount of PLA appeared to assist the release IDM in the early stages after 6 and 8 hours for PNP3$_{-12}$ and PNP2$_{-12}$ respectively. The release mechanism (Peppas EQN. 2.25) characteristic of non-Fickian behaviour, approached unity as the concentration of PLA increased. The release rate decreased as the percent of PLA incorporated into the gel increased (Figure 6.14 (a)). A possible explanation maybe hydrophobic interaction between the model drug and PLA component in the gel. Figure 6.154 (b) displays the relationship between the pore size and release rates, which indicate an increase in the rate of release as the pore size increases above the LCST, however composition appears to play an important role below the LCST.

181

6.5: Conclusions:

The degradation behaviour was significantly altered by incorporation of high MW PLA and the MW effect was composition dependent. Co-polymerisation of PNIPAM with PLA_{-12} led to a significant increase in the pore size and reduction in the crosslinking density relative to PNP-PLA_{-2} systems as previously seen in Section 4.12. The swelling kinetics therefore were also modified leading to a greater space for solute diffusion. As a result an effective reversal in the control of the rate of degradation was observed on switching temperature from below to above the LCST in comparison to that of the smaller MW PLA hydrogel series. All systems revealed a similar trend whereby the higher the PLA component incorporated in to the gel the faster the degradation behaviour both below and above the LCST.

Release studies varied from Fickian diffusion above the LCST to anomalous or case II diffusion below the LCST. All model drug compounds had relatively small molecular diameter relative to that of the mesh size of co-polymeric systems indicating degradation was not necessary for release to occur. The release kinetics were dependent on the temperature at which they were conducted with a higher rate of release overall below the LCST. IDM, a poorly soluble drug, revealed a faster rate of release above the LCST as a result of the increased mesh size of $PNP3_{-12}$. Another contributing factor of the fast release rate from $PNP3_{-12}$ at $37^{\circ}C$ could be the relative closeness of that temperature to the LCST. As a result the swelling ratio would be relatively large allowing diffusion of the drugs from a looser network compared to that of a fully collapsed network. However, drug physiochemical properties played an important role in the release behaviour both influencing rate and mechanism of release.

CHAPTER 7:

THE EFFECT OF DRUG PHYSCIOCHEMICAL PROPERTIES ON SWELLING/ DESWELLING KINETICS AND PULSATILE DRUG RELEASE FROM PNP2-2

7.1 INTRODUCTION:

As discussed in chapter 2, the majority of the published research focused on achieving thermoresponsive pulsatile drug delivery has involved heterogeneous PNIPAAM gels. Hydrophobic BMA is the most widely researched co-monomer introduced into PNIPAAM gels for pulsatile drug delivery. These delivery systems have proved successful in increasing the mechanical strength and have achieved "on-off" regulation of drug release in response to external temperature changes. Complete "on-off" regulation of drug release using poly (N-substituted acrylamide) co-polymers has been explained by the presence of a surface modulated polymeric skin layer formation. Altering the length and mobility of the alkyl side chains has controlled this dense skin layer process [Okano et al., 1990, and Bae et al., 1991, Yoshida et al., 1991, Gutowska et al., 1992].

Limited research is available on degradable pulsatile drug delivery systems. Thermoresponsive degradable polymeric micelle systems have been developed but not investigated for on-off regulation of drug release (Liu et al., 2003). Makino et al., (2000) achieved pulsatile release of estradiol from poly (lactide-co-glycolide) microspheres. Such systems cannot be controlled by stimuli to trigger pulsatile release. Instead control of pulsatile release from such systems was limited to the time needed for the systems to degrade. Recently degradable thermally sensitive micelles made from poly (N-isopropylacrylamide-co-N,N-dimethylacrylamide-b- poly(D,L- lactide-co-glycolide)) have been developed (Liu et al., 2005). Their findings indicated drug release could be tailored by altering the length of the PLGA block. The results showed drug release responded to environmental changes however the ability to control "on-off" release has not yet been investigated.

The present chapter examines pulsatile drug release from a novel thermoresposive biodegradable hydrogel. PNP2-2 was chosen as the tailored hydrogel to obtain better control over degradation and drug release. By introduction of PLA into the backbone of the gel, manipulation of the LCST was achieved to that near of body temperature (Section 4.4.2). The ability of PNIPAAM-co-PLA to thermally switch off drug release will be examined using a range of macromolecules and small molecular weight compounds. The extent to which the chosen model compounds or drug influenced the rate of swelling of the system, the drug diffusivity within the gel and diffusional release rates of the drug from the system as well as the size of the drug pulse seen following contraction will be examined. A range of probe molecules varying in physiochemical properties such as molecular weight, solubility, and chemical nature were chosen as model compounds. The hydrogels were loaded with drug solutions as described previously (Section 3.4) and their swelling/contraction rates examined.

7.2 INFLUENCE OF MODEL DRUGS ON SWELLING/DESWELLING

In chapter 4, the swelling and deswelling /contraction patterns of the unloaded PNP2$_{-2}$ disc in PB on switching temperature between 20°C and 37°C was shown in Figure 4.22 along with the corresponding swelling and contraction rates. The swelling (k_{s1}) was proportional to the square root of time during the first swelling period at 20°C (0-1hr) (Equation 2.22, Higuchi), whereas a decrease in the diffusion exponent was observed during the second swelling period at 20°C (4-7hr).

All studies undertaken in the following chapter involved the use of PNP2$_{-2}$ hydrogel system. The swelling and contraction patterns of the drug-loaded discs are shown in Figure 7.1(a-d) along with the corresponding pattern for the unloaded hydrogel (shown as a dashed line). The influence of the various drugs on the swelling contraction pattern was also quantified using the swelling rate constants (k_{s1}, k_{s2}) and the maximum contraction rates (k_{MC1}, k_{MC2}). The values obtained are shown in Table 7.1.

7.2.1 Small molecular weight compounds:

The effect of each of the hydrophobic drugs was to decrease the rate of swelling of the hydrogel while the reverse was seen in the case of diltiazem hydrochloride. The data in Table 7.1 indicates that during the first swelling period (k_{s1}), the swelling kinetics gave reasonable fits when described as diffusion controlled. There was no statistical difference in the swelling rate between diltiazem and indomethacin loaded hydrogels whereas a 1.5-fold increase in the rate of indomethacin-loaded hydrogel was observed in comparison to that of salicylic acid. The effect of the drug was to decrease the rate of diffusion of the medium into the hydrogel network at 20°C.

The swelling rate during period 2 was significantly greater than that during period 1. This effect can be attributed to the diminishing effect of the drug-matrix interaction over time as the outermost layer of the gel begins to swell and drug is released. A decrease in the diffusional exponent (n<0.5) during period 2 was seen of the order DH>DB>IDM>SA compared to that of the unloaded gel (Table 7.1). The change in the swelling rate constant is depicted in Figure 7.2 which shows a relationship (R^2= 0.9102) between the swelling rate constant during period 1 (k_{S1}) and diffusional exponent (n) for the swelling during period 2.

184
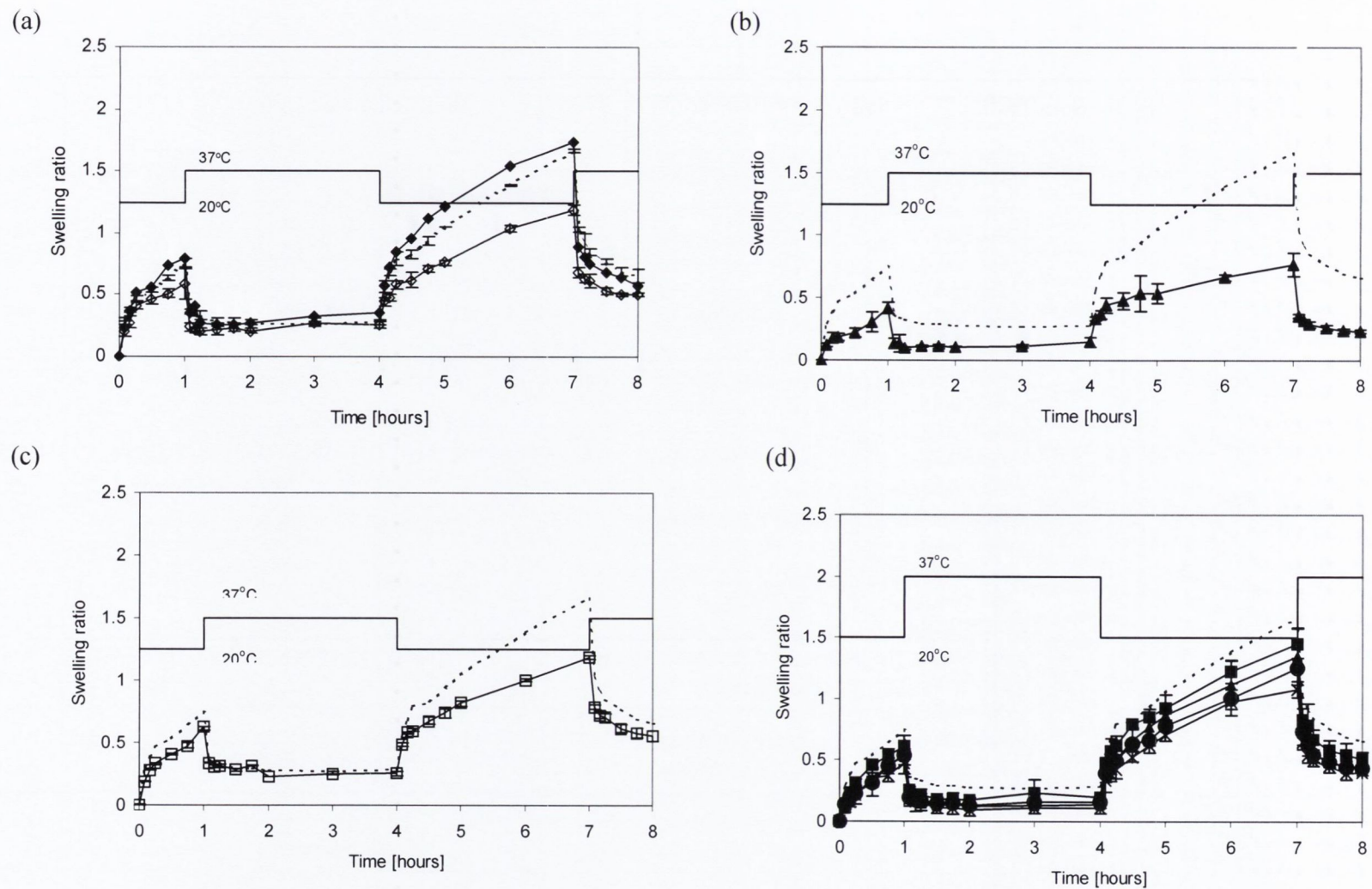
Figure 7.1: Swelling-contraction of unloaded hydrogel disc (---) on temperature switch between 20°C and 37°C for comparison with drug loaded systems (A) DH (♦), and DB (◊), (b) INDO (c) SA and (D) D4 (■), D10 (▲), D40 (●) and D70 (x).

Table 7.1: Swelling rate constants (k_s) and maximum contraction rates (k_{mc}) for the two swelling-contraction cycles (Fig 7.1(a-d).

	$M=k_d t^{0.5}$				$M=k_d t^{n}$					
	$(k_s 1)$ $(min^{-0.5})(x10^2)$	CD	$(k_s 2)$ $(min^{0.5})(x10^2)$	CD	Diffusional Exponent (n_1)	CD	Diffusional Exponent (n_2)	CD	k_{MC1} $(min^{-1})(x10^2)$	k_{MC2} $(min^{1})(x10^2)$
unloade	10.108±0.41	0.9538	13.53±0.93	0.7709	0.3616±0.022	0.9938	0.3188±0.044	0.9 189	8.50±0.19	13.15±0.32
DH	10.80±0.36	0.9715	14.90±0.97	0.7298	0.4292±0.005	0.9805	0.3076±0.095	0.9952	8.96±0.2	17.43±0.22
DB	8.18±0.37	0.9441	9.91±0.67	0.6921	0.3701±0.018	0.9794	0.3049±0.028	0.9966	7.53±0.1	10.16±0.0
IDM	7.67±0.26	0.9696	10.13±0.8	0.5100	0.4104±0.075	0.9844	0.2596±0.033	0.9690	6.77±0.0	8.31±0.01
S.A	4.88±0.22	0.9510	6.79±0.64	0.4083	0.5050±0.033	0.9510	0.2315±0.024	0.9783	6.37±0.079	8.29±0.02
D4	7.83±0.22	0.9828	11.83±0.70	0.7875	0.5848±0.028	0.9920	0.3246±0.015	0.9884	7.77±0.021	12.83±0.25
D10	6.45±0.23	0.9758	10.79±0.79	0.8960	0.6384±0.095	0.9974	0.3652±0.015	0.9903	7.35±. 064	12.78±0.14
D40	6.50±0.20	0.9800	9.90±0.50	0.8627	0.5822±0.011	0.9883	0.3541±0.026	0.9780	7.39±. 090	10.80±0.09
D70	5.82±0.19	0.9777	8.87±0.90	0.9035	0.5798±0.019	0.9858	0.3708±0.056	0.9877	6.54±0.154	8.79±0.021
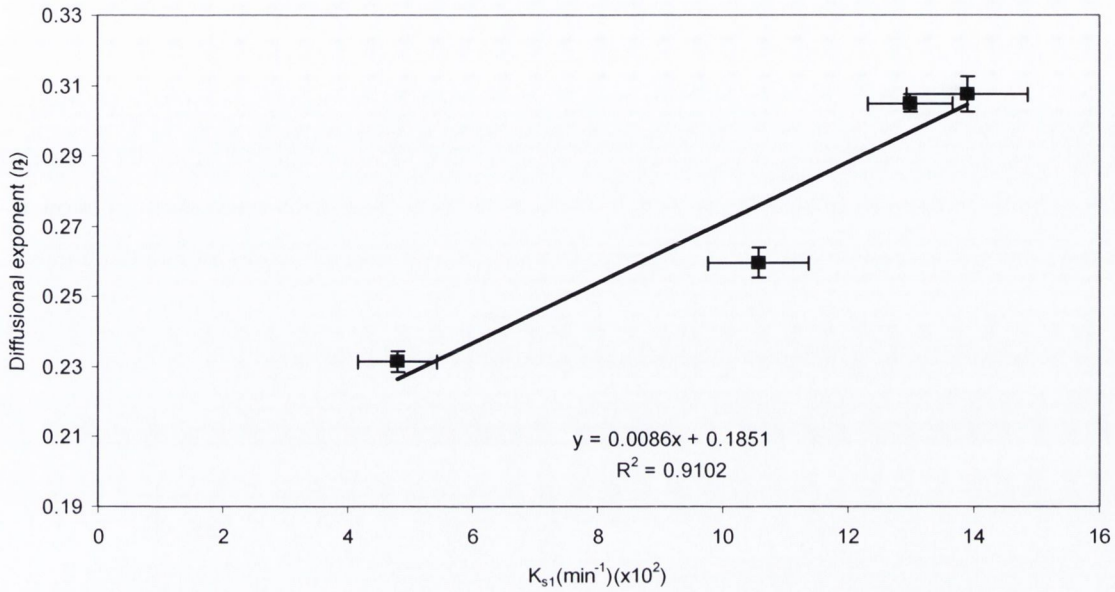
Figure 7.2: Relationship between the swelling rate constants (k_{s1}) and diffusional exponent (n_2) during the second swelling period.

The swelling level prior to temperature switch influenced the magnitude of contraction at the switch temperature. The rate of swelling decreased in the order DH>DB>IDM>SA whereby the lower the swelling at a particular time the smaller the magnitude of contraction. At 37°C, (the residual swelling volume), a similar trend was observed whereby the physicochemical properties of the drugs influenced the magnitude of the residual swelling volume. A noted increase in the swelling was observed in the case of DH whereas the remaining compounds decreased the swelling ratio relative to that of the unloaded hydrogel.

7.2.2 Dextran pulsatile swelling:

The loading of the series of dextrans ranging in molecular weight from 4000 to 70,000 Daltons suppressed the rate of swelling of the PNIPAAM-co-PLA$_{-2}$ hydrogel (Figure 7.1(d)). This effect was significantly increased ($p < 0.05$) the higher the molecular weight of dextran. Coughlan and Corrigan (2004) studied the swelling of dextran fractions in PNIPAAM and found an increase in the rate of swelling due to the hydrophilic nature of dextran. The decrease in the swelling of the dextran-loaded polymers could be attributed to binding of the dextran fractions in the PLA

component of the polymer. The binding of the dextran containing hydroxyl groups to the ester bond is sensitive to hydrolytic cleavage (Larson, 1998). Swelling during period 1 (0-1hrs) was characteristic of anomalous behaviour, suggesting a relaxation-controlled mechanism.

Both swelling periods at $20^{\circ}C$ were fitted to equation 2.25,(Higuchi 1961) in order to compare swelling rates. The swelling profiles gave a reasonable fit to the diffusion-controlled model. In each case the swelling rate constant during period 2 was significantly greater than that during period 1 and a decreasing trend (R^2=0.9692) was observed between the swelling rate constant and the logged molecular weight of each dextran fraction (Figure 7.3). The rate constant decreased from 7.83($\times 10^2$) ($min^{-0.5}$) to 5.82($\times 10^2$)($min^{-0.5}$) depending on the MW dextran loaded in the gel.
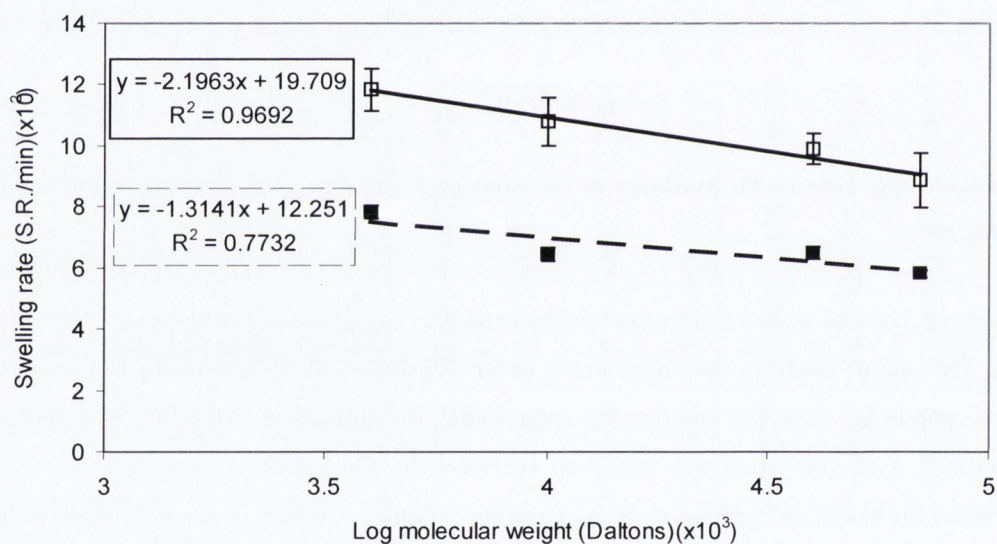
Figure 7.3: Relationship between the molecular weight of the dextrans and the swelling rate constant of loaded dextran hydrogel during swelling period 1(■) and period 2(□).

The residual volume at $37^{\circ}C$ following the first contraction period was similar or decreased in comparison to that of the unloaded hydrogel due to the presence of dextran. The effect is more apparent the higher the MW of dextran as indicated above.

The decrease in the rate of swelling caused by the dextrans molecules resulted in a smaller magnitude and rate of contraction on switching the temperature (Table 7.1). The higher the swelling level attained, the greater the magnitude and rate of contraction (Figure 7.1).

188

For all the drugs examined, a linear relationship existed between the total magnitude of contraction and the K_{MC} (Figure 7.4 (b)). In the case of the smaller molecular weight drugs a plot of swelling level prior to switch against the total contraction gave a R^2 value of 0.8324 while the dextran series gave a R^2 value of 0.9398 (Figure 7.4(a)). The swelling and contraction cycles of the thermoresponsive hydrogels were therefore shown to be strongly influenced by the physiochemical properties of the loaded drug.

(a)

(b)
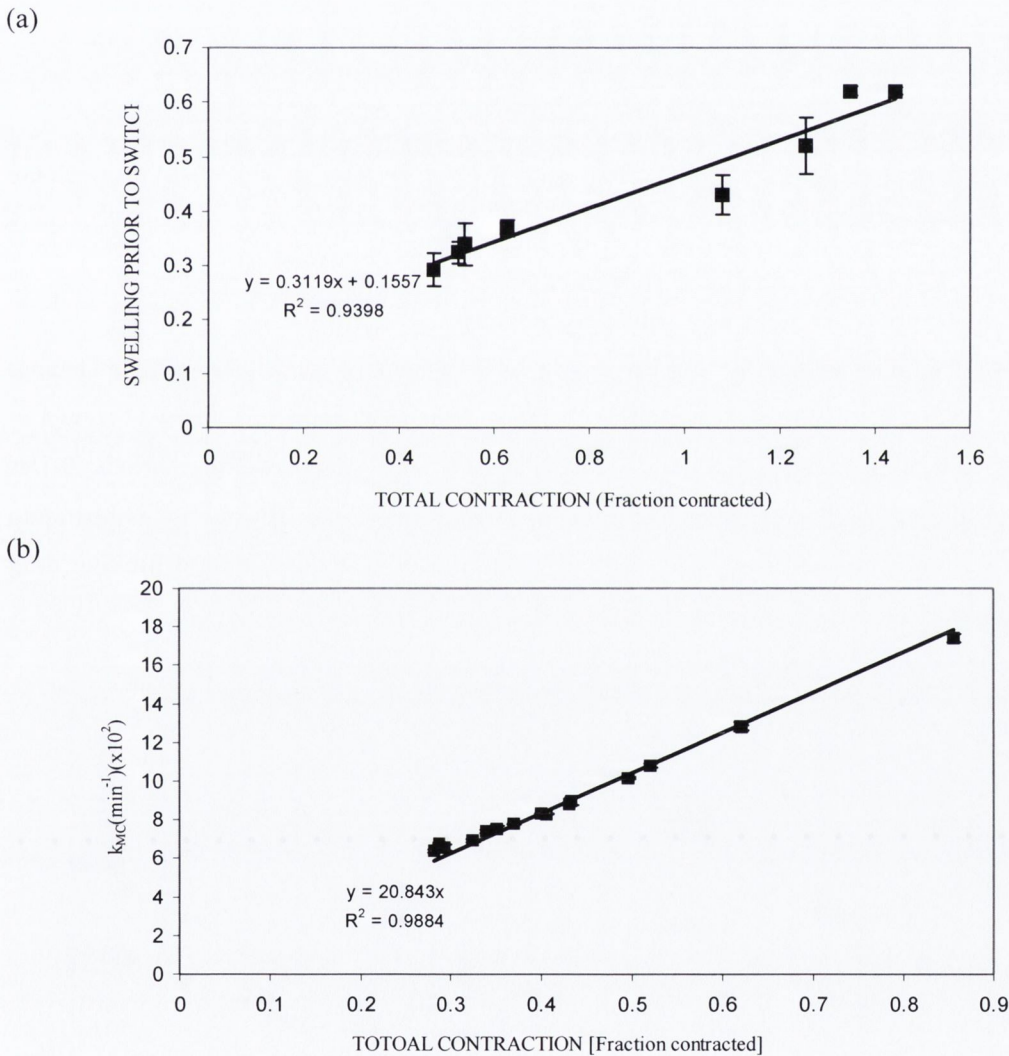
Figure 7.4: Relationship between total magnitude of contraction and the (a) fraction swollen prior to switch (b) maximum contraction rate (K_{MC}).

The hydrophilic model drug DH increased the rate of swelling of the hydrogel while other compounds decreased the rate of swelling for all drug-loaded hydrogels. The effects of the incorporated drugs influenced not only the rate of swelling but in turn influenced the swelling prior to switch and the magnitude of contraction. Polymer-drug interactions/binding may be playing an important role in the swelling kinetics. Tarvainen et al., (2006) loaded neutral and acidic drugs in to co-polymeric systems containing PLA and noted a catalytic effect on the degradation rate of the polymer system. In the following section, the effect of the level of swelling which in turn is related to the pore size and magnitude of contraction will be examined in relation to the pulsed drug delivery. Analysis of the drug release kinetics will be examined.

7.3 Pulsatile Drug Release

The effect of the temperature switch between 20°C and 37°C on the fraction and rate of drug release from the hydrogel was examined.

7.3.1 Pulsatile release of small molecular weight compounds

The cumulative fraction released and corresponding release rate of each of the small molecular weight compounds on switching the external temperature over an 8 hour time frame is shown in Figure 7.5 Release of the model compounds occurred at 20°C during both swelling periods (0-1hr, 4-7hr) as the hydrogel swelled allowing medium influx and thus drug diffusion. A temperature switch above the LCST caused a rapid deswelling or contraction of the hydrogel limiting drug diffusion (Figure 7.5)
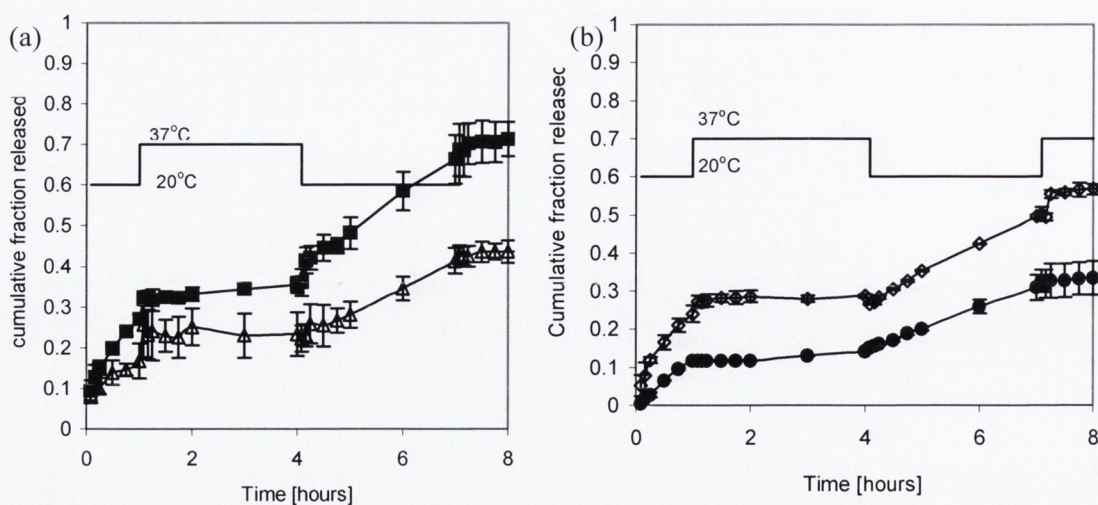
Figure 7.5: (a) Cumulative fraction released of (a) DH (■) and DB (Δ) and (b) cumulative fraction released of SA (◊) and INDO (●) on temperature switch between 20 °C and 37°C.

190

The fraction of drug released during the first swelling period was fitted to the Higuchi and Peppas equations (Equation 2.22, Higuchi) (Equation 2.25, Peppas) and the release parameters obtained (k_s, k_p) are given in Table 7.2 A reasonable representation of release was obtained and allowed the use of k_h to compare the different release profiles from the gel with the exception of IDM which approximated zero order kinetics.

Table 7.2: Release rate constant (k_h) at 20°C (Equation 2.22, Higuchi, 1961) and area under release rate curves versus time (AUC) obtained on temperature switch to 37°C. Also given are the coefficients of determination associated with the release rate constant (k_p) and diffusional coefficients (n) when release profiles were fitted to equation 2.25 (Peppas, 1985).

	$F=k_h t^{0.5}$		$F=k_p t^n$			
	(k_h) (min$^{-0.5}$)(x10^2)	C.D	(k_p) (min^{-1})(x10^2)	n ±s.d	C.D	(AUC) (fraction x 10^2)
SA	3.470±0.0005	0.9938	2.977±0.252	0.5429±0.030	0.9964	1.7673
IDM	----------------	--------	0.199±0.052	1.0040±0.067	0.9923	0.31635
DB	2.230±0.0014	0.8171	5.414±0.464	0.2493±0.026	0.9895	1.05418
DH	3.617±0.0007	0.9902	4.682±0.084	0.4275±0.005	0.9997	1.9477
D4	7.353±0.0055	0.8957	14.90±1.261	0.3002±0.025	0.9914	0.46831
D10	9.835±0.0075	0.8095	24.19±1.974	0.2446±0.023	0.9903	0.39073
D40	10.573±0.007	0.8210	27.29±1.276	0.2062±0.000	0.9964	0.63573
D70	12.670±0.008	0.8655	23.11±5.115	0.3148±0.063	0.9460	0.0764

Figure 7.6 (a-d) shows the experimental release rate of each of the model compounds from PNP2$_{-2}$ gels in response to stepwise temperature changes between 20°C and 37°C. At each temperature switch, a sharp peak was observed immediately after the temperature was increased. Drug is rapidly squeezed from the gel surface accompanying large volume changes due of contraction in the gel. The area under the release rate curve (AUC) was calculated in order to quantify the drug pulse seen on increasing the temperature (Table 7.2). For the hydrophobic series of drugs, the AUC was found to be proportional to the drug solubility (R^2=0.9476). In addition a linear relationship was seen between the release rate constant (k_h) and the AUC (R^2=0.9909). This in turn relates the magnitude of drug pulse to the solubility of the drug. This relationship suggests that the drug pulse was attributed to the presence of dissolved drug in the swelling front surrounding the drug core prior to temperature increase. Such drug was mechanically squeezed out as the polymer chains collapse.
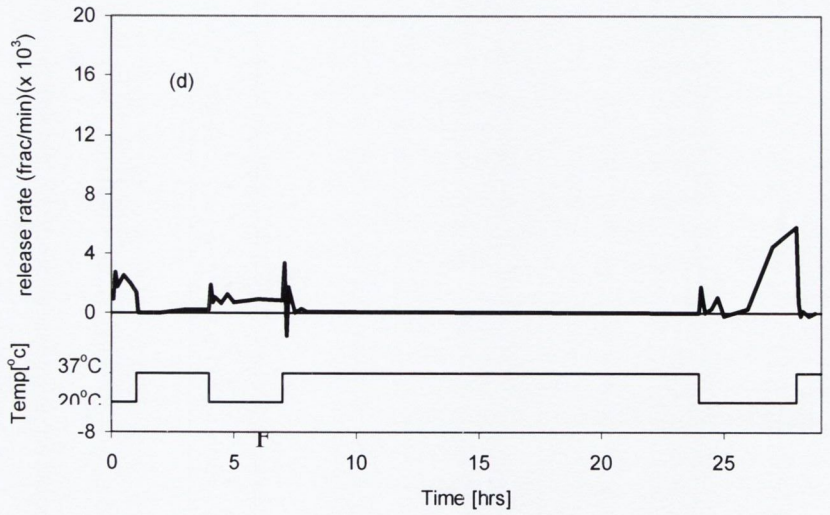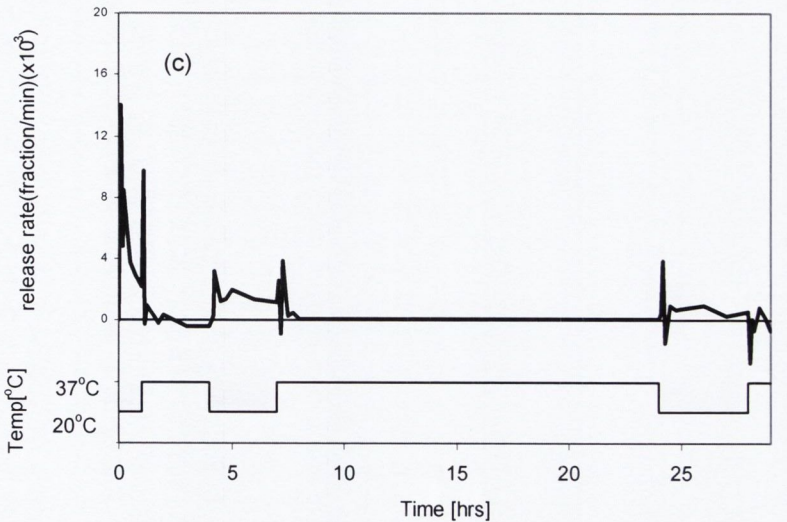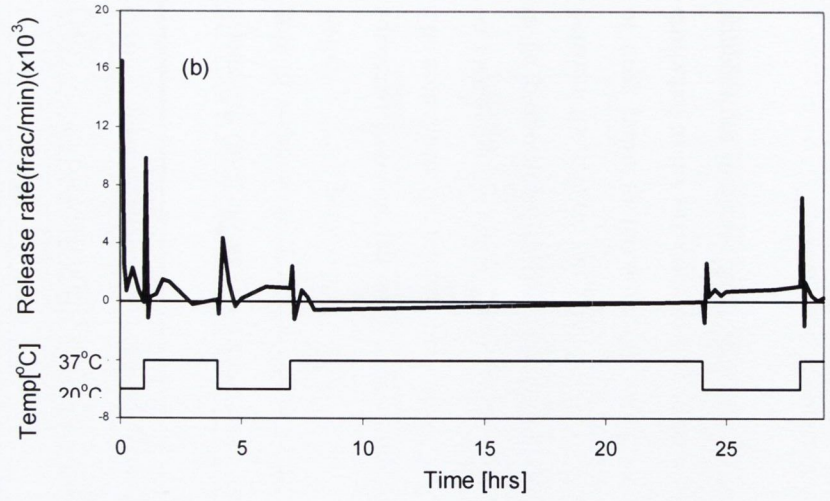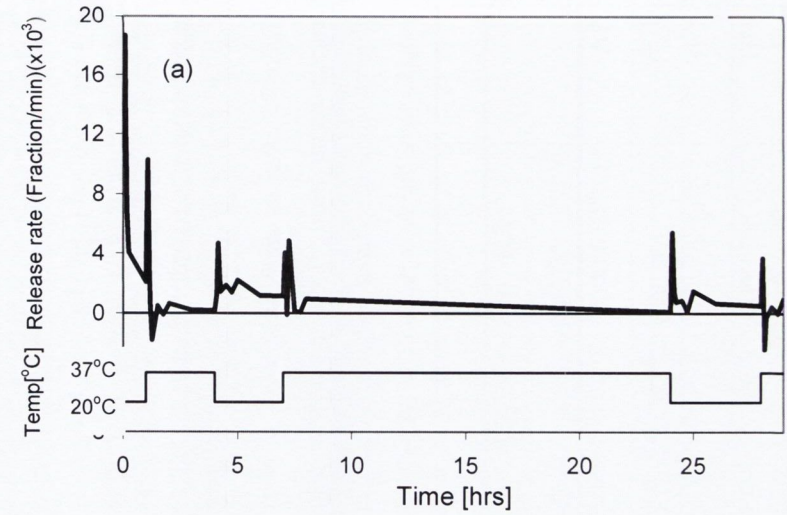
Figure 7.6: Corresponding release rates of (a) DH, (b) DB, (c) SA and (d) IDM on temperature switch between 20°C and 37°C (n=3).

192

On increasing temperature, all release profiles showed repeated fluctuations or sharp peaks after a lag time. Following temperature change, accumulation of internal pressure within the gel will occur in an attempt to extrude water from inside the shrinking gel. This resulted in a rapid outflow of medium to dissipate the pressure gradient after a certain time period. The intensities of these fluctuations diminished after a third cycle. At 37°C a negligible release rate was seen with all release profiles, except for the initial burst effect. These results imply that the release of small molecular weight compounds from the thermoresponsive PNP-PLA.2 hydrogel is predominately governed by the hydration of the gel. These results illustrate the effectiveness of these biodegradable thermoreponsive hydrogels as on-off regulators of controlled drug release.

Drug physiochemical properties played a significant role in the hydrogel release rate and transport mechanism at 20°C. Release data was fitted to EQN. 2.25 to give the diffusional exponent (n), which gave an indication of the release mechanism. In Table 7.2 it is shown that the values of the diffusional exponent (n) ranged from 0.20 to 1 depending on which model drug was been examined. Analysis of the release kinetics reveals that SA and IDM were both anomalous and Case 11 controlled. This is indicative of relaxation of the polymer or combined diffusion and degradation controlled mechanism. The release rate of indomethacin on temperature switch between 20 and 37°C did not show pulsed drug release on the first temperature change (Figure 7.6 (d)). In addition a large release was seen after 26hrs mid cycle of the third switch. This could be attributed to phase erosion whereby hydrolysis of PLA can lead to diffusion of the drug through the disrupted porous network.

Visual observation of the discs showed evidence of formation of a dense skin layer, which may be the cause of limited diffusion and dissolution of the drug. Furthermore the pore size, as measured by SEM at 37°C, revealed a pore size larger than the molecular diameter of the drugs. These results are suggestive of a dense skin layer formation. The change in the release rate was quantified by calculating the quasi steady state release rate constant (k_{ss}) and this was employed to compare release rates before and after temperature switch. The constant was defined as the average release rate at each temperature excluding the first thirty minutes after temperature switch. The proximity of this value to zero may be used to indicate the ability of the hydrogel to thermally shut off release. Figure 7.7 displays a bar chart of the kss of the model compounds.
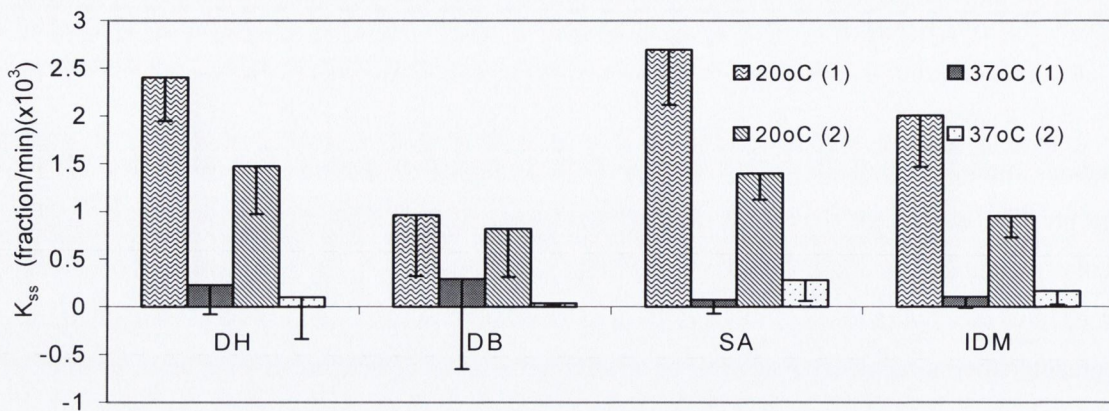
Figure 7.7: steady state release rate constants (kss) for the small molecular weight compounds after first temperature(1) and second temperature (2) switch; defined as the average release rate at each temperature, excluding first 30 min after temperature switch.

From The bar chart it can be observed that all systems approximated on–off release when the temperature was increased above the LCST. The error bars in proximity to or crossing the x-axis indicates the permeability of the drug from the gel decreased and drug release was effectively stopped.

7.3.2 Pulsatile release of dextran fractions from PNP2-2

The cumulative fraction released and the corresponding release rate of a series of dextrans on switching the external temperature is shown in Figure 7.8.
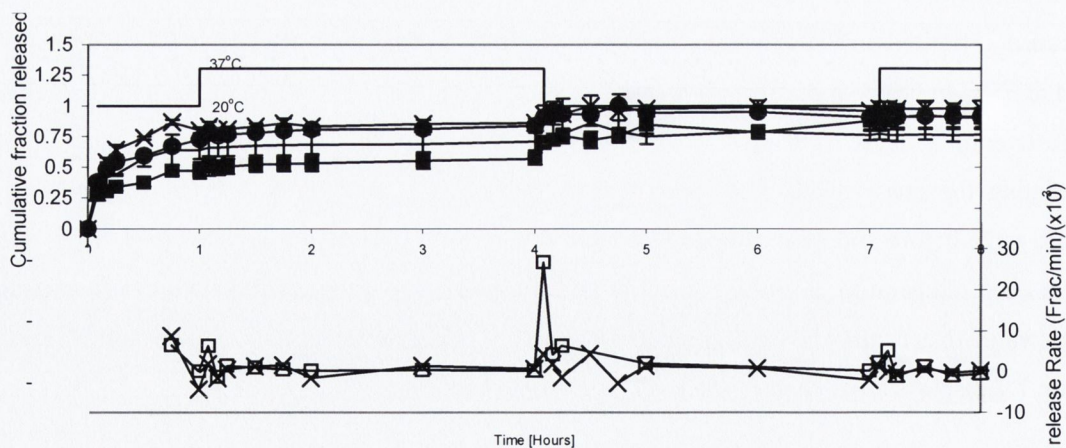
Figure 7.8: Cumulative amount of D4 (■), D10 (▲), D40 (●), and D70 (x) from PNP2-2 (top) and the swelling rate of D4 (□) and D70 (x) shown for clarity on temperature switch (bottom).

194

A pulsatile on-off release pattern was evident in this series with the pattern of release varying with molecular weight of the dextrans. During release period 1 (0-1hr) ~50to 90% of the total drug was released depending on the MW of the dextran. Hence limited drug was remaining for pulsatile drug delivery. After release period 2 (4-7 hrs) 100% drug release was achieved for all dextrans.

At higher temperatures (37°C) the cessation of drug delivery was achieved. All systems were successful for on-off pulsatile delivery, however a trend was noted whereby the higher the molecular weight of the dextran fraction the greater the release rate constant. Bulkier larger molecules would have been expected to have a slower release rate in comparison to that of smaller molecules.

In addition, the rate of swelling significantly decreased in PNP2$_{-2}$ gels the higher the MW dextrans incorporated into the gel (Section 7.4). A reduced influx of water into the gel would decrease the release rate. In chapter 4, the size exclusion technique found that a larger proportion of D4 would penetrate the core of the gel than that of D70. This suggests that the molecular diameter of the drug and reduced pore size of the gel due to the incorporation of PLA into the backbone of the gel resulted in a higher proportion of model drug at the interface of the glassy and rubbery phases of the swelling hydrogel. Since dextran is very soluble a high release rate would be seen, as the molecule would diffuse more rapidly from the outer surface of the gel. A linear relationship (R^2=0.9048) between the molecular weight and release rate constant was noted (Figure 7.9 (a)). In addition an inverse relationship between swelling rate constant and the release rate constant existed (Figure 7.9 (b)). The larger molecules therefore appear to be predominately entangled in the outer section of the hydrogel creating a molecular size dependant gradient.
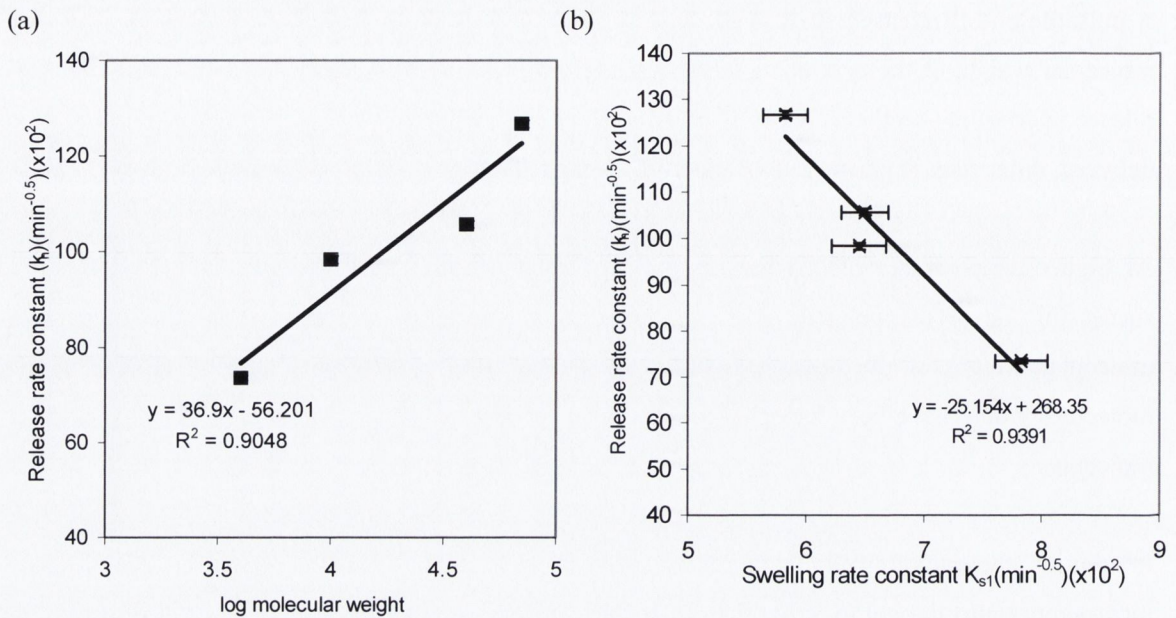
Figure 7.9: (a) Relationship between molecular weight and release rate constant (k_d) and (b) Relationship between the swelling rate (k_{s1}) constant and release rate constant (k_d) of the dextran fractions.

In order to quantify the drug pulse seen on temperature increase, the area under the release rate curve was calculated for the dextrans and is shown in Table 7.2. It is clear that the higher molecular weight of the series the less the amount of drug was squeezed out. The magnitude of drug pulse is consistent with a greater hindrance to transport larger drug molecules. These results are consistent with a lower diffusional coefficient compared to that of the smaller molecular weight compounds (Table 7.2). A trend was seen ($R^2=0.9672$) between the release rate constant and the AUC (Figure 7.10 (a)). Also a relationship ($R^2=0.9905$) existed between the swelling prior to switch and the AUC (Figure 7.10 (b)). In section 7.2.2, a notable decrease in the swelling rate, which in turn influenced the rate of contraction, was observed for the dextran series, the effect increasing the higher the molecular weight. The larger drug pulse can be attributed to a greater magnitude of contraction and also to a greater amount of drug present at the time of contraction.

In these studies rapid diffusion of dextran during the first swelling period from the outer region of the swollen hydrogel occurred. Dextran release in pulsatile studies is faster than release observed during non-pulsatile release experiments reported in chapter 5. This can be ascribed to different loading times employed for the individual studies. In the sustained release experiments undertaken, a loading time of 120hrs was employed whereas the drug-loading time for pulsatile release was

196

48hrs. Yu and Grainger (1995) also attributed a burst release of insulin from hydrogels due to incorporation of the drug in the surface layers during the solvent sorption method of loading. Coughlan and Corrigan (2004) similarly noted a molecular weight dependent gradient on pulsatile release of dextran molecules. This was attributed to both the loading and subsequent drying process

(a)   (b)
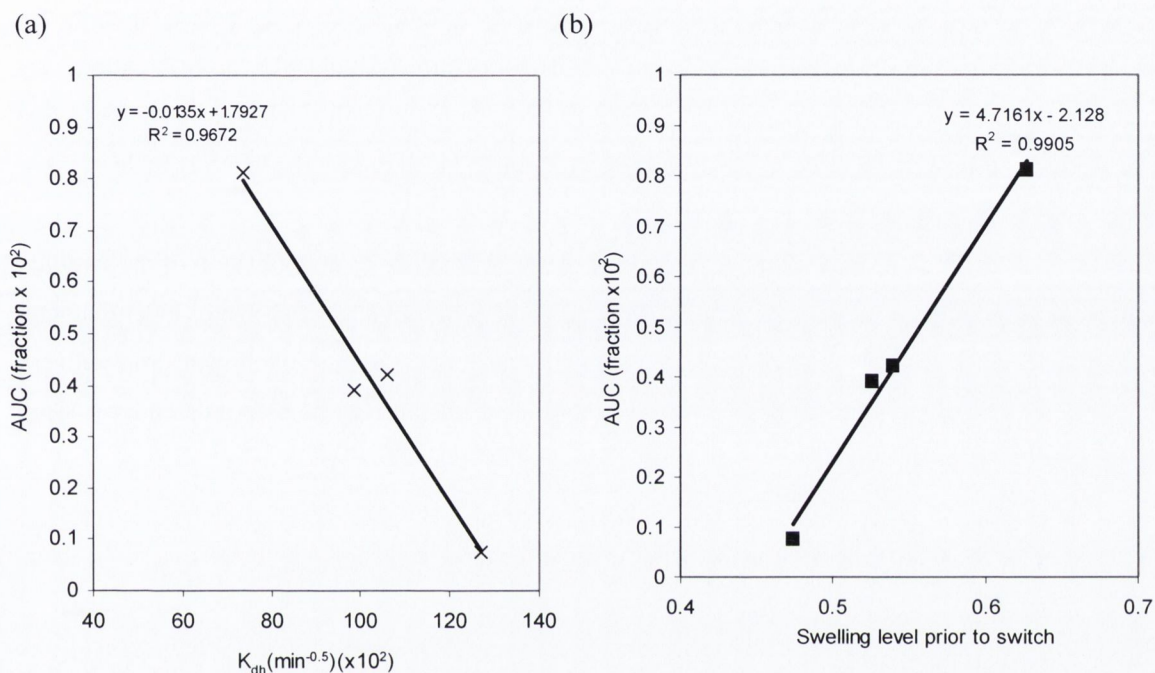
Figure 7.10 (a): Relationship between the release rate constant (k_h) and the area under the release rate curve and (b) relationship between the swelling level prior to switch and the area under the curve.

7.4: Conclusions:

These novel biodegradable hydrogels poly (N-isopropylacrylamide-co-PLA) (PNP2-2) are a potential new molecular structure to achieve intelligent drug delivery system. An increase in the LCST nearer to body temperature was achieved by the incorporation of PLA into the backbone of PNIPAAM. Increasing temperature appeared to induce formation of a dehydrated polymeric surface skin layer that stopped permeation. PNP2-2 gels shrink up to 80% their original volume on temperature switch suggesting the formation of a dense skin layer on the surface of the gel. In addition to the skin thickness, response to hydration and dehydration as a result of stepwise temperature change was rapid. This is reflected in the gradual decrease and a quick recovery of transmittance (Section 4.3.4). Therefore the incorporation of biodegradable hydrophobic co-

197

monomer PLA appears to strengthen the dense skin layer. This is further demonstrated by the effectiveness of thermal control of the smaller molecular weight drugs. On-off regulation of all drug compounds was achieved as demonstrated by the dramatic changes in the quasi steady state release constant (kss) both before and after temperature switch (Figure 7.7).

In the case of the dextran fractions, hydrogel contraction resulted in a drug pulse, whereby the magnitude of the drug pulse was related to the rate of contraction. A pulsatile "on-off" pattern was evident in this series with the pattern of release varying with the molecular weight. Release was likely governed by a molecular weight dependent gradient induced during the loading process.

Control of on-off drug release during temperature switch is possible by manipulation of the swelling behaviour (changing co-monomer content) of the gel, which in turn alters the size of inner diameter available for diffusion. PNIPAAM-co-PLA polymers constitute a unique intelligent drug delivery device whereby the geometry and pore size available for diffusion may be manipulated by varying molar ratios of reactants.

CHAPTER 8:

GENERAL DISCUSSION

8.1 INTRODUCTION

A novel series of thermoresponsive and biodegradable drug delivery systems were synthesised and characterised in the course of this project. Both structural parameters and the degradation behaviour were investigated relative to polymer composition and temperature. The potential use of these novel systems was examined using a range of model drugs in both sustained and pulsatile release. The effect of changing molar composition of the co-polymeric systems, MW of the PLA component and temperature was investigated in relation to the drug release process. The findings of the present work indicate a new drug delivery system, which may be tailored to meet specific criteria for drug release.

8.2 Thermoresponsive properties and swelling dynamics of hydrogels

Temperature sensitive hydrogels have been studied for drug delivery systems due to their unique thermoresponsive properties in water (Schild 1990, Galaev and Mattiasson, 1999). Kinetics and thermodynamics of the phase transition can be controlled by well-designed molecular parameters. Table 8.1 below summaries the composition and thermoresponsive behaviour of each system investigated.

Table 8.1: Hydrogel systems thermoresposive properties

Hydrogel	PNIPAAM:PLA (w/w) ratio	LCST(^{o}C)	S.R.$_{20}$	S.R.$_{37}$	P_x	Pores size (μm)(20°C)	Pore size (μm)(37°C)
PNP	100-0	28.41	8.53	0.1957	0.0164	8.52	0.8940
PNP1$_{-2}$	93-7	29.11	7.30	0.5326	0.0200	5.79	2.09
PNP2$_{-2}$	86-14	30.33	6.61	0.7842	0.0217	3.94	2.13
PNP3$_{-2}$	72-28	31.52	5.85	0.7400	0.0249	2.82	2.57
PNP1$_{-12}$	93-7	31.94	10.54	0.6212	0.0103	10.61	3.50
PNP2$_{-12}$	86-14	34.17	11.74	1.519	0.0090	11.06	7.18
PNP3$_{-12}$	72-28	36.69	14.14	4.450	0.0065	11.96	7.82

P_x= crosslinking density

S.R.= Swelling ratio

The main influence on S.R. is the molecular weight between crosslinks, which was altered in this case by changing the molecular weight of the macromers, and increasing the proportion of hydrophobic moiety PLA. Interestingly hydrogels of the same molar ratio composition but

higher MW PLA showed an increase in the equilibrium-swelling ratio; the most significant change seen in PNP3 system with a 2.4 (14.14/5.85) and 6-fold (4.45/0.74) difference at 20°C and 37°C respectively. Hydrogels with a smaller MW PLA produced gels with a tighter structure that hindered the mobility of the polymer chains and resisted the osmotic pressure of the swelling media. As a result the hydrogels swelled to a lesser extent and reached equilibrium much faster compared to gels with larger macromers.

It is known that PNIPAAM's tacticity has a major influence on PNIPAAM's LCST (Schild 1990). Other solution components can exert a significant and predictable effect on PNIPAAM's LCST (Section 1.6-1.7). In Chapter 4 it was observed that increasing PLA content increased the LCST, the effect becoming more pronounced the higher the MW. This result was attributed to polarity of the polymer favouring polymer-water interactions over polymer-polymer interactions. Similarly Chung et al., (1998) prepared a number of polar and non-polar end-modified PNIPAAM's. They prepared amine and hydroxyl terminated PNIPAAM oligomers and found that the hydroxyl group increased the PNIPAAM LCST more than the amino group.

The effect of molecular weight on the LCST in aqueous solution has also been explored by numerous authors (Furyk et al., 2006). An increase in the MW was shown to decrease the LCST of thermoresposive polymers (Schild and Tirrell, 1990). In the current work a decrease is observed in the LCST on increasing MW in both of the hydrogel series. However increasing the PLA content increases the LCST of the polymers (Table 8.1). Furthermore the higher MW PLA caused the greatest increase in the LCST. The Flory-Huggins theory has also been adapted to explain the effect of the molecular weight on the LCST (Equation 8.1).

$$\chi_c = \frac{1}{2}\left(1 + r^{-0.5}\right)^2$$
<div style="text-align:right">EQN8.1</div>

Where;
r is the ratio of molar volume of polymer over the molar volume of solvent
χ_c is polymer-solvent interaction parameter

The polymer-solvent interaction parameter, χ_c, changes as the size of the polymer changes since the ratio of molar volumes of polymer over solvent decreases as the degree of polymerisation decreases thus causing χ_c to increase (EQN 8.1).

8.3 Hydrogel swelling and degradation

Many studies have shown that microstrucutral design and chemical composition can be used to tailor improved polymeric matrices (Pillai and Panchagnula 2001). However few polymeric systems combining both smart and biodegradable properties have been synthesised and investigated in relation to drug delivery. An integral part of hydrogel properties is the swelling behaviour in water. The swelling behaviour of PNIPAAM-PLA gels was investigated in conjunction with both structural and environmental parameters. The effect of temperature, composition, molecular weight distribution and morphology on the rate of degradation of these novel intelligent-co-biodegradable hydrogels was investigated in both Chapter 5 and 6.

8.3.1 Effect of structural parameters:

Synthesising polymers with hydrolytically unstable ester groups accomplished degradation. Also by changing the molar ratio of monomers during polymerisation, control of the hydrogel degradation was achieved.

In the case of PNP-co-PLA$_2$ systems, below the LCST, the influence of composition of the molar ratio of PNP to PLA was to display a faster rate of degradation characteristic of zero order kinetics the higher the PLA component. Similarly Davis et al., (2003) showed that the mass loss of poly (LA-co-CA) (lactic acid-co-caproic acid) diethylene glycol based networks is a function of both hydrolysis kinetics and network structure.

The S.R increased as a function of time after which a decrease in mass was observed (Section 5.2). During degradation, two factors are of importance. Firstly, degradation causes an increase in the number of carboxylic acid chain ends, which are known to autocatalyse ester hydrolysis. Secondly, oligomers that are soluble in the surrounding aqueous medium can escape from the matrix. As degradation advances soluble oligomers close to the surface can leach out before they fully degrade whereas those remaining in the core of the matrix remain entrapped. This yields a low pH value in the core, which in turn results in accelerated degradation (Li and Vert 1994; van Dijk-Wolthuls, Tsang and Kettenes-van den BoschW.E. Hennink 1997). This could also be a contributing factor to the higher rate of degradation the higher the PLA content.

Changing the molecular weight between crosslinks of co-polymeric systems was also achieved by increasing the MW of the PLA component. A significant increase in pore size was observed for the PNP-co-PLA$_{12}$ hydrogel systems. This was attributed to a lower cross-linking density. However the increase in space available for solute diffusion did not lead to a greater rate of

degradation with respect to PNP-co-PlA$_{-2}$ systems. This was reflected in the [COOH] found within the degradation media at the end of the swelling studies (Section 8.3.3).

A faster rate of degradation was evident for all systems with a higher PLA content. Gel permeation chromatography (GPC) results for the linear polymers reveal a smaller MW polymer the higher the PLA content in the hydrogel networks (Chapter 4). This would be expected to lead to a faster rate of degradation. In addition introducing a higher MW PLA into the hydrogel would be expected to reduce the rate of degradation and this was found to be the case (Table 8.2).

The morphology of the hydrogels before and during hydrolytic degradation was observed by means of Scanning Electron Microscopy. Overall a greater increase in the average pore size was observed for the gels containing PLA$_{-12}$ in spite of a slower rate of degradation. This can be explained in terms of longer PLA chains within the polymer, reducing crosslinking density and increasing cyclisation on polymerisation; all are contributing factors to the network structure on increasing the MW. A looser network structure will lead to greater pore size on degradation as opposed to a tighter closely meshed network resulting in a larger number of pores when freshly polymerised (Section 4.2).

8.3.2 Effect of Temperature:

Variations in temperature will affect the Flory-Higgins interaction parameter, reducing swelling of the hydrogels with increasing temperature. While changes in swelling will directly affect the degradation of the hydrogels such that the reduction in swelling will reduce the degradation rate, it is the hydrolysis that is the primary factor governing the degradation of the lactide groups. The reaction rate constants for hydrolysis are usually temperature dependent with the rate of a reaction typically increasing with temperature. This is reflected in the linear PLA systems where degradation for both PLA$_{-2}$ and PLA$_{-12}$ were faster at 37°C than at 20°C (Chapter 5& 6). This produces two opposing forces that are at play in the degradation of hydrogels as a function of temperature. At low temperature the swelling and degradation are increased due to interaction parameter (i.e. the hydration state of the polymer) but the degradation rate decreased due to the lower temperature. In contrast at elevated temperatures the swelling is reduced but the degradation is increased. The complexity of the conditions of degradation are reflected in the fact that degradation appeared to be faster at 37°C for the PNP-coPLA$_{-12}$ gels while the opposite was seen for PNP-co-PLA$_{-2}$ hydrogel series with a faster degradation rate below the LCST. These results reveal that a combination of both swelling and temperature are important in the

role of degradation of the hydrogel series. Table 8.2 reveals the [COOH] present in the degradation media at both temperatures for both hydrogel series.

Table 8.2: The [COOH] present in the degradation media after 2 months for each hydrogel series. In addition the difference in the [COOH] is displayed between systems on increasing MW precursor PLA.

		Gels composed of PLA$_{-2}$		Gels composed of PLA$_{-12}$	
Gel 20°C	PNIPAAM:PLA (w/w)	[COOH] in external media (mol/L)	Mass loss (%)	[COOH] in external media (mol/L)	Mass loss (%)
PNP1	93-7	0.0195	21.50	0.0158	36.5
PNP2	86-14	0.0291	30.38	0.0075	17.5
PNP3	72-28	0.0333	40.00	0.0108	31.5
37°C					
PNP1	93-7	0.0066	13.34	0.0010	24.0
PNP2	86-14	0.0141	25.59	0.0125	24.5
PNP3	72-28	0.0191	33.05	0.0216	51.0

On examination of the results; an increase in [COOH] was seen on increasing lactide concentration within the polymer. The calculated difference in concentration of degraded acidic products at the end of the experiment (2 months) within the swelling media shows a faster rate of degradation at 20°C for PLA$_{-2}$ systems relative to that of the PLA$_{-12}$ systems indicating that the rate of degradation was faster for the smaller MW gels (Table 8.2). At 37°C the reverse is seen whereby increasing the MW of PLA unit in the addition to the amount incorporated into the gel leads to a faster rate of degradation for the PNP3$_{-12}$ gel. Overall on increasing the LA content a less significant difference is seen in the rate of degradation, which can be attributed to the higher degree of swelling of the PNP-co-PlA$_{-12}$ hydrogel systems. Table 8.2 also displays the mass loss determined after swelling experiments. The results were in good agreement with the concentration LA present within the external media whereby a greater increase in mass loss was observed the higher the LA concentration within the external media.

The degradation rate of the hydrogels under simulated physiological conditions was tuneable by the length and composition of the PLA monomer and also crosslinking degree. Therefore it is possible to tailor the rate to a large extent to meet diverse requirements for various applications in medical fields.

8.4 Hydrogel swelling and release studies

Thermoresponsive hydrogels have proved to be effective in sustained release and on-off release regulation. Drug release from thermoresponsive hydrogels can be controlled by utilisation of the drug diffusion process below the LCST or by use of the pulse of drug on temperature switch above the LCST. The effect of both swelling and degradation of polymer matrices on solute diffusion has been the subject of many studies (van Dijkhuizen-Radersma, Metairie, Roosma, de Groot and Bezemer 2005). The diffusion of solutes through these matrices depends on the size of the solute in relation to the mesh size of the polymer matrix. Some of the factors affecting the polymer mesh size are chain mobility, chain entanglements, cross-linking density, crystallinity and equilibrium degree of swelling. Degradation of the matrix may increase the diffusion co-efficient. In addition the release rate may alter due to erosion (mass loss) and/or pore formation. These factors in addition to polymer–drug interactions are important and will be discussed.

8.4.1 Hydrogel swelling and diffusional drug release

Several parameters such as pore size, degradability of hydrogel, hydrophobicity, concentration of a drug and the presence of specific interactions between hydrogels and incorporated drug can affect drug release from hydrogels (Jeong, Bae and Kim 2000; Coughlan, Quilty and Corrigan 2004). In the present work synthesis and evaluation of the role of hydrogel composition, network parameters, temperature and degradation on the drug release mechanisms were examined in relation to the range of novel smart-co-biodegradable gels.

The effect of temperature rise from 20°C to 37°C was shown in Chapter 5 to increase both the solubility and intrinsic dissolution rate of the pure drugs as expected. The environmental temperature however also significantly affected the hydrogel series with a decrease in both the rate and extent of hydrogel swelling at the higher temperature. The net effect of a temperature rise on release of the drugs from the hydrogels was a decrease in the release rate due to the influence of the mesh size on diffusion of the drugs. In addition the diffusional exponents were higher at 20°C than 37°C due to the greater contribution of the swelling process or increased hydrophilicity of the polymer on the rate of release.

The ability to prevent the release of the model compounds at constant temperature above the LCST (37°C) and stop release after a temperature "switch" to 37°C was examined in Chapter 7 with the chosen hydrogel system PNP2$_{-2}$. Figure 8.1 displays the quasi steady state release constants as previously described in Chapter 7. The proximity of the 37°C value to zero may be used to indicate the ability of the hydrogel to thermally shut off release.
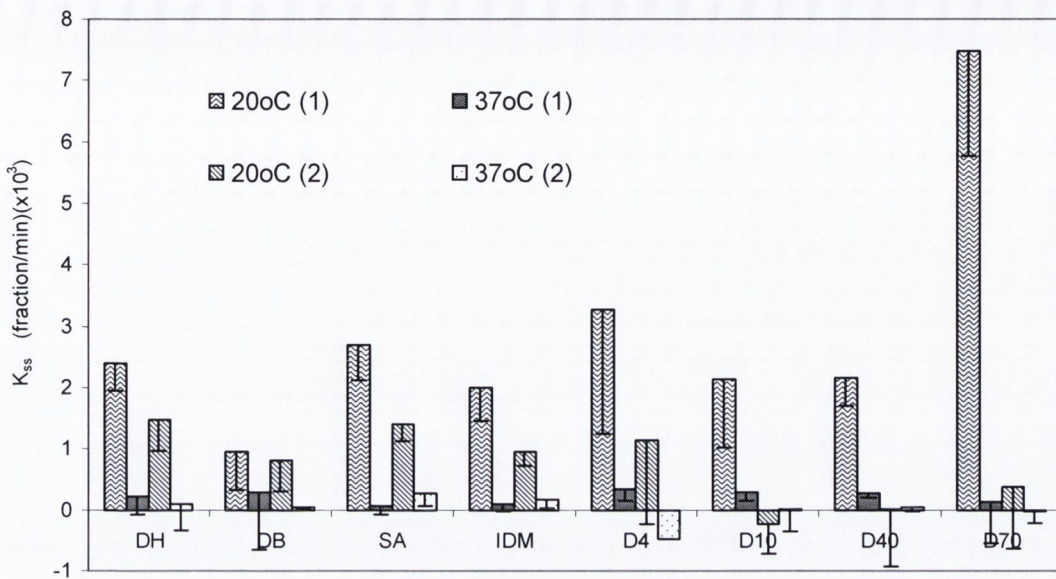
Figure 8.1: Steady state release rate constants (kss) for the model compounds: defined as the average release rate after the first temperature switch (1) and second temperature (2) switch: excluding the first 30min after temperature switch.

From the bar chart it can be observed that the small molecular weight compounds (~8Å) achieved an off state when temperature was raised above the LCST. The hydrogel PNP2$_{-2}$ was shown to have a pore size of 2.13µm in the shrunken state. Pulsatile release has previously been explained by the formation of a dense, less permeable surface layer of the gel, described as a "skin"-type barrier (Yoshida et al., 1991). This is a result of the outer surface of the gel being exposed to warmer water on increasing temperature therefore it immediately shrinks to form a surface layer more dense than the bulk matrix. In previous studies the length of the side alkyl chain has shown to control the thickness and density of the surface layer. The current hydrogel system showed evidence of the formation of a dense skin layer on deswelling. As a consequence, the small model drugs were successfully prevented from diffusing through the gel. This suggests that pore size is not an important factor in these release systems but the formation of skin-type barrier capable of stopping release on increasing temperature. The skin layer in the present system may be a specific effect due to the presence of the long chain hydrophobic co-monomers incorporated into the gel.

The magnitude of thermal control was also particularly dependent on drug size and pore size. In the case of the higher MW compounds a burst effect was seen in the early stages of release (>1hr) after which no further release was observed. This burst effect can be attributed to the model compound on the surface of the gel as the loading conditions did not permit the equilibrium permeation of the solute into the gel. This result is also reflected in the bar chart in Figure 8.1 where no release was observed during the second swelling period (Figure 8.1; 20°C (2)).

PNP2$_{-2}$ was also investigated in sustained release above the LCST (37°C) in Chapter 5. The solute size and shape, its relative hydrophilic and hydrophobic character and the availability of water molecules for hydrating the solute molecules are important factors governing solute permeation through any particular hydrogel (Rosiak et al., 1999). The release of the smaller molecular weight drugs was prevented to a limited extent. DH, SA and IDM had levelled off with only 0.67, 0.50 and 0.19 of the drug-loading fraction delivered. In the case of DH, a water-soluble drug, the fraction of pores assessable to the drug was found to be relatively large (Section 4.4.4). The release of IDM and SA, both hydrophobic model compounds, was dependent on the swelling ratio and polymer-drug interactions. In the case of the higher MW compounds a burst effect was seen in the early stages of release (>1hr) after which no further release was observed. Degradation controlled release would be the dominant factor in controlling the release of model compounds with a larger molecular diameter than that of the pore size.

In studying the diffusion in swollen hydrogels, it can be expected that the permeation of solutes through the hydrogel is dependent on the swelling ratio of the hydrogel and the solute molecular size. The quantity of the drug in solution increases with hydrogel hydration. The use of drugs for sustained release systems will therefore depend on the size of the drug, the pore size and the temperature at which the experiment is conducted. The chemical nature of the drug has also proved to be of importance as it may influence the rate of swelling or have a greater affinity for the drug delivery matrix.

The ability to alter the swelling kinetics and pore size of the hydrogel by increasing the PLA content was also shown in Chapter 5. Below the LCST, techniques such as SEM and size exclusion technique revealed a decrease in the pore size on increasing the amount of PLA$_{-2}$ incorporated into the gel. The reverse effect was observed above the LCST using the same experimental procedures. Hydrogels containing hydrophobic groups such as PLA will collapse in the presence of water, thus minimising their exposure to the water resulting in a smaller swelling ratio. A decrease in the rate of release of the small MW compounds on increasing PLA

content also showed that the pores at a molecular level were influenced in the same way by the presence of a hydrophobic moiety with a resulting effect on the drug release profiles.

In Chapter 6 it was observed that changing the molecular weight of the PLA precursor unit significantly altered the release rates. By varying the polymer chain length and the polymer composition it was possible to control the density and network crosslinking. This alteration in the crosslinking density led to significantly larger pore size and pore size distribution thus resulting in different permeabilities. Comparisons of the release rates of the small MW compounds are listed in Table 8.3 at 37°C and 20°C. Also shown in Table 8.4 are the pore sizes estimated using SEM (Chapter4).

Table 8.3: Comparison of the release rate constant of the small MW compounds of identical hydrogel composition using different MW PLA. Also shown are the ratios of the release rate constants at both 20 and 37°C between PNP-PLA$_{-2}$ and PNP-PLA$_{-12}$ polymeric systems.

DH	$k_{-2}(min^{-0.5})$ $(x10^2)(20°C)$	$k_2(min^{0.5})$ $(x10^2)(37°C)$	$k_{-12}(min^{-0.5})$ $(x10^2)(20°C)$	$k_{-12}(min^{-0.5})$ $(x10^2)(37°C)$	k_{-2}/k_{-12} $(20°C)$	k_{-2}/k_{-12} $(37°C)$
PNP1	4.16±0.320	0.999±0.020	3.84±0.003	2.05±0.020	1.0000	0.4945
PNP2	3.88±0.292	1.340±0.030	4.21±0.002	1.60±0.030	0.9200	0.8375
PNP3	2.96±0.002	1.544±0.020	5.26±0.002	4.23±0.020	0.5627	0.3646
SA						
PNP1	2.52±0.040	0.799±0.020	2.72±0.040	0.788±0.020	0.9264	1.0000
PNP2	2.54±0.040	0.953±0.073	3.14±0.040	1.289±0.730	0.8089	0.7390
PNP3	2.04±0.065	0.965±0.019	3.31±0.065	2.230±0.019	0.6163	0.4327
IDM						
PNP1	2.53±0.043	0.304±0.040	1.64±0.043	0.423±0.040	1.5400	0.7186
PNP2	2.11±0.050	0.408±0.075	1.60±0.050	1.109±0.075	1.3100	0.3678
PNP3	1.39±0.150	0.912±0.030	1.44±0.150	1.709±0.030	0.9652	0.5336

Interestingly below the LCST, increasing the mesh size did not have a large impact on the rate of release. Since the size of the molecular probe was small relative to the hydrogel pore size in the studies using PLA$_{-2}$ composed gels, hydrogel composition and drug–polymer interactions appeared to be dominant factors affecting the rate of release. Increasing the MW of PLA resulted in a decrease in the release of IDM despite the larger network. This is an indication of increased hydrophobic drug-polymer interactions within the PLA domains and the model compound IDM. In the case of SA and DH a significant increase was observed in the release rate using PNP3 hydrogel system on increasing the MW of PLA. On examination of Table 8.3

an increase of 9μm (Table 8.4) in the pore size is necessary to minimise drug-polymer interactions thereby increasing the rate of release of the solute through the matrix.

Table 8.4: Estimated pores size (μm) obtained using SEM for the co-polymeric systems at both 20°C and 37°C. Also shown is the increase in pore size on incorporating higher MW PLA into the thermoresposive drug delivery systems at 20°C and 37°C.

	Gels composed of PLA$_{-2}$		Gels composed of PLA$_{-12}$			
Gel	Pore size at 20°C (μm)	Pore size at 37°C (μm)	Pore size at 20°C (μm)	Pore size at 37°C (μm)	Increase in pore size (20°C) (μm)	Increase in pore size (37°C) (μm)
PNP1	5.79	2.09	10.61	3.50	4.82	1.41
PNP2	3.94	2.13	11.06	7.18	7.12	5.05
PNP3	2.82	2.57	11.96	7.88	9.14	5.25

At 37°C, when the hydrogel is in a collapsed state, the impact of the mesh size on the release rate was more evident. However overall an increase in the release rate was observed using PLA-$_{12}$ composed gels. The influence of drug solubility on hydrogel swelling was also examined. DH a hydrophilic drug was seen to increase the swelling rate attributable to the osmotic effect of the loaded drug on the swelling rate. It is likely that the solubility of DH greatly affected the dissolution rate since the drug substance is highly soluble in aqueous solution. This suggests that the drug almost instantaneously dissolved into the penetrating media leading to a faster drug release. In contrast the hydrophobic series (IDM<SA, DB) as well as the hydrophilic dextran series decreased the rate of swelling. Drugs that have a relatively low solubility can slow the swelling due to the presence of a drug diffusion front. However in the case of IDM, where hydrophobic interactions were likely a greater suppression of swelling and release was evident due to polymer-drug interactions. The dextran series (Chapter 7) was shown to interact with polymer matrix resulting in a decrease in swelling the higher the MW of the dextran fraction. As a result a poor correlation between molecular probe and hydrogel pore size was seen on release of the dextran fractions from PLA-$_2$ composed gels.

Thermoresponsive systems are designed to release drugs at temperatures below the LCST. However it may be desirable to design a system where the release occurs above a critical temperature. Such devices have applications in situations where the release of a substance is required at a critical temperature. Diinvard and D'emanuele, 1995 reported thermoreponsive

discs based on PNIPAAM and acrylamide exhibiting a LCST ~37°C. In the present work the biodegradable system could be manipulated to design a device capable of drug release at 37°C by increasing the MW and molar ratio of PLA.

Biodegradable systems offer an alternative approach to regulating drug release, as drug release from the matrices is also governed by the rate of degradation. In addition to the rate of swelling, the maximum degree of swelling as well as the size of the network and the size of the drug molecule dictates if and when a drug molecule is capable of leaving the network. It was shown in the case of the dextrans (chapter 5) that it is possible to incorporate large drugs into a tightly crosslinked network such that even at maximum swelling the molecules are unable to pass through the pores. In this case degradation should increase the network size and allow the drug to diffuse out. The relative rates of swelling and degradation are the most important parameters in determining the mechanism of drug release.

Apart from influencing the release rate, the hydrogel swelling properties and drug size were also shown to influence the release mechanism from these systems. The current work showed that the release mechanism of model compound from the various co-polymeric systems was dependent on swelling, polymer-drug interactions, solute size and rate of degradation as well as the temperature at which the experiments were conducted. The possibility therefore exists to design a thermoresponsive-co-biodegradable system with desirable swelling, degradation kinetics and pore sizes to achieve a particular release profile.

8.4.2 Hydrogel contraction and drug pulse

An important consequence of the influence of the drugs on the swelling rate is the subsequent change in the magnitude of hydrogel contraction following temperature switch above the LCST. The use of a drug pulse caused by hydrogel contraction can potentially control the drug release from a thermoresponsive hydrogel (Okano et al., 1990, and Bae et al., 1991, Yoshida et al., 1991, Gutowska et al., 1992).

In the case of small MW drugs; solubility of the drug determined the magnitude of the drug pulse after temperature switch. The pulse of the drugs can therefore be altered by knowledge of the extent of drug dissolution prior to temperature switch. The subsequent drug release rate from a system using a drug pulse could therefore be predicted. The higher MW dextrans displayed a poor relationship between pore size and molecular diameter during loading. A successful surface regulating system could be developed for larger macromolecules or proteins by manipulation of the hydrogel system. Since PLA induces a dense impermeable skin layer,

PNP2$_{-12}$ with a larger pore size (relative to the dextran series) below the LCST could achieve "on-off" release for larger compounds on temperature switch.

8.5 CONCLUSIONS

> ➢ A novel series of hydrogels with dual properties of both thermo-sensitivity (PNIPAAM) and degradation (PLA) were synthesised.

> ➢ The pore size of the hydrogel networks were dependent on hydrogel composition and the MW of PLA incorporated into the gel. PNP-PLA$_{-2}$ systems displayed a smaller pore size on increasing PLA content while PNP-PLA$_{-12}$ systems displayed an increase in pore size on increasing PLA content. These results were in turn reflective of the crosslinking density.

> ➢ Degradation was dependent on both structural and environmental conditions. A faster rate of degradation was seen in the higher the PLA content in all systems both below and above the LCST temperature. Degradation was faster for PNP-co-PLA$_{-2}$ systems below the LCST as a result of greater degree of swelling. In contrast PNP-co-PlA$_{-12}$ systems were faster above the LCST; the effect more pronounced the higher the PLA content. Overall PNP-co-PLA gels containing the lower MW PLA had faster degradation rates, which was reflected in [COOH] seen in the degradation media.

> ➢ Drug release experiments from PNP2$_{-2}$ were dependent on drug physiochemical properties such as size, pKa and polymer-drug interactions. The presence of the loaded drug influenced the swelling with the rate and extent of the swelling also dependent on temperature. Release of the model drugs above the LCST were dependent on the molecular size of the drug in solution relative to that of the pore size available for diffusion. The increase in temperature decreased the release rate of the smaller MW compounds whereas the larger molecules remained trapped in the hydrogel. Degradation control release could also be feasible above the LCST for poorly soluble drugs.

210

> ➢ The hydrogel composition influenced both the drug release rate and drug release mechanism. For all systems synthesised, increasing the amount of PLA revealed a trend towards zero order kinetics below the LCST. In addition the degree of swelling influenced the rate of drug release. A significant increase in the pore size of PNP-coPLA.$_{12}$ systems resulted in sustained release at both temperatures.

> ➢ The release rates of the model drugs were dependent on pores available for diffusion. The "enhanced skin layer" mentioned in the literature, which has been considered responsible for the on-off release on hydrogel contraction, was evident during temperature switch in the current work. PNP2.$_2$ proved successful in controlling on-off release of the smaller MW compounds. A temperature switch above the LCST caused a drug pulse, which was solubility dependent for the smaller compounds. The magnitude of the pulse of the dextran series decreased with molecular diameter of the drug, which was attributed to the relationship between the pore size and the molecular probe.

> ➢ The physical and chemical properties of the present hydrogel system can be engineered at a molecular level to optimise properties such as permeability (sustained release applications), environmental-release (pulastile drug release) and biodegradability (bioresorbable applications) for controlled drug delivery applications.

8.6 Future work:

The current thesis described a potential new thermoresonsive-co-biodegradable hydrogel system capable of meeting specific criteria for drug release by alteration of polymer network. Future work would be to examine the effect of increasing the molar composition of PLA within the gel network and investigate the resulting effect on degradation and drug release both below and above the LCST. The incorporation of drug into the polymer using appropriate solvents and the role of polymer degradation on subsequent drug release could be examined. In the current thesis pulsatile release using the co-polymeric system contained low molecular weight PLA; further work could incorporate larger MW PLA, as these systems are likely to give a better uptake of larger molecules. An interesting continuation of the work would be to investigate potential application of such a system in drug delivery devices.

REFERENCES:

Agarwal, M., Koelling, K. W. and Chalmers, J. J. (1998). "Characterization of the Degradation of Polylactic Acid Polymer in a Solid Substrate Environment." Biotechnol. Prog. **14**(3): 517-526.

am Ende, M. T., Hariharan, D. and Peppas, N. A. (1995). "Factors influencing drug and protein transport and release from ionic hydrogels." Reactive Polymers **25**(2-3): 127-137.

Anderson, J. M., Shive, M. S. (1997). "Biodegradation and biocompatibility of PLA and PLGA microspheres." Advanced Drug Delivery Reviews **28**(1): 5-24.

Andreopoulous , A. G., Hatzi, E., Doxastakis, M. (2001). "Controlled release of salicylic acid from poly(D,L-Lactide)." Journal of Material science : Materials in Medicine **12**: 233-239.

Ataman, M. (1987). "Properties of aqueous salt solutions of poly(ethylene oxide). Cloud points, θ temperatures." Colloid & Polymer Science **265**(1): 19-25.

Bae, Y., H., Okano, T., Hsu, R. and Kim, S. W. (1987). "Thermoresponsive polymers as on-off swithches for drug release." Makromol.Chem.,Rapid commun. **8**: 481-485.

Bae, Y. H., Okano, T. and Kim, S. W. (1991). ""On–Off' Thermocontrol of Solute Transport. I. Temperature Dependence of Swelling of N-Isopropylacrylamide Networks Modified with Hydrophobic Components in Water." Pharmaceutical Research **8**(4): 531-537.

Bae, Y. H., Teruo, O. and Wan, K. S. (1990). "Temperature dependence of swelling of crosslinked poly(N,N-alkyl substituted acrylamides) in water." Journal of Polymer Science Part B: Polymer Physics **28**(6): 923-936.

Baltes, T., Garret-Flaudy,F., Freitag, R. (1999). "Investigation of the LCST of polyacrylamides as a function of molecular parameters and the solvent composition." Journal of Polymer Science Part A: Polymer Chemistry **37**(15): 2977-2989.

Barbani, N., Bertoni, F., Ciardelli, G., Cristallini, C., Silvestri, D., Coluccio, M. L. and Giusti, P. (2005). "Bioartificial materials based on blends of dextran and poly(vinyl alcohol-co-acrylic acid)." European Polymer Journal **41**(12): 3004-3010.

Beltran, S., Baker, J. P., Hooper, H. H., Blanch, H. W. and Prausnitz, J. M. (1991). "Swelling equilibria for weakly ionizable, temperature-sensitive hydrogels." Macromolecules 24(2): 549-551.

Brazel, C. S. and Peppas, N. A. (1999a). "Mechanisms of solute and drug transport in relaxing, swellable, hydrophilic glassy polymers." Polymer 40(12): 3383-3398.

Brazel, C. S. and Peppas, N. A. (1999b). "Dimensionless analysis of swelling of hydrophilic glassy polymers with subsequent drug release from relaxing structures." Biomaterials 20(8): 721-732.

Brazel, C. S. and Peppas, N. A (2000). Modeling of drug release from swellable polymers. European Journal of Pharmaceutics and Biopharmaceutics 49: 47-58

Bromberg, L. (1997). "Zein-Poly(N-isopropylacrylamide) Conjugates." J. Phys. Chem. B 101(4): 504-507.

Bromberg, L. E. and Ron, E. S. (1998). "Temperature-responsive gels and thermogelling polymer matrices for protein and peptide delivery." Advanced Drug Delivery Reviews 31(3): 197-221.

Brownlee, M. and Cerami, A. (1979). "A Glucose-Controlled Insulin-Delivery System: Semisynthetic Insulin Bound to Lectin." Science 206(4423): 1190-1191.

Canal, T., Peppas, N.A. (1989). "Correlation between mesh size and equilibrium degree of swelling of polymeric networks." Journal of Biomedical Materials Research 23(10): 1183-1193.

Çatiker, E., Gümüsderelioglu, M. , Güner, A. (2000). "Degradation of PLA, PLGA homo- and copolymers in the presence of serum albumin: a spectroscopic investigation." Polymer International 49(7): 728-734.

Caulfield, M. J., Hao, X., Qiao, G. G. and Solomon, D. H. (2003). "Degradation on polyacrylamides. Part I. Linear polyacrylamide." Polymer 44(5): 1331-1337.

Caykara, T. and Akcakaya, I. (2006). "Synthesis and network structure of ionic poly(N,N-dimethylacrylamide-co-acrylamide) hydrogels: Comparison of swelling degree with theory." European Polymer Journal **42**(6): 1437-1445.

Caykara, T.Kiper, S., Demirel, G. (2006). Network and volume phase transition behaviour of Poly (N-isopropylacrylamide) hydrogels: Journal of Applied Polymer Science 101: 1756-1762

Chaterji, S., Kwon, I. K. and Park, K. (2007). "Smart polymeric gels: Redefining the limits of biomedical devices." Progress in Polymer Science **32**(8-9): 1083-1122.

Cheng, S.-X., Zhang,Jian-Tao., Zhuo, Ren-Xi (2003). "Macroporous poly(N-isopropylacrylamide) hydrogels with fast response rates and improved protein release properties." Journal of Biomedical Materials Research Part A **67A**(1): 96-103.

Chenite, A., Chaput, C., Wang, D., Combes, C., Buschmann, M. D., Hoemann, C. D., Leroux, J. C., Atkinson, B. L., Binette, F. and Selmani, A. (2000). "Novel injectable neutral solutions of chitosan form biodegradable gels in situ." Biomaterials **21**(21): 2155-2161.

Cheung, H.-Y., Lau, K.-T., Lu, T.-P. and Hui, D. (2007). "A critical review on polymer-based bio-engineered materials for scaffold development." Composites Part B: Engineering **38**(3): 291-300.

Chiellini, F., Petrucci, F., Ranucci, E., Solaro., R. (2002). "Bioerodible hydrogels based on 2-hydroxyethyl methacrylate: Synthesis and characterization." Journal of Applied Polymer Science **85**(13): 2729-2741.

Chung, J. E., Yokoyama, M., Aoyagi, T., Sakurai, Y. and Okano, T. (1998). "Effect of molecular architecture of hydrophobically modified poly(N-isopropylacrylamide) on the formation of thermoresponsive core-shell micellar drug carriers." Journal of Controlled Release **53**(1-3): 119-130.

Coughlan, D. C. and Corrigan, O. I. (2006). "Drug-polymer interactions and their effect on thermoresponsive poly(N-isopropylacrylamide) drug delivery systems." International Journal of Pharmaceutics **313**(1-2): 163-174.

Coughlan, D. C., Quilty, F. P. and Corrigan, O. I. (2004). "Effect of drug physicochemical properties on swelling/deswelling kinetics and pulsatile drug release from thermoresponsive poly(N-isopropylacrylamide) hydrogels." Journal of Controlled Release **98**(1): 97-114.

Coviello, T., Matricardi, P., Marianecci, C. and Alhaique, F. (2007). "Polysaccharide hydrogels for modified release formulations." Journal of Controlled Release **119**(1): 5-24.

Crank, J. (1975). The mathematics of diffusion, 2nd ed., Clarendon Press, Oxford.

Cruise, G. M., Scharp, D. S. and Hubbell, J. A. (1998). "Characterization of permeability and network structure of interfacially photopolymerized poly(ethylene glycol) diacrylate hydrogels." Biomaterials **19**(14): 1287-1294.

Cunliffe, D., Kirby, A. and Alexander, C. (2005). "Molecularly imprinted drug delivery systems." Advanced Drug Delivery Reviews **57**(12): 1836-1853.

D'Emanuele, A. and Dinarvand, R. (1995). "Preparation, characterisation, and drug release from thermoresponsive microspheres." International Journal of Pharmaceutics **118**(2): 237-242.

Davis, K. A., Burdick, J. A. and Anseth, K. S. (2003). "Photoinitiated crosslinked degradable copolymer networks for tissue engineering applications." Biomaterials **24**(14): 2485-2495.

de Jong, S. J., Arias, E. R., Rijkers, D. T. S., van Nostrum, C. F., Kettenes-van den Bosch, J. J. and Hennink, W. E. (2001). "New insights into the hydrolytic degradation of poly(lactic acid): participation of the alcohol terminus." Polymer **42**(7): 2795-2802.

Del Arco, M., Cebadera E., Gutiérrez, S. , Martín, C., Montero, M. J., Rives, V., Rocha, J., Sevilla, M. A. (2004). "Mg,Al layered double hydroxides with intercalated indomethacin: Synthesis, characterization, and pharmacological study." Journal of Pharmaceutical Sciences **93**(6): 1649-1658.

Dhara, D. and Chatterji, P. R. (2000). "Swelling and deswelling pathways in non-ionic poly(N-isopropylacrylamide) hydrogels in presence of additives." Polymer **41**(16): 6133-6143.

Diez-Pena, E., Fructos, P., Fructos, G., Quijada-Garrido, I., Barrales-Rienda, J. M. (2004). "The influence of the copolymer composition on the diltiazem hydrochloride release from a series of pH-sensitive poly[(N-isopropylacrylamide)-co-(methacrylic acid)] hydrogels." AAPS PharmSciTech **5**(2): 1-8.

Dinarvand, R. and D'Emanuele, A. (1995). "The use of thermoresponsive hydrogels for on-off release of molecules." Journal of Controlled Release **36**(3): 221-227.

Dirk Kuckling, H.-J. P. A., Karl-Friedrich Arndt ,Long Ling, Wolf D. Habicher (2000). "Temperature and pH dependent solubility of novel poly(N-isopropylacrylamide)-copolymers." Macromolecular Chemistry and Physics **201**(2): 273-280.

Dittgen, M., Durrani,M.,Lehmann,K. (1997). "Acrylic polymers. A review of Pharmacetical apllications." S.T.P. Pharma.Sci. **7**: 403-457.

Dong, L.-C., Hoffman, A.S., Yan, Q.I. (1994). "Dextran permeation through poly (N-isopropylacrylamide) hydrogels." journal of Biomaterials Science -- Polymer Edition **5**: 473-484.

Dragana Neradovic, W. L. J. H. J. J. K.-v. d. B. W. E. H. (1999). "Poly(N-isopropylacrylamide) with hydrolyzable lactic acid ester side groups: a new type of thermosensitive polymer." Macromolecular Rapid Communications **20**(11): 577-581.

Eeckman, F., Amighi, K. and Moes, A. J. (2001). "Effect of some physiological and non-physiological compounds on the phase transition temperature of thermoresponsive polymers intended for oral controlled-drug delivery." International Journal of Pharmaceutics **222**(2): 259-270.

Eliassaf, J. (1978). "Aqueous solutions of poly(N-isopropylacrylamide)." Journal of Applied Polymer Science **22**(3): 873-874.

Feil, H., Bae, Y. H., Feijen, J. and Kim, S. W. (1992). "Mutual influence of pH and temperature on the swelling of ionizable and thermosensitive hydrogels." Macromolecules **25**(20): 5528-5530.

Feil, H., Bae, Y. H., Feijen, J. and Kim, S. W. (1993). "Effect of comonomer hydrophilicity and ionization on the lower critical solution temperature of N-isopropylacrylamide copolymers." Macromolecules **26**(10): 2496-2500.

Fitzgerald, J. F. and Corrigan, O. I. (1996). "Investigation of the mechanisms governing the release of levamisole from poly-lactide-co-glycolide delivery systems." Journal of Controlled Release **42**(2): 125-132.

Flory , P. J. (1953). Principles of polymer chemistry.The George Fisher Baker non-resident lectureship in chemistry at Cornell University. Ithaca, Cornell University Press. .

Furyk, S., Zhang, Y., Ortiz-Acosta, D., Cremer, P.S., Bergbreiter, D.E. (2006). "Effects of end group polarity and molecular weight on the lower critical solution temperature of poly(<I>N</I>-isopropylacrylamide)." Journal of Polymer Science Part A: Polymer Chemistry **44**(4): 1492-1501.

Galaev, I. Y. and Mattiasson, B. (1999). "`Smart' polymers and what they could do in biotechnology and medicine." Trends in Biotechnology **17**(8): 335-340.

Gallagher, K. M. and Corrigan, O. I. (2000). "Mechanistic aspects of the release of levamisole hydrochloride from biodegradable polymers." Journal of Controlled Release **69**(2): 261-272.

Ghandehari, H., Kopeckova, P. and Kopecek, J. (1997). "In vitro degradation of pH-sensitive hydrogels containing aromatic azo bonds." Biomaterials **18**(12): 861-872.

Gil, E. S. and Hudson, S. M. (2004). "Stimuli-reponsive polymers and their bioconjugates." Progress in Polymer Science **29**(12): 1173-1222.

Gopferich, A. (1996). "Mechanisms of polymer degradation and erosion." Biomaterials **17**(2): 103-114.

Gopferich, A. (1997). "Polymer Bulk Erosion." Macromolecules **30**(9): 2598-2604.

Goulet, P. J. G. and Aroca, R. F. (2004). "Chemical adsorption of salicylate on silver - A systematic approach to the interpretation of surface-enhanced vibrational spectra." Canadian Journal of Chemistry **82**(6): 987-997.

Greenhalgh, D. J., Williams A. C., Timmins, P., York, P. (1999). "Solubility parameters as predictors of miscibility in solid dispersions." Journal of Pharmaceutical Sciences **88**(11): 1182-1190.

Gunatillake, P., Mayadunne, R., Adhikari, R. and El-Gewely, M. R. (2006). Recent developments in biodegradable synthetic polymers. Biotechnology Annual Review, Elsevier. **Volume 12:** 301-347.

Guo, K. and Chu, C.-C. (2007). "Biodegradation of unsaturated poly(ester-amide)s and their hydrogels." Biomaterials **28**(22): 3284-3294.

Guo, X. and Szoka, F. C. (2001). "Steric Stabilization of Fusogenic Liposomes by a Low-pH Sensitive PEG-Diortho Ester-Lipid Conjugate." Bioconjugate Chem. **12**(2): 291-300.

Gupta, P., Vermani, K. and Garg, S. (2002). "Hydrogels: from controlled release to pH-responsive drug delivery." Drug Discovery Today **7**(10): 569-579.

Gutowska, A., Bae, Y. H., Feijen, J. and Kim, S. W. (1992). "Heparin release from thermosensitive hydrogels." Journal of Controlled Release **22**(2): 95-104.

Gutowska, A., Bae, Y. H., Jacobs, H., Feijen, J. and Kim, S. W. (1994). "Thermosensitive Interpenetrating Polymer Networks: Synthesis, Characterization, and Macromolecular Release." Macromolecules **27**(15): 4167-4175.

Han, D. K. and Hubbell, J. A. (1997). "Synthesis of Polymer Network Scaffolds from L-Lactide and Poly(ethylene glycol) and Their Interaction with Cells." Macromolecules **30**(20): 6077-6083.

Hancock, B. C., York, P. and Rowe, R. C. (1997). "The use of solubility parameters in pharmaceutical dosage form design." International Journal of Pharmaceutics **148**(1): 1-21.

Hassan, C. M., Doyle, F. J. and Peppas, N. A. (1997). "Dynamic Behavior of Glucose-Responsive Poly(methacrylic acid-g-ethylene glycol) Hydrogels." Macromolecules **30**(20): 6166-6173.

Hatefi, A. and Amsden, B. (2002). "Biodegradable injectable in situ forming drug delivery systems." Journal of Controlled Release **80**(1-3): 9-28.

Heller, J., Chang, A. C., Rood, G. and Grodsky, G. M. (1990). "Release of insulin from pH-sensitive poly(ortho esters)." Journal of Controlled Release **13**(2-3): 295-302.

Heller, J., Helwing, R. F., Baker, R. W. and Tutte, M. E. (1983). "Controlled release of water-soluble macromolecules from bioerodible hydrogels." Biomaterials **4**(4): 262-266.

Hennink, W. E. and van Nostrum, C. F. (2002). "Novel crosslinking methods to design hydrogels." Advanced Drug Delivery Reviews **54**(1): 13-36.

Higuchi, T. (1961). "Rate of release of medicaments from ointment bases containing drugs in suspension." Journal of Pharmaceutical Sciences **50**(10): 874-875.

Higuchi, W. I. (1962). "Analysis of data on the medicament release from ointments." Journal of Pharmaceutical Sciences **51**(8): 802-804.

Hiljanen-Vainio, M., Varpomaa, P., Seppälä, J., Törmälä P. (1996). "Modification of poly(L-lactides) by blending: mechanical and hydrolytic behavior." Macromolecular Chemistry and Physics **197**(4): 1503-1523.

Hinrichs, W. L. J., Schuurmans-Nieuwenbroek, N. M. E., van de Wetering, P. and Hennink, W. E. (1999). "Thermosensitive polymers as carriers for DNA delivery." Journal of Controlled Release **60**(2-3): 249-259.

Hixson, A. W. and Crowell, J. H. (1931). "Dependence of Reaction Velocity upon surface and Agitation." Ind. Eng. Chem. **23**(8): 923-931.

Ho, S.-M. and Young, A. M. (2006). "Synthesis, polymerisation and degradation of poly(lactide-co-propylene glycol) dimethacrylate adhesives." European Polymer Journal **42**(8): 1775-1785.

Hoffman, A. S. (1987). "Applications of thermally reversible polymers and hydrogels in therapeutics and diagnostics." Journal of Controlled Release **6**(1): 297-305.

Hoffman, A. S. (2002). "Hydrogels for biomedical applications." Advanced Drug Delivery Reviews **54**(1): 3-12.

Hoffman, A. S., Afrassiabi, A. and Dong, L. C. (1986). "Thermally reversible hydrogels: II. Delivery and selective removal of substances from aqueous solutions." Journal of Controlled Release **4**(3): 213-222.

Hopfenberg, H. B., Hsu K. C. (1978). "Swelling-controlled, constant rate delivery systems." Polymer Engineering & Science **18**(15): 1186-1191.

Huang, G., Gao, J., Hu, Z., St. John, J. V., Ponder, B. C. and Moro, D. (2004). "Controlled drug release from hydrogel nanoparticle networks." Journal of Controlled Release **94**(2-3): 303-311.

Huang, X. and Lowe, T. L. (2005). "Biodegradable Thermoresponsive Hydrogels for Aqueous Encapsulation and Controlled Release of Hydrophilic Model Drugs." Biomacromolecules **6**(4): 2131-2139.

Huang, X., Nayak, B. R., Lowe T. L. (2004). "Synthesis and characterization of novel thermoresponsive-co-biodegradable hydrogels composed of N-isopropylacrylamide, poly(L-lactic acid), and dextran." Journal of Polymer Science Part A: Polymer Chemistry **42**(20): 5054-5066.

Huh, K. M., Cho, Y.W., Park, K. (2003). "PLGA-PEG Block Copolymers for Drug Formulations " Drug delivery technology **3**: Article 152

Iannace, S., Maffezzoli, A., Leo, G. and Nicolais, L. (2001). "Influence of crystal and amorphous phase morphology on hydrolytic degradation of PLLA subjected to different processing conditions." Polymer **42**(8): 3799-3807.

Ichikawa, H. and Fukumori, Y. (2000). "A novel positively thermosensitive controlled-release microcapsule with membrane of nano-sized poly(N-isopropylacrylamide) gel dispersed in ethylcellulose matrix." Journal of Controlled Release **63**(1-2): 107-119.

Inoue, T., Chen, G., Nakamae, K. and Hoffman, A. S. (1997). "A hydrophobically-modified bioadhesive polyelectrolyte hydrogel for drug delivery." Journal of Controlled Release **49**(2-3): 167-176.

Ito, Y., Casolaro, M., Kono, K. and Imanishi, Y. (1989). "An insulin-releasing system that is responsive to glucose." Journal of Controlled Release **10**(2): 195-203.

Jafari, S., Modarress, H. (2005). "A study on swelling and complex formation of acrylic acid and methacrylic acid hydrogels with polyethylene glycol." Iranian polymer journal **14**(10): 863-873.

Jagur-Grodzinski, J. (1999). "Biomedical application of functional polymers." Reactive and Functional Polymers **39**(2): 99-138.

Jennie Baier Leach, K. A. B. C. W. P. J. C. E. S. (2003). "Photocrosslinked hyaluronic acid hydrogels: Natural, biodegradable tissue engineering scaffolds." Biotechnology and Bioengineering **82**(5): 578-589.

Jeong, B. and Bae, Y. H. (1997). "Biodegradable block copolymers as injectable drug-delivery systems." Nature **388**(6645): 860.

Jeong, B., Bae, Y. H. and Kim, S. W. (1999). "Thermoreversible Gelation of PEG-PLGA-PEG Triblock Copolymer Aqueous Solutions." Macromolecules **32**(21): 7064-7069.

Jeong, B., Bae, Y. H. and Kim, S. W. (2000). "Drug release from biodegradable injectable thermosensitive hydrogel of PEG-PLGA-PEG triblock copolymers." Journal of Controlled Release **63**(1-2): 155-163.

Jeong, B., Kim, S. W. and Bae, Y. H. (2002). "Thermosensitive sol-gel reversible hydrogels." Advanced Drug Delivery Reviews **54**(1): 37-51.

Johnson, B. D., Beebe, D. J. and Crone, W. C. (2004). "Effects of swelling on the mechanical properties of a pH-sensitive hydrogel for use in microfluidic devices." Materials Science and Engineering: C **24**(4): 575-581.

Johnson, S. L. and Rumon, K. A. (1965). "Infrared Spectra of Solid 1:1 Pyridine-Benzoic Acid Complexes; the Nature of the Hydrogen Bond as a Function of the Acid-Base Levels in the Complex." J. Phys. Chem. **69**(1): 74-86.

Ju, H. K., Kim, S. Y. and Lee, Y. M. (2001). "pH/temperature-responsive behaviors of semi-IPN and comb-type graft hydrogels composed of alginate and poly(N-isopropylacrylamide)." Polymer **42**(16): 6851-6857.

Juodkazis, S., Mukai, N., Wakaki, R., Yamaguchi, A., Matsuo, S. and Misawa, H. (2000). "Reversible phase transitions in polymer gels induced by radiation forces." Nature **408**(6809): 178.

Kabiri, K., Omidian, H., Hashemi, S. A. and Zohuriaan-Mehr, M. J. (2003). "Synthesis of fast-swelling superabsorbent hydrogels: effect of crosslinker type and concentration on porosity and absorption rate." European Polymer Journal **39**(7): 1341-1348.

Kaneko, Y., Sakai, K., Kikuchi, A., Yoshida, R., Sakurai, Y. and Okano, T. (1995). "Influence of Freely Mobile Grafted Chain Length on Dynamic Properties of Comb-Type Grafted Poly(N-isopropylacrylamide) Hydrogels." Macromolecules **28**(23): 7717-7723.

Katono, H., Maruyama, A., Sanui, K., Ogata, N., Okano, T. and Sakurai, Y. (1991). "Thermo-responsive swelling and drug release switching of interpenetrating polymer networks composed of poly(acrylamide-co-butyl methacrylate) and poly (acrylic acid)." Journal of Controlled Release **16**(1-2): 215-227.

Kikuchi, A. and Okano, T. (2002). "Pulsatile drug release control using hydrogels." Advanced Drug Delivery Reviews **54**(1): 53-77.

Kim, I.-S., Jeong, Y.-I., Cho, C.-S. and Kim, S.-H. (2000). "Core-shell type polymeric nanoparticles composed of poly(-lactic acid) and poly(N-isopropylacrylamide)." International Journal of Pharmaceutics **211**(1-2): 1-8.

Kim, T. H. and Park, T. G. (2004). "Critical effect of freezing/freeze-drying on sustained release of FITC-dextran encapsulated within PLGA microspheres." International Journal of Pharmaceutics **271**(1-2): 207-214.

Kister, G., Cassanas, G. and Vert, M. (1998). "Effects of morphology, conformation and configuration on the IR and Raman spectra of various poly(lactic acid)s." Polymer **39**(2): 267-273.

Kister, G., Cassanas, G., Vert, M., Pauvert B., Térol, A. (1995). "Vibrational analysis of poly(L-lactic acid)." Journal of Raman Spectroscopy **26**(4): 307-311.

Kitano, S., Koyama, Y., Kataoka, K., Okano, T. and Sakurai, Y. (1992). "A novel drug delivery system utilizing a glucose responsive polymer complex between poly (vinyl alcohol) and poly (N-vinyl-2-pyrrolidone) with a phenylboronic acid moiety." Journal of Controlled Release **19**(1-3): 161-170.

Kohori, F., Sakai, K., Aoyagi, T., Yokoyama, M., Sakurai, Y. and Okano, T. (1998). "Preparation and characterization of thermally responsive block copolymer micelles comprising poly(N-isopropylacrylamide-b--lactide)." Journal of Controlled Release **55**(1): 87-98.

Kopecek, J. (2003). "Smart and genetically engineered biomaterials and drug delivery systems." European Journal of Pharmaceutical Sciences **20**(1): 1-16.

Kost, J. and Langer, R. (1991). "Responsive polymeric delivery systems." Advanced Drug Delivery Reviews **6**(1): 19-50.

Kost, J. and Langer, R. (2001). "Responsive polymeric delivery systems." Advanced Drug Delivery Reviews **46**(1-3): 125-148.

Kost, J., Leong, K. and Langer, R. (1989). "Ultrasound-Enhanced Polymer Degradation and Release of Incorporated Substances." Proceedings of the National Academy of Sciences of the United States of America **86**(20): 7663-7666.

Kost, J., Noecker, R., Enora, K. and Robert, L. (1985). "Magnetically controlled release systems: Effect of polymer composition." Journal of Biomedical Materials Research **19**(8): 935-940.

Kost, J., Wolfrum,J., Langer, R. (1987). "Magnetically enhanced insulin release in diabetic rats." Journal of Biomedical Materials Research **21**(12): 1367-1373.

Krsko, P. and Libera, M. (2005). "Biointeractive hydrogels." Materials Today **8**(12): 36-44.

Kugita, H., Inoue, H., Ikezaki, M., Konda, M., Takeo, S., (1971). "Synthesis of !1,5-benzothiazepine derivatives III." Chem.Pharm. Bull **19**: 595-602.

Kurisawa, M., Yokoyama, M. and Okano, T. (2000). "Gene expression control by temperature with thermo-responsive polymeric gene carriers." Journal of Controlled Release **69**(1): 127-137.

Kwon, G. S., You Han, B., Cremers, H., Feijen, J. and Sung Wan, K. (1992). "Release of macromolecules from albumin-heparin microspheres." International Journal of Pharmaceutics **79**(1-3): 191-198.

Kwon, I. C. and Bae, H. (1991). "Electrically erodible polymer gel for controlled release of drugs." Nature **354**(6351): 291.

Larsen, C. (1989). "Dextran prodrugs -- structure and stability in relation to therapeutic activity." Advanced Drug Delivery Reviews **3**(1): 103-154.

Lee, K. H., Jee,J.G., Jhon M.S. and Ree, T. (1978). "Solute Transport Through Crosslinked Poly(2-Hydroxyethyl Methacrylate) Membrane." J. of Bioengineering, **2**: 269.

Lee, P. I. and Kim, C.-J. (1991). "Probing the mechanisms of drug release from hydrogels." Journal of Controlled Release **16**(1-2): 229-236.

Lee, S. B., Song, S.-C., Jin, J.-I., Jin, J.-I. and Sohn, Y. S. (2000). "Solvent effect on the lower critical solution temperature of biodegradable thermosensitive poly(organophosphazenes)." Polymer Bulletin **45**(4): 389-396.

Lee, W.-F. and Yeh, Y.-C. (2005). "Studies on preparation and properties of NIPAAm/hydrophobic monomer copolymeric hydrogels." European Polymer Journal **41**(10): 2488-2495.

Li, L., Portela, J. R., Vallejo, D. and Gloyna, E. F. (1999). "Oxidation and Hydrolysis of Lactic Acid in Near-Critical Water." Ind. Eng. Chem. Res. **38**(7): 2599-2606.

Li, Q., Wang, J., Shahani, S., Sun, D. D. N., Sharma, B., Elisseeff, J. H. and Leong, K. W. (2006). "Biodegradable and photocrosslinkable polyphosphoester hydrogel." Biomaterials **27**(7): 1027-1034.

Li, S. M., Rashkov, I., Espartero, J. L., Manolova, N. and Vert, M. (1996). "Synthesis, Characterization, and Hydrolytic Degradation of PLA/PEO/PLA Triblock Copolymers with Long Poly(L-lactic acid) Blocks." Macromolecules **29**(1): 57-62.

Li, S. M. and Vert, M. (1994). "Morphological Changes Resulting from the Hydrolytic Degradation of Stereocopolymers Derived from L- and DL-Lactides." Macromolecules **27**(11): 3107-3110.

Li Yan, Q. and You Han, B. (2006). "Polymer Architecture and Drug Delivery." Pharmaceutical Research **23**(1): 1-30.

Lin, C.-C. and Metters, A. T. (2006). "Hydrogels in controlled release formulations: Network design and mathematical modeling." Advanced Drug Delivery Reviews **58**(12-13): 1379-1408.

Lin, H. H. and Cheng, Y. L. (2001). "In-Situ Thermoreversible Gelation of Block and Star Copolymers of Poly(ethylene glycol) and Poly(N-isopropylacrylamide) of Varying Architectures." Macromolecules **34**(11): 3710-3715.

Liu, S. Q., Tong, Y. W. and Yang, Y.-Y. (2005). "Incorporation and in vitro release of doxorubicin in thermally sensitive micelles made from poly(N-isopropylacrylamide-co-N,N-dimethylacrylamide)-b-poly(d,l-lactide-co-glycolide) with varying compositions." Biomaterials **26**(24): 5064-5074.

Liu, S. Q., Yang, Y. Y., Liu, X. M. and Tong, Y. W. (2003). "Preparation and Characterization of Temperature-Sensitive Poly(N-isopropylacrylamide)-b-poly(D,L-lactide) Microspheres for Protein Delivery." Biomacromolecules **4**(6): 1784-1793.

Loh, X. J., Goh, S. H. and Li, J. (2007). "Hydrolytic degradation and protein release studies of thermogelling polyurethane copolymers consisting of poly[(R)-3-hydroxybutyrate], poly(ethylene glycol), and poly(propylene glycol)." Biomaterials **28**(28): 4113-4123.

Lowe, T. L., Nayak, B.R., Huang, X. (2003). "Engineering biodegadable-co-responsive hydrogels for drug delivery." Proceed. Int. Symp.Control. Rel. bioact. Mater. **30**: 707-708.

Lu, S. and Anseth, K. S. (2000). "Release Behavior of High Molecular Weight Solutes from Poly(ethylene glycol)-Based Degradable Networks." Macromolecules **33**(7): 2509-2515.

Luckachan, G. E. and Pillai, C. K. S. (2006). "Chitosan/oligo L-lactide graft copolymers: Effect of hydrophobic side chains on the physico-chemical properties and biodegradability." Carbohydrate Polymers **64**(2): 254-266.

Makino, K., Hiyoshi, J. and Ohshima, H. (2001). "Effects of thermosensitivity of poly (N-isopropylacrylamide) hydrogel upon the duration of a lag phase at the beginning of drug release from the hydrogel." Colloids and Surfaces B: Biointerfaces **20**(4): 341-346.

Mamada, A., Tanaka, T., Kungwatchakun, D. and Irie, M. (1990). "Photoinduced phase transition of gels." Macromolecules **23**(5): 1517-1519.

Mandal, T. K. (2000). "Swelling-controlled release system for the vaginal delivery of miconazole." European Journal of Pharmaceutics and Biopharmaceutics **50**(3): 337-343.

Maris, B., Verheyden, L., Van Reeth, K., Samyn, C., Augustijns, P., Kinget, R. and Van den Mooter, G. (2001). "Synthesis and characterisation of inulin-azo hydrogels designed for colon targeting." International Journal of Pharmaceutics **213**(1-2): 143-152.

Martens, P. and Anseth, K. S. (2000). "Characterization of hydrogels formed from acrylate modified poly(vinyl alcohol) macromers." Polymer **41**(21): 7715-7722.

Martin, A. (1993). Physical pharmacy, 4th Edition, Lea & Febiger, Philadelphia

Metters, A. T., Anseth, K. S. and Bowman, C. N. (1999). Optimization of synthetic hydrogel biomaterials through control of microstructure.

Metters, A. T., Anseth, K. S. and Bowman, C. N. (2000). "Fundamental studies of a novel, biodegradable PEG-b-PLA hydrogel." Polymer **41**(11): 3993-4004.

Meyer, D. E., Shin, B. C., Kong, G. A., Dewhirst, M. W. and Chilkoti, A. (2001). "Drug targeting using thermally responsive polymers and local hyperthermia." Journal of Controlled Release **74**(1-3): 213-224.

Meyvis, T. K. L., De Smedt, S. C., Demeester, J. and Hennink, W. E. (2000). "Influence of the Degradation Mechanism of Hydrogels on Their Elastic and Swelling Properties during Degradation." Macromolecules **33**(13): 4717-4725.

Miyajima, M., Koshika, A., Okada, J. i. and Ikeda, M. (1999). "Effect of polymer/basic drug interactions on the two-stage diffusion-controlled release from a poly(-lactic acid) matrix." Journal of Controlled Release **61**(3): 295-304.

Miyata, T., Uragami, T. and Nakamae, K. (2002). "Biomolecule-sensitive hydrogels." Advanced Drug Delivery Reviews **54**(1): 79-98.

Mullarney, M. P., Seery, T. A. P. and Weiss, R. A. (2006). "Drug diffusion in hydrophobically modified N,N-dimethylacrylamide hydrogels." Polymer **47**(11): 3845-3855.

Mwangi, J. W. and Ofner, C. M. (2004). "Crosslinked gelatin matrices: release of a random coil macromolecular solute." International Journal of Pharmaceutics **278**(2): 319-327.

Nakayama, M., Okano, T., Miyazaki, T., Kohori, F., Sakai, K. and Yokoyama, M. (2006). "Molecular design of biodegradable polymeric micelles for temperature-responsive drug release." Journal of Controlled Release **115**(1): 46-56.

Nath, N. and Chilkoti, A. (2001). "Interfacial Phase Transition of an Environmentally Responsive Elastin Biopolymer Adsorbed on Functionalized Gold Nanoparticles Studied by Colloidal Surface Plasmon Resonance." J. Am. Chem. Soc. **123**(34): 8197-8202.

Nayak, S. (2004). Design, synthesis and characterisation of multiresponsive microgels. School of chemistry and biochemistry, Georgia Institute of technology, Doctor of Philosophy

Nerest, W., Brunner,E., (1904). "Theorie der reackionsgeschwindigkeit in heterogenen systemen." Z.Phys.Chem., **47**: 52-55; 56-102.

Noyes, A. A. and Whitney, W. R. (1897). "The rate of solution of solid substances in their own solutions." J. Am. Chem. Soc. **19**(12): 930-934.

Okano, T., Bae, Y. H., Jacobs, H. and Kim, S. W. (1990). "Thermally on-off switching polymers for drug permeation and release." Journal of Controlled Release **11**(1-3): 255-265.

Olewnik, E., Czerwinski, W. and Nowaczyk, J. (2007). "Hydrolytic degradation of copolymers based on l-lactic acid and bis-2-hydroxyethyl terephthalate." Polymer Degradation and Stability **92**(1): 24-31.

Omidian, H., Hashemi, S. A., Sammes, P. G. and Meldrum, I. (1998). "A model for the swelling of superabsorbent polymers." Polymer **39**(26): 6697-6704.

Otake, K., Inomata, H., Konno, M. and Saito, S. (1990). "Thermal analysis of the volume phase transition with N-isopropylacrylamide gels." Macromolecules **23**(1): 283-289.

Park, K., Shalaby, W. and Park, H. (1993). Biodegradable Hydrogels for Drug Delivery, Lancaster, PA, Technomic.

Park, T. G. and Hoffman, A. S. (1993). "Sodium chloride-induced phase transition in nonionic poly(N-isopropylacrylamide) gel." Macromolecules **26**(19): 5045-5048.

Peng, T. and Cheng, Y. L. (2001). "PNIPAAm and PMAA co-grafted porous PE membranes: living radical co-grafting mechanism and multi-stimuli responsive permeability." Polymer **42**(5): 2091-2100.

Peppas, N. A. (1986). Hydrogels in medicine and Pharmacy, Fundamentals. CRC Press, Inc.Boca Raton, Florida.

Peppas, N. A., Huang, Y., Torres-Lugo, M., Ward, J. H. and Zhang, J. (2000). "Physiochemical foundations and structural design of hydrogels in medicine and biology." Annual Review of Biomedical Engineering **2**(1): 9-29.

Peppas, N. A. and Khare, A. R. (1993). "Preparation, structure and diffusional behavior of hydrogels in controlled release." Advanced Drug Delivery Reviews **11**(1-2): 1-35.

Peppas, N. A. and Lustig, S. R. (1985). "The Role of Cross-links, Entanglements, and Relaxations of the Macromolecular Carrier in the Diffusional Release of Biologically Active Materialsa. Conceptual and Scaling Relationships." Annals of the New York Academy of Sciences **446**(1): 26-40.

Peppas, N. A., Merrill, E.W. (1977). "Crosslinked poly(vinyl alcohol) hydrogels as swollen elastic networks." Journal of Applied Polymer Science **21**(7): 1763-1770.

Pharmacetical handbook (1980), Society of Great Britain, 19th edition, the pharmaceutical press, London ,U.K. (ED. Ainley Wade)

Pillai, O. and Panchagnula, R. (2001). "Polymers in drug delivery." Current Opinion in Chemical Biology **5**(4): 447-451.

Ping-Yang Yeh, P. K., ccaron, kova, J., rcaron, ich, K., ccaron and ek (1995). "Degradability of hydrogels containing azoaromatic crosslinks." Macromolecular Chemistry and Physics **196**(7): 2183-2202.

Proikakis, C. S., Mamouzelos, N. J., Tarantili, P. A. and Andreopoulos, A. G. (2006). "Swelling and hydrolytic degradation of poly(d,l-lactic acid) in aqueous solutions." Polymer Degradation and Stability **91**(3): 614-619.

Proikakis, C. S., Tarantili, P. A. and Andreopoulos, A. G. (2006). "The role of polymer/drug interactions on the sustained release from poly(dl-lactic acid) tablets." European Polymer Journal **42**(12): 3269-3276.

Qiu, Y. and Park, K. (2001). "Environment-sensitive hydrogels for drug delivery." Advanced Drug Delivery Reviews **53**(3): 321-339.

Rama Rao, G. V., Krug, M. E., Balamurugan, S., Xu, H., Xu, Q. and Lopez, G. P. (2002). "Synthesis and Characterization of Silica-Poly(N-isopropylacrylamide) Hybrid Membranes: Switchable Molecular Filters." Chem. Mater. **14**(12): 5075-5080.

Rapoport, N. (2007). "Physical stimuli-responsive polymeric micelles for anti-cancer drug delivery." Progress in Polymer Science **32**(8-9): 962-990.

Ritger, P. L. and Peppas, N. A. (1987). "A simple equation for description of solute release II. Fickian and anomalous release from swellable devices." Journal of Controlled Release **5**(1): 37-42.

Rosen, S. L. (1993

). Fundamental properties of polymeric materials. "2nd Ed.,. New York, Wiley-Interscience Pub.,.

Rosiak, J. M. and Yoshii, F. (1999). "Hydrogels and their medical applications." Nuclear Instruments and Methods in Physics Research Section B: Beam Interactions with Materials and Atoms **151**(1-4): 56-64.

Rost, M. and Quist, P. O. (2003). "Dissolution of USP prednisone calibrator tablets: Effects of stirring conditions and particle size distribution." Journal of Pharmaceutical and Biomedical Analysis **31**(6): 1129-1143.

Ruel-Gariepy, E. and Leroux, J.-C. (2004). "In situ-forming hydrogels--review of temperature-sensitive systems." European Journal of Pharmaceutics and Biopharmaceutics **58**(2): 409-426.

Rzaev, Z. M. O., Dincer, S. and Piskin, E. (2007). "Functional copolymers of N-isopropylacrylamide for bioengineering applications." Progress in Polymer Science **32**(5): 534-595.

Saito, S. and Kitamura, K. (1971). "Counterion effect of tetraalkylammonium and long-chain alkylammonium salts in the interaction with nonionic polymers." Journal of Colloid and Interface Science **35**(2): 346-353.

Saito, S., Konno, M., Inomata, H. (1992). "Volume phase transition of N-alkylacrylamide gels." Advances in polymer science **109**: 207-232.

Salgado-Rodriguez, R., Licea-Claverie, A. and Arndt, K. F. (2004). "Random copolymers of N-isopropylacrylamide and methacrylic acid monomers with hydrophobic spacers: pH-tunable temperature sensitive materials." European Polymer Journal **40**(8): 1931-1946.

Sato, S. and Kim, S. W. (1984). "Macromolecular diffusion through polymer membranes." International Journal of Pharmaceutics **22**(2-3): 229-255.

Savas, H. and Guven, O. (2001). "Investigation of active substance release from poly(ethylene oxide) hydrogels." International Journal of Pharmaceutics **224**(1-2): 151-158.

Sawhney, A. S., Pathak, C. P., Hubbell, J.A. (1993). "Bioerodible hydrogels based on photopolymerized poly(ethylene glycol)-co-poly(.alpha.-hydroxy acid) diacrylate macromers." Macromolecules **26**(4): 581-587.

Schild, H. G. (1992). "Poly(N-isopropylacrylamide): experiment, theory and application." Progress in Polymer Science **17**(2): 163-249.

Schild, H. G. and Tirrell, D. A. (1990). "Microcalorimetric detection of lower critical solution temperatures in aqueous polymer solutions." J. Phys. Chem. **94**(10): 4352-4356.

Schild, H. G. and Tirrell, D. A. (1991). "Interaction of poly(N-isopropylacrylamide) with sodium n-alkyl sulfates in aqueous solution." Langmuir **7**(4): 665-671.

Schliecker, G., Schmidt, C., Fuchs, S. and Kissel, T. (2003). "Characterization of a homologous series of ,-lactic acid oligomers; a mechanistic study on the degradation kinetics in vitro." Biomaterials **24**(21): 3835-3844.

Schliecker, G., Schmidt, C., Fuchs, S., Wombacher, R. and Kissel, T. (2003). "Hydrolytic degradation of poly(lactide-co-glycolide) films: effect of oligomers on degradation rate and crystallinity." International Journal of Pharmaceutics **266**(1-2): 39-49.

Schmaljohann, D. (2006). "Thermo- and pH-responsive polymers in drug delivery." Advanced Drug Delivery Reviews **58**(15): 1655-1670.

Serra, L., Domenech, J. and Peppas, N. A. (2006). "Drug transport mechanisms and release kinetics from molecularly designed poly(acrylic acid-g-ethylene glycol) hydrogels." Biomaterials **27**(31): 5440-5451.

Seymour, L. W., Duncan, R., Duffy, J., Ng, S. Y. and Heller, J. (1994). "Poly (ortho ester) matrices for controlled release of the antitumour agent 5-fluorouracil." Journal of Controlled Release **31**(2): 201-206.

Shah, N. M., Pool, M. D.Metters, A. T. (2006). "Influence of Network Structure on the Degradation of Photo-Cross-Linked PLA-b-PEG-b-PLA Hydrogels." Biomacromolecules **7**(11): 3171-3177.

Shalaby, W. S. W., Blevins, W. E. and Park, K. (1992). "In vitro and in vivo studies of enzyme-digestible hydrogels for oral drug delivery." Journal of Controlled Release **19**(1-3): 131-144.

Si-Xue Cheng, J.-T. Z. R.-X. Z. (2003). "Macroporous poly(N-isopropylacrylamide) hydrogels with fast response rates and improved protein release properties." Journal of Biomedical Materials Research Part A **67A**(1): 96-103.

Singh, B., Sharma, N. and Chauhan, N. (2007). "Synthesis, characterization and swelling studies of pH responsive psyllium and methacrylamide based hydrogels for the use in colon specific drug delivery." Carbohydrate Polymers **69**(4): 631-643.

Sokolsky-Papkov, M., Agashi, K., Olaye, A., Shakesheff, K. and Domb, A. J. (2007). "Polymer carriers for drug delivery in tissue engineering." Advanced Drug Delivery Reviews **59**(4-5): 187-206.

Sousa, R. G., Magalhaes, W. F. and Freitas, R. F. S. (1998). "Glass transition and thermal stability of poly(N-isopropylacrylamide) gels and some of their copolymers with acrylamide." Polymer Degradation and Stability **61**(2): 275-281.

Sriamornsak, P., Thirawong, N. and Korkerd, K. (2007). "Swelling, erosion and release behavior of alginate-based matrix tablets." European Journal of Pharmaceutics and Biopharmaceutics **66**(3): 435-450.

Stammen, J. A., Williams, S., Ku, D. N. and Guldberg, R. E. (2001). "Mechanical properties of a novel PVA hydrogel in shear and unconfined compression." Biomaterials **22**(8): 799-806.

Suwa, K., Yamamoto, K., Akashi, M., Takano, K., Tanaka, N. and Kunugi, S. (1998). "Effects of salt on the temperature and pressure responsive properties of poly(N-vinylisobutyramide) aqueous solutions." Colloid & Polymer Science **276**(6): 529-533.

Suzuki, A. and Tanaka, T. (1990). "Phase transition in polymer gels induced by visible light." Nature **346**: 345-347.

Swami, S. N. (2004). Radiation synthesis for polymeric hydrogels for swelling-controlled drug release studies, University of Western Sydney, New South Wales, Australia.

Tanaka, T., Inoue, H., Date, T., Okamura, K., Aoe, K., Takeda, M., Hiroshi, K., Murata, S., Yamaguchi, T., Kikkawa, K., Nakajima, S., Nagao,T. (1992). "Synthesis of the optically active transisomers of diltiazem and their cardiovascular effects and Ca-antagonistic activity." Chem. Pharm. Bull **40**: 1476-1480.

Tarvainen, T., Karjalainen, T., Malin, M., Pohjolainen, S., Tuominen, J., Seppala, J. and Jarvinen, K. (2002). "Degradation of and drug release from a novel 2,2-bis(2-oxazoline) linked poly(lactic acid) polymer." Journal of Controlled Release **81**(3): 251-261.

Tarvainen, T., Malin, M., Barragan, I., Tuominen, J., Seppala, J. and Jarvinen, K. (2006). "Effects of incorporated drugs on degradation of novel 2,2'-bis(2-oxazoline) linked poly(lactic acid) films." International Journal of Pharmaceutics **310**(1-2): 162-167.

Tokuhiro, T., Amiya, T., Mamada, A. and Tanaka, T. (1991). "NMR study of poly(N-isopropylacrylamide) gels near phase transition." Macromolecules **24**(10): 2936-2943.

Tomic, S. L., Micic, M. M., Filipovic, J. M. and Suljovrujic, E. H. (2007). "Swelling and drug release behavior of poly(2-hydroxyethyl methacrylate/itaconic acid) copolymeric hydrogels obtained by gamma irradiation." Radiation Physics and Chemistry **76**(5): 801-810.

Torchilin, V. P., Tischenko E. G., Smirnov,V. N., Chazov E. I. (1977). "Immobilization of enzymes on slowly soluble carriers." Journal of Biomedical Materials Research **11**(2): 223-235.

Uenoyama, S. and Hoffman, A. S. (1988). "Synthesis and characterization of acrylamide-N-isopropyl acrylamide copolymer grafts on silicone rubber substrates." International Journal of Radiation Applications and Instrumentation. Part C. Radiation Physics and Chemistry **32**(4): 605-608.

Ulijn, R. V., Bibi, N., Jayawarna, V., Thornton, P. D., Todd, S. J., Mart, R. J., Smith, A. M. and Gough, J. E. (2007). "Bioresponsive hydrogels." Materials Today **10**(4): 40-48.

van de Wetering, P., Metters, A. T., Schoenmakers, R. G. and Hubbell, J. A. (2005). "Poly(ethylene glycol) hydrogels formed by conjugate addition with controllable

swelling, degradation, and release of pharmaceutically active proteins." Journal of Controlled Release **102**(3): 619-627.

van Dijk-Wolthuis, W. N. E., Tsang, S. K. Y. and Kettenes-van den BoschW.E. Hennink, J. J. (1997). "A new class of polymerizable dextrans with hydrolyzable groups: hydroxyethyl methacrylated dextran with and without oligolactate spacer." Polymer **38**(25): 6235-6242.

van Dijkhuizen-Radersma, R., Metairie, S., Roosma, J. R., de Groot, K. and Bezemer, J. M. (2005). "Controlled release of proteins from degradable poly(ether-ester) multiblock copolymers." Journal of Controlled Release **101**(1-3): 175-186.

Van Krevelen, D. (1990). Properties of polymers: Their correlation with chemical structure, Elsevier, New York.

van Nostrum, C. F., Veldhuis, T. F. J., Bos, G. W. and Hennink, W. E. (2004). "Hydrolytic degradation of oligo(lactic acid): a kinetic and mechanistic study." Polymer **45**(20): 6779-6787.

VanDurme, K., Rahier, H. and VanMele, B. (2005). "Influence of Additives on the Thermoresponsive Behavior of Polymers in Aqueous Solution." Macromolecules **38**(24): 10155-10163.

Wada, N., Kajima, Y., Yagi, Y., Inomata, H. and Saito, S. (1993). "Effect of surfactant on the phase transition of N-alkylacrylamide gels." Langmuir **9**(1): 46-49.

Wang, C.-H., Fan, K.-R. and Hsiue, G.-H. (2005). "Enzymatic degradation of PLLA-PEOZ-PLLA triblock copolymers." Biomaterials **26**(16): 2803-2811.

Wang, L.-Q., Tu, K., Li, Y., Zhang, J., Jiang, L. and Zhang, Z. (2002). "Synthesis and characterization of temperature responsive graft copolymers of dextran with poly(N-isopropylacrylamide)." Reactive and Functional Polymers **53**(1): 19-27.

Weidner, J. (2001). "Drug delivery and drug targeting: Drug targeting using thermally responsive polymers and local hyperthermia." Drug Discovery Today **6**(23): 1239-1241.

Wolkers, W. F., Oliver, A. E., Tablin, F. and Crowe, J. H. (2004). "A Fourier-transform infrared spectroscopy study of sugar glasses." Carbohydrate Research **339**(6): 1077-1085.

Wu, X. S., Hoffman, A. S. and Yager, P. (1992). "Synthesis and characterization of thermally reversible macroporous poly(N-isopropylacrylamide) hydrogels." Journal of Polymer Science Part A: Polymer Chemistry **30**(10): 2121-2129.

Xian-Zheng Zhang, D.-Q. W. G.-M. S. C.-C. C. (2003). "Novel Biodegradable and Thermosensitive Dex-AI/PNIPAAm Hydrogel." Macromolecular Bioscience **3**(2): 87-91.

Xue Shen Wu, A. S. H. P. Y. (1992). "Synthesis and characterization of thermally reversible macroporous poly(N-isopropylacrylamide) hydrogels." Journal of Polymer Science Part A: Polymer Chemistry **30**(10): 2121-2129.

Xue, W. and Hamley, I. W. (2002). "Thermoreversible swelling behaviour of hydrogels based on N-isopropylacrylamide with a hydrophobic comonomer." Polymer **43**(10): 3069-3077.

XXIV, U. S. P. (2000). United States Pharmacopoeial Convention, Rockville, Maryland.

Yamada, N., Okano, T., Sakai,H., Karikusa, F., Sawasaki,Y., Sakurai,Y. (1990). "Thermo-responsive polymeric surfaces; control of attachment and detachment of cultured cells." Die Makromolekulare Chemie, Rapid Communications **11**(11): 571-576.

Yasuda, H., Ikenberry, L. D. Lamaze, C. E. (1969). "Permeability of solutes through hydrated polymer membranes. Part II. Permeability of water soluble organic solutes." Die Makromolekulare Chemie **125**(1): 108-118.

Yasuda, H., Lamaze, C. E., Ikenberry, L. D. (1968). "Permeability of solutes through hydrated polymer membranes. Part I. Diffusion of sodium chloride." Die Makromolekulare Chemie **118**(1): 19-35.

Yasukawa, T., Ogura, Y., Sakurai, E., Tabata, Y. and Kimura, H. (2005). "Intraocular sustained drug delivery using implantable polymeric devices." Advanced Drug Delivery Reviews 57(14): 2033-2046.

Yoshida, R., Kaneko, Y., Sakai, K., Okano, T., Sakurai, Y., Bae, Y. H. and Kim, S. W. (1994). "Positive thermosensitive pulsatile drug release using negative thermosensitive hydrogels." Journal of Controlled Release 32(1): 97-102.

Yoshida, R., Okuyama, Y., Sakai, K., Okano, T. and Sakurai, Y. (1994). "Sigmoidal swelling profiles for temperature-responsive poly(N-isopropylacrylamide-co-butyl methacrylate) hydrogels." Journal of Membrane Science 89(3): 267-277.

Yoshida , R., Sakai K., Okano, T., Sakurai, Y. (1991). "A new model for Zero order release I. HYdrophobic drug release from hydrophilic polymeric matricies." Polymer journal 23(9): 1111-1121.

Yoshida , R., Sakai K., Okano, T., Sakurai, Y. (1994). "Modulating the phase transition and thermosensitivity in N-isopropylacrylamide copolymer gels." Journal of biomaterials science. Polymer edition 6: 585-598.

Yoshida, R. and Uchida, K. (1995). "Comb-type grafted hydrogels with rapid de-swelling response to temperature changes." Nature 374(6519): 240.

Yu, H. and Grainger, D. W. (1995). "Modified release of hydrophilic, hydrophobic and peptide agents from ionized amphiphilic gel networks." Journal of Controlled Release 34(2): 117-127.

Yu, H., Grainger, David W. (1993). "Thermo-sensitive swelling behavior in crosslinked N-isopropylacrylamide networks: Cationic, anionic, and ampholytic hydrogels." Journal of Applied Polymer Science 49(9): 1553-1563.

Yui, N., Okano, T. and Sakurai, Y. (1993). "Photo-responsive degradation of heterogeneous hydrogels comprising crosslinked hyaluronic acid and lipid microspheres for temporal drug delivery." Journal of Controlled Release 26(2): 141-145.

238

Zhang, J. and Peppas, N. A. (2002). "Morphology of poly(methacrylic acid)/poly(N-isopropyl acrylamide) interpenetrating polymeric networks." Journal of Biomaterials Science -- Polymer Edition **13**(5): 511-525.

Zhang, R., Liu, J., He, J., Han, B., Zhang, X., Liu, Z., Jiang, T. and Hu, G. (2002). "Compressed CO_2-Assisted Formation of Reverse Micelles of PEO-PPO-PEO Copolymer." Macromolecules **35**(21): 7869-7871.

Zhang, Y. and Chu, C.-C. (2002). "The Effect of Molecular Weight of Biodegradable Hydrogel Components on Indomethacin Release from Dextran and Poly(DL)lactic Acid Based Hydrogels." Journal of Bioactive and Compatible Polymers **17**(2): 65-85.

Zhang, Y. and Chu, C.-C. (2002). "In vitro Release Behavior of Insulin from Biodegradable Hybrid Hydrogel Networks of Polysaccharide and Synthetic Biodegradable Polyester." J Biomater Appl **16**(4): 305-325.

Zhang, Y., Chu, C.-C. (2001). "Biodegradable dextran-polylactide hydrogel network and its controlled release of albumin." Journal of Biomedical Materials Research **54**(1): 1-11.

Zhang, Y., Ma, L. and Yang, J. (2004). "Kinetics of esterification of lactic acid with ethanol catalyzed by cation-exchange resins." Reactive and Functional Polymers **61**(1): 101-114.

Zhang, Y., Won, C.Y., Chu, C.C. (2000). "Synthesis and characterization of biodegradable hydrophobic-hydrophilic hydrogel networks with a controlled swelling property." Journal of Polymer Science Part A: Polymer Chemistry **38**(13): 2392-2404.

Zhang, Y., Won, C.Y., Chu, C.C. (1999). "Synthesis and characterization of biodegradable network hydrogels having both hydrophobic and hydrophilic components with controlled swelling behavior." Journal of Polymer Science Part A: Polymer Chemistry **37**(24): 4554-4569.

Zhong, X., Wang, Y.-X. and Wang, S.-C. (1996). "Pressure dependence of the volume phase-transition of temperature-sensitive gels." Chemical Engineering Science **51**(12): 3235-3239.

APPENDICES

Appendix I:

SYNTHESIS OF HYDROGELS

The exact quantities of chemicals used are as outlined in the Tables below. The number of moles of PLA macromer was calculated for one repeating unit. Summation of NIPAAM and PLA macromer represents 100% reactant.

Table 1:SYNTHESIS OF 100-0 NIPAAM-PLA

Chemical	moles	Ratio (%)	Quantity
NIPAAM	0.025mol	100	2.829g
PLA Macromer	----------	-----------	---------
AIBN	$2.50E10^{-4}$	1	41mg + 1ml DMF
BIS	$1.00E10^{-3}$	4	154mg
TEMED	$2.26E10^{-3}$	9	0.34ml
Volume DMF	----------	------------	8ml

Table 2: Table1SYNTHESIS OF 93-7 NIPAAM-PLA

Chemical	moles	ratio	Quantity
NIPAAM	0.02375mol	93	2.68g
PLA Macromer	$1.75E10^{-3}$	7	0.4425g
AIBN	$2.50E10^{-4}$	1	41mg + 1ml DMF
BIS	$1.00E10^{-3}$	4	154mg
TEMED	$2.26E10^{-3}$	9	0.34ml
Volume DMF	----------------	----------------	8ml

Table 3: Table1SYNTHESIS OF 86-14 NIPAAM-PLA

Chemical	moles	ratio	Quantity
NIPAAM	0.0225mol	86	2.546g
PLA Macromer	$3.5E10^{-3}$	14	0.885g
AIBN	$2.50E10^{-4}$	1	41mg + 1ml DMF
BIS	$1.00E10^{-3}$	4	154mg
TEMED	$2.26E10^{-3}$	9	0.34ml
Volume DMF	----------------	----------------	8ml

Table 4: Table1SYNTHESIS OF 72-28 NIPAAM-PLA

Chemical	moles	ratio	Quantity
NIPAAM	0.020mol	72	2.2632g
PLA Macromer	0.007mol	28	1.77g
AIBN	$2.50E10^{-4}$	1	41mg + 1ml DMF
BIS	$1.00E10^{-3}$	4	154mg
TEMED	$2.26E10^{-3}$	9	0.34ml
Volume DMF	----------------	--------------	8ml

Appendix II:

Calibration Curves

(A) Calibration curves in the form y = mx + c, where y is the absorbance at a given wavelength and x is the concentration (mg/ml)

Drug Assays (U.V):		
DH (238nm)	Y =51.264x+0.0104	R^2=0.9952
DB (238nm)	Y= 55.791x + 0.010	R^2=0.9998
SA (296nm)	Y= 24.061x -0.0006	R^2=0.9995
IDM (318nm)	Y= 19.323x -0.011	R^2=0.9993

(B)

Drug Assays (Flurometry)		
Excitation wavelength=490nm		
Emission Wavelength=520nm		
D4	Y= 120453x + 272.53	R^2=0.9726
D10	Y= 585347x +406.87	R^2=0.9899
D40	Y= 507627x +3.4667	R^2=0.9811
D70	Y= 717047x –661.43	R^2=0.9956

(C) Calibration curve for GPC using polystyrene standards in DMF

Gel Permeation Chromatography (GPC)	
<u>In DMF</u>	
$Log_e^{(Molecular\ weight)}$ = -0.3173x +9.0396	R^2=0.985

Appendix III

Pure Drug Dissolution Profiles
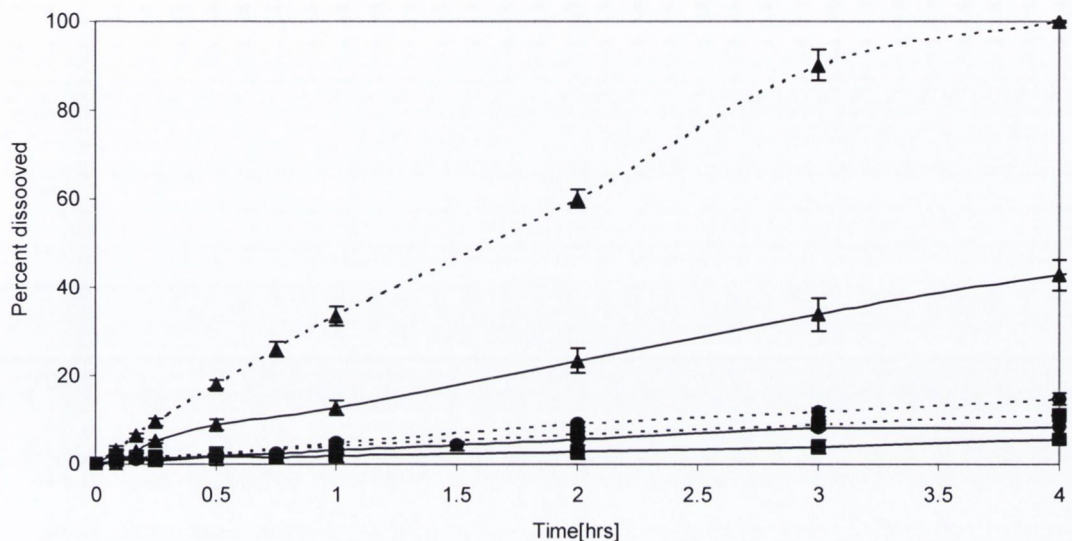
Figure1: Plot of dissolution of pure drugs (100mg) over time in PB at 20°C (solid line) and 37°C (Dashed line) where ▲ is SA, ● is DB and ■ is IDM.
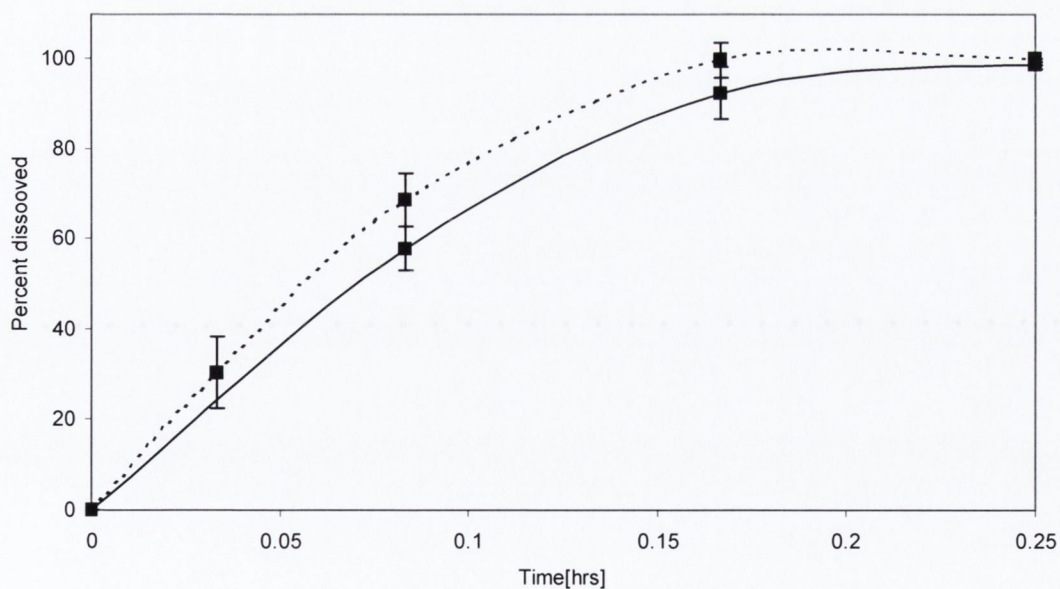
Figure2: Plot of dissolution of pure drug (100mg) DHCl over time in PB at 20°C (solid line) and 37°C (Dashed line).

Appendix IV

Values of the different polymer parameters used for calculation of the molecular weight between cross-links

Parameters used to calculate the molecular weight between crosslinks:

Hydrogel	Q (S.R.)	V_{2s}	Mn (daltons)	*d (g/cm^3)	V_{2r}	χ
PNP	8.26	0.1036	20141	1.046	0.2308	0.30
PNP1$_{-2}$	7.36	0.1139	15276	1.052	0.2516	0.34
PNP2$_{-2}$	6.61	0.1219	10965	1.055	0.2752	0.34
PNP3$_{-2}$	5.85	0.1352	7858	1.058	0.3206	0.34
PNP1$_{-12}$	10.54	0.0786	20028	1.100	0.2422	0.34
PNP2$_{-12}$	11.74	0.0707	15040	1.120	0.2596	0.34
PNP3$_{-12}$	14.46	0.0564	14265	1.126	0.2879	0.34

* d= density

Appendix V

XRD of the various polymer systems composed of PLA MW 2000
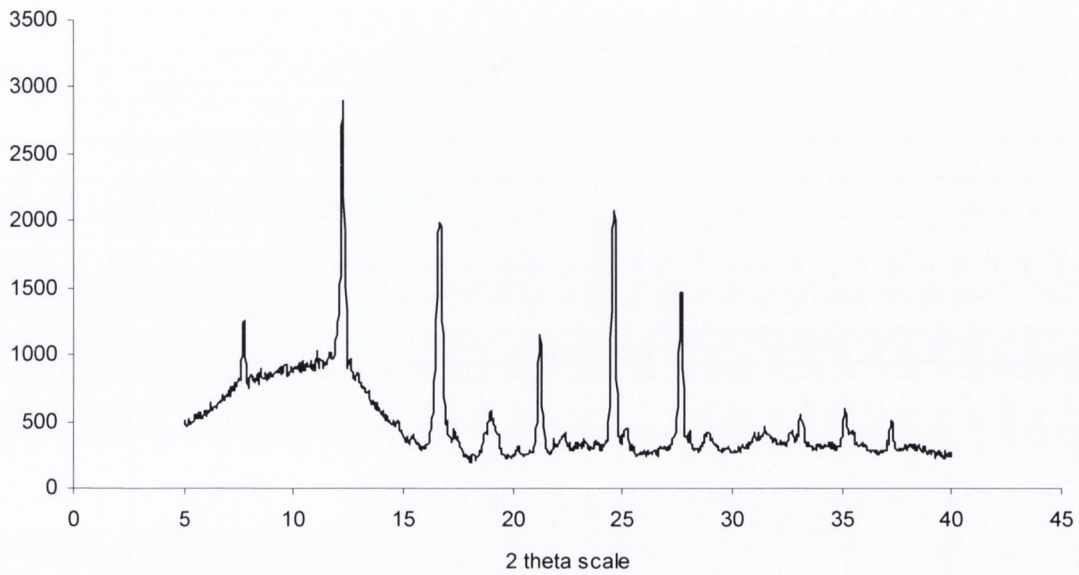
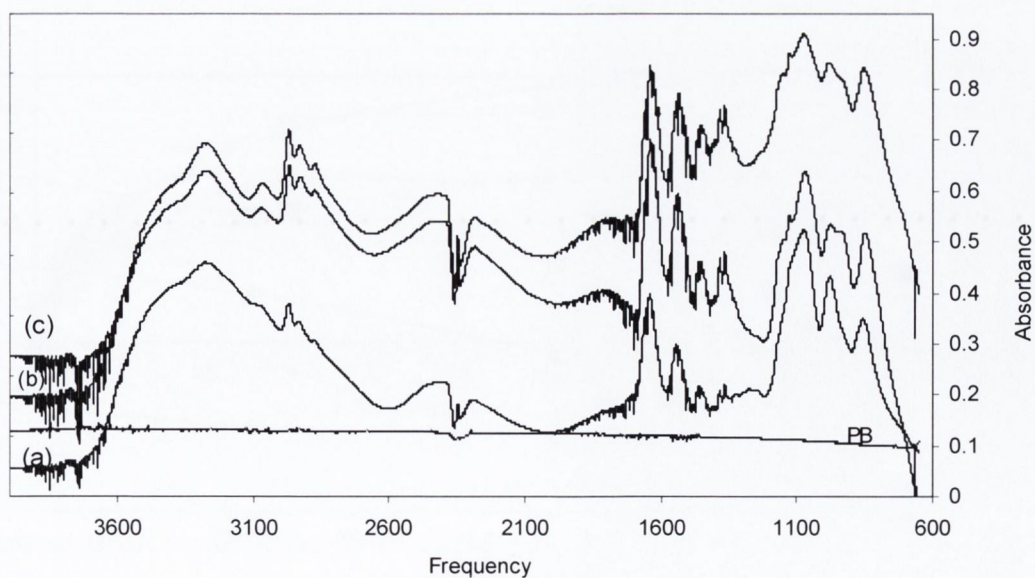X-ray diffraction pattern of PLA diacrylate macromer

(a)
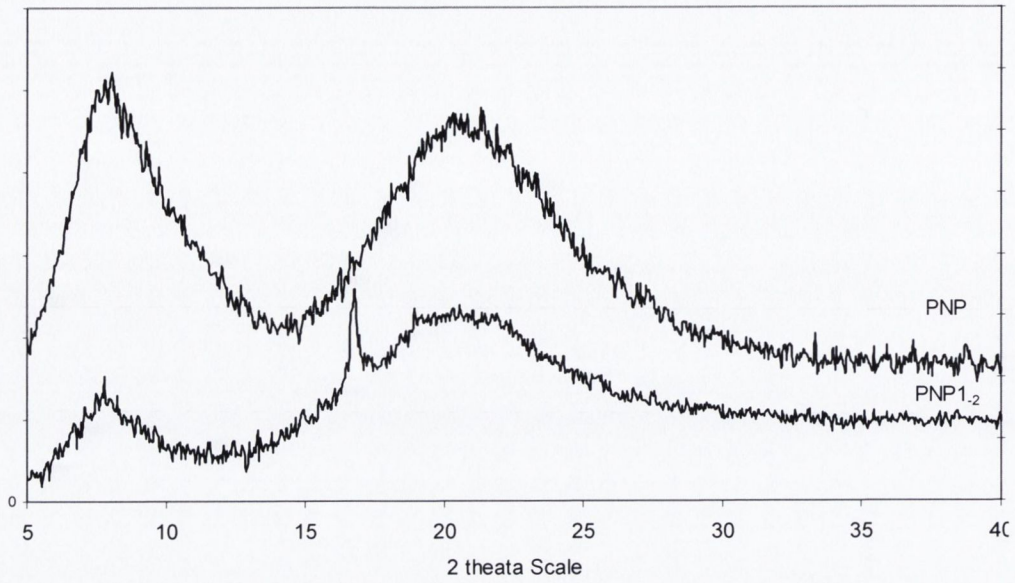
(b)
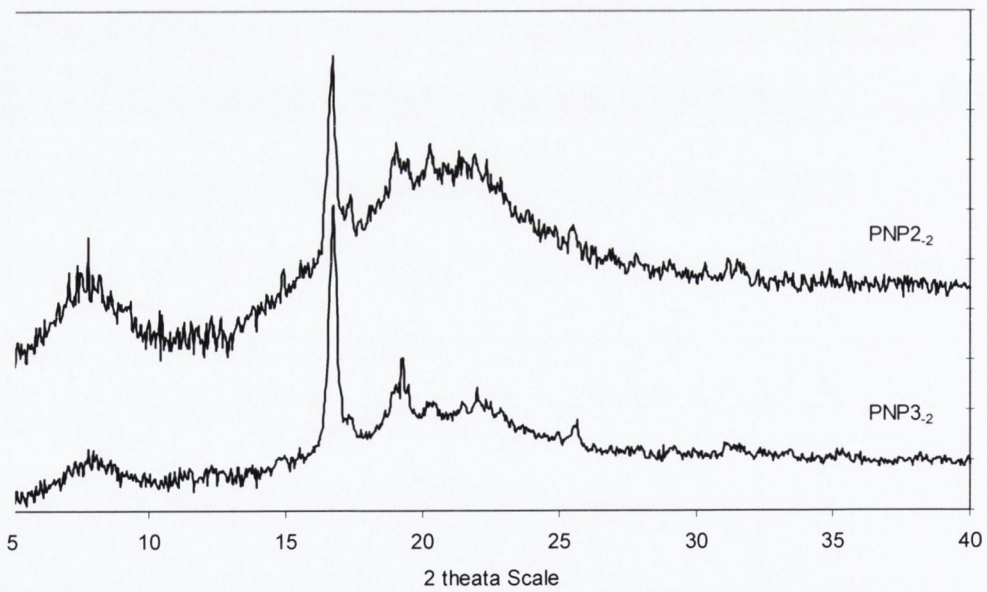
X-ray diffraction patterns of (a) PNP, PNP1$_{-2}$, (b) PNP2$_{-2}$ and PNP3$_{-2}$ polymer

Appendix VI

FTIR analysis of degradation media
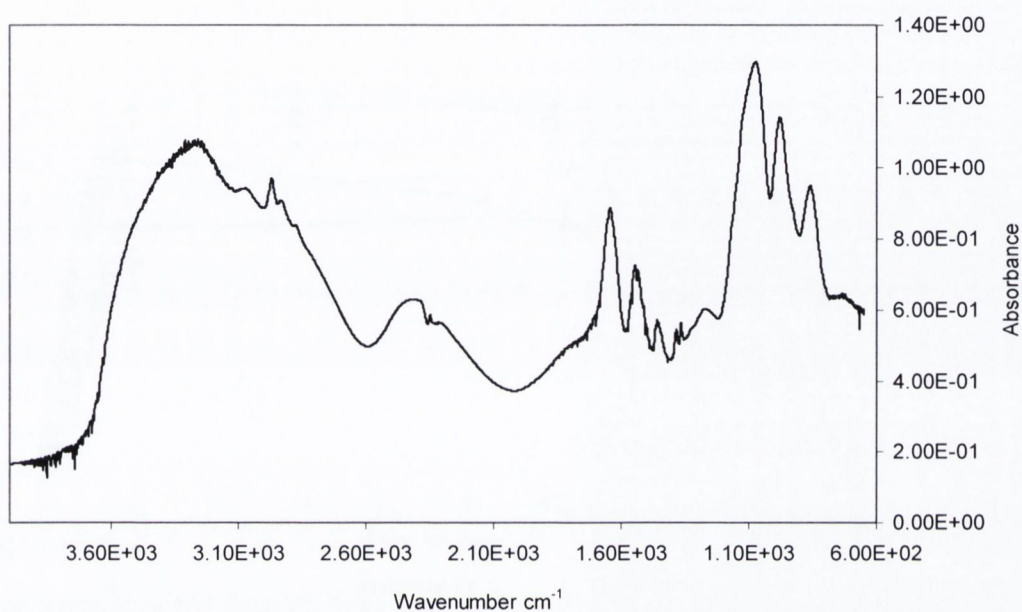
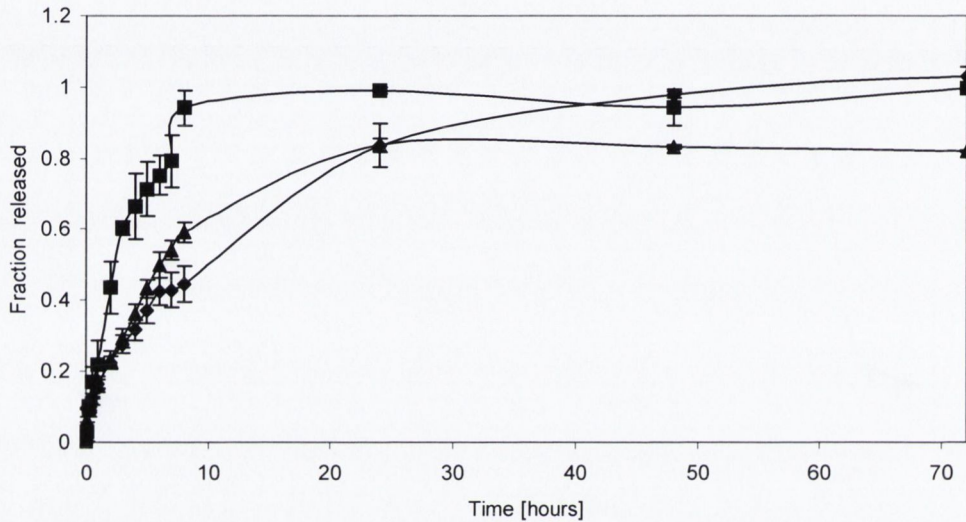
FTIR analysis of PNP swelling medium after 2 months at 20°C

FTIR analysis of (a) PNP1$_{-2}$, (b) PNP2$_{-2}$ and (c) PNP3$_{-2}$ swelling media after 2 months at 20°C.

Also shown PB medium in which experiments were conducted.

Appendix VII

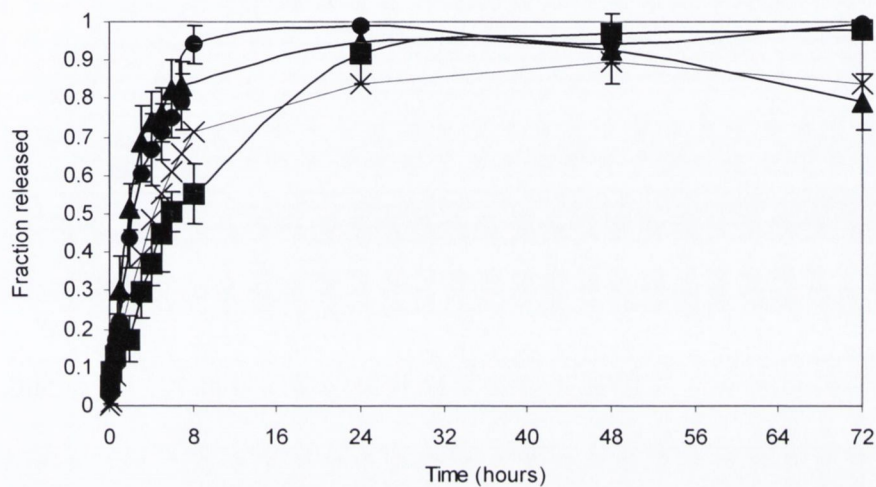# Release profiles of a range of small model drugs from PNP-2$_{-2}$ hydrogel system
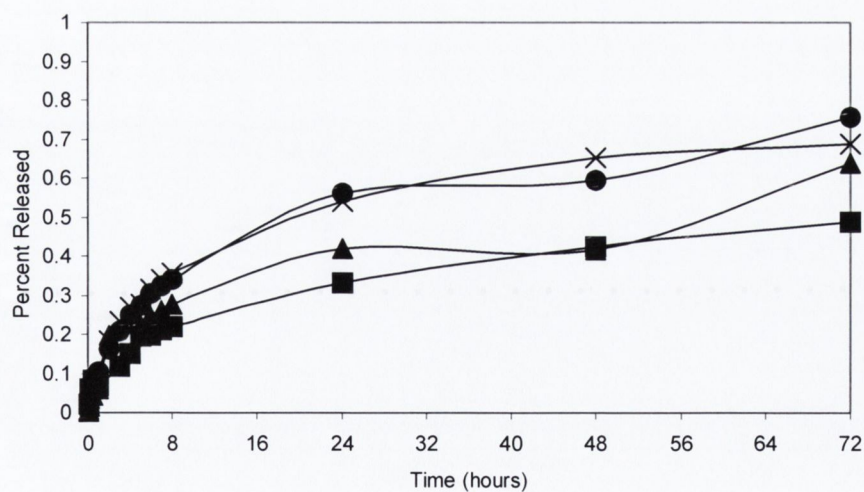

Release profiles of DH (■), SA (▲) and IDM (♦) from PNP2$_{-2}$ at 20°C
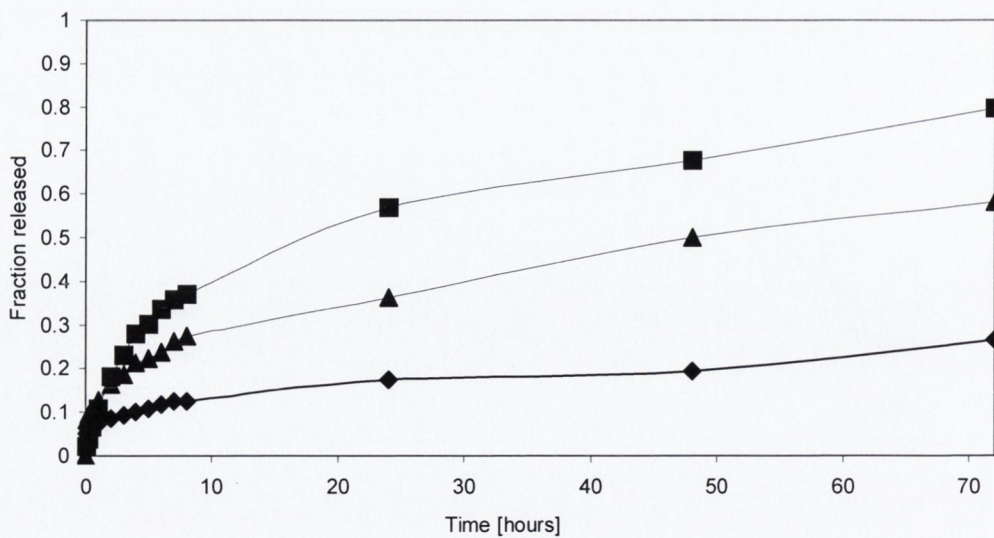
Release profiles of DH (■), SA (▲) and IDM (♦) from PNP2$_{-2}$ at 37°C
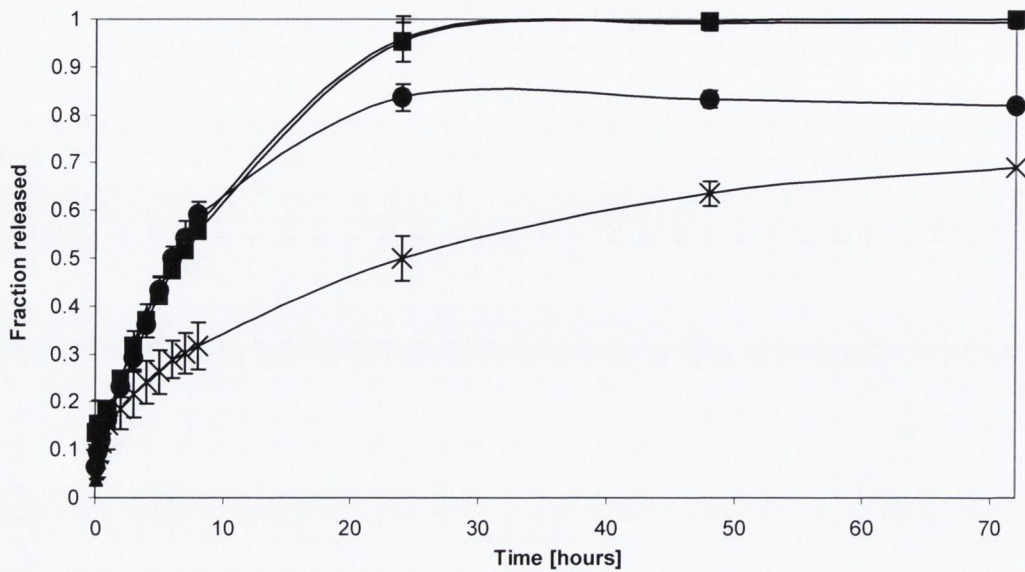
Appendix VIII

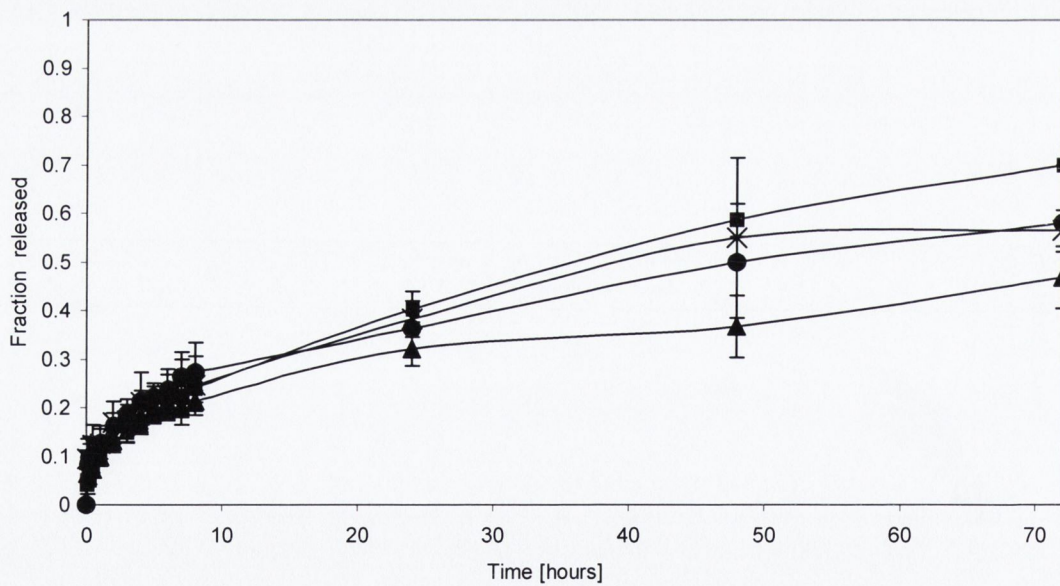# Release profiles of Small Model drugs from PNP-PLA$_{-2}$ hydrogel systems

Fraction released of DH from PNP (■), PNP1$_{-2}$, (▲) PNP2$_{-2}$ (●) and PNP3$_{-2}$ (x) at 20°C.

Fraction released of DH from PNP (■), PNP1$_{-2}$, (▲) PNP2$_{-2}$ (●) and PNP3$_{-2}$ (x) at 37°C.

Fraction released of SA from PNP (■), PNP1$_{-2}$, (▲) PNP2$_{-2}$ (●) and PNP3$_{-2}$ (x) at 20°C.

Fraction released of SA from PNP (■), PNP1$_{-2}$, (▲) PNP2$_{-2}$ (●) and PNP3$_{-2}$ (x) at 37°C.